# Environmental Influences on Distribution and Abundance of Capelin (*Mallotus villosus*) in the Gulf of Alaska

David W. McGowan

A dissertation

submitted in partial fulfillment of the

requirements for the degree of

Doctor of Philosophy

University of Washington

2018

Reading Committee:

Dr. John K. Horne, Chair

Dr. David A. Beauchamp

Dr. Olav Ormseth

Dr. Sandra L. Parker-Stetter

Program Authorized to Offer Degree:

School of Aquatic and Fishery Sciences

University of Washington

**Abstract**

Environmental influences on distribution and abundance of capelin (*Mallotus villosus*) in the Gulf of Alaska

David W. McGowan

Chair of the Supervisory Committee:

Professor John K. Horne

School of Aquatic and Fishery Sciences

To support ecosystem-based management of Alaska's marine resources, there is a need to improve our understanding of how climate-related perturbations in ocean conditions and long-term warming affect distributions and abundances of planktivorous fish that function as a mid-trophic link within marine food webs. Capelin (*Mallotus villosus*) is an important small pelagic fish species in boreal-Arctic marine ecosystems. Spatial and temporal changes in capelin distributions affect their availability as prey to piscivorous seabirds, marine mammals, and commercially important fish. Compared to Atlantic populations, there is limited information describing fluctuations in capelin distributions and abundances in the Alaskan North Pacific.

This dissertation examined environmental influences on distributions and relative abundance of age-1+ capelin over the Gulf of Alaska (GOA) continental shelf to assess variability in capelin biomass and availability to predators. Acoustic, oceanographic, and trawl sampling were conducted in summer and fall of 2011 and 2013 as part of the Gulf of Alaska Integrated Ecosystem Research Program to characterize spatial and temporal variability in

distributions of capelin and other forage fish species over the central (CGOA) and eastern (EGOA) shelf and slope. Environmental factors that influenced occurrence and density of capelin in summer 2013 were identified at spatial resolutions associated with systematic sampling at discrete stations and continuous sampling along transects. Additional data from an independent fisheries-oceanographic survey were used to investigate effects of temperature on spatiotemporal variability in capelin distributions and densities during a period of warm and cold years between 2000 and 2013.

GOA capelin have concentrated over the shelf south and east of the Kodiak Archipelago in the CGOA since at least the mid-2000s. Distributions were influenced by increased vertical mixing and bathymetry. Model results indicated that over shallow submarine banks (< 100 m bottom depth) capelin concentrated in areas with relatively higher water column stratification associated with enhanced primary production. In deeper troughs (≥ 100 m), capelin were most likely to occur in waters between 8 and 9° C, concentrated in areas that were less stratified and associated with higher production. Mean densities of capelin were not directly related to interannual differences in temperature. Observed differences in distributions and relative abundance of capelin between the western (WGOA) and CGOA regions were attributed to either displacement of capelin along the shelf, expansion of distributions during warm years and contraction during cold years, or spatiotemporal differences in capelin mortality due to shifts in predator distributions. Interannual variability in the relative abundance of capelin in the WGOA was correlated with the winter Pacific Decadal Oscillation (PDO) index lagged by 1 year. This suggests that GOA capelin abundance may be influenced by climate-related processes linked to North Pacific sea surface temperature anomalies that affect capelin survival during their first year of life.

# TABLE OF CONTENTS

# LIST OF FIGURES

# LIST OF TABLES

# ACKNOWLEDGMENTS

First, I thank my amazing wife, Veronica, for her love and support… and patience… throughout this project. The hardships associated with the pursuit of a graduate degree fall hardest on those we love most, and this dissertation would not exist without her unwavering support and encouragement. Sweetheart, I can never truly thank you for all that you have done for me throughout our 15 years together. You are my inspiration and will always be the light that makes me strive to be a better father to our beautiful Benjamin, husband that you deserve, and contributor to our community. Never have I been more excited for the three of us to continue rolling along together on this journey. Likewise, the love and support from my parents and brothers have provided me the foundation to pursue my dreams while continually reminding me of what really matters in life.

Next, I wish to thank my advisor, John, for his mentorship and continually challenging me to see the forest through the trees. I also thank my committee members: Sandy, for her sound guidance and feedback; Olav, for his efforts to secure the data and financial support essential to this project's success; and Dave, for helping me grasp the complexities of marine food webs and trophic dynamics. This dissertation was shaped and greatly improved by numerous colleagues from the GOAIERP, NOAA, and UW. I'd like to thank Jim Thorson for patiently guiding me through the world of TMB and spatial models, and to Lauren Rogers and Mark Zimmermann for their contributions to Chapters 3 and 4. I am grateful for having worked with a talented, collaborative group of scientists at SAFS and in the Fisheries Acoustics Research Lab, with special thanks to Dale Jacques and Beth Phillips. Finally, this dissertation was made possible through the financial support of the North Pacific Research Board and SAFS.

# Chapter 1. INTRODUCTION

Climate-related changes to marine ecosystems are projected to affect marine organisms, food webs, fisheries, and fishery-dependent communities in the northern hemisphere (Drinkwater et al., 2010; Hollowed et al., 2013a). These ecological, economic, and social effects are predicted to occur as a result of climate-related variability in primary production (Arrigo and van Dijken, 2011; Perrette et al., 2011), species distributions (Hollowed et al., 2013b; Perry et al., 2005; Pershing et al., 2015), community composition (Grebmeier et al., 2006), and the partitioning of energy between demersal and pelagic communities (Grebmeier et al., 2006; Moore and Stabeno, 2015). To support ecosystem-based management of marine resources, there is a need for resource managers to improve their understanding of how climate-related perturbations in ocean conditions and long-term warming influence the distribution and abundance of mid-trophic, planktivorous fish (Hollowed et al., 2013a) that modulate the transfer of energy from primary producers to upper trophic species (Pikitch et al., 2014).

Planktivorous fish are often collectively referred to as forage fish; these include small, schooling pelagic fish (*e.g.* clupeids, osmerids), early life stages of piscivorous fish (*e.g.* gadids), and mesopelagic fish (*e.g.* myctophids) species (Pikitch et al., 2012; Springer and Speckman, 1997). Forage fish serve as key prey for many seabirds, marine mammals, and commercially important fish species (Dragoo et al., 2012; Womble and Sigler, 2006; Yang et al., 2005). As predators, forage fish can regulate the biomass (Freon et al., 2005; Gjøsæter et al., 2002; Micheli, 1999) and species composition (Cury et al., 2000; Frank et al., 2011) of their zooplankton prey, and may potentially influence recruitment of their predators by consuming fish eggs and larvae (Fauchald, 2010; Kornilovs et al., 2001).

Capelin (*Mallotus villosus*) are an important forage fish species in boreal-Arctic waters

across the northern hemisphere. Distributed in all oceans at latitudes of approximately 45 to 80° N (Carscadden et al., 2013a; Logerwell et al., 2015; Pahlke, 1985), capelin occupy waters that extend from the nearshore, across the continental shelf and to the upper slope. Capelin are small pelagic fish that live less than 5 years (Carscadden and Vilhjálmsson, 2002; Gjøsæter, 1998; Vilhjálmsson, 2002). Spawning can occur from spring through summer, varying by region and local temperatures (Gjøsæter, 1998; Pahlke, 1985; Rose, 2005). In the Atlantic, spawning occurs on gravel beaches in the intertidal or in deeper waters (<150 m bottom depth) (Carscadden and Vilhjálmsson, 2002; Rose, 2005; Vilhjálmsson, 1994, 2002), while only beach spawning is believed to occur in the Pacific (Blackburn et al., 1981; Pahlke, 1985; Rose, 2005). Capelin are demersal spawners on beaches, depositing eggs in gravel (Carscadden and Vilhjálmsson, 2002). The duration of egg incubation is temperature-dependent, varying from weeks in 7° C water to months in 2° C waters (Carscadden et al., 2013a; Gjøsæter, 1998). After hatching, larvae are pelagic and primarily transported away from spawning locations to offshore nursery areas over the shelf (Doyle et al., 2002; Gjøsæter, 1998; Rose, 2005). The larval phase lasts for approximately 12 months before metamorphosis to the adult form (Gjøsæter, 1998). With the exception of capelin that are retained within coastal fjords (*e.g.* Arimitsu et al., 2008), most capelin remain offshore in feeding areas until they mature as age-2+ fish, after which they migrate back to coastal waters to spawn and die (Gjøsæter, 1998; Vilhjálmsson, 2002).

A mobile and gregarious pelagic species, capelin distributions are spatially and temporally heterogeneous (Carscadden et al., 2013a; Ingvaldsen and Gjøsæter, 2013; Rose, 2005), which affects their availability as prey to apex predators. Capelin function in an intermediate trophic role as predators of zooplankton and prey for piscivorous fish, seabirds, and marine mammals. Spatial and temporal changes in capelin distributions and densities affect their

availability as prey to piscivorous seabirds (Carscadden et al., 2002; Sydeman et al., 2017), marine mammals (Gjøsæter et al., 2009; Simard et al., 2002; Whitehead and Carscadden, 1985), and commercially important fish (Ciannelli and Bailey, 2005; Rose and O'Driscoll, 2002; Vilhjálmsson, 2002).

In Hjort's (1914) classic review of cod and herring fisheries in the North Atlantic, he described how environmentally-driven variability in capelin distributions and migration patterns affects the availability of capelin to fisheries and as prey to other commercially and ecologically important species. During the 100+ years that have followed, fluctuations in capelin distributions and abundances have been well documented in the Barents Sea, Icelandic, and Northwest Atlantic populations (Carscadden et al., 2013b, 2013a; Gjøsæter, 1998; Vilhjálmsson, 2002). Decades of extensive monitoring and collection of fisheries and oceanographic data to support commercial capelin fisheries in the Atlantic (*e.g.* Carscadden et al., 2013a; Gjøsæter, 1998) have facilitated investigations on the potential role of directed fisheries on population crashes, and how environmental processes influence capelin population dynamics and distributions during different life stages (*e.g.* Carscadden et al., 2013b; Frank et al., 1996; Ingvaldsen and Gjøsæter, 2013; Olafsdottir and Rose, 2012). Studies on Atlantic capelin populations also highlight how the strength of capelin-predator relationships, including Atlantic cod (*Gadus morhua*) (Horne and Schneider, 1994; Piatt, 1990; Rose and Leggett, 1990) and seabirds (Fauchald, 2009; Fauchald and Erikstad, 2002), vary as a function of scale.

Compared to Atlantic populations, there has been no directed monitoring and limited research and management of Pacific capelin populations. Research products that describe changes in capelin distributions and abundances in the North Pacific have typically been derived from studies designed for other species. This lack of historical information is attributed to the

absence of a directed capelin fishery, and to the fact that bottom trawl gear used in existing abundance surveys for groundfish is poorly suited to detect changes in capelin and other small pelagic species' distributions (Ormseth, 2012).

Despite limited monitoring, interdecadal abundance fluctuations have been observed in Pacific capelin (Anderson and Piatt, 1999; Mueter and Norcross, 2002; Ormseth, 2012), and are believed to have negatively impacted predators. After the late 1970s regime shift (Francis et al., 1998), declines in production and abundances of piscivorous seabirds and marine mammals were attributed to reductions of capelin and other forage species in predator diets (Anderson and Piatt, 1999; Merrick et al., 1997; Piatt and Anderson, 1996). The recognition that changes in the availability and species composition of prey may impact managed predators (Ormseth, 2012; Springer and Speckman, 1997) prompted investigations of how physical and biological processes influence the distribution and abundance of capelin and other small pelagic species in the North Pacific (*e.g.* Arimitsu et al., 2008; Hollowed et al., 2012; Parker-Stetter et al., 2016).

Recent interdisciplinary research efforts in Alaska have attributed a wide range of environmental factors to changes in offshore and coastal capelin distributions. In the eastern Bering Sea (EBS), the relative abundance of capelin in surface waters (upper 30 m) was significantly higher during years with relatively colder water (2006-2011), with distributions concentrated in the northern EBS and extended to lower latitudes compared to observations from warm years (2003-2005) (Andrews et al., 2015). Capelin in surface waters during cold years were predicted to occur in relatively cooler, less saline waters above the pycnocline where densities would be highest over bottom depths between 60 to 80 m (Parker-Stetter et al., 2016). In the Gulf of Alaska (GOA), changes in capelin distributions over the shelf south and east of the Kodiak Archipelago have been attributed to oceanographic conditions (Hollowed et al., 2007;

Logerwell et al., 2007), composition and distribution of zooplankton prey, and potential competition with juvenile walleye pollock (*Gadus chalcogrammus*, hereafter pollock) (Logerwell et al., 2010; Wilson et al., 2006). Within interior waters of Glacier Bay in Southeast Alaska, capelin have been associated with areas near tidewater glaciers that are hypothesized to serve as cold-water refugia during periods of ocean warming (Arimitsu et al., 2008).

Recognizing that changes in marine food webs affect species of anthropogenic importance, ecosystem-based management is expanding the research aperture to include non-commercial but ecologically important species such as capelin and other forage species (Francis et al., 2007; Link, 2002; Pikitch et al., 2004). To protect key food web components, new fisheries targeting forage fish species (including capelin) were prohibited in the North Pacific by the North Pacific Fisheries Management Council (NPFMC) in 1998 (Ormseth, 2012). A management framework has been adopted by the NPFMC to include indicators of marine ecosystem status to assess both historical and present ecosystem states (Livingston et al., 2005). Since 2000, Ecosystem Status indicators have been used to provide updated information on the status and trends of ecosystem components by trophic level to the NPFMC (Zador and Yasumishii, 2017). In 2016, an index of capelin relative abundance developed from predator diets was adopted as an Ecosystem Status indicator for the western GOA (Zador and Yasumishii, 2016). Currently, Ecosystem Status indicators contribute to Alaska's Integrated Ecosystem Assessment (IEA, https://www.integratedecosystemassessment.noaa.gov) used to support ecosystem-based management by aiding managers in understanding how environmental factors influence managed species, and to consider potential effects of fishing or other human activities on the ecosystem.

In response to anomalously warm ocean conditions in the Northeast Pacific from 2014-16 (the "Warm Blob", Bond et al., 2015), resource managers are also seeking information on how temperature-related changes in distributions and abundances of capelin and other forage species during marine heatwaves and temperature regime shifts affect their availability as prey to upper trophic predators (Zador and Yasumishii, 2017). Temperature variability and climate-related changes to marine ecosystems have previously been associated with fluctuations in distributions and abundances of capelin in the Pacific (Anderson and Piatt, 1999; Andrews et al., 2015), Arctic (Carscadden et al., 2013a; Logerwell et al., 2015), and Atlantic (Carscadden et al., 2013a; Ingvaldsen and Gjøsæter, 2013; Rose, 2005) Oceans. Despite having a wide thermal tolerance (-1.5 to 14° C), small changes in sea temperatures (~1° C) have been associated with changes in capelin distributions that spanned 100s km (Rose, 2005). Temperature has been associated with changes in the timing and path of migrations to spawning areas around Iceland (Olafsdottir and Rose, 2012, 2013), as well as with spawn timing and the selection of spawning habitat in the Northwest Atlantic (Carscadden et al., 1989; Davoren et al., 2012; Nakashima and Wheeler, 2002). There is also evidence that capelin distributions and population dynamics are influenced by indirect effects of temperature variability linked to changes in distributions, abundances, and/or species compositions of zooplankton prey related to temperature regime shifts (Orlova et al., 2010) or sea ice dynamics (Buren et al., 2014), as well as to changes in distributions and abundances of predators (Hjermann et al., 2004).

Temperature increases have been associated with a northward shift in capelin distributions around Iceland (Carscadden et al., 2013a; Valdimarsson et al., 2012). In response to projected increases in sea temperatures and loss of sea ice (IPCC, 2007), capelin distributions in the Barents and Bering Seas are also predicted to shift northward into the Arctic (Carscadden

et al., 2013a; Hollowed et al., 2013b; Huse and Ellingsen, 2008). In the North Pacific, empirical evidence partially supports this predicted northward shift, where the southern range of capelin in surface waters (<30 m) of the EBS shifted from the Aleutian Islands in cold years to north of approximately 60° N in warm years (Andrews et al., 2015). Limited field studies in the Chukchi and Beaufort Seas have observed interannual variability in capelin range and abundance, but differences in distribution and density were not directly associated with water temperatures (De Robertis et al., 2017b; Logerwell et al., 2015).

In contrast to capelin populations that are expected to shift northward during periods of increased warming, the GOA capelin population is likely more vulnerable to anomalous warming events and long-term increases in sea temperatures. Northward movement in the GOA is blocked above 60° N by the Alaska coast, potentially limiting suitable habitat during periods of increased warming and constraining capelin distributions to waters that may serve as cold water refugia (*e.g.* Arimitsu et al., 2008). While capelin are distributed across the GOA shelf and within coastal embayments, the core of the population is believed to be located over the Kodiak shelf (Ormseth et al., 2016). Support for this observation is found in the recovery of capelin after the population collapsed following the late 1970s regime shift (Anderson and Piatt, 1999; Francis et al., 1998). As the population recovered, increasing catch rates in the National Marine Fisheries Service Alaska Fisheries Science Center (AFSC) Groundfish Assessment Program's summer GOA Continental Shelf and Slope bottom trawl survey showed that capelin distributions expanded across the GOA from waters around Kodiak (Mueter and Norcross, 2002; Ormseth, 2012). Temperature-related habitat reductions may lead to distributional shifts, reduced biomass, and potentially another collapse of the GOA population if sufficient habitat is not available. Negative impacts to GOA capelin may also result from indirect effects of

increased variability in ocean conditions or climate-related warming that influence changes in the timing, magnitude, and/or species composition of plankton blooms (Stabeno et al., 2016b; Strom et al., 2006, 2016; Waite and Mueter, 2013), shifts in water mass distributions due to fluctuations in the Alaska Coastal Current (Hermann et al., 2016; Ladd et al., 2016; Stabeno et al., 2016a) and eddies (Ladd, 2007; Ladd et al., 2007), and changes in distributions, abundances, and species compositions of zooplankton prey (Batten et al., 2017; Coyle et al., 2013; Pinchuk et al., 2008), other invertebrates (*e.g.* Li et al., 2016), and predators (*e.g.* Ciannelli and Bailey, 2005; Hjermann et al., 2004).

This dissertation examined environmental influences on age-1+ capelin distributions and relative abundance over the GOA shelf to assess variability in capelin biomass and availability to predators. The objectives of this dissertation were to: 1) characterize spatial and temporal variability in distributions of capelin and other forage fish species over the GOA shelf; 2) quantify the influence of physical and biological factors on capelin occurrence and density at different spatial resolutions; and 3) investigate effects of temperature on spatiotemporal variability in capelin distributions and densities.

In Chapter 2, spatial and temporal variability in species composition and distributions of forage fish was characterized using acoustic-trawl data from summers and falls of 2011 and 2013 in the eastern (EGOA) and central (CGOA) regions of the GOA. Potential effects on forage fish predators and distribution/abundance survey efforts were then inferred from the quantitative pattern description. This study was conducted as part of the Gulf of Alaska Integrated Ecosystem Research Program (GOAIERP - http://www.nprb.org/gulf-of-alaska-project). The GOAIERP was an inter-disciplinary effort to investigate how physical and biological processes

in the GOA marine ecosystem determine the survival of five commercially and ecologically important demersal species during their first year of life.

Physical and biological factors that influenced capelin distributions in the CGOA during the GOAIERP surveys were evaluated in Chapter 3. Recognizing that the relative influence of explanatory factors on capelin distributions may be scale-dependent (Schneider, 1994), acoustic measurements of capelin density were analyzed at two spatial resolutions: station (37 km) and transect (0.5 km). Specific objectives of this chapter were to: 1) quantify the influence of physical and biological factors on capelin occurrence and density; and 2) compare the relative importance of factors that explain variance in capelin distributions at two spatial resolutions.

Given that the GOAIERP surveys were only conducted in two years and Chapter 3's analysis of environmental factors that influenced capelin distributions was limited to one year of GOAIERP data, Chapter 4 investigated responses of capelin to temperature variability over the GOA shelf using seven years of fisheries-oceanographic survey data collected during warm and cold years. Conducted by the AFSC Ecosystems and Fisheries-Oceanography Coordinated Investigations Program, the late-summer small-mesh trawl survey was designed to monitor the distribution and abundance of age-0 pollock prior to the onset of winter, and to investigate influences of oceanographic conditions and zooplankton prey on variability in densities of pollock and other small pelagic fishes. Specific objectives of this chapter were to: 1) quantify spatiotemporal changes in capelin occurrence and positive catch rates related to temperature-related covariates; 2) characterize shifts in capelin distributions and mean densities during warm and cold years; and 3) quantify relationships between annual mean capelin densities with an alternate GOA-based capelin index and large-scale climate indices.

Key findings from this dissertation are summarized in Chapter 5 to provide insights on capelin distributions and habitat preferences in the GOA. Recommendations are presented for improved monitoring of capelin and forage fish in the GOA, and for analytic approaches developed for GOA-based survey data. Future research needs are identified to inform resource managers on the response of capelin to climate-related changes to the GOA and in an effort to improve assessments of potential effects on commercially important species.

# Chapter 2. VARIABILITY IN SPECIES COMPOSITION AND DISTRIBUTION OF FORAGE FISH IN THE GULF OF ALASKA

## 2.1 INTRODUCTION

In pelagic marine ecosystems, planktivorous fish occupy an intermediate trophic position where they function as both predator and prey, facilitating the transfer of energy from primary producers to piscivores. Collectively referred to as forage fish, these include small, schooling pelagic fish, early life stages of piscivorous fish, and mesopelagic fish species (Springer and Speckman, 1997). Forage fish serve as the primary prey for many seabirds, marine mammals, and commercially important fish species. As predators, forage fish can regulate the biomass (Freon et al., 2005; Gjøsæter et al., 2002; Micheli, 1999) and species composition (Cury et al., 2000; Frank et al., 2011) of their zooplankton prey, and may potentially influence recruitment of their predators by consuming fish eggs and larvae (Fauchald, 2010; Kornilovs et al., 2001). Throughout the Northeast Pacific, the forage fish community is comprised of small pelagic species such as capelin (*Mallotus villosus*) and Pacific herring (*Clupea pallasii*, hereafter herring), juvenile groundfish such as walleye pollock (*Gadus chalcogrammus*, hereafter pollock) and Pacific cod (*Gadus macrocephalus*), juvenile salmonids, and mesopelagic fish (*e.g.* myctophids) species (Mecklenburg et al., 2002; Springer and Speckman, 1997).

Forage fish exhibit high spatial and temporal variability in their population abundance and distribution, arising from differences in life history patterns among species. Fluctuations in the abundance of small pelagic species primarily result from high recruitment variability and relatively short life spans (Freon et al., 2005). Spawning stocks comprised of only 1 or 2 age classes cannot withstand multiple years of poor recruitment (Freon et al., 2005; Pikitch et al., 2012; Springer and Speckman, 1997), making these species more susceptible to large variations

in abundance compared to longer-lived species. Reduced abundance may result in contracted distributions (Hay et al., 2001; Ingvaldsen and Gjøsæter, 2013; MacCall, 1990); while strong recruitment can rapidly increase abundance and/or expand distributions (*e.g.* Bertrand et al., 2004; Chavez et al., 2003; Schwartzlose et al., 1999). In high latitude ecosystems, abrupt changes in abundance and/or distribution have been observed in populations of small pelagic species including capelin (Anderson and Piatt, 1999; Carscadden et al., 2013b, 2013a) and herring (*Clupea* spp.) (Hay et al., 2001). Variability in abundances of a planktivorous stage in a longer-lived, piscivorous fish species (*e.g.* age-0 gadoids) are weakly related to the age structure and biomass of the spawning stock (Szuwalski et al., 2015).

Independent of abundance, distributions of forage fish may also be influenced by physical and biological processes that operate across a range of spatial and temporal scales (Freon et al., 2005; Hunt et al., 1999; Ingvaldsen and Gjøsæter, 2013). The distribution and intensity of oceanographic gradients, or the distribution and duration of increased nutrient mixing, varies over scales ranging from 100s m to 100s km, and persist for hours to months (*e.g.* Stabeno et al., 2004; Cheng et al., 2012; Ladd et al., *in review*). This environmental variability changes the availability of preferred habitat or prey , which can influence forage fish distributions (*e.g.* Arimitsu et al., 2008; Obradovich et al., 2014; Speckman et al., 2005). Vertical structure in the water column can also influence forage fish distributions by limiting habitat (Bertrand et al., 2010; Sogard and Olla, 1998), concentrating prey (Hunt et al., 1999; Grados et al., 2012), or providing refuge from predators (Hrabik et al., 2006). Predators can directly influence forage fish distributions (*e.g.* a "halo" of local prey depletion, Ashmole, 1963; Lewis et al., 2001), or indirectly by causing anti-predator behavioral responses, such as shifts in vertical position (*e.g.* Hrabik et al., 2006; Mowbray, 2002; Scheuerell and Schindler, 2003).

Spatial and temporal variability in the species composition and distribution of a forage fish community may affect their availability to predators and abundance estimation surveys that are conducted to monitor changes in the forage base. The potential effects on a predator will depend on the predator's foraging behavior, spatial constraints, and energetic demands. Variability in the aggregation of forage fish will affect predators that use search behaviors sensitive to patch size, distance between patches, and/or prey density (*e.g.* Benoit-Bird et al., 2013; Fauchald, 2009). Mobile predators are less affected by a shift in the horizontal distribution of prey compared to a central place forager (Orians and Pearson, 1979), while a vertical shift in prey distribution would have different effects on fish compared to air-breathing predators, divers compared to surface feeders, or between predators with different thermal tolerances and/or light sensitivities. A change in the species composition of a forage fish community may reduce a predator's net energy intake due to differences in energy density among forage fish species (*e.g.* Vollenweider et al., 2011), and vulnerability to predation that potentially limits a predator's growth, fitness, and/or reproductive success (*e.g.* Gjøsæter et al., 2009; Cury et al., 2011; Robinson et al., 2015). Potential effects of spatial and temporal variability in forage fish distributions on survey abundance estimates will depend on the timing, spatial extent, sampling gear, and sampling resolution of the survey. Variability in the timing or pathway of migrations (Olafsdottir and Rose, 2013, 2012) or climate-induced shifts in distribution (Carscadden et al., 2013a; Perry et al., 2005) may result in incomplete survey coverage of the population domain. Changes in vertical distribution may result in biased measurements of horizontal distribution and abundance in surveys that exclusively use fixed-depth sampling gear (*e.g.* McQuinn, 2009; Parker-Stetter et al., 2013). A systematic survey based on equally-spaced point samples may not

detect variability in forage fish aggregation patterns at spatial scales that differ from the resolution of point samples.

Despite their ecological importance, information on the distribution and community structure of forage fish over the GOA continental shelf and slope is limited (Ormseth, 2012). To support ecosystem-based management of Alaska's marine resources, characterization of spatial and temporal variability in forage fish distributions is needed to improve our understanding of how changes in forage fish biomass and availability potentially affect predators in the GOA (Livingston et al., 2005). In this study, an acoustic-trawl survey was conducted in the summer and fall of 2011 and 2013 to quantify variability in species composition and distributions of forage fish in the central and eastern regions of the GOA.

## 2.2 METHODS

### 2.2.1 Study area & sampling design

This study was conducted during the summer (July-August) and fall (September-October) of 2011 and 2013. During each season, the eastern and central regions of the GOA were surveyed (Fig. 2.1). The eastern GOA (EGOA) region extended along the Southeast Alaska coast, from Cross Sound to Cape Ommaney (southern tip of Baranof Island). The central GOA (CGOA) region extended from the southeast side of Kodiak Island to the mouth of Amatuli Trough.

The survey sampled parallel transects orthogonal to the coast that extended from coastal waters over the continental slope (200 to 2000 m bottom depth) to basin waters beyond the 2000 m isobath (Fig. 2.1). Each region's sampling grid was comprised of fixed stations spaced equidistant to each other along transects. In the CGOA, 53 stations spaced at 37.04 km (20 nmi)

intervals were sampled along 10 transects (4 to 6 stations per transect depending on width of the shelf). In the EGOA, the sampling grid in 2011 was composed of 52 stations spaced 18.52 km (10 nmi) apart along 13 transects (4 stations each). In 2013, the EGOA sampling grid was increased to 72 stations along 8 transects (9 stations each) to expand its spatial extent to approximately 150 km offshore. All EGOA stations remained spaced at 18.52 km along each transect, while spacing between the 5 southernmost transects (A to K) increased to 37.04 km. In addition to the two primary sampling grids, single transect lines including 4 fixed stations were sampled off Kayak Island (spaced 14.82 km apart) and Yakutat (the two nearshore stations were spaced 18.52 km apart, then 37.04 km spacing to outermost stations – Fig. 2.1) to provide limited sampling in the area between the two primary sampling grids.

### 2.2.2 **Data collection**

#### 2.2.2.1. *Acoustic data collection*

Acoustic data were collected during seasonal cruises in 2011 and 2013 from the F/V *Northwest Explorer* and the NOAA Ship *Oscar Dyson* (Table 2.1). Simrad ES60 echosounders (Kongsberg, Norway) and hull-mounted, splitbeam transducers operating at 38 and 120 kHz (7° beamwidths measured at half-power points; transmitted power 2000 W and 200 W) were used on the *Northwest Explorer*, with the 120 kHz only available in 2013. Acoustic data were collected on the *Oscar Dyson* using Simrad EK60 echosounders and centerboard-mounted, splitbeam transducers operating at 18, 38, 70, 120, and 200 kHz; only 38 (7° beamwidth; 2000 W) and 120 (7° beamwidth; 500 W) data were used in this study. Acoustic sampling used a pulse duration of 1.024 ms and a transmit rate of 1 pulse every 1-7 seconds depending on recording depth (1 s per 600 m) on the *Northwest Explorer*. On the *Oscar Dyson*, the echosounder operated at a pulse

duration of 0.512 ms and transmit rate of 1 pulse every 1.4 s. Data were continuously collected during daytime hours (sunrise to sunset) along each transect at a speed of approximately 5 m/s (~ 10 knots ) on the *Northwest Explorer* and 6.2 m/s (12 knots) on the *Oscar Dyson*. Prior to the start of summer surveys, all echosounders were calibrated using a 38.1 mm tungsten carbide sphere following Foote et al. (1987). In fall 2013, 120 kHz data were recorded at an uncalibrated power setting on the *Northwest Explorer*, and those data were not used in the analysis.

2.2.2.2. *Trawl sampling*

Fish were sampled using a 198 m rope trawl (Cantrawl model 400, Cantrawl Nets LTD, Richmond, BC, Canada) with a 1.2 mm mesh codend liner. Trawls were towed at 1.6 ± 0.26 m/s (mean ± SE, range 0.8 to 2.5 m/s). Surface trawls (in which additional floats were attached to headrope) were conducted at each station along transects (Fig. 2.1). Additional midwater trawls were conducted opportunistically to identify acoustic targets at headrope depths ranging from 10 to 250 m. Gear and time limitations precluded the trawl from being fished at depths exceeding 250 m. To monitor headrope depth and measure the net opening during trawling, a Simrad FS900 trawl sonar was used on the *Northwest Explorer* and a Simrad FS70 trawl sonar was used on the *Oscar Dyson*. The net opening vertical height averaged 34.7 ± 4.3 m (range 24.2 to 44.3 m) during surface trawls and 16.9 ± 2.4 m (range 12.8 to 22.7 m) during midwater trawls. The horizontal spread of the net averaged 39.5 ± 2.8 m (range 29 to 48 m) during surface trawls, and 62.6 ± 8 m (range 36.9 to 79.9 m) during midwater trawls. Surface trawls were fished for 30 minutes once the trawl sonar confirmed the net was fully opened. Midwater trawl fishing times averaged approximately 20 minutes (range 4 to 35 minutes) based on acoustic densities observed on the echosounder and trawl sonar displays. Trawl catches were sorted by species. For each species or age-group (*i.e.* juvenile or adult), length and weight were individually measured for up

to 50 fish, and an additional subsample of up to 200 fish were counted and bulk weighed to estimate the total number of fish in larger catches. Pollock less than 130 mm standard length were classified as age-0 (Brodeur and Wilson, 1996a).

2.2.2.3. *Acoustic data pre-processing*

The 38 kHz data were analyzed for the 2011 survey, and 38 and 120 kHz data for analysis of the 2013 survey. ES60 data were corrected to remove the triangle-wave error sequence following Keith et al. (2005). All other acoustic data processing was completed using Echoview v5.4 (Echoview Software Pty Ltd). A surface exclusion line was set at 10 m on the *Northwest Explorer* and 15 m on the *Oscar Dyson* to account for transducer depth (4.9 and 9.1 m), and to exclude data within twice the near-field of the 38 kHz transducer (Simmonds and MacLennan, 2005). The seafloor was detected in the 38 kHz data using the bottom detection algorithm in Echoview, followed by visual inspection and manual correction. A bottom exclusion line was set 1 m above the acoustically-detected seafloor to exclude the acoustic deadzone (Ona and Mitson, 1996). Only data between the surface and bottom exclusion lines were analyzed. 38 kHz data were analyzed to a maximum depth of 500 m, and the 120 kHz data to a maximum depth of 250 m. All acoustic data were visually inspected to exclude electrical noise spikes or ping dropouts (*i.e.* transmissions in which a bottom echo was not received at the transducer). Volumes of excluded data were removed/not included from estimates of integrated backscatter. Ambient and vessel-generated noise were removed using the "background noise removal" operator in Echoview based on methods described by De Robertis and Higginbottom (2007). For each frequency, logarithmic measurements of mean volume-backscattering strength (MVBS, dB re 1 $m^{-1}$ - hereafter dB) (MacLennan et al., 2002) were averaged in the linear domain within a matrix of 20 pings (horizontal) by 10 m (vertical) cells. A -110 dB maximum

noise threshold and a minimum signal-to-noise ratio filter of 10 dB were applied to each analytic cell.

### 2.2.3 **Acoustic data classification**

Acoustic backscatter data were classified into single or mixed species categories. Data collected during each survey was assigned to one of the following backscatter categories: surface, mesopelagic, piscivores, capelin, herring, age-0 pollock, forage fish mix, forage fish/piscivore mix, macrozooplankton, and unknown (Table 2.2). All single or mixed species categories were classified to a maximum depth of 250 m, similar to the depth limit of midwater trawl samples and the 120 kHz data, with the exception of the mesopelagic layer and unknown categories which were classified to 500 m. Data classification was conducted following a multistep procedure (Fig. 2.2) that discriminated macrozooplankton from fish (2013 data only), identified surface and mesopelagic layers, and then created analysis regions for single or multispecies fish aggregations by matching observed backscatter patterns and vertical distributions to species compositions in trawl catches.

#### 2.2.3.1. *Discriminating macrozooplankton from fish*

Classification of acoustic data was consistent between the 2011 and 2013 surveys, with the exception of macrozooplankton. Addition of the 120 kHz frequency in the 2013 survey facilitated discrimination of macrozooplankton from fish using frequency-dependent differences in MVBS between 120 and 38 kHz data ($\Delta MVBS_{(120\text{-}38)}$, measured in the logarithmic domain) (Kang et al., 2002). Backscatter measurements from each frequency within the upper 250 m of the water column were averaged into 20 pings (horizontal) by 3 m (vertical) cells. Cells with $\Delta MVBS_{(120\text{-}38)}$ values greater than 8.6 dB were classified as macrozooplankton, while all other

cells were classified as "fish" (Fig. 2.2). The $\Delta MVBS_{(120-38)}$ 8.6 dB value is 1 standard deviation greater than the $\Delta MVBS_{(120-38)}$ for eulachon (*Thaleichthys pacificus*, 5.8 ± 2.8 dB), the highest difference value among common North Pacific fish species observed by De Robertis et al. (2010). Copepods (*Neocalanus* spp., Murase et al., 2009) and euphausiids (*Euphausia pacifica*, Kang et al., 2002; McKelvey and Wilson, 2006; Murase et al., 2009; and *Thysanoessa* spp., De Robertis et al., 2010) in the North Pacific have $\Delta MVBS_{(120-38)}$ values greater than 10 dB. The large bin size and the 8.6 dB difference value increased the likelihood that any cell containing fish would not be classified as macrozooplankton. This approach could result in some macrozooplankton being misclassified as fish, which would bias macrozooplankton estimates low. The magnitude of this bias is lower than having fish misclassified as macrozooplankton due to the large difference in target strengths between taxa. The 120 kHz data were used to assign backscatter values to macrozooplankton cells, while a Boolean operator masked "fish" cells by assigning them a -999 dB value (the equivalent of 0 in the linear domain).

2.2.3.2. *Layer detection*

The 38 kHz data were used to further classify the 20 ping x 3 m "fish" cells identified by $\Delta MVBS_{(120-38)}$ to all other backscatter categories (Fig. 2.2). To classify "fish" cells, 20 ping x 3 m cells were re-assigned 38 kHz backscatter values to the original measurement resolution of 1 ping (horizontal) by 0.187 m (vertical). Macrozooplankton cells were assigned a -999 dB value. Acoustic backscatter associated with surface and mesopelagic layers within the water column were identified using the "schools detection" SHAPES algorithm in Echoview (Barange, 1994; Coetzee, 2000), with parameter settings: 300 m minimum total length and maximum horizontal linking distance; 10 m minimum candidate length; and 5 m minimum total school height, minimum candidate height, and maximum vertical linking distance. The surface layer was

comprised of backscatter located in the upper portion of the water column that was primarily sampled by the surface trawl. The mesopelagic layer was comprised of backscatter primarily located below the 250 m depth limit of the midwater trawl. To detect schools as continuous layers, a -90 dB data threshold was applied to backscatter within the upper 50 m (classified as surface layer) and a -80 dB threshold to backscatter between a depth range of 150 to 500 m (mesopelagic layer). When a continuous layer extended beyond these depth boundaries, the school detection depth range was extended to include the layer. Backscatter located between 250 to 500 m and not associated with a layer (*e.g.* dense aggregations at shelf breaks) were classified as unknown due to a lack of midwater trawl samples below 250 m. Prior to the next classification step, surface and mesopelagic layers were removed (*i.e.* masked) and reassigned a -999 dB value.

2.2.3.3. *Discriminating aggregations*

All remaining backscatter was classified using trawl samples associated with homogenous echogram patterns. Backscatter patterns observed during trawls in which one classification category accounted for at least 90% of the catch (by number) were treated as a characteristic echogram pattern for that category. A -67 dB data threshold was applied to exclude jellyfish and remaining macrozooplankton (Parker-Stetter et al., 2013) from fish backscatter. Analysis regions were created and classified (capelin and herring) when similar echogram patterns were observed in acoustic data. Echogram patterns associated with trawl samples comprised of multiple species (forage fish mix) or overlapping patterns of two or more categories were classified as mixed categories (forage fish mix, forage fish/piscivore mix). Observed backscatter patterns that were not sampled by trawls were classified as unknown. Analysis regions for capelin, herring, forage fish mix, forage fish / piscivores mix, and unknown

backscatter were masked and assigned a -999 dB value prior to proceeding to the final classification step.

2.2.3.4. *Depth stratification*

Analysis regions for age-0 pollock and piscivores were stratified by depth. Trawl data for age-0 pollock and piscivores during the summer 2013 survey indicated that the two categories were vertically separated across most of the EGOA and CGOA at a depth of 100 m. An editable line was initially set at 100 m depth, and then adjusted to maintain continuity of patterns consistent with age-0 pollock and piscivores in areas where trawl samples indicated a change in vertical distribution (*e.g.* shallow waters inside the 100 m isobath). All remaining backscatter between 10 m and the edited 100 m line was classified as age-0 pollock. Backscatter between the edited 100 m line and either a depth of 250 m or the bottom exclusion line, whichever was shallower, were classified as piscivores. Although age-0 pollock were mostly absent in all 2011 and fall 2013 surveys, the edited 100 m line was used as the upper boundary for piscivore analysis regions in all surveys. When age-0 pollock were absent, backscatter above the edited 100 m line and not assigned to other categories was classified as unknown.

2.2.3.5. *Acoustic data exports*

Along-transect estimates of acoustic density, (nautical area scattering coefficient, $s_A$, $m^2$ $nmi^{-2}$, MacLennan et al., 2002), for each fish classification category (Table 2.2) were integrated through the water column from the surface exclusion line (*i.e. Northwest Explorer* = 10 m; *Oscar Dyson* = 15 m) to 250 m in 200 m horizontal bins. Mesopelagic and unknown backscatter were both integrated to a maximum depth of 500 m. At the 200 m horizontal resolution, each bin contained a minimum of 5 pings when the echosounder was operated at the slowest pulse rate of 1 ping per 7 seconds. A -80 dB data threshold was applied to the macrozooplankton category

(Ressler et al., 2012), and a -75 dB threshold was applied to the surface and mesopelagic categories to include weak scatterers associated with each group (*e.g.* small squids and jellyfish in the surface layer; mesopelagic fish lacking gas-filled swimbladders). A -67 dB data threshold was applied to all other fish categories.

### 2.2.4 **Identifying scales of variability**

The choice of horizontal resolution to characterize distributions of age-0 pollock, capelin, herring, and mesopelagic backscatter categories (collectively referred to as forage fish categories) was determined by identifying scales that maximize variability in distributions of acoustic density, $s_A$. A wavelet analysis was conducted to quantify significant scales of variability along individual transects for each forage fish backscatter category by survey (*e.g.* Grados et al., 2012). The frequency of occurrence of significant scales was summed across transects for each forage fish category during all surveys to determine the smallest scale that was most prevalent among all forage fish categories. Acoustic density estimates for each forage fish category were then horizontally binned at this resolution and exported using the same data thresholds as the original data exports (see 2.2.3.5).

The following background information describes how wavelet analysis identifies significant scales of variability in spatial data. Wavelet functions locally decompose a data series in the frequency domain as a function of space and scale (Bradshaw and Spies, 1992). Similar to Fourier transforms, the wavelet space-scale decomposition identifies dominant periods that account for variance in the series (Torrence and Compo, 1998) that are converted to spatial scales (Fig. 2.3). Acoustic density estimates for each forage fish category from each transect were treated as independent one-dimensional time series. Continuous wavelet transforms were

calculated using the complex Morlet wavelet (wave number = 6) to optimize detection and localization of scale (Mi et al., 2005; Torrence and Compo, 1998). With a Morlet wavelet, the relationship between period ($\lambda$) and scale ($s$) is nearly equal, $\lambda = 1.03s$ (Mi et al., 2005; Torrence and Compo, 1998). The wavelet coefficient (WC) indicates the amount of energy at a specific scale and location. The wavelet power spectrum (WPS) is the square of the WC , and describes the distribution of variance across the data series as a function of scale (Mi et al., 2005; Torrence and Compo, 1998). To enable comparison across scales, wavelet power was normalized by the global wavelet variance (*i.e.* the average WPS for all points at a specific scale). Edge effects were minimized by adding zeros to the end of each data series to bring the total length of the series up to the next power of two (Torrence and Compo, 1998). Significance testing of the WPS at the 95% confidence level was conducted using a modeled red noise (*i.e.* autoregressive lag-1) background spectrum (Torrence and Compo, 1998). The global wavelet spectrum (GWS) summarizes the wavelet variance as a function of scale, with concentrations of variance indicated by peaks in the spectrum (Mi et al., 2005; Saunders et al., 2005). GWS variance peaks greater than the 95% confidence level are defined as significant scales of variability (referred to as significant scales). Significant scales based on WPS values outside the cone of influence (Torrence and Compo, 1998) were excluded.

Computation of wavelet functions and significance testing was completed in Matlab v8.1.0.604 (The MathWorks Inc.) using an adapted Matlab package provided by C. Torrence and G. Compo (http://paos.colorado.edu/research/wavelets/). Wavelet plots and summary of wavelet outputs were completed in R v3.1.2 (The R Foundation) using the "biwavelet" package (version 0.17.5) provided by T. Gouhier and A. Grinsted (http://github.com/tgouhier/biwavelet).

### 2.2.5 **Forage fish distributions**

Forage fish distributions were characterized using metrics to quantify differences in horizontal and vertical distributions among forage fish backscatter categories. The metrics include: an index of spatial aggregation or dispersion; identification of locations where forage fish aggregate; measuring changes in acoustic density relative to distance from shore and bathymetry; and measuring changes in vertical distribution between isobaths. Distributions for each category were characterized by region (CGOA/EGOA), season (summer/fall), and year (2011/2013). Data from the Kayak Island and Yakutat transects were not included in the pattern description. All metrics were calculated using acoustic estimates binned at the resolution identified by the wavelet analysis (section 2.4, referred to as analysis resolution).

#### 2.2.5.1. *Characterizing aggregation/dispersion in forage fish distributions*

The L-function, a derivative of the Ripley's K-function (Ripley, 1981), was used to determine if forage fish were spatially aggregated, dispersed, or randomly distributed. The K-function, a measurement of covariation between paired points, is transformed to the L-function to indicate if points are more significantly clustered or dispersed than a random distribution as a function of distance, *d* (Fortin and Dale, 2005). Acoustic density estimates, $s_A$, for each forage fish backscatter category and survey were treated as a two-dimensional point pattern, in which each point was compared to other points across the region. This contrasts with the wavelet analysis where each transect was analyzed as an independent series. Observed *L(d)* values weighted by $s_A$ were calculated using the ArcGIS v10.0 (Environmental Systems Research Institute, Inc.) "Multi-Distance Spatial Cluster Analysis (Ripley's K-function)" tool (http://resources.arcgis.com). Starting at a distance of 1 km, *L(d)* values were estimated for 100 distance bands in 1.5 km increments. Monte Carlo simulations were used to estimate 90%

confidence limits around an expected random distribution of points. An observed value greater than the upper confidence limit and expected value indicates that points are significantly clustered at that distance (*i.e.* scale). Observed values less than the lower confidence limits and expected values indicate scales at which points are significantly dispersed.

Spatial scales at which aggregation was greatest were identified by plotting the difference between observed and expected values (referred to as diffK values) as a function of scale. Based on this study's 37.04 km spacing between transects, a peak in diffK value within a lag distance range of 1 to 37 km would indicate that the scale of aggregation was determined by the along-transect length of an aggregation, independent of values from adjacent transects. A sharp increase in diffK values at a lag distance of 38.5 to 41.5 km would result if neighboring values on an adjacent transect contributed to the aggregation. In contrast, a relatively small change in diffK values at lag distances greater than 37 km would indicate the scale of aggregation primarily reflected the along-transect length of an aggregation. To make seasonal and interannual comparisons of diffK values within each region, similar domain boundaries and transect spacing are required. To maintain an equal domain, the following transects were excluded from the Ripley's K analysis: 181, 185, 213, and 217 in the CGOA, and B, D, F, H, J, L, and the outer-most transect in the EGOA that ran parallel to shore during the summer 2013 survey (referred to as the "80s" transect line). The fall 2013 CGOA survey was excluded from this analysis due to a lack of sampling that resulted from the United States federal government shutdown on October 1, 2013.

2.2.5.2. *Identifying spatially-explicit aggregations*

Specific locations that may be associated with high densities of forage fish were identified using the Local Moran's I index (Anselin, 1995) to detect the position of fish

aggregations. Similar to the Ripley's K, the Local Moran's I was calculated using acoustic density, $s_A$, for each forage fish category. Significant aggregations of high density values were identified using the ArcGIS "Cluster and Outlier Analysis (Anselin Local Moran's I)" tool. To identify nonstationary features in the pattern (Anselin, 1995), the tool calculates a Local Moran's I index value and z-score for each observation by measuring a point's contribution to the global Moran's I statistic. A positive index value with a z-score > 1.96 indicates that the observation is significant ($\alpha = 0.05$) surrounded by similar values that form a cluster (*i.e.* an aggregation). The Local Moran's I was computed using an inverse distance with a 40 km Euclidian distance limit to include neighboring observations from adjacent transects. To maintain equal spacing between transects, the following transects were excluded: the 181 CGOA transect in summer 2011 and the B, D, F, H, J, L, and 80s EGOA transects. The fall 2013 CGOA survey was also excluded from this analysis due to a lack of sampling.

2.2.5.3. *Characterization of horizontal and vertical forage fish distributions*

Horizontal distributions for each backscatter category were summarized as a function of distance from shore and bathymetry. To analyze changes in density relative to distance from shore, acoustic density, $s_A$, were averaged in 1 km increments. Distance from shore was measured from the middle of each acoustic bin to the closest point on the coastline (National Atlas of the United States, 2014) in ArcGIS using the "near" tool. To analyze changes in density relative to bathymetry, acoustic densities were averaged in 10 m bottom depth increments for shallow observations (30 to 200 m bottom depth), and in 100 m depth increments for observations over deeper water (> 200 m bottom depth). Bottom depth for each acoustic bin was determined by averaging depths of the acoustically-detected bottom for all samples (*i.e.* pings) within a bin. The magnitude of forage fish acoustic density (mean $s_A$ values) was characterized

as: "low" < 10 $m^2$ $nmi^{-2}$, 10 ≤ "medium" < 100 $m^2$ $nmi^{-2}$, 100 ≤ "high" < 1,000 $m^2$ $nmi^{-2}$, and "very high" ≥ 1,000 $m^2$ $nmi^{-2}$. The use of these categories should not be interpreted as numeric densities (*i.e.* number fish $m^{-2}$) due to differences in acoustic backscatter properties and differences in data processing between species.

Spatial and temporal changes in forage fish density and vertical distribution were examined relative to bathymetry only where fish were present (*i.e.* $s_A > 0$, referred to as nonzero density) (Bez and Rivoirard, 2001; Woillez et al., 2007). This approach also accounts for limitations in the survey design, where the frequency of zero density values in a sample is sensitive to changes in the extent of the survey domain (Table 2.1 and Fig. 2.1), and acoustic classification (*i.e.* backscatter assigned to the forage fish mix, forage fish/piscivore mix, or unknown categories). Horizontal changes in forage fish nonzero density relative to bathymetry were summarized by averaging nonzero densities between isobaths (bottom depth ranges for isobath categories: < 100 m, 100-199 m, 200-499 m, 500-999 m, 1,000-1,999 m, and > 2,000 m). Vertical distributions for each forage fish category were summarized as a function of bathymetry. Acoustic data were partitioned in 1 m vertical depth layers, and estimates of $s_A$ for each forage fish category were exported using the same data thresholds as the original data exports (see 2.3.5). The mean vertical location, or center of mass (CM) in the water column within each acoustic bin, was derived following Urmy et al. (2012) , in which a weighted mean of volumetric density (volume-backscattering coefficient, $s_v$, $m^{-1}$, MacLennan et al., 2002) was calculated from all depth layers using Python v2.7 (Python Software Foundation). CM values for each forage fish category were averaged by isobath category to characterize changes in vertical distribution relative to bathymetry.

Notched boxplots and pairwise comparisons were used to quantify differences in forage fish density and vertical distributions between isobaths and surveys. Notched boxplots (*i.e.* a visual narrowing of the box around the median) provides a statistical measure of differences between medians of samples (McGill et al., 1978). The width of the notch is 1.58 times the interquartile range of the sample divided by the square root of the sample size (Chambers et al., 1983). Notches that do not overlap are considered significantly different at the 95% confidence level. Multiple two-sample comparisons were conducted within each classification category using the Wilcoxon rank-sum test (Zar, 2010) to measure differences in median nonzero density and CM between isobath categories and surveys. A two-tailed null hypothesis that each set of medians were equal was tested at $\alpha = 0.05$ significance level. Samples with less than 30 observations were not tested.

## 2.3 RESULTS

### 2.3.1 Trawl and acoustic sampling

A total of 83 midwater trawls were sampled, with 41 in 2011 and 42 in 2013 (Table 2.3). Among these samples, 47 trawls (19 in 2011 and 28 in 2013) contained one backscatter category that accounted for at least 90% of the catch (by number) (Table 2.4). These samples were used to match representative echogram patterns for classification of backscatter categories (Table 2.2). Of the 382 surface trawl samples collected (Table 2.3), 16 trawls (4 in 2011 and 12 in 2013) were also used to classify acoustic data (Table 2.4).

Classification of acoustic backscatter to categories is summarized for each survey in Table 2.5 using mean acoustic density, mean $s_A$, and the mean proportion of backscatter (weighted by $s_A$) assigned to each category. Total backscatter was higher in 2013 (mean $s_A$

range: 557 to 1,471 $m^2$ $nmi^{-2}$) than in 2011 (mean $s_A$ range: 113 to 170 $m^2$ $nmi^{-2}$) in both seasons and regions. The surface layer provided a combined abundance index of salmon, epipelagic fish, jellyfish, squid, and other macroinvertebrates. Surface trawl data characterizing species and length compositions of the surface layer are summarized in (Rhea-Fournier et al., 2016). The surface layer accounted for less than 12 % of total backscatter in all surveys (range 0.6 to 11.5 % total backscatter). The mesopelagic layer was primarily comprised of myctophids, such as the northern lanternfish (*Stenobrachius leucopsarus*). Mesopelagics accounted for the largest proportion of total backscatter in 3 of 4 EGOA surveys (range 66.3 to 76.5 % total backscatter, not including fall 2011), and a relatively large fraction of backscatter in the CGOA (range 21.3 to 34 % total backscatter, not including fall 2013). Changes in mesopelagic density should be interpreted with caution as they cannot necessarily be attributed to changes in abundance due to potential bias associated with species-specific and ontogenetic differences in scattering properties among mesopelagic fish and invertebrates (Davison, 2011; Davison et al., 2015). The piscivores category was primarily comprised of groundfish species (*e.g.* pollock, rockfish, and arrowtooth flounder) greater than 158 mm in length. Piscivores accounted for a high proportion of total backscatter during all surveys in the CGOA (range 28.5 to 40.3 % total backscatter) and in the EGOA over the shelf and at the shelf break in waters less than 500 m bottom depth (range 21.4 to 56.3% total backscatter < 500 m). The age-0 pollock category was comprised of pollock 26 to 88 mm in length. Age-0 Pacific cod (45 to 77 mm) co-occurred with age-0 pollock in summer 2013, primarily over Albatross bank. Surface and midwater catches indicated that cod densities were consistently an order of magnitude lower than pollock densities and were classified under the age-0 pollock category. Backscatter was only assigned to the age-0 pollock category in summer 2013, accounting for less than 6 % of total backscatter in both regions.

Herring sampled from the trawl were 72 to 289 mm in length. Backscatter was only assigned to the herring category in EGOA fall surveys of both years, with discrete aggregations observed in less than 5 % of total samples (*i.e.*200 m acoustic bins) in 2011 ($n$ = 109) and less than 1 % of samples in 2013 ($n$ =20). Capelin sampled from the trawl were 54 to 204 mm in length. Backscatter was only assigned to the capelin category in the CGOA, and accounted for 13.4 to 35.1 % of total backscatter in CGOA waters less than 500 m bottom depth. The forage fish mix category was comprised of at least two or more of the following species: capelin, herring, age-0 pollock, and/or age-0 Pacific cod. Limited observations of other forage species include eulachon, longfin smelt (*Spirinchus thaleichthys*), surf smelt (*Hypomesus pretiosus*), and Pacific sandfish (*Trichodon trichodon*). Backscatter was only assigned to the forage fish mix category in the fall 2013 EGOA and both CGOA fall surveys, accounting for 9.6 and 11.2 % (CGOA and EGOA) of total backscatter inside 500 m bottom depths in 2013. The forage fish/piscivore mix category includes at least one forage fish and one piscivorous fish species, and only accounted for a small fraction of total backscatter (< 5 %) among all surveys. Acoustic measurements of macrozooplankton in 2013 are primarily comprised of euphausiids, copepods, and amphipods. Proportions of total backscatter were not calculated for macrozooplankton because density estimates were derived from 120 kHz data. Backscatter that was classified as unknown varied widely between surveys (range 1.4 to 48.1% total backscatter). Distribution maps of acoustic density, $s_A$, for each backscatter category in 200 m horizontal bins are provided in Appendix A.

Two sources of supplemental data were reviewed to assess if this study's backscatter classification was consistent. As part of the GOAIERP, zooplankton and ichthyoplankton communities were sampled at each station by obliquely towing a 60 cm bongo net with 0.5 mm mesh to a maximum depth of 200 m. During summer 2011 and 2013, juvenile myctophids were

collected in 12 bongo samples (A. Matarese, NMFS-AFSC, unpublished data). Acoustic data collected during each of these bongo tows were reviewed to determine if the net passed through the acoustically-detected mesopelagic layer. In all 12 observations, the minimum depth of the mesopelagic layer was shallower than 200 m, indicating myctophid species were available to the bongo net. Supplemental acoustic and trawl data collected by the National Marine Fisheries Service (NMFS) Alaska Fisheries Science Center (AFSC) Midwater Assessment and Conservation Engineering (MACE) Program during the 2013 summer GOA pollock acoustic-trawl (AT) survey (D. Jones, NMFS-AFSC, per. com.) were also reviewed. Conducted from the *Oscar Dyson*, the MACE summer pollock AT survey overlapped with the CGOA study area from 11-26 July, 2013 prior to the summer CGOA survey (Table 2.1). A total of 15 trawl samples and corresponding acoustic data were reviewed. Echogram patterns and trawl catches from 13 samples were consistent with this study's classification for capelin, piscivores, and forage fish/piscivores mix backscatter categories. Echogram patterns for the other 2 trawl samples (aggregations of pollock > 160 mm in length over Barnabus Trough) were not observed during the summer 2013 CGOA survey, and therefore had no impact on this study's classification.

### 2.3.2 **Scales of variability**

Significant periods were detected in all forage fish distributions (*i.e.* age-0 pollock, capelin, herring, and mesopelagic backscatter categories), indicating spatial structure across a range of scales (Fig. 2.4). The occurrence of significant periods at scales less than 4 km (*i.e.* fine) was more frequent across transects and surveys for each species group than the occurrence of significant periods at scales greater than 8 km (*i.e.* coarse). Herring had the fewest (n = 5) and

narrowest range of significant periods (0.41 to 0.55 km), likely reflecting the limited number of discrete, monospecific schools observed during all surveys (Table 2.5). Distributions of age-0 pollock and capelin had similar distinct modes of fine- (pollock = 0.41 to 1.34 km, capelin = 0.41 to 3.54 km) and coarse-scale structure (pollock = 14.17 to 60.76 km, capelin = 8.14 to 60.76 km). The bimodal peaks in distribution scales likely correspond to aggregations of fish schools (fine-scales), and the width of submarine banks in the CGOA and the EGOA shelf (coarse-scales). Significant periods of mesopelagic distribution scales occurred between 0.41 to 11.51 km, consistent with observed chord distances of high density shoals within the mesopelagic layer. There was higher seasonal and interannual variability in significant periods in mesopelagic distributions, resulting in a broader range of significant periods compared to age-0 pollock and capelin distributions (Fig. 2.4).

The significant period most prevalent across transects and surveys for all forage fish categories ranged from 0.44 to 0.55 km. Therefore a resolution of 0.5 km was selected for analysis of all forage fish distributions.

### 2.3.3 **Forage fish distributions**

Seasonal and interannual changes in species composition and distribution of forage fish communities were observed within and between the CGOA and EGOA regions. In the CGOA (Fig. 2.5), the forage fish community was primarily comprised of capelin over the shelf and mesopelagics beyond the shelf break in both years. Age-0 pollock were abundant across the shelf in summer 2013, but rarely observed during other CGOA surveys. A low density, mixed aggregation of age-0 pollock and capelin at the northwest end of the 201 and 205 transects in fall 2011 was the only observed concentration of age-0 pollock verified by trawl samples in 2011.

Herring aggregations were not observed in midwater trawl catches in the CGOA. Infrequent, surface trawl catches of small numbers of herring (< 10 fish per trawl) were the only indication of their presence (Rhea-Fournier et al., 2016).

In the EGOA (Fig. 2.6), mesopelagics were the only forage fish group consistently present in summer and fall of both years. Age-0 pollock were distributed over shelf, slope, and basin waters in summer 2013, but were nearly absent in the fall and throughout 2011. A small number of age-0 pollock were caught in midwater trawls off nearshore stations on the Yakutat and M transects, mixed with other forage fish species in fall 2013. Herring aggregations were observed during fall surveys, both in dense monospecific or mixed aggregations with other forage and/or piscivorous fish (*e.g.* adult pollock, rockfish). Herring were primarily distributed over the shelf or within the Yakobi Sea Valley off Cross Sound (Fig. 2.1). A herring aggregation was also observed over slope waters within the mesopelagic layer. Summer observations of herring were rare in both years, limited to a small number of fish caught in surface trawls over the shelf. Capelin observations were limited in the EGOA. In summer 2011, capelin occurred in a mixed aggregation along with longfin smelt (*Spirinchus thaleichthys*) and pollock (≥ 305 mm in length) within the Yakobi Sea Valley on the L transect. In fall 2013, high density aggregations of capelin co-occurred with herring over the shelf northwest of the Yakobi Sea Valley on the M transect. Even though capelin did not occur in midwater or surface trawl catches in summer 2013, large osmerids were observed in the stomachs of Chinook salmon (*Oncorhynchus tshawytscha*) collected from the surface trawl at the nearshore station on the M transect (E. Fergusson, NMFS-AFSC, unpublished data).

2.3.3.1. *Characterizing distribution of forage fish aggregations*

The Ripley's K analysis indicated that distributions of all forage fish were aggregated, but that there was considerable variability in the scale and location of aggregations between and within species (Fig. 2.7, Fig. 2.8). In the CGOA (Fig. 2.7), bimodal peaks in diffK values indicated that the distribution of mesopelagic densities were significantly aggregated at lag distances of 13 to 14.5 km and 41.5 km, suggesting both along- and across-transect structure in their distributions across seasons and years. Capelin distributions were more aggregated in 2011 than 2013, but had similar peaks in diffK values at lag distances of 8.5 to 11.5 km and 41.5 km during both summer surveys. Capelin were less aggregated at more coarse scales during the fall 2011 survey. A steady decline in diffK values from a peak at 8.5 km reflected a lack of influence from adjacent aggregations on neighboring transects. This interpretation is supported by differences in the location of significant aggregations identified by the local Moran's I analysis. Unlike summer distributions in which significant aggregations were clustered over Portlock and Albatross Banks (Fig. 2.1), capelin were more patchily distributed during fall 2011. Age-0 pollock distributions were aggregated at similar scales and magnitude as capelin in summer 2013. Although there was extensive spatial overlap of capelin and age-0 pollock, separation between significant aggregations for these species was observed in some areas (*e.g.* over Portlock Bank on the 205 transect).

In the EGOA (Fig. 2.8), mesopelagic distributions were weakly aggregated at peak lag distances of 7 to 10 km in both seasons and years. A second significant peak at 44.5 km was present in both 2013 surveys, likely reflecting the extension of the survey range offshore (Fig. 2.1). In contrast to mesopelagics, distributions of herring and age-0 pollock densities were more aggregated and patchily distributed. Age-0 pollock were strongly aggregated at peak lag distances of 7 to 8.5 km. Herring distributions were primarily aggregated at 40 to 41.5 km, with

a second significant peak at 2.5 km observed in fall 2013. Significant aggregations of herring and age-0 pollock were primarily located over the shelf or just beyond the shelf break, while the location of significant aggregations of mesopelagics varied over slope and basin waters.

2.3.3.2. *Density relative to distance from shore*

Seasonal and interannual changes in forage fish acoustic density, $s_A$, relative to distance from shore was observed within and between regions (Fig. 2.9). Within the CGOA, peak densities of capelin were distributed 100 km from shore in summer 2011 ($s_A = 91.9 \pm 14.5$ $m^2$ $nmi^{-2}$), 90 km in summer 2013 ($s_A = 658.6 \pm 159.5$ $m^2$ $nmi^{-2}$), and 20 km in fall of both years (2011: $s_A = 102.7 \pm 23.0$ $m^2$ $nmi^{-2}$, 2013: $s_A = 525.2 \pm 155.2$ $m^2$ $nmi^{-2}$). High densities of capelin occurred in 10 depth bins from 10 to 140 km in summer 2013. In contrast, capelin densities were lower in 2011 across the shelf, with only low and medium densities occurring in summer from 30 to 140 km and in fall from 30 to 130 km. Similar to capelin, peak densities of mesopelagics were higher in summer 2013 ($s_A = 1555.7 \pm 347.3$ $m^2$ $nmi^{-2}$ at 200 km) than in both seasons of 2011 (summer: $s_A = 222.6 \pm 36.0$ $m^2$ $nmi^{-2}$at 190 km, fall: $s_A = 121.4 \pm 8.9$ $m^2$ $nmi^{-2}$ at 200 km). Medium and high densities of mesopelagics were also distributed further offshore in summer 2011 ($\geq$ 90 km and $\geq$ 190 km, respectively) compared to distributions of medium and high densities in fall 2011 ($\geq$ 70 km and $\geq$ 90 km) and high densities in summer 2013 ($\geq$ 80 km). Peak density of age-0 pollock ($s_A = 81.7 \pm 11.6$ $m^2$ $nmi^{-2}$) occurred 60 km from shore. Medium densities of age-0 pollock were broadly distributed from 10 to 110 km and at 150 km.

In the EGOA, peak densities of mesopelagics were lower in 2011 (summer: $s_A = 273.6 \pm 23.3$ $m^2$ $nmi^{-2}$ at 70 km, fall: $s_A = 71.6 \pm 5.8$ $m^2$ $nmi^{-2}$ at 60 km) than in 2013 (summer: $s_A = 790.0 \pm 69.2$ $m^2$ $nmi^{-2}$ at 190 km, fall: $s_A = 2549.0 \pm 213.4$ $m^2$ $nmi^{-2}$ at 140 km). High densities of mesopelagics occurred closer to shore in both seasons of 2013 (20 km compared to 40 km in

2011), and were broadly distributed out to 210 km in summer 2013 and 180 km in fall 2013. While a seasonal decline in mesopelagic densities was observed in 2011, a seasonal increase occurred in 2013, with very high densities distributed from 50 to 160 km in fall 2013. Age-0 pollock densities were highest close to shore, with a peak density at 30 km ($s_A$ = 243.7 ± 84.2 $m^2$ $nmi^{-2}$), and declined further offshore where they fluctuated between low and medium densities to 210 km. Similar to pollock, peak herring densities were also close to shore in fall of both years (2011: $s_A$ = 6.4 ± 4.0 $m^2$ $nmi^{-2}$ at 20 km, 2013: $s_A$ = 78.1 ± 76.5 $m^2$ $nmi^{-2}$ at 30 km). While herring densities were lower in 2011 (2011: $s_A$ = 0.2 to 6.4 $m^2$ $nmi^{-2}$, 2013: $s_A$ = 12.4 to 78.1 $m^2$ $nmi^{-2}$) they were distributed nearly twice as far offshore (2011: 10 to 70 km, 2013: 10 to 30 km).

Regional comparisons of the distribution of high and/or peak densities of mesopelagics and age-0 pollock indicated that they were located closer to shore in the EGOA than in the CGOA (Fig. 2.9). Although age-0 pollock peak densities were higher in the EGOA ($s_A$ = 243.7 ± 84.2) than in the CGOA ($s_A$ = 81.7 ± 11.6), medium densities of pollock were consistently distributed from 10 to 110 km in the CGOA, whereas pollock were more concentrated from 10 to 60 km in the EGOA. With the exception of summer 2011, high and/or peak densities of capelin and herring were located relatively close to shore (≤ 30 km).

2.3.3.3. *Density relative to bottom depth*

Seasonal and interannual changes in forage fish density relative to bottom depth were observed within and between regions (Fig. 2.9). In general, capelin and mesopelagic distributions were correlated with bathymetry; capelin to bottom depths of 240 m or shallower, and mesopelagics to bottom depths greater than 210 m. Over bottom depths greater than 500 m, mesopelagic densities were relatively constant within each survey and did not exhibit pronounced changes relative to a specific depth. One exception was an increase from high to

very high mesopelagic densities in the EGOA that occurred over bottom depths greater than 1,000 m in fall 2013. In the CGOA, peak capelin densities occurred over shallow banks (< 100 m) in summer 2011 ($s_A$ = 79.9 ± 17.5 $m^2$ $nmi^{-2}$ at 80 m) and both seasons of 2013 (summer: $s_A$ = 739.9 ± 208.6 $m^2$ $nmi^{-2}$ at 50 m, fall: $s_A$ = 422.7 ± 121.2 $m^2$ $nmi^{-2}$ at 70 m), while similar peak densities occurred at 70 m ($s_A$ = 65.2 ± 12.6 $m^2$ $nmi^{-2}$) and 140 m ($s_A$ = 66.5 ± 31.8 $m^2$ $nmi^{-2}$) in fall 2011. Capelin distributed over deeper waters (100 to 240 m) associated with troughs had relatively lower densities in both summer 2011 ($s_A$ < 15 $m^2$ $nmi^{-2}$) and 2013 ($s_A$ < 92 $m^2$ $nmi^{-2}$) than observed over banks.

Unlike capelin and mesopelagics, age-0 pollock, and to a lesser extent herring, were horizontally distributed across the full depth range of both regions. Similar to capelin, age-0 pollock densities were correlated with changes in bathymetry. In the CGOA, medium densities of age-0 pollock only occurred over bottom depths of 50 to 200 m, with a high density peak over 80 m ($s_A$ = 142.2 ± 17.0 $m^2$ $nmi^{-2}$). Age-0 pollock in the EGOA exhibited a different distribution, in which medium densities occurred over a wide range of bottom depths from 100 to 1,800 m, with a peak density occurring over 400 m ($s_A$ = 510.6 ± 148.9 $m^2$ $nmi^{-2}$) and high densities over 700 to 800 m bottom depths. Among the limited herring observations, densities of similar magnitude were observed in three distinct bathymetric regions within the EGOA in fall 2011: over the inner areas of the shelf ($s_A$ = 14.3 ± 14.3 $m^2$ $nmi^{-2}$ at 140 m), within the Yakobi Sea Valley ($s_A$ = 13.1 ± 10.3 $m^2$ $nmi^{-2}$ at 400 m), and beyond the shelf break ($s_A$ = 4.02 ± 2.7 $m^2$ $nmi^{-2}$ at 1,200 m). In fall 2013, herring schools were observed over the shelf, with peaks at 130 m ($s_A$ = 83.2 ± 52.1 $m^2$ $nmi^{-2}$) and 200 m ($s_A$ = 229.4 ± 229.4 $m^2$ $nmi^{-2}$) bottom depths.

2.3.3.4. *Horizontal and vertical distributions of fish relative to bathymetry*

Changes in nonzero density and vertical distribution of forage fish are summarized by isobath categories (Fig. 2.10). Results for individual Wilcoxon rank-sum tests are provided in text. Comparisons that reflect results from two or more Wilcoxon tests reference summary tables of comparisons in Tables 6-9. In 5 of the 7 surveys, nonzero densities of mesopelagics were positively correlated with bottom depth. With the exception of the EGOA fall 2011 and summer 2013 distributions, mesopelagic nonzero densities were lowest between the 200 and 500 m isobaths, and then increased over deeper water before stabilizing (Wilcoxon rank-sum, $\alpha$ = 0.05 two-tailed, Table 2.6). Median nonzero densities of mesopelagics were significantly higher during 2013 within each isobath category (Wilcoxon rank-sum, $\alpha = 0.05$ two-tailed, Table 2.7), with peak mesopelagic density observed in fall 2013 over bottom depths greater than 1,000 m (median $s_A \geq 1{,}521.6$ m$^2$ nmi$^{-2}$) in the EGOA.

Nonzero densities of capelin, age-0 pollock, and herring were typically higher over shallow waters associated with the shelf, declining over deeper water beyond the shelf break outside the 500 m isobath (Fig. 2.10). Over the shelf, median nonzero densities of capelin were significantly higher inside the 100 m isobath in summer of both years (Table 2.6), with the peak capelin density (median $s_A = 411.1$ m$^2$ nmi$^{-2}$) occurring in summer 2013 (Table 2.7). In fall, capelin nonzero density inside the 100 m isobath significantly declined from summer maxima to similar levels in fall of both years. Density increased from summer to fall in 2011 within the 100 to 200 m isobaths ($W = 2{,}025$, $n_{2GOA11,\ 100\text{-}200m} = 71$, $n_{4GOA11,\ 100\text{-}200m} = 89$, $P < 0.05$), to levels higher than those observed in shallower waters ($W = 9{,}748$, $n_{4GOA11,\ <100m} = 271$, $n_{4GOA11,\ 100\text{-}200m} = 89$, $P < 0.05$). Median nonzero density of age-0 pollock inside the 100 m isobath (median $s_A = 21.6$ m$^2$ nmi$^{-2}$) was also significantly higher compared to all other isobath categories in the CGOA (median $s_A \leq 5.2$ m$^2$ nmi$^{-2}$, Table 2.6). In the EGOA, peak age-0 pollock nonzero

densities (median $s_A \geq 32.9$ m$^2$ nmi$^{-2}$) occurred over a broader bottom depth range inside 500 m (Table 2.6). Outside the 100 m isobath, median nonzero densities of age-0 pollock in the EGOA were significantly higher than in the CGOA within each isobath category (Table 2.7). No statistical comparisons of median nonzero density of herring across depths or between years were possible due to small sample sizes ($n < 30$) in 4 of 5 isobath categories (Table 2.6).

Although nonzero densities of capelin and age-0 pollock were concentrated inshore of the 500 m isobath (Fig. 2.10), there were significant differences in vertical distributions within and between species (Wilcoxon rank-sum, $\alpha = 0.05$ two-tailed, Tables 8-9). The median center of mass (CM) of capelin inside the 100 m isobath (median CM = 55 m) was significantly shallower than outside 100 m (median CM $\geq$ 110 m) in summer 2013, and in both seasons in 2011 (Table 2.8). There were no significant differences in capelin CM within isobath groups between years and seasons, with the exception of summer 2013 and fall 2011 within 100 to 200 m and inside 100 m in fall 2013 with the other CGOA surveys (Table 2.9).

Vertical distributions of age-0 pollock differed between regions. In the CGOA, age-0 pollock CM decreased from a depth of 31 m inside the 100 m isobath to 44 m between the 100 and 200 m isobaths ($W = 210{,}693$, $n_{2GOA13,<100m} = 860$, $n_{2GOA13,\ 100\text{-}200m} = 1{,}016$, $P < 0.05$), but then increased to 33 m between the 200 and 500 m isobaths ($W = 251{,}169$, $n_{2GOA13,100\text{-}200m} = 1{,}016$, $n_{2GOA13,\ 200\text{-}500m} = 365$, $P < 0.05$). Over deeper waters, age-0 pollock were vertically distributed over a 1$^{st}$ and 3rd quartile depth range of 13 to 93 m (Fig. 2.10). In the EGOA, the median CM was significantly deeper within each isobath group than in the CGOA between the 100 to 2,000 m isobaths (Table 2.9). The vertical position of age-0 pollock was shallower within the 100 and 200 m isobaths (median CM = 59 m) compared to within the 200 to 500 m isobaths (median CM = 73 m) ($W = 15{,}267$, $n_{1GOA13,100\text{-}200m} = 332$, $n_{1GOA13,\ 200\text{-}500m} = 153$, $P < 0.05$),

stabilized at a maximum median CM depth of 82 m between the 500 to 1,000 m isobaths ($W$ = 5,700, $n_{1GOA13,\ 200\text{-}500m}$ = 153, $n_{1GOA13,500\text{-}1,000m}$ = 82, $P$ = 0.25), and then was shallower beyond the 1,000 and 2,0000 m isobaths at median CM depths of 65 and 59 m ($W$ = 10,570.5, $n_{1GOA13,500\text{-}1,000m}$ = 82, $n_{1GOA13,\ 1,000\text{-}2,000m}$ = 218, $P < 0.05$).

Vertical distributions of mesopelagics varied seasonally and regionally between a CM interquartile range of 241 to 336 m depth in the CGOA and 214 to 405 m in the EGOA (Fig 10). Mesopelagics within the Yakobi Sea Valley were as shallow as 125 m. Vertical distributions of herring within the 100 to 200 m isobaths were similar between years (median CM = 111 and 112). Although sample sizes were too small for statistical comparison, the median CM decreased from 158 to 172 m between the 200 to 1,000 m isobaths in fall 2011. Between the 1,000 and 2,000 m isobaths, discrete herring schools were located at a median CM of 165 m within the mesopelagic layer. The midwater trawl that collected these samples was paired with a surface trawl in which no herring were caught, making it unlikely that herring in the midwater sample were caught near the surface as the net was deployed or recovered.

## 2.4 DISCUSSION

Ecosystem-based management of marine resources requires understanding how changes in the abundance and distribution of forage fish will potentially affect predators of commercial and ecological importance (Livingston et al., 2005). In this study, interannual, seasonal, and spatial variability in species composition and distributions of forage fish in the GOA were observed. The forage fish community in 2011 can be characterized by the absence of age-0 pollock and lower densities of capelin, herring, and mesopelagics, compared to observations in 2013. Seasonal changes in community composition are attributed to the transport of age-0

pollock from offshore waters in summer 2013 to nearshore nursery areas in fall, and to immigration of herring over the eastern GOA shelf in fall of both years. Forage fish distribution patterns varied within and between regions due to intra- and interspecific differences in horizontal and vertical distributions that were strongly correlated with bottom depth ranges. Spatial and temporal variability in the species composition and distributions of forage fish likely resulted in reduced foraging opportunities for predators in 2011 compared to 2013. Differences in forage fish distribution patterns between species may also affect surveys attempting to monitor changes in forage fish abundance and distribution.

### 2.4.1 **Characterization of forage fish community composition and distribution patterns**

Spatial and temporal differences were observed in the abundance and distribution of forage fish in the GOA. Forage fish densities were significantly higher for all species in 2013 compared to 2011. Age-0 pollock were nearly absent throughout 2011, but were abundant across the GOA in summer 2013 and limited to coastal waters in the subsequent fall. Capelin were the dominant forage fish over the CGOA shelf in the summer and fall of both years. Dense aggregations of herring were observed over the EGOA shelf in fall of both years, but were absent in summer and rarely observed in the CGOA. Mesopelagics were the only forage fish category present during all surveys, yet their density and vertical distribution varied between regions both seasonally and between years.

#### 2.4.1.1. *Interannual variability*

Interannual differences in capelin density and the lack of age-0 pollock observations in 2011 were also detected in other resource assessment surveys conducted in the GOA by the NMFS-AFSC's Resource Assessment and Conservation Engineering Division (RACE) and

Alaska Department of Fish and Game (ADFG). Capelin abundance was significantly higher in 2013 than 2011 in this study, which is consistent with abundance estimates from the AFSC Groundfish Assessment Program's summer GOA Continental Shelf and Slope bottom trawl (BT) survey (Ormseth, 2012). The 2013 capelin biomass estimate was the second highest recorded in the BT survey since 1984 (Ormseth, 2012). Acoustic densities for age-0 pollock in 2013 were high when compared to catch-per-unit-effort (CPUE) values from the AFSC Ecosystems and Fisheries-Oceanography Coordinated Investigations (EcoFOCI) Program's late-summer small-mesh trawl survey. Conducted over the Kodiak shelf since 2005 and in the western GOA (WGOA) since 2000, age-0 pollock CPUE in 2013 was the highest observed in the EcoFOCI trawl survey time series, while CPUE in 2011 was among the lowest (Zador, 2013). The small-mesh demersal survey, conducted by NMFS and the ADFG in nearshore bays around Kodiak and along the Alaska Peninsula coastline in the WGOA, also recorded the highest CPUEs for juvenile pollock (< 20 cm) in 2013 since 1979 (Zador, 2014), while CPUE in 2011 was below average (Zador, 2012). The pronounced difference in age-0 pollock abundance in 2011 and 2013 was also evident in initial measurements of year class strength. The MACE winter Shelikof Strait pollock AT survey observed considerably fewer age-1 pollock from the 2011 cohort in 2012 (95 million fish) compared to age-1's from the 2013 cohort that were observed in the 2014 survey (576 million fish) (Dorn et al., 2014).

There is evidence that 2011 was an anomalous year in the GOA, and may account for the lack of pollock and lower acoustic densities of other forage fish species compared to observations in 2013. Ship-based measurements of chlorophyll-*a* collected during the GOAIERP spring (April-May) oceanographic survey and by satellite-based composite ocean color imagery indicated dramatically lower concentrations of chlorophyll in 2011 compared to

2013 (median 29 versus 62 mg $m^{-2}$) (Stabeno et al., 2016b). Pronounced differences in phytoplankton community composition were also observed in 2011 compared to 2013 (Strom et al., 2016). The weak spring bloom in 2011 coincided with low mesozooplankton biomass relative to a 7 year average measured by continuous plankton recorders over the CGOA shelf (Zador, 2012). In contrast, the spring bloom in 2013 was characterized as being typical when compared to long-term satellite imagery (Stabeno et al., 2016b), and being early and intense based on phytoplankton photosynthetic characteristics (Strom et al., 2016). Measurements taken during the AFSC BT survey indicated that there was no obvious differences in water temperature and stratification patterns between 2011 and 2013 (Zador, 2013). This suggests that interannual differences observed in forage fish communities in this study may be a result of changes in the environment that occurred prior to the start of the summer survey.

2.4.1.2. *Seasonal variability*

In 2013, a seasonal shift in age-0 pollock abundance altered the forage fish community composition. Pollock were distributed across both regions in summer, but were rare in fall and only observed near coastal areas off Yakutat and Cross Sound in the EGOA. The pronounced shift in age-0 pollock abundance likely reflects their transport from offshore waters to nearshore nursery areas (*e.g.* Brodeur and Wilson, 1996a; Hinckley et al., 1991; Smart et al., 2012); with the timing of settlement in nearshore waters expected to occur in late-summer/early-fall. Age-0 pollock distributions in 2013 were consistent with these general patterns, with most age-0 pollock emigrating from the shelf to nearshore nurseries by the end of August in 2013.

In contrast to the seasonal inshore movement of age-0 pollock, the occurrence of herring over the EGOA shelf in fall of both years may indicate a migration from coastal waters to offshore overwintering grounds. Herring have been extensively monitored within Alaska state

waters (< 3 nmi from shore) by ADFG (*e.g.* Hebert, 2014; Hollowell et al., 2015), yet information on herring distributions over the EGOA shelf is lacking. Within the inner waters of southeastern Alaska, herring descend to deeper waters in fall once the water column destratifies (Carlson, 1980; Csepp et al., 2011; Sigler and Csepp, 2007). Similarly, herring in the eastern Bering Sea (EBS) feed over the shelf in summer and overwinter offshore near the Pribilof Islands (Funk, 1990). In the western Atlantic, Iceland, and North Sea, some Atlantic herring (*Clupea harengus*) populations also migrate to deeper coastal waters or over the shelf to overwinter (Hay et al., 2001). Observations of herring within the mesopelagic layer in fall 2011 trawl samples suggests that they are not limited to the shelf, and opens the possibility that a portion of the population may overwinter over the EGOA slope.

The presence of dense aggregations of capelin in summer and fall over the CGOA shelf in both years suggests a non-migratory distribution. The length frequency distribution of capelin caught in this study indicates that these fish were primarily immature age-1 and age-2 fish (*cf.* Brown, 2002). Since the 1980s, catches of capelin over the Kodiak shelf from the AFSC BT survey have higher CPUEs than other areas of the GOA (Ormseth, 2012), suggesting that the CGOA shelf may serve as a feeding area for juveniles. It is unknown if capelin remain over the CGOA shelf in winter. If capelin in the Northeast Pacific are consistent with capelin in the Northwest Atlantic, Iceland, and Barents Sea (Carscadden et al., 2013a), then they are predicted to remain offshore over the GOA shelf until they mature at age-2 or age-3, and then migrate to coastal waters to spawn near beaches in late spring and early summer (Brown, 2002; Pahlke, 1985).

2.4.1.3. *Spatial variability*

Forage fish distribution patterns reflect intra- and interspecific differences in spatial distributions within and between regions. In the CGOA, capelin and age-0 pollock densities were concentrated inside the 100 m isobath, but spatial separation between these species was apparent from the distribution of aggregations identified by the local Moran's I analysis. Capelin were concentrated along the edges of banks and troughs, while age-0 pollock were distributed both along the edges and over the top of banks. Vertical separation between these species was common over both banks and troughs, with capelin consistently deeper. Variability in the distribution of capelin and age-0 pollock in this and other studies suggests that both species are sensitive to changes in the environment. Spatial separation between these species may be indicative of interspecific differences in habitat preferences, prey resource utilization, and/or predator avoidance that have been the focus of prior studies in the GOA (e.g. Logerwell et al., 2010; Wilson et al., 2006). For example, the aggregation of capelin near outer margins of Portlock and Albatross Banks may indicate a preference for areas of relatively high primary production and cooler water. In summer, strong tidal mixing of relatively warm, iron-rich coastal water with cold, nutrient-rich slope water transported up troughs enhances primary production over banks compared to troughs, while waters over the bank remain relatively cooler along edges compared to the top (Cheng et al., 2012; Ladd et al., 2005; Stabeno et al., 2004). Changes in distributions of capelin and age-0 pollock over the Kodiak shelf and in the WGOA have been attributed to oceanographic conditions and the location of water masses (Hollowed et al., 2007; Logerwell et al., 2007), areas of relatively weak currents (Wilson, 2009), and the composition and distribution of zooplankton prey (Logerwell et al., 2010; Wilson et al., 2006). Similarly, spatial variability among capelin populations in the Atlantic have been associated with abundance, water temperature and the location of water masses, and the extent of sea ice (*e.g.*

Frank et al., 1996; Ingvaldsen and Gjøsæter, 2013; Olafsdottir and Rose, 2012). Although capelin and age-0 pollock have been hypothesized to potentially compete for shared prey resources (Logerwell et al., 2010; Wilson et al., 2006), vertical distributions of capelin in summer were not different in 2011, when pollock were absent, compared to 2013, when pollock were abundant.

Even though capelin were the dominant forage fish species over the CGOA shelf in summer and fall of both years, observations of capelin in the EGOA were rare and only occurred in summer 2011 and fall 2013. The limited observations of capelin in the EGOA are potentially due to bathymetric and oceanographic differences compared to the CGOA. The narrow EGOA shelf is much deeper than the shallow banks and troughs that penetrate the broad CGOA shelf where capelin densities were highest. Aggregations of capelin were observed within the Yakobi Sea Valley in summer 2011 and over the relatively shallow shelf, northwest of Cross Sound in fall 2013. This area receives well mixed, nutrient-rich waters from Cross Sound (Stabeno et al., 2016b). North of Cross Sound, capelin distributions within Glacier Bay have been associated with areas near tidewater glaciers that are relatively cooler, more turbid, have higher dissolved oxygen, and lower chlorophyll levels (Arimitsu et al., 2008). An association with colder water may partially explain why capelin are not as abundant in the inner waters of Southeast Alaska compared to other forage species (Csepp et al., 2011). The frequent occurrence of capelin in diets of rhinoceros auklets (*Cerorhinca monocerata*) sampled at St. Lazaria Island in 2011 and 2013 (Slater and Fety, 2015) suggests that capelin were present in the region, but likely distributed inshore of the study area.

Compared to distribution patterns in the CGOA, age-0 pollock in the EGOA were concentrated in higher densities located closer to shore over deeper waters near the shelf break or

within the Yakobi Sea Valley. The vertical distribution of age-0 pollock in the EGOA was significantly deeper than in the CGOA out to the 1,000 m isobath, occupying maximum depths of 125 m. This maximum depth falls within daytime vertical distributions of age-0 pollock in summer and fall reported for the Northeast Pacific that spanned from surface waters to 150 m (Bailey, 1989; Brodeur and Wilson, 1996b; Parker-Stetter et al., 2015). Variability in vertical distributions of age-0 pollock were associated with bottom depth in this study, often occurring over relatively short horizontal distances due to strong bathymetric gradients in both regions. Variability in vertical position may serve an important role in transport of age-0 pollock over 100s of km to nearshore nursery areas (Smart et al., 2013). The horizontal movement of fish located at shallow depths (*i.e.* above the pycnocline) would be more susceptible to wind-forced circulation, while subsurface currents would have a greater effect on the trajectory of fish occupying deeper waters (Duffy-Anderson et al., 2015).

Mesopelagics in the EGOA were also distributed relatively close to shore compared to distributions in the CGOA, and occasionally at shallow depths (≥ 125 m) within the Yakobi Sea Valley. Catches of myctophids in the AFSC BT survey have also typically occurred off the Yakobi Sea Valley, near the southern tip of Baranof Island, and near the shelf break off Kayak Island and Yakutat (Ormseth, 2014). The relatively close proximity of mesopelagics to within 20 km from the EGOA coast and shallow vertical distribution within the Yakobi Sea Valley may provide an important energy source to coastal piscivores (*e.g.* Robards et al., 2003; Slater and Fety, 2015) given the high energy density and lipid content of mesopelagic species (Van Pelt et al., 1997; Vollenweider et al., 2011).

### 2.4.2 **Potential effects of forage fish variability on predators**

The absence of age-0 pollock in 2011 and interannual differences in acoustic densities of all other forage fish species suggests that foraging opportunities for GOA predators were less favorable in 2011 compared to 2013. The anomalously weak spring bloom, observed differences in phytoplankton community composition (Stabeno et al., 2016b; Strom et al., 2016), and lower mesozooplankton biomass (Zador, 2012) suggest that poor foraging conditions persisted from spring through fall in 2011. Seabird recruitment failures were observed across the GOA in 2011, as well as a higher occurrence of "mushy" (*i.e.* high flesh water content) halibut in lower Cook Inlet (Zador, 2012). In contrast to 2011, higher forage fish densities, and high summer abundance of age-0 pollock observed in this and other surveys, likely increased predator foraging opportunities in 2013. Seabird production in the western GOA was categorized as good or above average for most monitored species in 2013, and there was a decrease in "mushy" halibut (Zador, 2014).

In 2011, foraging predators required greater energy expenditures to locate and capture prey compared to 2013. Predator foraging success can be sensitive to local prey density and vertical position (Benoit-Bird et al., 2013). Piatt et al. (2007) demonstrated that the allocation of time spent foraging and incubating chicks by murres, and the breeding success of black-legged kittiwakes (*Rissa tridactyla*) exhibited strong non-linear relationships with prey density. Vertical shifts of prey to greater depths reduces potential encounter rates with prey as reaction distances of visual foragers decreases under low light (Vogel and Beauchamp, 1999). Diving and epipelagic predators are further constrained by the vertical distribution of prey due to physiological costs of diving and limited time available to search for prey per dive when swimming to greater depths (Acevedo-Gutiérrez et al., 2002; Wilson et al., 1992). Age-0

pollock were observed at shallower depths than most other forage fish species, with juvenile salmon in the surface layer being the one notable exception. When age-0 pollock were absent, diving and epipelagic predators would have to dive deeper to forage during daytime. Higher energy density and lipid content among capelin, herring, and myctophids compared to age-0 pollock (Vollenweider et al., 2011) would potentially offset some of these increased foraging costs. Yet, widespread recruitment failures among seabirds across the GOA in 2011 indicate that the prey supply was insufficient (Zador, 2012).

Reduced abundance of capelin over the CGOA shelf could potentially impact coastal predators the following year when predators are dependent on a concentrated input of energy to coincide with their breeding season (Gjøsæter et al., 2009; Sigler et al., 2004; Womble et al., 2009). Summer abundance of immature capelin can be viewed as an indicator of spawning stock biomass for the subsequent spring (*e.g.* Carscadden et al., 2013a). Observed low densities of immature capelin in 2011 may have subsequently resulted in reduced prey availability in coastal areas in spring 2012 as fewer mature capelin would have been expected to complete their nearshore spawning migration.

Despite the spatial and temporal differences in GOA forage fish communities, the area around Cross Sound and the Yakobi Sea Valley appears to be an ecological "hot spot" (Sydeman et al., 2006). The sea valley provides a pathway for slope water into Cross Sound, where strong tidal mixing and gap winds result in higher primary production, which is then transported to the outflow side of the canyon and over the shallow shelf northwest of Cross Sound (Ladd and Cheng, 2016; Stabeno et al., 2016b). Peak acoustic densities of macrozooplankton, primarily comprised of euphausiids, were observed within the sea valley in summer 2013. Age-0 pollock formed a dense shoal several kilometers in length, the largest observed aggregation of age-0

pollock during the study. This large aggregation contrasted to relatively smaller patches (< 600 m) of age-0 pollock that occurred on nearly all other GOA transects. Aggregations of other species or length classes of pollock were also observed within the sea valley, including capelin, longfin smelt, pollock (≥ 298 mm in length), and mesopelagics in summer 2011; herring and mesopelagics in fall 2011; pollock (≥ 418 mm), mesopelagics, and macrozooplankton in summer 2013; and herring, pollock (≥ 183 mm), mesopelagics, and macrozooplankton in fall 2013. Most of these aggregations were vertically distributed between 80 to 200 m, including the deepest age-0 pollock and shallowest mesopelagic occupied depths of approximately 125 m. The weakest flows occurred within this depth range on the south side of the canyon where slope water flowed into Cross Sound (Stabeno et al., 2016b). Fish and macrozooplankton may have concentrated at these depths to maintain their positions in an area characterized by high water flow. The consistency of these patterns can be important to predators, as the Cross Sound area may serve as a critical feeding ground during periods when prey resources are limited over the EGOA shelf, such as those observed in 2011 and fall of 2013.

### 2.4.3 **Study limitations**

This study's characterization of forage fish distributions in the two regions was potentially limited by the absence of some forage fish species from the pattern description, classification of acoustic data to species, and the loss of data due to logistic constraints. Juvenile salmon were not included in the analysis of GOA forage fish. Juvenile salmon are primarily distributed in the upper 50 m of the water column (Orsi and Wertheimer, 1995), often concentrating within 15 m of the surface (Beamish et al., 2000; Emmett et al., 2004; Farley et al., 2005). The shallow vertical distribution of juvenile salmon, and co-occurrence with adult

salmon and other epipelagic fish and invertebrate species, prevented acoustic estimates of salmon to species and/or length classes in this study. This group of species was assigned to the surface category. Juvenile salmon distribution patterns based on GOAIERP surface trawl data are described by Shotwell and Moss (2013).

This study's description of GOA forage fish is also potentially limited by infrequent observations of eulachon and the absence of Pacific sand lance (*Ammodytes hexapterus*) in trawl samples. The absence is attributed to the extent of the survey domain and not the catchability of the Cantrawl net. From 2007 to 2013, AFSC BT survey catches of eulachon were concentrated to the west of the CGOA study area within the Shelikof Sea Valley, within Amatuli Trough (partially covered by the CGOA grid), and inside Sitka Sound (Ormseth, 2012). Sand lance typically occur in shallow, coastal and intertidal waters (Blackburn and Anderson, 1997; Haynes et al., 2008; Johnson et al., 2008). In Prince William Sound, sand lance primarily occurred close to shore in less than 40 m bottom depth, and were not observed over depths greater than 60 m (Ostrand et al., 2005). Offshore, AFSC BT survey catches of sand lance have historically occurred over Albatross Bank, but were mostly absent from bottom trawl catches in 2007 to 2013 (Ormseth, 2012). It is unlikely that aggregations of eulachon or sand lance went undetected in trawl samples throughout the duration of this study. In fall 2013, small numbers of eulachon (8 to 24 fish per trawl) were caught in 3 midwater samples. In previous surface trawl-based studies in the EBS that used the same Cantrawl net, sand lance comprised 2% of non-salmonid catches (approximately 11,400 sand lance) during the fall 2002 survey (Farley et al., 2005). Although known to burrow in substrate (Meyer et al., 1979), sand lance are primarily distributed in the water column during daytime (Hobson, 1986), making them accessible to both the Cantrawl net and acoustic sampling (*e.g.* Ostrand et al., 2005). The lack of eulachon and

sand lance observations in this study are therefore unlikely due to net selectivity of the Cantrawl net.

The analysis was further constrained by the ability to classify acoustic data to species. The proportion of acoustic backscatter categorized as mixed species and/or unclassified varied between surveys due to uncertainty in trawl selectivity and the lack of trawl samples for some high density aggregations. The classification method used in this study depended on the collection of relatively homogenous trawl samples (> 90% of the catch by number of fish). Mixed species catches were not used to apportion backscatter by percent composition due to an inability to correct for trawl selectivity (*e.g.* Williams et al., 2011). The inability to correct for the selectivity bias prevented describing distributions of low density species, such as age-0 Pacific cod, that co-occurred in mixed aggregations with a dominant species, such as age-0 pollock. Logistic constraints associated with equipment failures, poor weather, and decreased sampling time on shorter days in fall also reduced the number of trawl samples available to verify observed echogram patterns. As a result, a higher proportion of backscatter in some surveys was classified as unknown, limiting interpretation of observed changes in forage fish distributions.

The U.S. government shutdown in 2013 resulted in the loss of 10 survey days in the fall CGOA survey, limiting sampling effort to only the southern portion of the survey grid over the shelf. Less than 460 km of transect were sampled, compared to at least 1,700 km in all other CGOA surveys. No samples were collected over waters deeper than 500 m, preventing any meaningful coverage of mesopelagics.

### 2.4.4 **Considerations for survey design**

Observed spatial and temporal variability in forage fish distributions highlight factors that should be considered in future monitoring of the GOA forage fish community. Survey design elements that have to be examined include timing (*i.e.* season), spatial extent, gear selection, and sample resolution. Design choices will differ if surveys target individual species. Compromises are required if the goal is to conduct a forage fish survey.

The optimal time to monitor interannual differences in the distribution and abundance of forage fish is July and August. Age-0 pollock are widely distributed across the shelf and slope in summer where they overlap with capelin and mesopelagics. A secondary advantage is a summer survey would coincide with groundfish assessment surveys (*i.e.* MACE summer pollock AT survey, AFSC summer BT survey, and AFSC longline survey) and breeding season surveys for seabirds (Dragoo et al., 2015) and pinnipeds (Womble et al., 2009; Womble and Sigler, 2006). Stomach and bill-load samples are typically collected during these surveys, which are used to characterize foraging habits and energy intake of predators (*e.g.* Kettle et al., 2015; Yang et al., 2005). Temporal overlap of a dedicated forage fish survey with these long-running surveys would allow for quantifying changes in the forage base with predator abundances, distributions, growth, prey selection, and reproductive success. A summer survey would also be consistent with international efforts to survey capelin populations off Iceland and in the Barents Sea when immature age-1 and -2 fish are distributed offshore (Carscadden et al., 2013b).

Although distributions varied among species in this study, observed spatial distributions can be used to delineate the spatial extent of a forage fish survey. The relative stability of mesopelagic density within each isobath suggests that it would be inefficient to extend a survey grid by a fixed distance offshore; a depth-stratified survey design would provide an estimate of

relative abundance between major isobaths. Similarly, even though age-0 pollock were observed in low densities over the EGOA basin, all significant aggregations identified by the local Moran's I analysis were located within the 200 m isobath in the CGOA and within the 1,000 m isobath in the EGOA. Extending a forage fish survey beyond the 2,000 m isobath would not be an efficient allocation of resources if the objective of the survey was to produce an index of forage fish availability over shelf and slope habitats. On the other hand, the concentration of age-pollock and capelin over CGOA banks and age-pollock within the Yakobi Sea Valley in the EGOA highlight the importance of identifying specific locations or habitats where fish aggregate. Areas where fish aggregate may warrant increased sampling effort to generate accurate biomass estimates.

Survey gear and sampling resolution should be selected to ensure that forage fish are sampled through their full vertical range at horizontal scales that maximize variability in their distributions. In this study, high variability in the vertical distribution of age-0 pollock and capelin between isobath groups and regions highlights the necessity of sampling the whole water column. Continuous horizontal sampling will be necessary to sample forage fish distributions at spatial scales structured at less than 1 km. High resolution, continuous samples across large survey areas are collected by acoustic technologies which are appropriate for this survey. Acoustic samples are constrained by surface and bottom exclusions, discrimination of species, and determining length composition within mixed aggregations (Simmonds and MacLennan, 2005), but all acoustic surveys include direct samples such as midwater trawls. The importance of juvenile salmon as forage fish and the periodic occurrence of large catches of herring in surface trawl catches highlight the value of integrating near surface and midwater trawls with multifrequency acoustic sampling.

A forage fish survey should also include species not well sampled in this study. The lack of summer observations of herring during this study suggests that herring are unlikely to be well sampled in an offshore summer survey unless the survey area was extended into coastal embayments (Ormseth et al., 2016). Inclusion of eulachon, sand lance, and age-0 Pacific cod may require expansion of the survey domain or to incorporate sampling methodologies that increase the likelihood they would be caught. For sand lance, this includes identifying when they occupy pelagic waters and are available to both acoustic and trawl sampling (Greenstreet et al., 2006).

### 2.4.5 **Conclusion**

To support an ecosystem-based management of marine resources in the GOA (Ormseth, 2012), accurate estimates of forage fish abundance and distribution are needed to track the forage base utilized by piscivorous fish, seabirds, and marine mammals. This requirement is amplified during periods of anomalous ocean conditions, such as the observed low densities of forage fish in 2011; that are expected to occur more frequently in response to changing climate conditions. A long-term monitoring program designed for forage fish in the GOA can be accomplished through a multispecies summer survey utilizing acoustic (*e.g.* echosounder) and pelagic trawl technologies.

## 2.5 TABLES

**Table 2.1** - Season ("S" = summer; "F" = fall), dates, survey area "E" = eastern Gulf of Alaska region; "Y" = Yakutat transect; "K" = Kayak Island transect; "C" = central GOA region, vessel ("NWE" = F/V *Northwest Explorer*; "OD" = NOAA Ship *Oscar Dyson*), and distance length of acoustic transect sampled for each survey. Refer to Fig. 2.1 for survey area locations.

| Survey | Season | Date | Survey Area | Vessel | Distance (km) |
|---|---|---|---|---|---|
| 1GOA11 | S | Jul 3-17, 2011 | E | NWE | 1,115 |
| 2GOA11 | S | Aug 2-21, 2011 | Y, K, C | NWE | 2,648 |
| 3GOA11 | F | Sep 8-22, 2011 | E, K | NWE | 882 |
| 4GOA11 | F | Sep 25-Oct 8, 2011 | C | NWE | 1,728 |
| 1GOA13 | S | Jul 3-21, 2013 | E | NWE | 1,861 |
| 2GOA13 | S | Aug 3-21, 2013 | Y, K, C | NWE | 2,621 |
| 3GOA13 | F | Sep 6-24, 2013 | K, Y, E | NWE | 1,506 |
| 4GOA13 | F | Sep 24-28, 2013 | C | OD | 459 |

**Table 2.2** – Backscatter category definitions for acoustic data. Survey(s) in which backscatter was assigned to each category are listed, along with the category water column depth range. Reported lengths are from this study's trawl samples and ages are inferred from literature-based length-age relationships.

(* Note, minimum depth for all categories during 4GOA13 survey is 15 m)

| Category | Survey | | | | * Depth Range (m) | Acoustic Threshold (dB) | Definition |
|---|---|---|---|---|---|---|---|
| | 1GOA11 | 2GOA11 | 3GOA11 | 4GOA11 | | | |
| | 1GOA13 | 2GOA13 | 3GOA13 | 4GOA13 | | | |
| Surface | x | x | x | x | 10 - 50 | -75 | May include but not limited to adult and juvenile salmon, epipelagic fish, squid, jellyfish |
| | x | x | x | x | | | |
| Mesopelagic | x | x | x | x | 125 – 500 | -75 | Primarily comprised of myctophids and other mesopelagic fish. |
| | x | x | x | x | | | |
| Piscivores | x | x | x | x | 10 – 250 | -67 | Includes all groundfish > 158 mm in length |
| | x | x | x | x | | | |
| Age-0 Pollock | | | | | 10 – 125 | -67 | Pollock < 88 mm in length; may also include age-0 Pacific cod in 2GOA13 |
| | x | x | | | | | |
| Herring | | | x | | 10 – 250 | -67 | Pacific herring ≥ 71 mm in length |
| | | | x | | | | |
| Capelin | | x | | x | 10 – 250 | -67 | Age-1+ capelin (≥ 59 mm in length) (Pahlke 1985; Brown 2001) |
| | | x | x | x | | | |
| Forage Fish Mix | | | | x | 10 -250 | -67 | Includes two or more of these species: capelin, herring, age-0 pollock, and/or eulachon |
| | | | x | x | | | |
| Forage Fish/ Piscivores Mix | x | x | x | | 10 – 250 | -67 | Includes at least one forage fish and one piscivore species |
| | | x | x | x | | | |
| Macrozooplankton | | | | | 10 – 250 | -80 | Primarily euphausiids, copepods, and/or amphipods – 2013 only |
| | x | x | x | x | | | |
| Unknown | x | x | x | x | 10 - 500 | -67 | All backscatter that cannot be assigned to a category |
| | x | x | x | x | | | |

**Table 2.3** – Trawl samples by survey. "ST" = surface trawl; "MWT" = midwater trawl.

| Survey | ST | MWT |
|---|---|---|
| 1GOA11 | 52 | 11 |
| 2GOA11 | 54 | 10 |
| 3GOA11 | 40 | 10 |
| 4GOA11 | 37 | 10 |
| 1GOA13 | 71 | 11 |
| 2GOA13 | 55 | 19 |
| 3GOA13 | 63 | 10 |
| 4GOA13 | 10 | 2 |

**Table 2.4**– Number of trawl samples in which one classification category accounted for more than 90% of the catch by number. "ST" = surface trawl; "MWT" = midwater trawl; "FF" = forage fish.

| Classification category | 2011 | | 2013 | |
|---|---|---|---|---|
| | *ST* | *MWT* | *ST* | *MWT* |
| Age-0 Pollock | 0 | 0 | 6 | 8 |
| Capelin | 3 | 6 | 2 | 4 |
| Herring | 1 | 1 | 1 | 1 |
| FF Mix | 0 | 3 | 3 | 2 |
| FF/Piscivores Mix | 0 | 6 | 0 | 6 |
| Piscivores | 0 | 10 | 0 | 6 |
| Mesopelagic | 0 | 3 | 0 | 1 |

**Table 2.5** – Summary of acoustic data classification by year, season, and region. *N* = the number of 200 m acoustic bins where acoustic density, $s_A$ ($m^2$ $nmi^{-2}$), was greater than zero (*i.e.* nonzero density). Mean density and standard error ($s_A \pm SE$) for each survey: "□ " = mean $s_A$ among all samples; "□ ($s_A > 0$)" = mean nonzero density for *N* samples. The $s_A$-weighted mean proportion of 38 kHz backscatter assigned to each category (% $s_A$) is summarized as follows for each survey: "Total" = proportion of all backscatter; "< 500" = proportion of backscatter over bottom depths less than 500 m. Backscatter categories: "T" = all 38 kHz backscatter; "MP" = mesopelagic, "PO" = age-0 pollock; "CA" = capelin; "HE" = herring; "FF" = forage fish mix; "FP" = forage fish/piscivores mix; "PI" = piscivores; "Surf" = surface; "UN" = unknown backscatter; "MZ" = macrozooplankton (not included in proportion of total backscatter).

| Category | | 2011 | | | | | 2013 | | | | |
|---|---|---|---|---|---|---|---|---|---|---|---|
| | | | $s_A \pm SE$ ($m^2$ $nmi^{-2}$) | | % $s_A$ | | | $s_A \pm SE$ ($m^2$ $nmi^{-2}$) | | % $s_A$ | |
| | | *N* | [illegible] | [illegible] $_{(s_A > 0)}$ | *Total* | *< 500* | *N* | [illegible] | [illegible] $_{(s_A > 0)}$ | *Total* | *< 500* |
| **Summer EGOA** | T | 3,179 | 170 ± 5 | - | - | - | 5,684 | 707 ± 9 | - | - | - |
| | MP | 1,733 | 112 ± 3 | 206 ± 5 | 66.3 | 23 | 4,739 | 538 ± 7 | 646 ± 7 | 76.1 | 39.5 |
| | PO | 0 | 0 | 0 | 0 | 0 | 3,526 | 39 ± 3 | 62 ± 5 | 5.5 | 20.3 |
| | FP | 34 | 0.5 ± 0.1 | 45 ± 9 | 0.3 | 0.8 | 0 | 0 | 0 | 0 | 0 |
| | PI | 1,735 | 35 ± 4 | 64 ± 7 | 20.5 | 56.3 | 2,977 | 39 ± 4 | 74 ± 8 | 5.4 | 28.7 |
| | SU | 2,887 | 13 ± 1 | 14 ± 1 | 7.5 | 8.8 | 5,616 | 81 ± 2 | 82 ± 2 | 11.5 | 9.2 |
| | UN | 2,846 | 9 ± 1 | 10 ± 1 | 5.5 | 11.2 | 4,477 | 10 ± 0.3 | 13 ± 0.4 | 1.4 | 2.2 |
| | MZ | - | - | - | - | - | 5,164 | 97 ± 5 | 107 ± 6 | - | - |
| | | * No backscatter assigned to CA, HE, or FF | | | | | * No backscatter assigned to CA, HE, or FF | | | | |
| **Summer CGOA** | T | 7,472 | 128 ± 9 | - | - | - | 7,339 | 681 ± 21 | - | - | - |
| | MP | 1,268 | 27 ± 1 | 160 ± 4 | 21.3 | 3.9 | 1,345 | 195 ± 8 | 1,062 ± 34 | 28.6 | 5.4 |
| | PO | 0 | 0 | 0 | 0 | 0 | 6,438 | 29 ± 1 | 33 ± 2 | 4.2 | 5.6 |
| | CA | 800 | 13 ± 1 | 125 ± 9 | 10.5 | 13.4 | 1,383 | 179 ± 14 | 949 ± 68 | 26.3 | 35.1 |
| | FP | 145 | 0.9 ± 0.2 | 45 ± 9 | 0.7 | 0.9 | 116 | 3 ± 0.7 | 185 ± 38 | 0.4 | 0.6 |
| | PI | 4,056 | 36 ± 3 | 67 ± 6 | 28.5 | 36.1 | 6,177 | 214 ± 12 | 254 ± 15 | 31.4 | 42 |
| | SU | 6,658 | 12 ± 1 | 13 ± 1 | 9.2 | 8.8 | 5,558 | 19 ± 0.7 | 25 ± 0.9 | 2.8 | 3 |
| | UN | 5,821 | 38 ± 8 | 49 ± 10 | 29.8 | 36.9 | 1,567 | 43 ± 7 | 202 ± 34 | 6.3 | 8.3 |
| | MZ | - | - | - | - | - | 7,071 | 90 ± 2 | 94 ± 2 | - | - |
| | | * No backscatter assigned to HE or FF | | | | | * No backscatter assigned to HE or FF | | | | |
| **Fall EGOA** | T | 2,515 | 135 ± 18 | - | - | - | 4,420 | 1,471 ± 27 | - | - | - |
| | MP | 1,374 | 36 ± 1 | 67 ± 2 | 26.9 | 5.6 | 2,965 | 1,125 ± 19 | 1,677 ± 21 | 76.5 | 11 |
| | HE | 109 | 2 ± 1 | 44 ± 21 | 1.4 | 1.7 | 20 | 9 ± 7 | 2,076 ± 1,453 | 0.6 | 5 |
| | FF | 0 | 0 | 0 | 0 | 0 | 212 | 21 ± 5 | 440 ± 109 | 1.4 | 11.2 |
| | FP | 119 | 6 ± 1 | 125 ± 16 | 4.4 | 6.1 | 160 | 5 ± 1 | 126 ± 25 | 0.3 | 2.4 |
| | PI | 1,302 | 24 ± 2 | 46 ± 3 | 17.5 | 23.6 | 1,654 | 40 ± 3 | 108 ± 7 | 2.7 | 21.4 |
| | SU | 1,130 | 2 ± 0.1 | 5 ± 0.2 | 1.7 | 0.6 | 4,234 | 122 ± 3 | 128 ± 3 | 8.3 | 12.7 |
| | UN | 2,225 | 65 ± 18 | 73 ± 21 | 48.1 | 62.4 | 4,280 | 148 ± 16 | 153 ± 16 | 10.1 | 36.2 |
| | MZ | - | - | - | - | - | - | - | - | - | - |
| | | * No backscatter assigned to PO or CA | | | | | * No backscatter assigned to PO or CA, MZ uncalibrated | | | | |
| **Fall CGOA** | T | 4,846 | 113 ± 5 | - | - | - | 1,303 | 557 ± 47 | - | - | - |
| | MP | 912 | 38 ± 1 | 204 ± 4 | 34 | 3.9 | 20 | 3 ± 1 | 190 ± 23 | 0.5 | 0.4 |
| | CA | 689 | 17 ± 2 | 121 ± 12 | 15.2 | 22.5 | 134 | 117 ± 21 | 1,137 ± 177 | 21 | 21 |
| | FF | 231 | 0.3 ± 0.04 | 5 ± 1 | 0.2 | 0.3 | 52 | 54 ± 12 | 1,344 ± 251 | 9.6 | 9.6 |
| | FP | 0 | 0 | 0 | 0 | 0 | 66 | 32 ± 8 | 636 ± 138 | 5.8 | 5.8 |
| | PI | 2,264 | 46 ± 4 | 98 ± 8 | 40.3 | 59.5 | 478 | 188 ± 34 | 512 ± 91 | 33.7 | 33.8 |
| | SU | 1,854 | 1 ± 0.1 | 3 ± 0.3 | 1 | 0.9 | 632 | 3 ± 0.7 | 7 ± 1 | 0.6 | 0.6 |
| | UN | 4,258 | 10 ± 2 | 12 ± 2 | 9.3 | 12.9 | 1,292 | 160 ± 21 | 161 ± 21 | 28.7 | 28.8 |
| | MZ | - | - | - | - | - | 1,114 | 64 ± 6 | 75 ± 7 | - | - |
| | | * No backscatter assigned to PO or HE | | | | | * No backscatter assigned to PO or HE | | | | |

**Table 2.6** – Results of Wilcoxon rank-sum tests for differences of median acoustic density, $s_A$ ($m^2$ $nmi^{-2}$), across isobaths within each survey by forage fish group. Results reflect two-tailed tests at $\alpha = 0.05$ significance level. (Note, ** indicates sample size too small for statistical comparison)

| Survey | Species | Isobath (m) | *N* | Median Density ($s_A$) | 100-200 m | | 200-500 m | | 500-1,000 m | | 1,000-2,000 m | | > 2,000 m | |
|---|---|---|---|---|---|---|---|---|---|---|---|---|---|---|
| | | | | | *W* | *p*-value | *W* | *p*-value | *W* | *p*-value | *W* | *p*-value | *W* | *p*-value |
| 1GOA11 | Mesopelagics | 200-500 | 122 | 82.9 | - | - | - | - | 4,160 | < 0.001 | 18,997 | 0.001 | 3,739 | < 0.001 |
| | | 500-1,000 | 112 | 184.0 | - | - | - | - | - | - | 25,331 | 0.005 | 5,326 | 0.581 |
| | | 1,000-2,000 | 385 | 124.9 | - | - | - | - | - | - | - | - | 15,319 | 0.063 |
| | | > 2,000 | 91 | 169.8 | - | - | - | - | - | - | - | - | - | - |
| 2GOA11 | Capelin | < 100 | 308 | 37.2 | 16,590 | < 0.001 | ** | ** | - | - | - | - | - | - |
| | | 100-200 | 71 | 5.1 | - | - | ** | ** | - | - | - | - | - | - |
| | | 200-500 | 4 | 0.2 | - | - | - | - | - | - | - | - | - | - |
| | Mesopelagics | 200-500 | 89 | 75.1 | - | - | - | - | 5,967 | 0.002 | 7,244 | 0.003 | 1,599 | 0.184 |
| | | 500-1,000 | 174 | 136.8 | - | - | - | - | - | - | 18,377 | 0.858 | 4,035 | 0.295 |
| | | 1,000-2,000 | 209 | 125.4 | - | - | - | - | - | - | - | - | 4,671 | 0.512 |
| | | > 2,000 | 42 | 130.1 | - | - | - | - | - | - | - | - | - | - |
| 3GOA11 | Herring | 100-200 | 7 | 17.3 | - | - | ** | ** | ** | ** | ** | ** | - | - |
| | | 200-500 | 41 | 1.8 | - | - | - | - | ** | ** | ** | ** | - | - |
| | | 500-1,000 | 7 | 0.7 | - | - | - | - | - | - | ** | ** | - | - |
| | | 1,000-2,000 | 17 | 3.2 | - | - | - | - | - | - | - | - | - | - |
| | Mesopelagics | 200-500 | 105 | 51.9 | - | - | - | - | 3,509 | 0.2892 | 12,353 | 0.5065 | 3,576 | 0.0271 |
| | | 500-1,000 | 80 | 36.2 | - | - | - | - | - | - | 11,889 | 0.5806 | 3,180 | 0.8251 |
| | | 1,000-2,000 | 226 | 44.8 | - | - | - | - | - | - | - | - | 12,613 | 0.182 |
| | | > 2,000 | 763 | 43.6 | - | - | - | - | - | - | - | - | - | - |
| 4GOA11 | Capelin | < 100 | 271 | 7.5 | 9,748 | 0.007 | - | - | - | - | - | - | - | - |
| | | 100-200 | 89 | 26.2 | - | - | - | - | - | - | - | - | - | - |
| | Mesopelagics | 200-500 | 45 | 104.1 | - | - | - | - | 2,589 | 0.007 | 1,886 | < 0.001 | ** | ** |
| | | 500-1,000 | 156 | 207.2 | - | - | - | - | - | - | 10,369 | 0.004 | ** | ** |
| | | 1,000-2,000 | 163 | 228.4 | - | - | - | - | - | - | - | - | ** | ** |
| | | > 2,000 | 11 | 298.2 | - | - | - | - | - | - | - | - | - | - |

**Table 2.6 (cont'd)-**

| Survey | Species | Isobath (m) | *N* | Median Density ($s_A$) | 100-200 m | | 200-500 m | | 500-1,000 m | | 1,000-2,000 m | | > 2,000 m | |
|---|---|---|---|---|---|---|---|---|---|---|---|---|---|---|
| | | | | | *W* | *p*-value | *W* | *p*-value | *W* | *p*-value | *W* | *p*-value | *W* | *p*-value |
| 1GOA13 | Mesopelagics | 200-500 | 107 | 815.9 | - | - | - | - | 7,621 | < 0.001 | 20,338 | < 0.001 | 101,560 | < 0.001 |
| | | 500-1,000 | 90 | 328.2 | - | - | - | - | - | - | 8,831 | < 0.001 | 33,965 | < 0.001 |
| | | 1,000-2,000 | 270 | 405.4 | - | - | - | - | - | - | - | - | 153,658 | < 0.001 |
| | | > 2,000 | 1,485 | 541.5 | - | - | - | - | - | - | - | - | - | - |
| | Pollock | < 100 | 4 | 51.3 | ** | ** | ** | ** | ** | ** | ** | ** | ** | ** |
| | | 100-200 | 332 | 39.0 | - | - | 24,896 | 0.727 | 18,582 | < 0.001 | 51,322 | < 0.001 | 309,668 | < 0.001 |
| | | 200-500 | 153 | 32.9 | - | - | - | - | 8,507 | < 0.001 | 23,668 | < 0.001 | 139,588 | < 0.001 |
| | | 500-1,000 | 82 | 9.9 | - | - | - | - | - | - | 9,923 | 0.141 | 59,715 | < 0.001 |
| | | 1,000-2,000 | 218 | 5.5 | - | - | - | - | - | - | - | - | 143,776 | < 0.001 |
| | | > 2,000 | 1,103 | 2.7 | - | - | - | - | - | - | - | - | - | - |
| 2GOA13 | Capelin | < 100 | 389 | 411.1 | 62,144 | < 0.001 | 36,365 | < 0.001 | - | - | - | - | - | - |
| | | 100-200 | 173 | 7.5 | - | - | 6,493 | < 0.001 | - | - | - | - | - | - |
| | | 200-500 | 107 | 28.6 | - | - | - | - | - | - | - | - | - | - |
| | Mesopelagics | 200-500 | 76 | 379.4 | - | - | - | - | 4,109 | < 0.001 | 4,958 | < 0.001 | 1,264 | < 0.001 |
| | | 500-1,000 | 170 | 794.7 | - | - | - | - | - | - | 17,735 | 0.566 | 4,506 | 0.840 |
| | | 1,000-2,000 | 216 | 835.8 | - | - | - | - | - | - | - | - | 5,760 | 0.889 |
| | | > 2,000 | 54 | 896.8 | - | - | - | - | - | - | - | - | - | - |
| | Pollock | < 100 | 860 | 21.6 | 610,626 | < 0.001 | 267,854 | < 0.001 | 103,776 | < 0.001 | 128,367 | < 0.001 | 38,094 | < 0.001 |
| | | 100-200 | 1,016 | 5.2 | - | - | 283,191 | < 0.001 | 113,692 | < 0.001 | 145,384 | < 0.001 | 42,318 | < 0.001 |
| | | 200-500 | 365 | 1.1 | - | - | - | - | 28,288 | 0.003 | 38,111 | < 0.001 | 9,843 | 0.164 |
| | | 500-1,000 | 132 | 0.7 | - | - | - | - | - | - | 11,772 | 0.059 | 2,971 | 0.525 |
| | | 1,000-2,000 | 158 | 0.5 | - | - | - | - | - | - | - | - | 2,846 | 0.009 |
| | | > 2,000 | 48 | 1.1 | - | - | - | - | - | - | - | - | - | - |
| 3GOA13 | Herring | 100-200 | 13 | 211.5 | - | - | - | - | - | - | - | - | - | - |
| | Mesopelagics | 200-500 | 105 | 224.9 | - | - | - | - | 1,169 | < 0.001 | 1,262 | < 0.001 | 5,337 | < 0.001 |
| | | 500-1,000 | 80 | 947.2 | - | - | - | - | - | - | 4,608 | < 0.001 | 15,807 | < 0.001 |
| | | 1,000-2,000 | 226 | 1,521.6 | - | - | - | - | - | - | - | - | 81,076 | 0.173 |
| | | > 2,000 | 763 | 1,742.5 | - | - | - | - | - | - | - | - | - | - |
| 4GOA13 | Capelin | < 100 | 68 | 4.1 | ** | ** | - | - | - | - | - | - | - | - |
| | | 100-200 | 2 | 71.1 | - | - | - | - | - | - | - | - | - | - |

**Table 2.7** – Results of Wilcoxon rank-sum tests for differences of median acoustic density, $s_A$ ($m^2$ $nmi^{-2}$), across surveys within isobaths by forage fish group. Results reflect two-tailed tests at $\alpha = 0.05$ significance level. See Appendix 11 for sample size and median density values. (Note, ** indicates sample size too small for statistical comparison)

| Species | Isobath (m) | Survey | 2GOA11 | | 3GOA11 | | 4GOA11 | | 1GOA13 | | 2GOA13 | | 3GOA13 | | 4GOA13 | |
|---|---|---|---|---|---|---|---|---|---|---|---|---|---|---|---|---|
| | | | *W* | *p*-value | *W* | *p*-value | *W* | *p*-value | *W* | *p*-value | *W* | *p*-value | *W* | *p*-value | *W* | *p*-value |
| Capelin | < 100 | 2GOA11 | - | - | - | - | 56,477 | < 0.001 | - | - | 19,373 | < 0.001 | - | - | 11,835 | 0.093 |
| | | 4GOA11 | - | - | - | - | - | - | - | - | 10,898 | < 0.001 | - | - | 8,781 | 0.549 |
| | | 2GOA13 | - | - | - | - | - | - | - | - | - | - | - | - | 18,637 | < 0.001 |
| | 100-200 | 2GOA11 | - | - | - | - | 2,025 | < 0.001 | - | - | 4,916 | 0.014 | - | - | ** | ** |
| | | 4GOA11 | - | - | - | - | - | - | - | - | 9,552 | 0.001 | - | - | ** | ** |
| | | 2GOA13 | - | - | - | - | - | - | - | - | - | - | - | - | ** | ** |
| | 200-500 | 2GOA11 | - | - | - | - | - | - | - | - | ** | ** | - | - | - | - |
| Herring | 200-500 | 3GOA11 | - | - | - | - | - | - | - | - | - | - | ** | ** | - | - |
| Mesopelagics | 200-500 | 1GOA11 | 5,692 | 0.549 | 6,745 | < 0.001 | 2,739 | 0.984 | 1,561 | < 0.001 | 2,125 | < 0.001 | 3,140 | < 0.001 | - | - |
| | | 2GOA11 | - | - | 4,502 | < 0.001 | 2,000 | 0.992 | 1,051 | < 0.001 | 1,417 | < 0.001 | 2,429 | < 0.001 | - | - |
| | | 3GOA11 | - | - | - | - | 1,188 | 0.003 | 664 | < 0.001 | 895 | < 0.001 | 968 | < 0.001 | - | - |
| | | 4GOA11 | - | - | - | - | - | - | 537 | < 0.001 | 723 | < 0.001 | 1,224 | < 0.001 | - | - |
| | | 1GOA13 | - | - | - | - | - | - | - | - | 5,486 | < 0.001 | 8,722 | < 0.001 | - | - |
| | | 2GOA13 | - | - | - | - | - | - | - | - | - | - | 4,950 | 0.006 | - | - |
| | 500-1,000 | 1GOA11 | 11,957 | 0.001 | 7,900 | < 0.001 | 9,677 | 0.133 | 3,332 | < 0.001 | 1,855 | < 0.001 | 541 | < 0.001 | - | - |
| | | 2GOA11 | - | - | 11,483 | < 0.001 | 12,080 | 0.085 | 3,904 | < 0.001 | 2,065 | < 0.001 | 508 | < 0.001 | - | - |
| | | 3GOA11 | - | - | - | - | 2,424 | < 0.001 | 703 | < 0.001 | 246 | < 0.001 | 46 | < 0.001 | - | - |
| | | 4GOA11 | - | - | - | - | - | - | 3,905 | < 0.001 | 2,081 | < 0.001 | 543 | < 0.001 | - | - |
| | | 1GOA13 | - | - | - | - | - | - | - | - | 2,865 | < 0.001 | 1,028 | < 0.001 | - | - |
| | | 2GOA13 | - | - | - | - | - | - | - | - | - | - | 6,280 | 0.330 | - | - |
| | 1,000-2,000 | 1GOA11 | 40,034 | 0.921 | 89,812 | < 0.001 | 20,985 | < 0.001 | 18,470 | < 0.001 | 7,622 | < 0.001 | 2,323 | < 0.001 | - | - |
| | | 2GOA11 | - | - | 51,210 | < 0.001 | 9,778 | < 0.001 | 7,287 | < 0.001 | 2,930 | < 0.001 | 715 | < 0.001 | - | - |
| | | 3GOA11 | - | - | - | - | 3,235 | < 0.001 | 1,912 | < 0.001 | 936 | < 0.001 | 480 | < 0.001 | - | - |
| | | 4GOA11 | - | - | - | - | - | - | 8,836 | < 0.001 | 3,296 | < 0.001 | 556 | < 0.001 | - | - |
| | | 1GOA13 | - | - | - | - | - | - | - | - | 15,131 | < 0.001 | 5,230 | < 0.001 | - | - |
| | | 2GOA13 | - | - | - | - | - | - | - | - | - | - | 12,062 | < 0.001 | - | - |
| | > 2,000 | 1GOA11 | 2,404 | 0.017 | 6,128 | < 0.001 | ** | ** | 19,178 | < 0.001 | 400 | < 0.001 | 2,518 | < 0.001 | - | - |
| | | 2GOA11 | - | - | 3,002 | < 0.001 | ** | ** | 2,455 | < 0.001 | 2 | < 0.001 | 444 | < 0.001 | - | - |
| | | 3GOA11 | - | - | - | - | ** | ** | 959 | < 0.001 | - | < 0.001 | 178 | < 0.001 | - | - |
| | | 4GOA11 | - | - | - | - | - | - | ** | ** | ** | ** | ** | ** | - | - |
| | | 1GOA13 | - | - | - | - | - | - | - | - | 26,119 | < 0.001 | 158,870 | < 0.001 | - | - |
| | | 2GOA13 | - | - | - | - | - | - | - | - | - | - | 9,542 | < 0.001 | - | - |

**Table 2.7 (cont'd)**

| Species | Isobath (m) | Survey | 2GOA11 | | 3GOA11 | | 4GOA11 | | 1GOA13 | | 2GOA13 | | 3GOA13 | | 4GOA13 | |
|---|---|---|---|---|---|---|---|---|---|---|---|---|---|---|---|---|
| | | | *W* | *p*-value | *W* | *p*-value | *W* | *p*-value | *W* | *p*-value | *W* | *p*-value | *W* | *p*-value | *W* | *p*-value |
| Pollock | < 100 | 1GOA13 | - | - | - | - | - | - | - | - | ** | ** | - | - | - | - |
| | 100-200 | 1GOA13 | - | - | - | - | - | - | - | - | 274,305 | < 0.001 | - | - | - | - |
| | 200-500 | 1GOA13 | - | - | - | - | - | - | - | - | 49,864 | < 0.001 | - | - | - | - |
| | 500-1,000 | 1GOA13 | - | - | - | - | - | - | - | - | 9,103 | < 0.001 | - | - | - | - |
| | 1,000-2,000 | 1GOA13 | - | - | - | - | - | - | - | - | 28,040 | < 0.001 | - | - | - | - |
| | > 2,000 | 1GOA13 | - | - | - | - | - | - | - | - | 37,354 | < 0.001 | - | - | - | - |

**Table 2.8** – Results of Wilcoxon rank-sum tests for differences of median center of mass across surveys within isobaths by forage fish group. Results reflect two-tailed tests at $\alpha = 0.05$ significance level. (Note, ** indicates sample size too small for statistical comparison)

| Survey | Species | Isobath (m) | *N* | Center of Mass (m) | 100-200 m | | 200-500 m | | 500-1,000 m | | 1,000-2,000 m | | > 2,000 m | |
|---|---|---|---|---|---|---|---|---|---|---|---|---|---|---|
| | | | | | *W* | *p*-value | *W* | *p*-value | *W* | *p*-value | *W* | *p*-value | *W* | *p*-value |
| 1GOA11 | Mesopelagics | 200-500 | 122 | 288.6 | - | - | - | - | 8,129 | 0.012 | 28,522 | < 0.001 | 8,201 | < 0.001 |
| | | 500-1,000 | 112 | 263.4 | - | - | - | - | - | - | 23,191 | 0.223 | 6,965 | < 0.001 |
| | | 1,000-2,000 | 385 | 258.9 | - | - | - | - | - | - | - | - | 22,445 | < 0.001 |
| | | > 2,000 | 91 | 251.8 | - | - | - | - | - | - | - | - | - | - |
| 2GOA11 | Capelin | < 100 | 308 | 54.9 | 4,924 | < 0.001 | ** | ** | - | - | - | - | - | - |
| | | 100-200 | 71 | 124.6 | - | - | ** | ** | - | - | - | - | - | - |
| | | 200-500 | 4 | 153.5 | - | - | - | - | - | - | - | - | - | - |
| | Mesopelagics | 200-500 | 89 | 291.3 | - | - | - | - | 5,382 | < 0.001 | 6,571 | < 0.001 | 1,513 | 0.080 |
| | | 500-1,000 | 174 | 311.8 | - | - | - | - | - | - | 18,356 | 0.873 | 4,092 | 0.229 |
| | | 1,000-2,000 | 209 | 312.4 | - | - | - | - | - | - | - | - | 4,756 | 0.393 |
| | | > 2,000 | 42 | 296.6 | - | - | - | - | - | - | - | - | - | - |
| 3GOA11 | Herring | 100-200 | 7 | 111.8 | - | - | ** | ** | ** | ** | ** | ** | - | - |
| | | 200-500 | 41 | 155.7 | - | - | - | - | ** | ** | ** | ** | - | - |
| | | 500-1,000 | 7 | 172.3 | - | - | - | - | - | - | ** | ** | - | - |
| | | 1,000-2,000 | 17 | 168.8 | - | - | - | - | - | - | - | - | - | - |
| | Mesopelagics | 200-500 | 105 | 287.1 | - | - | - | - | 1,126 | < 0.001 | 6,742 | < 0.001 | 2,210 | 0.006 |
| | | 500-1,000 | 80 | 349.1 | - | - | - | - | - | - | 15,273 | 0.001 | 4,299 | < 0.001 |
| | | 1,000-2,000 | 226 | 333.6 | - | - | - | - | - | - | - | - | 13,212 | 0.042 |
| | | > 2,000 | 763 | 313.3 | - | - | - | - | - | - | - | - | - | - |
| 4GOA11 | Capelin | < 100 | 271 | 54.5 | 342 | < 0.001 | - | - | - | - | - | - | - | - |
| | | 100-200 | 89 | 110.2 | - | - | - | - | - | - | - | - | - | - |
| | Mesopelagics | 200-500 | 45 | 292.7 | - | - | - | - | 3,960 | 0.191 | 3,249 | 0.242 | ** | ** |
| | | 500-1,000 | 156 | 294.8 | - | - | - | - | - | - | 9,703 | < 0.001 | ** | ** |
| | | 1,000-2,000 | 163 | 304.0 | - | - | - | - | - | - | - | - | ** | ** |
| | | > 2,000 | 11 | 294.4 | - | - | - | - | - | - | - | - | - | - |

**Table 2.8 (cont'd)-**

| Survey | Species | Isobath (m) | *N* | Center of Mass (m) | 100-200 m | | 200-500 m | | 500-1,000 m | | 1,000-2,000 m | | > 2,000 m | |
|---|---|---|---|---|---|---|---|---|---|---|---|---|---|---|
| | | | | | *W* | *p*-value | *W* | *p*-value | *W* | *p*-value | *W* | *p*-value | *W* | *p*-value |
| 1GOA13 | Mesopelagics | 200-500 | 107 | 238.1 | - | - | - | - | 992 | < 0.001 | 7,699 | < 0.001 | 23,848 | < 0.001 |
| | | 500-1,000 | 90 | 301.6 | - | - | - | - | - | - | 17,486 | < 0.001 | 83,519 | < 0.001 |
| | | 1,000-2,000 | 270 | 274.0 | - | - | - | - | - | - | - | - | 153,748 | < 0.001 |
| | | > 2,000 | 1,485 | 288.0 | - | - | - | - | - | - | - | - | - | - |
| | Pollock | < 100 | 4 | 37.3 | ** | ** | ** | ** | ** | ** | ** | ** | ** | ** |
| | | 100-200 | 332 | 58.6 | - | - | 15,267 | < 0.001 | 8,878 | < 0.001 | 31,157 | 0.006 | 175,940 | 0.280 |
| | | 200-500 | 153 | 73.2 | - | - | - | - | 5,700 | 0.249 | 19,118 | 0.016 | 106,971 | < 0.001 |
| | | 500-1,000 | 82 | 81.7 | - | - | - | - | - | - | 10,571 | 0.015 | 57,314 | < 0.001 |
| | | 1,000-2,000 | 218 | 65.4 | - | - | - | - | - | - | - | - | 130,207 | 0.053 |
| | | > 2,000 | 1,103 | 58.8 | - | - | - | - | - | - | - | - | - | - |
| 2GOA13 | Capelin | < 100 | 389 | 54.6 | 612 | < 0.001 | 9 | < 0.001 | - | - | - | - | - | - |
| | | 100-200 | 173 | 115.1 | - | - | 1,887 | < 0.001 | - | - | - | - | - | - |
| | | 200-500 | 107 | 166.2 | - | - | - | - | - | - | - | - | - | - |
| | Mesopelagics | 200-500 | 76 | 260.4 | - | - | - | - | 7,461 | 0.052 | 7,505 | 0.267 | 941 | < 0.001 |
| | | 500-1,000 | 170 | 250.9 | - | - | - | - | - | - | 14,161 | < 0.001 | 1,792 | < 0.001 |
| | | 1,000-2,000 | 216 | 265.6 | - | - | - | - | - | - | - | - | 3,084 | < 0.001 |
| | | > 2,000 | 54 | 281.7 | - | - | - | - | - | - | - | - | - | - |
| | Pollock | < 100 | 860 | 30.9 | 210,693 | < 0.001 | 151,055 | 0.298 | 70,768 | < 0.001 | 55,315 | < 0.001 | 12,660 | < 0.001 |
| | | 100-200 | 1,016 | 44.3 | - | - | 251,169 | < 0.001 | 97,301 | < 0.001 | 78,986 | 0.747 | 19,283 | 0.014 |
| | | 200-500 | 365 | 32.7 | - | - | - | - | 29,184 | < 0.001 | 23,966 | 0.002 | 5,582 | < 0.001 |
| | | 500-1,000 | 132 | 20.3 | - | - | - | - | - | - | 7,940 | < 0.001 | 1,818 | < 0.001 |
| | | 1,000-2,000 | 158 | 44.8 | - | - | - | - | - | - | - | - | 3,119 | 0.063 |
| | | > 2,000 | 48 | 68.4 | - | - | - | - | - | - | - | - | - | - |
| 3GOA13 | Herring | 100-200 | 13 | 109.4 | - | - | - | - | - | - | - | - | - | - |
| | Mesopelagics | 200-500 | 105 | 257.9 | - | - | - | - | 808 | < 0.001 | 345 | < 0.001 | 2,165 | < 0.001 |
| | | 500-1,000 | 80 | 375.3 | - | - | - | - | - | - | 4,485 | < 0.001 | 21,606 | < 0.001 |
| | | 1,000-2,000 | 226 | 398.0 | - | - | - | - | - | - | - | - | 103,050 | < 0.001 |
| | | > 2,000 | 763 | 387.4 | - | - | - | - | - | - | - | - | - | - |
| 4GOA13 | Capelin | < 100 | 68 | 18.1 | ** | ** | - | - | - | - | - | - | - | - |
| | | 100-200 | 2 | 72.8 | - | - | - | - | - | - | - | - | - | - |

**Table 2.9** – Results of Wilcoxon rank-sum tests for differences of median center of mass across surveys within isobaths by forage fish group. Results reflect two-tailed tests at $\alpha = 0.05$ significance level. (Note, ** indicates sample size too small for statistical comparison)

| Species | Isobath (m) | Survey | 2GOA11 | | 3GOA11 | | 4GOA11 | | 1GOA13 | | 2GOA13 | | 3GOA13 | | 4GOA13 | |
|---|---|---|---|---|---|---|---|---|---|---|---|---|---|---|---|---|
| | | | *W* | *p*-value | *W* | *p*-value | *W* | *p*-value | *W* | *p*-value | *W* | *p*-value | *W* | *p*-value | *W* | *p*-value |
| Capelin | < 100 | 2GOA11 | - | - | - | - | 40,602 | 0.573 | - | - | 62,294 | 0.366 | - | - | 13,791 | < 0.001 |
| | | 4GOA11 | - | - | - | - | - | - | - | - | 56,328 | 0.133 | - | - | 11,983 | < 0.001 |
| | | 2GOA13 | - | - | - | - | - | - | - | - | - | - | - | - | 17,330 | < 0.001 |
| | 100-200 | 2GOA11 | - | - | - | - | 3,442 | 0.333 | - | - | 5,666 | 0.343 | - | - | ** | ** |
| | | 4GOA11 | - | - | - | - | - | - | - | - | 5,979 | 0.003 | - | - | ** | ** |
| | | 2GOA13 | - | - | - | - | - | - | - | - | - | - | - | - | ** | ** |
| | 200-500 | 2GOA11 | - | - | - | - | - | - | - | - | ** | ** | - | - | - | - |
| Herring | 200-500 | 3GOA11 | - | - | - | - | - | - | - | - | - | - | ** | ** | - | - |
| Mesopelagics | 200-500 | 1GOA11 | 4,230 | 0.006 | 4,256 | 0.209 | 1,646 | < 0.001 | 9,935 | < 0.001 | 5,499 | 0.028 | 7,265 | 0.081 | - | - |
| | | 2GOA11 | - | - | 3,599 | 0.683 | 1,742 | 0.221 | 7,260 | < 0.001 | 4,327 | 0.002 | 5,723 | 0.007 | - | - |
| | | 3GOA11 | - | - | - | - | 1,419 | 0.078 | 5,791 | < 0.001 | 3,390 | 0.124 | 4,460 | 0.304 | - | - |
| | | 4GOA11 | - | - | - | - | - | - | 4,138 | < 0.001 | 2,560 | < 0.001 | 3,375 | < 0.001 | - | - |
| | | 1GOA13 | - | - | - | - | - | - | - | - | 2,356 | < 0.001 | 3,405 | < 0.001 | - | - |
| | | 2GOA13 | - | - | - | - | - | - | - | - | - | - | 4,006 | 0.964 | - | - |
| | 500-1,000 | 1GOA11 | 3,263 | < 0.001 | 961 | < 0.001 | 4,854 | < 0.001 | 2,087 | < 0.001 | 10,863 | 0.045 | 749 | < 0.001 | - | - |
| | | 2GOA11 | - | - | 3,712 | < 0.001 | 17,908 | < 0.001 | 8,108 | 0.637 | 24,624 | < 0.001 | 1,828 | < 0.001 | - | - |
| | | 3GOA11 | - | - | - | - | 10,774 | < 0.001 | 5,368 | < 0.001 | 12,332 | < 0.001 | 1,733 | < 0.001 | - | - |
| | | 4GOA11 | - | - | - | - | - | - | 5,407 | 0.003 | 19,608 | < 0.001 | 1,295 | < 0.001 | - | - |
| | | 1GOA13 | - | - | - | - | - | - | - | - | 12,458 | < 0.001 | 1,044 | < 0.001 | - | - |
| | | 2GOA13 | - | - | - | - | - | - | - | - | - | - | 1,122 | < 0.001 | - | - |
| | 1,000-2,000 | 1GOA11 | 12,811 | < 0.001 | 2,089 | < 0.001 | 8,965 | < 0.001 | 42,532 | < 0.001 | 35,142 | 0.002 | 323 | < 0.001 | - | - |
| | | 2GOA11 | - | - | 4,615 | < 0.001 | 9,588 | 0.013 | 3,138 | < 0.001 | 37,342 | < 0.001 | 1,159 | < 0.001 | - | - |
| | | 3GOA11 | - | - | - | - | 3,063 | < 0.001 | 2,995 | < 0.001 | 51,987 | < 0.001 | 5,242 | < 0.001 | - | - |
| | | 4GOA11 | - | - | - | - | - | - | 3,580 | < 0.001 | 30,646 | < 0.001 | 352 | < 0.001 | - | - |
| | | 1GOA13 | - | - | - | - | - | - | - | - | 31,652 | 0.105 | 400 | < 0.001 | - | - |
| | | 2GOA13 | - | - | - | - | - | - | - | - | - | - | 107 | < 0.001 | - | - |
| | > 2,000 | 1GOA11 | 203 | < 0.001 | 1,447 | < 0.001 | ** | ** | 1,065 | < 0.001 | 567 | < 0.001 | 136 | < 0.001 | - | - |
| | | 2GOA11 | - | - | 1,381 | 0.228 | ** | ** | 0,946 | < 0.001 | 1,612 | < 0.001 | 905 | < 0.001 | - | - |
| | | 3GOA11 | - | - | - | - | ** | ** | 72,311 | < 0.001 | 2,646 | 0.005 | 5,285 | < 0.001 | - | - |
| | | 4GOA11 | - | - | - | - | - | - | ** | ** | ** | ** | ** | ** | - | - |
| | | 1GOA13 | - | - | - | - | - | - | - | - | 41,132 | 0.747 | 14,340 | < 0.001 | - | - |
| | | 2GOA13 | - | - | - | - | - | - | - | - | - | - | 316 | < 0.001 | - | - |

**Table 2.9 (cont'd)**

| Species | Isobath (m) | Survey | 2GOA11 | | 3GOA11 | | 4GOA11 | | 1GOA13 | | 2GOA13 | | 3GOA13 | | 4GOA13 | |
|---|---|---|---|---|---|---|---|---|---|---|---|---|---|---|---|---|
| | | | *W* | *p*-value | *W* | *p*-value | *W* | *p*-value | *W* | *p*-value | *W* | *p*-value | *W* | *p*-value | *W* | *p*-value |
| Pollock | < 100 | 1GOA13 | - | - | - | - | - | - | - | - | ** | ** | - | - | - | - |
| | 100-200 | 1GOA13 | - | - | - | - | - | - | - | - | 241,847 | < 0.001 | - | - | - | - |
| | 200-500 | 1GOA13 | - | - | - | - | - | - | - | - | 49,997 | < 0.001 | - | - | - | - |
| | 500-1,000 | 1GOA13 | - | - | - | - | - | - | - | - | 8,996 | < 0.001 | - | - | - | - |
| | 1,000-2,000 | 1GOA13 | - | - | - | - | - | - | - | - | 21,051 | < 0.001 | - | - | - | - |
| | > 2,000 | 1GOA13 | - | - | - | - | - | - | - | - | 25,556 | 0.685 | - | - | - | - |

## 2.6 FIGURES

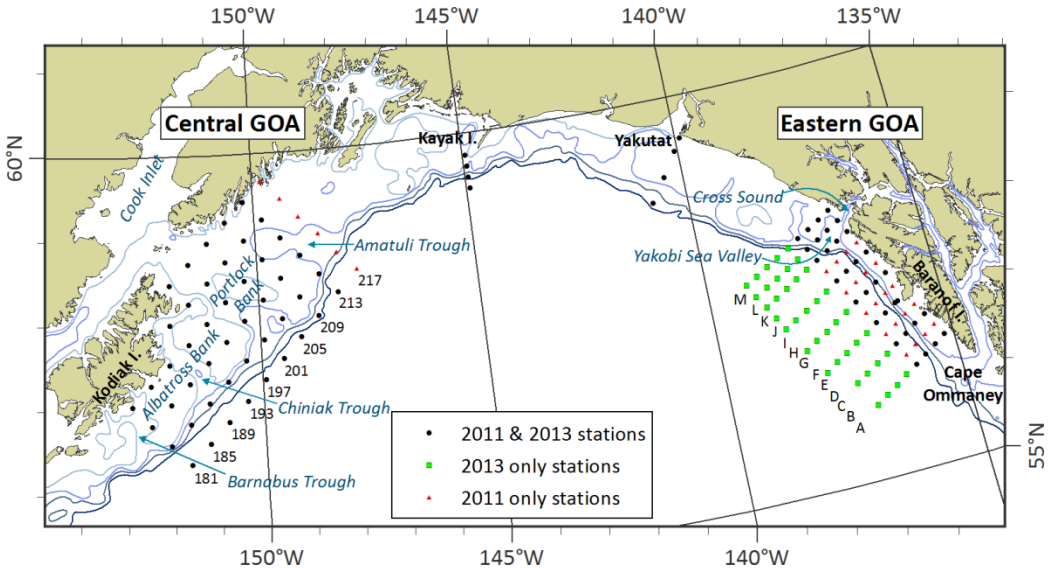


**Figure 2.1** – Survey coverage map for 2011 & 2013. Individual transects are labeled in the CGOA (181 to 217) and EGOA (A to M). Key geographic features are labeled in black, bathymetric features labeled in blue.

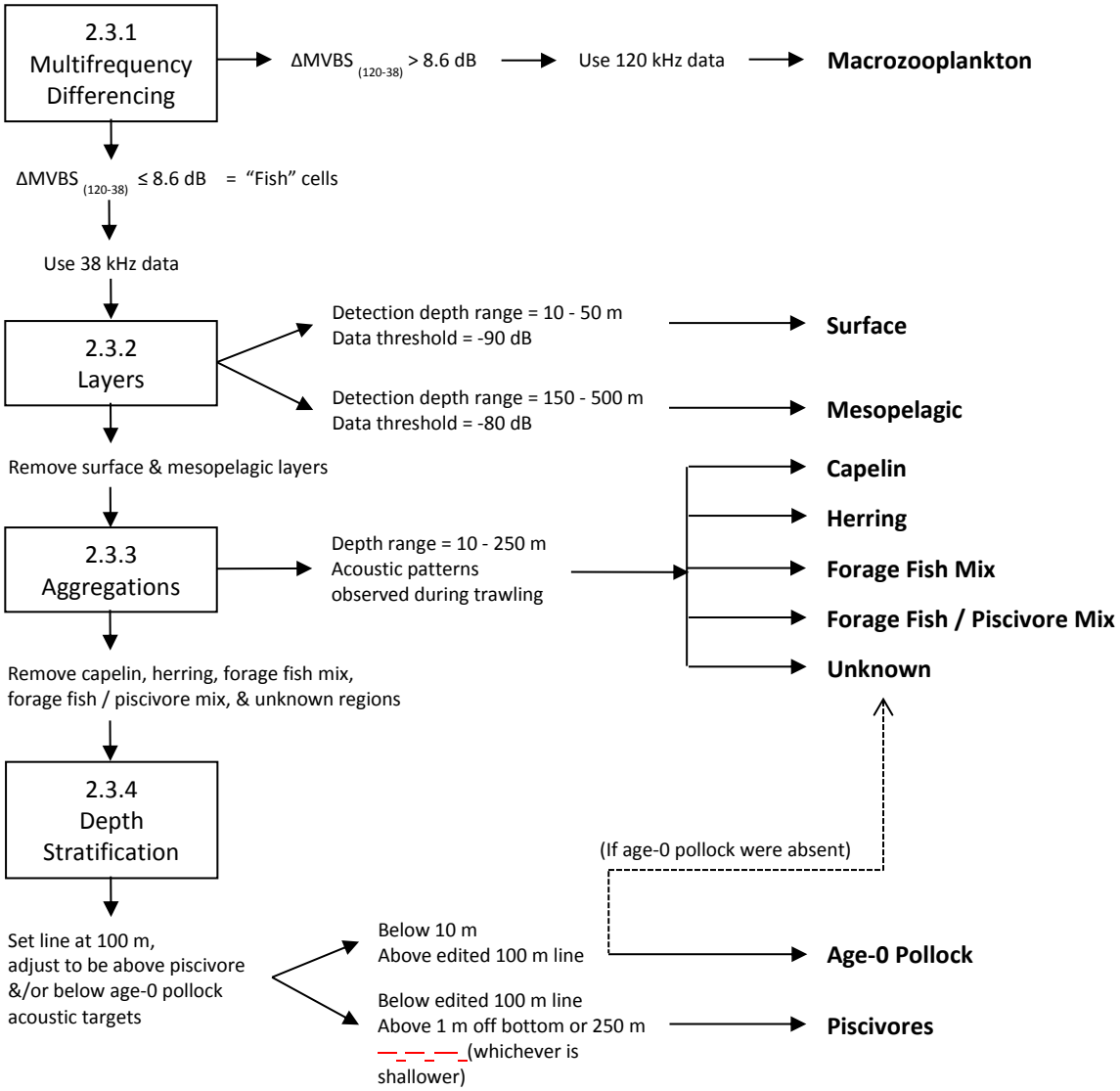


**Figure 2.2** – Classification procedure for acoustic backscatter data. Key classification steps are indicated in boxes and numbered according to Methods subheadings. Backscatter categories are in bold. Note the depth range minimum of 10 m refers to the surface exclusion line on the *Northwest Explorer*. A minimum depth range of 15 m was used for data collected on the *Oscar Dyson*.

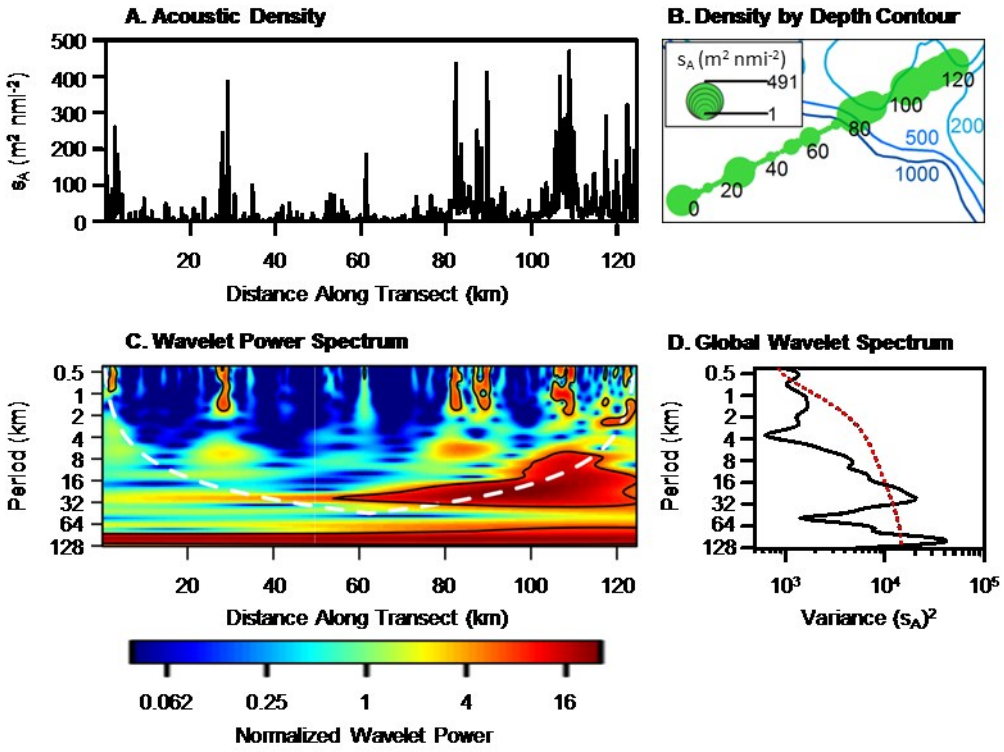


**Figure 2.3** – An example of a local decomposition of estimates of acoustic density ($s_A$, $m^2$ $nmi^{-2}$) along a single transect to identify significant scales of variability using wavelet analysis. A) Age-0 pollock densities in 200 m horizontal bins along transect L in the EGOA during the summer 2013 survey. B) Density measurements from plot (A) projected over bottom depth contours. Numbers 0 to 120 (black) coincide with distance along transect in plots (A) & (C), while numbers 200 to 1000 (shades of blue) indicate isobaths (m). C) The wavelet power spectrum for plot (A) normalized by the global wavelet variance. Black contour lines indicate the 95% confidence level using a red-noise (*i.e.* autoregressive lag-1) background spectrum. White dashed line indicates cone of influence boundary. (D) Global wavelet power spectrum (black line) and 95% confidence level (red dashed line) for plot (C).

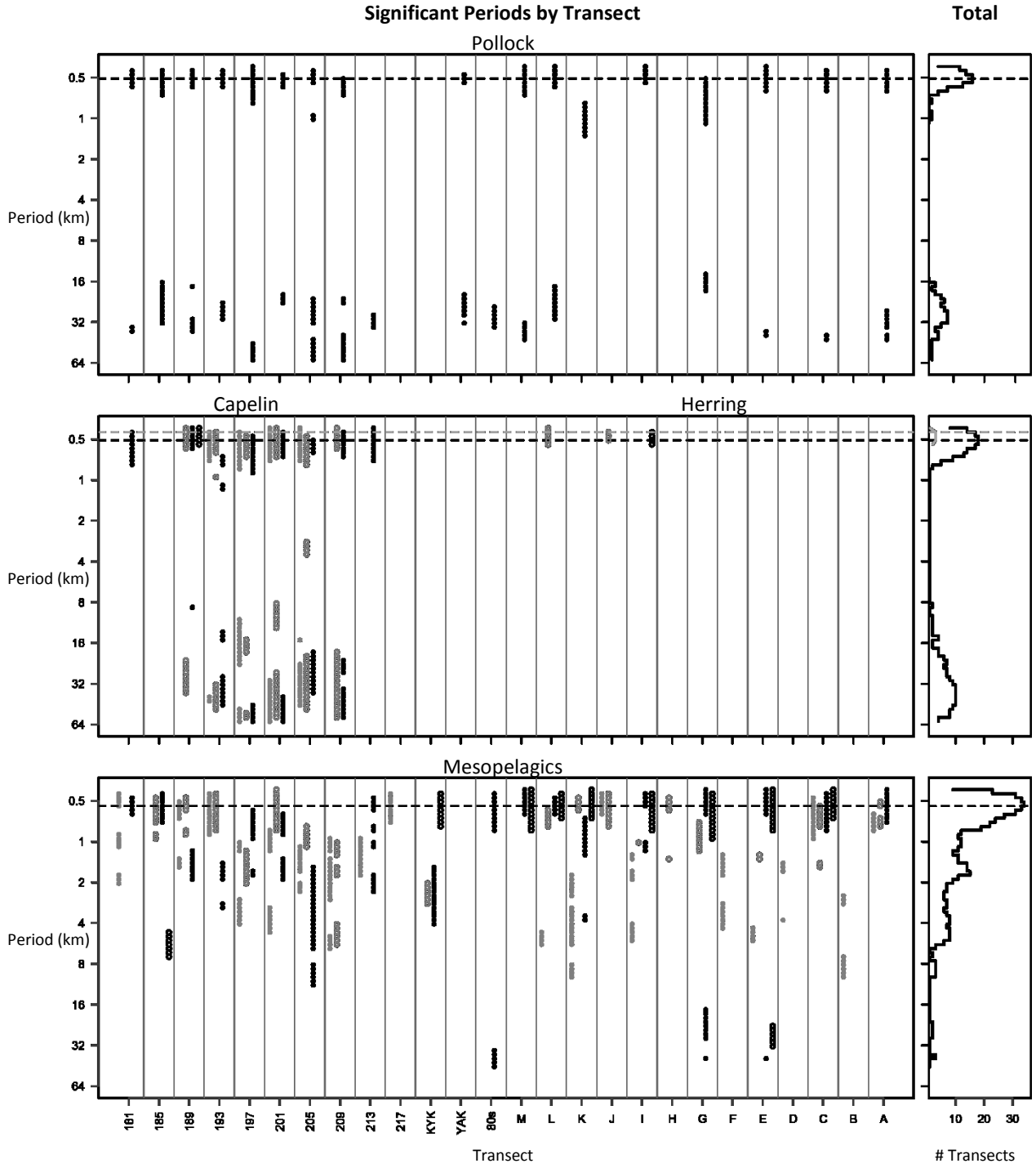


**Figure 2.4** – Summary of significant periods for each forage fish group by transect identified by wavelet analysis. Note the y-axis is an octave scale. Periods in which the global wavelet spectrum variance peak was greater than the 95% confidence level are considered significant spatial scales of variability. For each transect, significant periods are indicated by year (gray

circles = 2011, black circles = 2013) and season (closed circles = summer, open circles = fall) for each forage fish group. Cumulative frequency distributions (right panel) indicate the peak period (dashed line) that was most prevalent across all surveys for each forage fish group (herring values are indicated by gray lines).

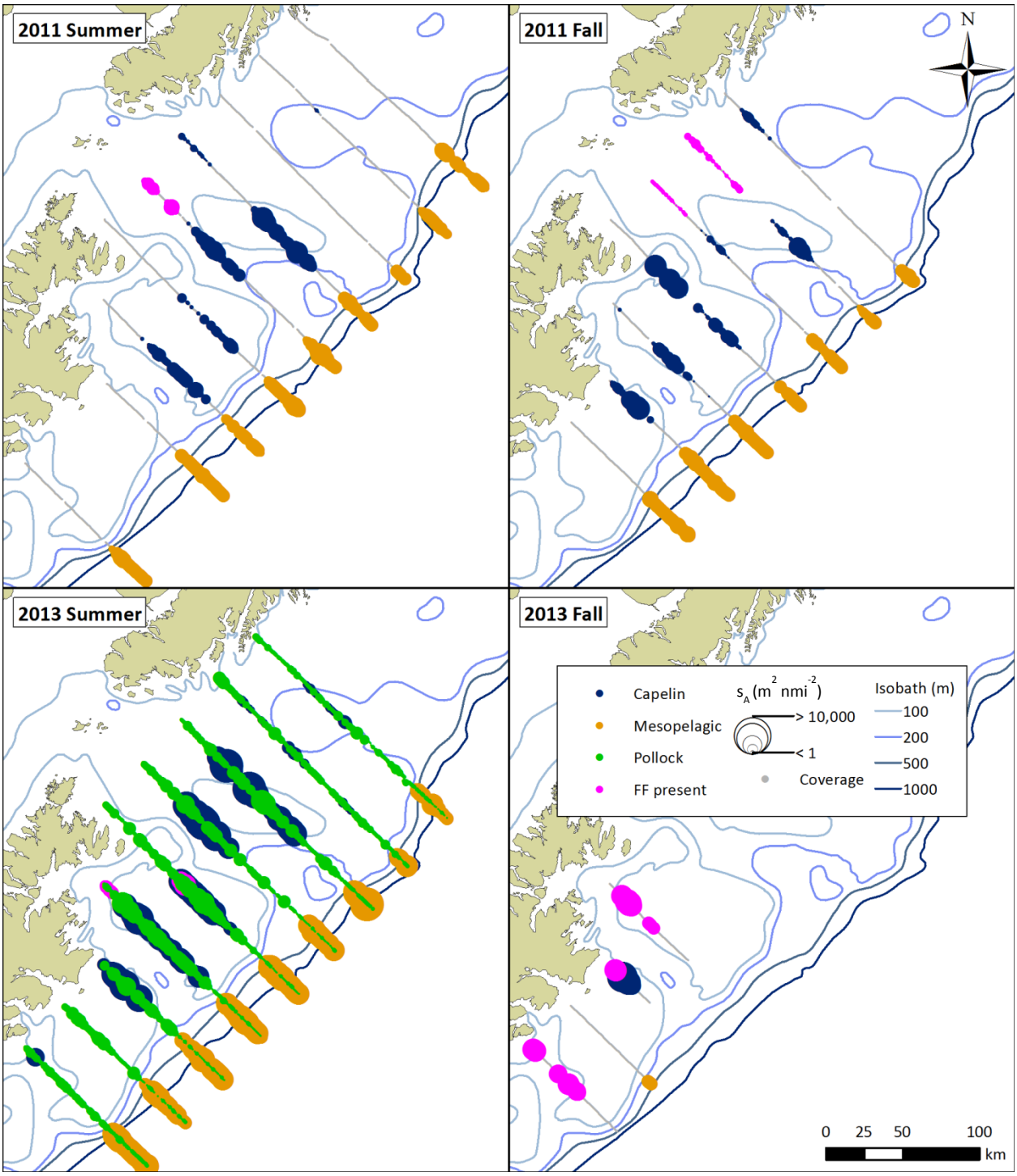


**Figure 2.5** - Distribution of forage fish in the CGOA by year and season. Acoustic density estimates, $s_A$ ($m^2$ $nmi^{-2}$), are in 500 m horizontal bins. "FF present" = forage fish mix and forage fish / piscivores mix backscatter categories.

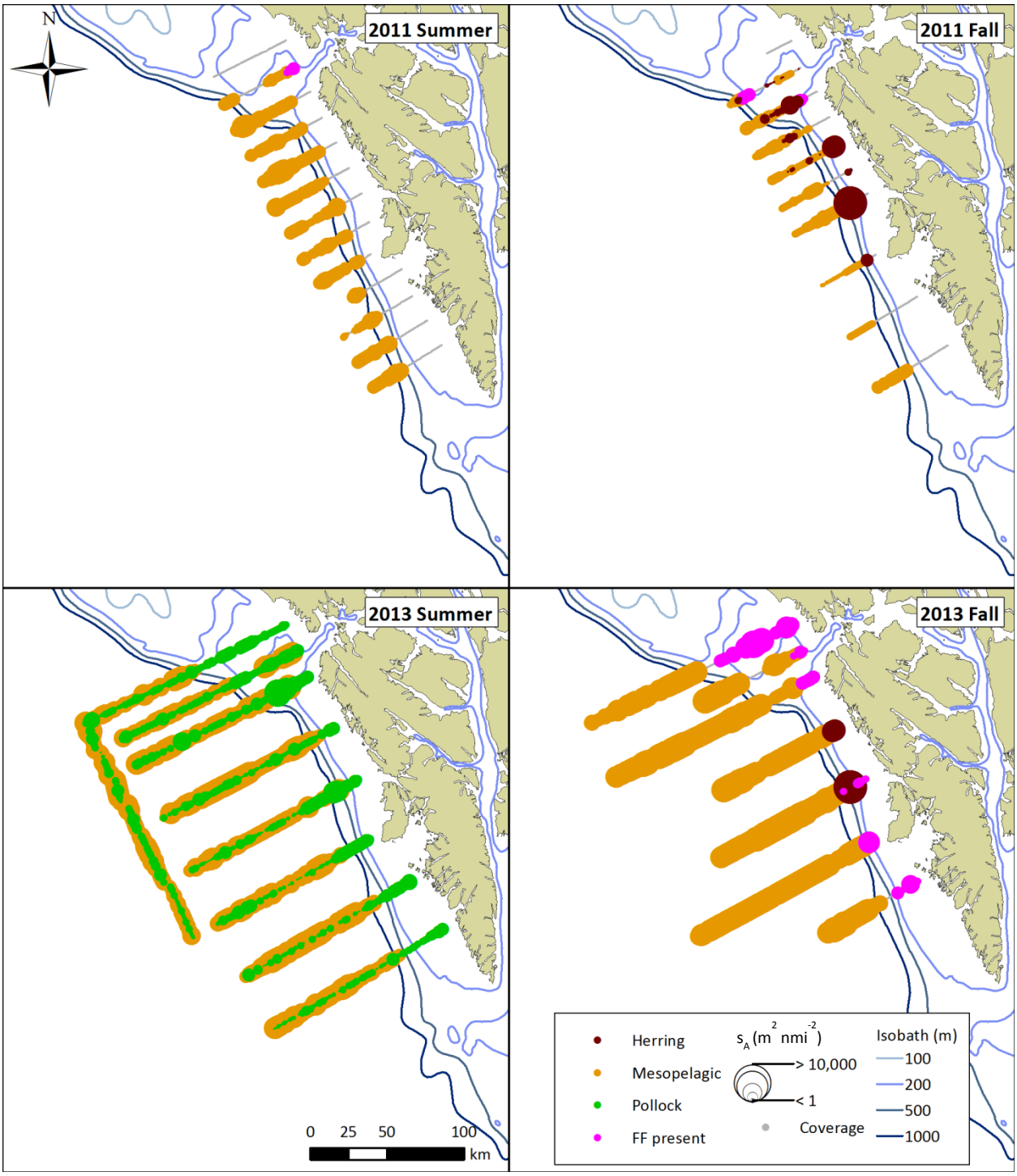


**Figure 2.6** - Distribution of forage fish in the EGOA by year and season. Acoustic density estimates, $s_A$ ($m^2$ $nmi^{-2}$), are in 500 m horizontal bins. "FF present" = forage fish mix and forage fish / piscivores mix backscatter categories.

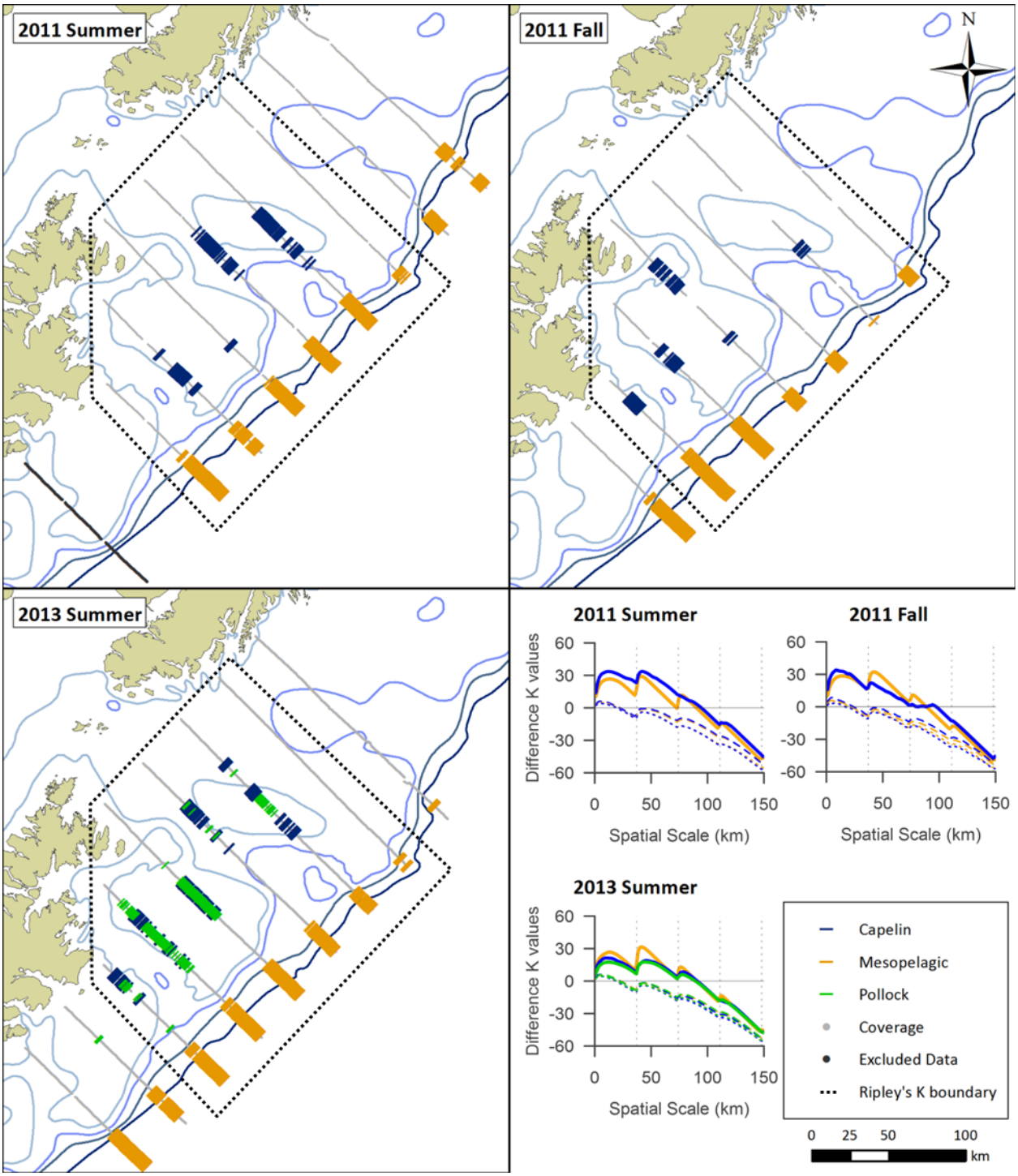


**Figure 2.7** – Distribution of significant aggregations for each forage fish category by year and season in the CGOA. The dotted line indicates the Ripley's K analysis domain boundary on each map, while black dots indicate transects excluded from the Local Moran's I analysis. A measure

of aggregation for each species group is shown in the inserted line graphs, in which the difference in observed versus expected Ripley's K values are plotted as a function of spatial scale across each domain. Note, vertical dotted lines indicate 37.04 km (20 nmi) spacing between transects. Positive values above the dashed line indicate the forage fish species/group distribution is more spatially aggregated at a 95% significance level than a random distribution at that scale. Negative values below the dotted line indicate the forage fish species/group is significantly dispersed at a 95% significance level.

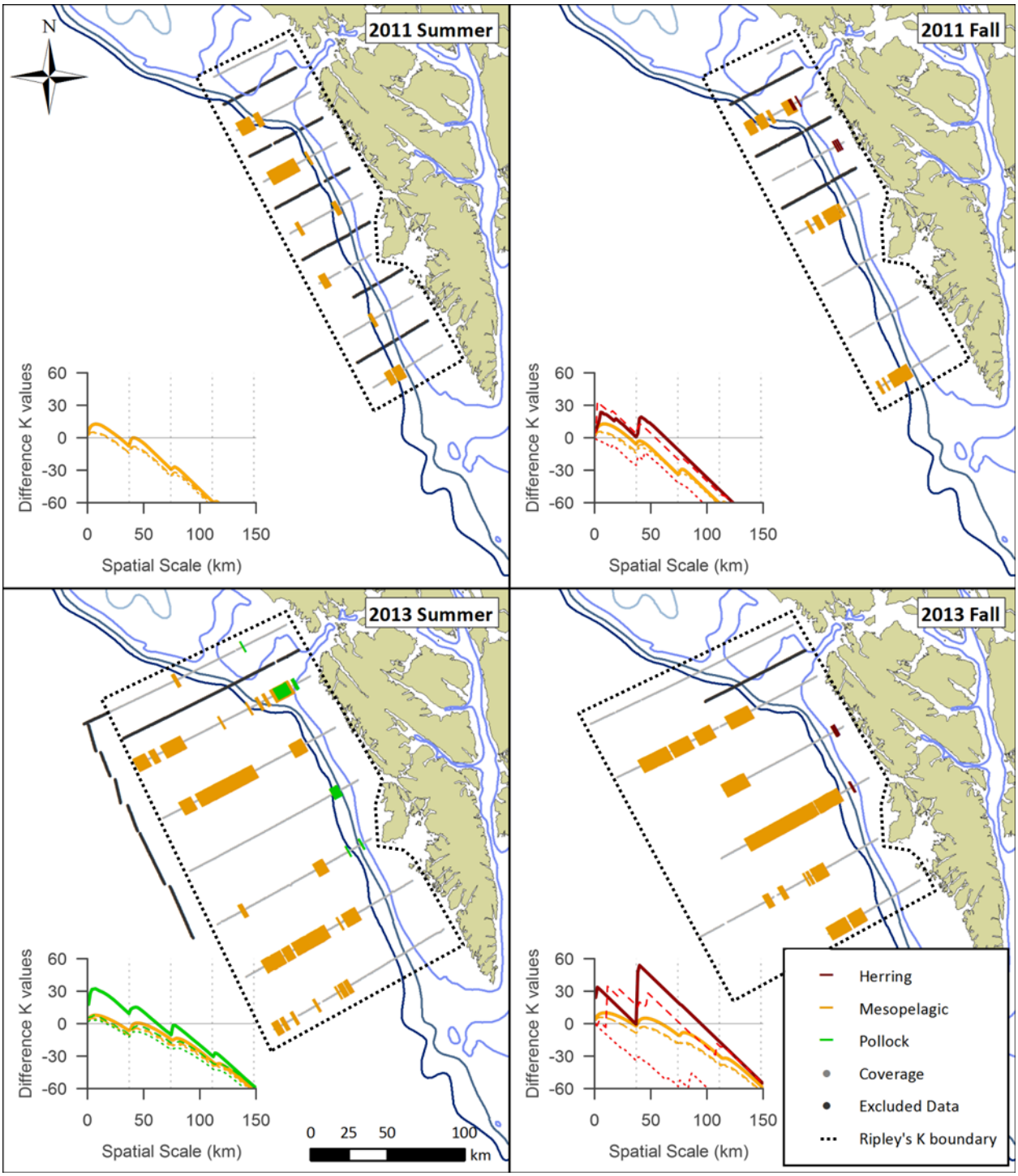


**Figure 2.8** – Distribution of significant aggregations for each forage fish category by year and season in the EGOA. The dotted line indicates the Ripley's K analysis domain boundary on each map, while black dots indicate transects excluded from the Local Moran's I analysis. A measure

of aggregation for each species group is shown in the inserted line graphs, in which the difference in observed versus expected Ripley's K values are plotted as a function of spatial scale across each domain. Note, vertical dotted lines indicate 37.04 km (20 nmi) spacing between transects. Positive values above the dashed line indicate the forage fish species/group distribution is more spatially aggregated at a 95% significance level than a random distribution at that scale. Negative values below the dotted line indicate the forage fish species/group is significantly dispersed at a 95% significance level.

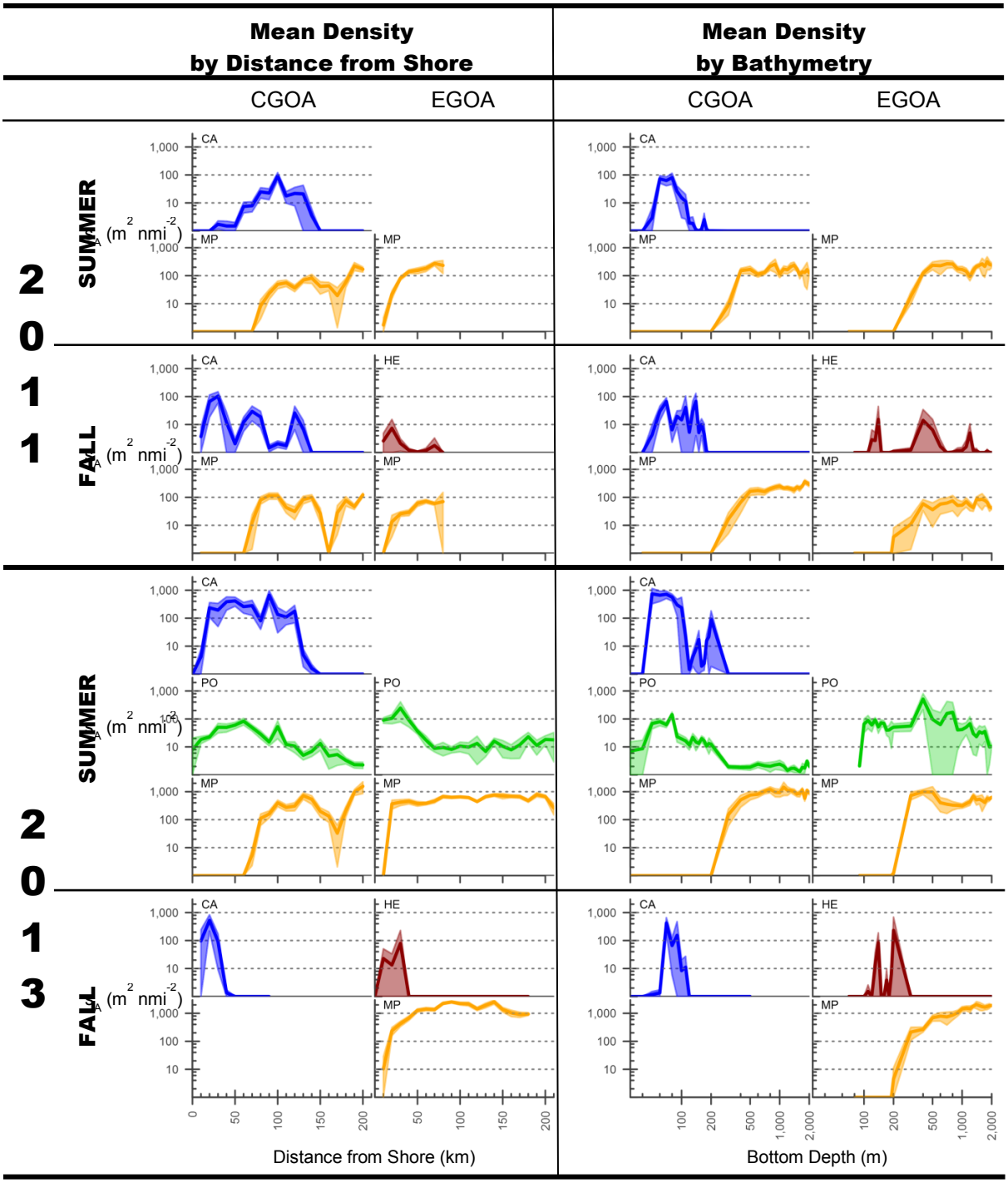


**Figure 2.9** –Forage fish horizontal distribution patterns by year, season, and region for each forage fish category. On the left side, mean acoustic density, $s_A$ ($m^2$ $nmi^{-2}$), is shown by distance from shore (km). Plots on the right side show mean density by bottom depth (m). Shaded areas

indicate 95% confidence interval. CA = capelin (blue); HE = herring (red); MP = macrozooplankton (orange); PO = age-0 pollock (green).

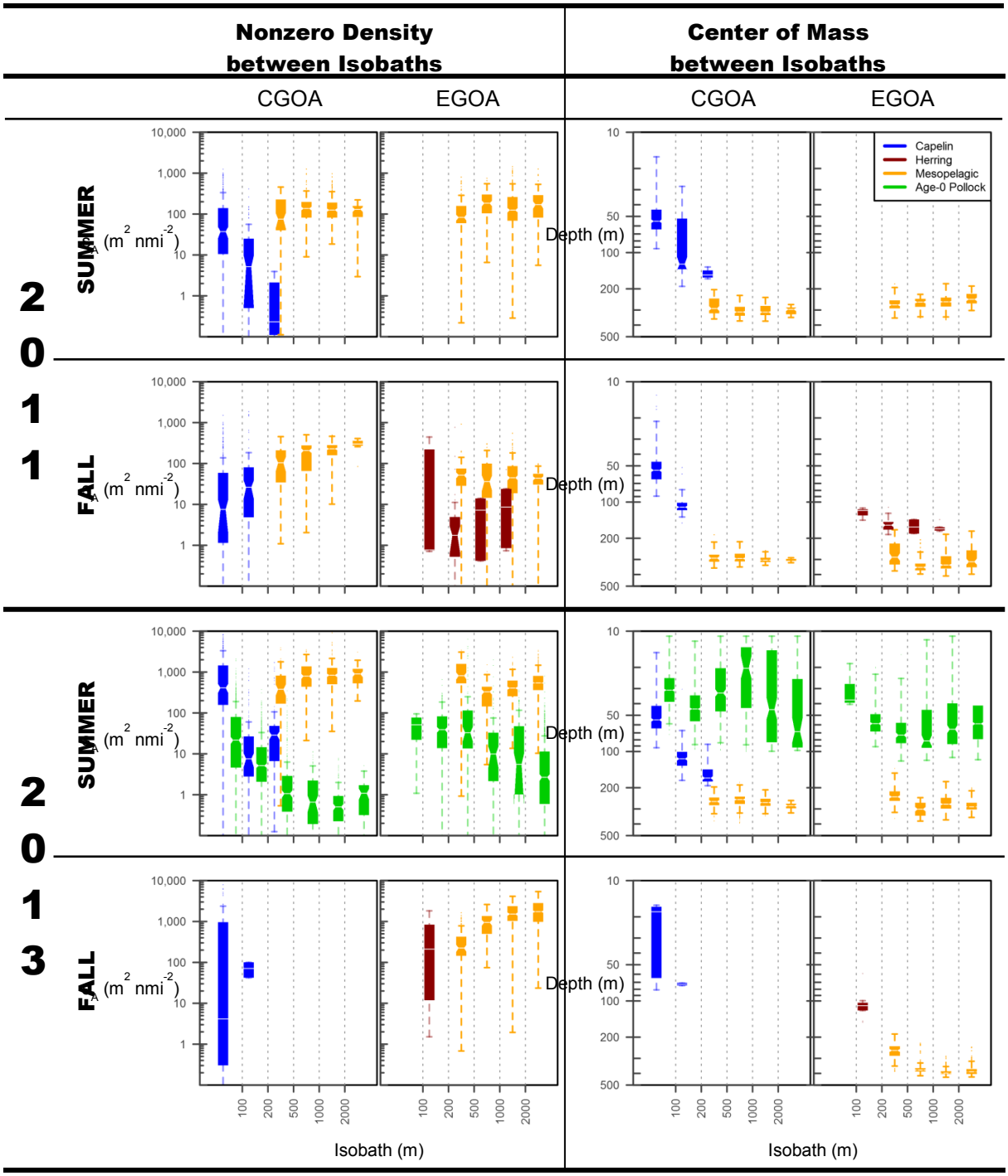


**Figure 2.10** – Distributions for each forage fish category between isobaths by year, season, and region. Box plots on left side show horizontal distributions of acoustic density, $s_A$ ($m^2$ $nmi^{-2}$), when fish were present (*i.e.* nonzero density) between isobaths for backscatter assigned to each

forage fish category. Box plots on the right side show vertical distributions (*i.e.* center of mass, m) between isobaths for each forage fish category. Box plot notches that do not overlap indicate strong evidence of differences between medians at the 95% confidence level. Box plots are not notched if $n < 30$ or during the CGOA fall 2013 survey due to limited survey coverage of the study area.

# Chapter 3. INFLUENCE OF ENVIRONMENTAL FACTORS ON CAPELIN OCCURRENCE AND DENSITY IN THE CENTRAL GULF OF ALASKA

## 3.1 INTRODUCTION

In northern, high-latitude ecosystems, capelin (*Mallotus villosus*) are an important mid-trophic link within marine food webs. A mobile and gregarious small pelagic species, capelin are spatially and temporally heterogeneous (Gjøsæter, 1998; Rose, 2005; Vilhjálmsson, 2002), and function as a predator of zooplankton and prey for piscivorous fish, seabirds, and marine mammals. As a result, fluctuations in capelin distributions and abundances modulate the transfer of energy from lower to upper trophic levels in marine food webs throughout boreal waters (Gjøsæter et al., 2009; Hjermann et al., 2010; Vilhjálmsson, 2002).

Understanding how capelin biology, population dynamics, and distributions are influenced by environmental processes has been a research focus spanning decades in the Atlantic. Fluctuations in capelin distributions and abundances are well documented in the Barents Sea, Icelandic, and Northwest Atlantic populations (Carscadden et al., 2013b, 2013a; Gjøsæter, 1998; Vilhjálmsson, 2002), with fisheries and oceanographic data to support commercial capelin fisheries (e.g. Carscadden et al., 2013a; Gjøsæter, 1998). These data have facilitated investigations on the potential role of directed fisheries on population crashes, and how environmental processes influence capelin population dynamics and distributions during different life stages (e.g. Carscadden et al., 2013b; Frank et al., 1996; Ingvaldsen and Gjøsæter, 2013; Olafsdottir and Rose, 2012). Studies on Atlantic capelin populations also highlight how the strength and direction of capelin-predator relationships, including Atlantic cod (*Gadus*

*morhua*) (Horne and Schneider, 1994; Piatt, 1990; Rose and Leggett, 1990) and seabirds (Fauchald, 2009; Fauchald and Erikstad, 2002), vary as a function of scale.

Compared to Atlantic populations, information is limited describing changes in Pacific capelin distributions and abundances. This lack of information is attributed to the absence of a directed capelin fishery, and existing abundance surveys for demersal fish species are poorly suited for detecting changes in capelin and other small pelagic species' distributions (Ormseth, 2012). Despite limited monitoring, interdecadal abundance fluctuations have been observed in the GOA (Anderson and Piatt, 1999; Ormseth, 2012), and are believed to have impacted predators. After the late 1970s regime shift (Francis et al., 1998), declines in production and abundances of piscivorous seabirds and marine mammals were attributed to reductions of capelin and other forage species in predator diets (Anderson and Piatt, 1999; Merrick et al., 1997; Piatt and Anderson, 1996). Recognition that changes in the availability and species composition of prey may affect managed predators (Ormseth, 2012; Springer and Speckman, 1997) prompted investigations of how physical and biological processes influence the distribution and abundance of capelin and other small pelagic species in the Northeast Pacific (e.g. Arimitsu et al., 2008; Hollowed et al., 2012; Parker-Stetter et al., 2016).

Recent interdisciplinary research efforts in Alaska have attributed a wide range of environmental factors to changes in offshore and coastal distributions of capelin. In the Gulf of Alaska (GOA), changes in capelin distributions over the continental shelf east of Kodiak Island have been attributed to oceanographic conditions and the location of water masses (Hollowed et al., 2007; Logerwell et al., 2007), composition and distribution of zooplankton prey, and potential competition with juvenile walleye pollock (*Gadus chalcogrammus*, hereafter pollock) (Logerwell et al., 2007, 2010; Wilson et al., 2006). GOA-based analyses have also shown

differences in capelin diets within and among years that were associated with the body length of capelin and type of water mass (Logerwell et al., 2010; Wilson et al., 2006). Within Glacier Bay in southeast Alaska, capelin have been associated with areas near tidewater glaciers (Arimitsu et al., 2008). In the eastern Bering Sea (EBS), the relative abundance of capelin in surface waters (upper 30 m) was significantly higher during years with colder water (2006-2011), during which distributions were concentrated in the northeastern Bering Sea and extended south compared to observations from warm years (2003-2005) (Andrews et al., 2015). Capelin located in surface waters during cold years were predicted in relatively cooler, less saline waters above the pycnocline where densities would be highest over bottom depths between 60 to 80 m (Parker-Stetter et al., 2016).

This study was conducted to identify physical and biological factors that influence distributions of capelin in the GOA over the shelf east of Kodiak Island. This investigation was facilitated by a fisheries-oceanographic survey that measured distributions of pelagic fishes and macrozooplankton. As part of the Gulf of Alaska Integrated Ecosystem Research Program (GOAIERP, http://www.nprb.org/gulf-of-alaska-project), acoustic-trawl surveys were conducted in summer and fall 2011 and summer 2013. GOAIERP was an interdisciplinary effort to investigate how recruitment dynamics of five key groundfish species are influenced by physical and biological processes during their first year of life (Moss et al., 2016b). Recognizing that the relative influence of explanatory factors on distributions of capelin may be scale-dependent (Schneider, 1994), I analyzed data at station (37 km) and transect (0.5 km) spatial resolutions. My specific objectives were to: 1) quantify the influence of physical and biological factors on occurrence and density of capelin; and 2) compare the relative importance of factors that explain variance in distributions of capelin at two spatial resolutions.

## 3.2 METHODS

### 3.2.1 Study area and survey design

Data were collected in the central GOA (CGOA) during GOAIERP acoustic-trawl surveys on the F/V *Northwest Explorer* in summer (5-21 August) and fall (25 September to 8 October) 2011, and summer (6-21 August) 2013 (see Chapter 2, Table 2.1 for details). The study area extended from the southeast side of Kodiak Island to the mouth of Amatuli Trough (Fig. 3.1). Acoustic measurements were taken along parallel transects orthogonal from the coast (< 50 m bottom depth) to basin waters beyond the 2000 m depth contour. Midwater trawls were conducted opportunistically along transects to sample observed acoustic targets. Surface trawl and oceanographic measurements were sampled at fixed stations spaced equidistant at 37 km (20 nmi) along 10 transects that ranged from 111 to 185 km in length (4 to 6 stations per transect) depending on the width of the shelf. All sampling was conducted during daytime hours (i.e. 30 minutes after sunrise to 30 minutes before sunset).

### 3.2.2 Data collection and processing

*3.2.2.1. Acoustic and trawl data*

Acoustic data were collected using a Simrad ES60 echosounder (Kongsberg Maritime) with hull-mounted, split-beam transducers operating at 38 and 120 (added in 2013) kHz. Prior to the start of summer surveys, both frequencies were calibrated using a 38.1 mm tungsten carbide sphere following Foote et al. (1987). Fish were sampled at surface (0-30 m) and midwater depths (30-250 m) using a 198 m midwater rope trawl (Cantrawl model 400, Cantrawl Nets Ltd) with a 1.2 mm mesh cod-end liner. Trawl samples were used to validate the species and length compositions of observed acoustic patterns to partition backscatter (*i.e.* reflected sound) to

single- or mixed-species classification categories: capelin, piscivorous fish (groundfish species > 158 mm, *e.g.* age-1+ pollock), age-0 pollock, macrozooplankton (*e.g.* euphausiids and amphipods), capelin/age-0 pollock mix (hereafter forage fish mix), capelin/age-0 pollock/piscivores mix (hereafter forage fish/piscivores mix), and unknown (see Chapter 2, section 2.2.3. for details). Backscatter observed during trawls in which one classification category accounted for at least 90% of the catch (by number) was treated as a characteristic echogram pattern for subsequent visual classification of that category. The forage fish mix and forage fish/piscivores mix categories were comprised of backscatter that could not be assigned to capelin, age-0 pollock, or piscivorous fish categories; this occurred when trawl samples indicated that echogram patterns were comprised of multiple forage fish species, or when echogram patterns of two or more categories overlapped. Backscatter was only assigned to one classification category, and patterns that were not sampled by trawls were classified as unknown and excluded from analysis. Categorized backscatter for capelin and piscivorous fish were available for all CGOA surveys. Backscatter data for age-0 pollock and macrozooplankton were only available in summer 2013 due to the rare occurrence of age-0 pollock and lack of 120 kHz data needed to acoustically discriminate macrozooplankton from fish in 2011 (see Chapter 2, section 2.2.3. for details). Along-transect estimates of acoustic density (nautical area scattering coefficient (NASC), $s_A$, $m^2$ $nmi^{-2}$, MacLennan et al., 2002) for each classification category were calculated by integrating backscatter through the water column from 10 m below the surface to a maximum depth of 250 m or 1 m above bottom. The 10-m upper limit accounted for transducer depth (4.9 m) and excluded data from within twice the near-field of the 38 kHz transducer (Simmonds and MacLennan, 2005). Data below 250 m were excluded due to a lack of trawl samples for species validation. Data within 1 m of the bottom were excluded to account for the

acoustic deadzone (Ona and Mitson, 1996). Acoustic density estimates were integrated and exported in 0.2 km horizontal bins, the minimum resolution of acoustic data. Each 0.2 km bin contained a minimum of 5 pings when the echosounder was operated at the slowest pulse rate of 1 ping per 7 seconds when sampling was conducted over deep water (>4000 m). Wavelet analysis (Bradshaw and Spies, 1992; Torrence and Compo, 1998) of the 0.2 km GOAIERP acoustic data (see Chapter 2 for details) determined that a 0.5 km horizontal resolution maximized variability in capelin distributions and was used in further analyses. Additional details of acoustic data collection, processing, and classification can be found in Chapter 2 of this dissertation.

*3.2.2.2. Oceanographic data*

Oceanographic data were collected at each station. A Sea-Bird SBE 911 plus (Sea-Bird Electronics) was used to measure conductivity, temperature, and depth (CTD) on the downcast to 200 m or 10 above bottom, whichever was shallower. CTD measurements were error-checked and integrated in 1 m depth intervals at the University of Alaska Fairbanks in Fairbanks, AK (2011 data) and the Pacific Marine Environmental Laboratory (PMEL) in Seattle, WA (2013 data) (*cf.* Stabeno et al., 2016b). *In situ* chlorophyll-*a* concentrations were measured from water samples collected on the CTD upcast at 10 m intervals from 50 m depth to the surface. Trapezoidal integration was used to approximate integrated chlorophyll from 0-50 m *(cf.* Strom et al., 2016).

*3.2.2.3. Bathymetric data*

To investigate the affiliation of capelin with bathymetric features, high resolution bathymetry data (Zimmermann and Prescott, 2015) for the CGOA shelf were used to determine the proximity of acoustic samples to the edges of shallow, submarine banks by measuring the

shortest distance from each sample's midpoint to the 100 m bottom depth contour (*Edge*) in ArcGIS v10.3 (Environmental Systems Research Institute, Inc). Enhanced vertical mixing and primary production occur near the edges of Albatross and Portlock Banks, primarily due to strong tidal mixing that supplies cold, nutrient-rich bottom water from adjacent troughs to the euphotic zone over banks throughout summer (Cheng et al., 2012; Mordy et al., 2016). This variable was added as it was observed that capelin densities were highest over waters less than 100 m bottom depth in summer of both years (Chapter 2), and appeared to concentrate near the edges of Portlock and Albatross Banks.

### 3.2.3 **Response and predictor indices**

Response variables occurrence (*P*) and density (*D*) were used to evaluate factors influencing capelin distributions (Table 3.1). Capelin occurrence was a binary variable (present: $P=1$; absent: $P=0$) derived from acoustic density estimates ($s_A$) for capelin, forage fish mix, and forage fish/piscivores mix classification categories (see Table 2.2 in Chapter 2). Capelin were considered present in an acoustic sample when the $s_A$ value was greater than 0 for any of the three categories. Capelin density (*D*) was a continuous measure of nonzero acoustic density (i.e. where fish were present, capelin $s_A > 0$). Using categorical and continuous response variables accounts for limitations in survey design, where the frequency of zero density values in a sample is sensitive to changes in the extent of the survey domain (Fig. 3.1), and acoustic classification (i.e. backscatter assigned to multi-species or unknown classification categories). Density estimates for forage fish mix and forage fish/piscivores mix categories were not included in analyses of capelin nonzero densities because backscatter could not be apportioned to species from trawl catches due to an inability to correct for net selectivity (e.g. De Robertis et al., 2017a;

Williams et al., 2011). Data for all response and predictor indices were limited to observations in waters shallower than 500 m depth over the CGOA shelf or adjacent to the shelf break.

Predictor indices used in this study represent the environment where capelin occur, while minimizing collinearity among covariates (Table 3.1). Bathymetric features were represented by acoustic-based bottom depth (*BtmD*) measurements and the proximity of acoustic samples to the nearest edge of banks (*Edge*) derived from the Zimmermann and Prescott (2015) data. Oceanographic predictor indices included: surface temperature (*TmpS*), measured 1 m below surface; bottom temperature (*TmpB*) and salinity (*SalB*), measured at 200 m or approximately 10 m above bottom; and water column stratification represented by the difference between surface and bottom temperature (*TmpD*). Primary production was characterized using integrated chlorophyll-*a* (*Chla*) from 0 to 50 m. Acoustic-based, biological predictor indices included: predator density (*Pred*) using the piscivorous fish classification category; a competitor (*Comp*) represented by the age-0 pollock category; and prey density (*Prey*) using data from the macrozooplankton category. *Chla*, *Pred*, *Comp*, and *Prey* were log-transformed prior to analysis to linearize their relationship with response variables (Zuur et al., 2009).

### 3.2.4 **Analysis resolution**

The influence of physical and biological factors on capelin distributions over the CGOA shelf were analyzed at two spatial resolutions (hereafter analysis resolution) to differentiate continuous acoustic sampling along transects (hereafter transect-based) from discrete sampling at fixed stations (hereafter station-based). Transect-based analyses used continuous data at a spatial resolution of 0.5 km between midpoints of adjacent samples ($n$=2320 samples in summer 2011; $n$=1636 in fall 2011; $n$=2268 in summer 2013). Station-based analyses examined data at a

spatial resolution of 37 km between samples; using both oceanographic measurements from stations ($n$=32 stations sampled in summer 2011; $n$=28 in fall 2011; $n$=37 in summer 2013) and a subset of acoustic samples that were converted to discrete measurements of mean acoustic density at each station. Mean acoustic density was calculated at each station by averaging all 0.2 km resolution samples located within 0.5 km from a station's CTD cast location and collected the same day as the CTD cast. For stations with less than 3 acoustic samples within 0.5 km of the CTD cast due to logistical constraints, the closest 3 acoustic samples were used. The small number of acoustic samples used to estimate mean acoustic density at each station (3 to 6, 0.2 km samples) was intended to represent the area swept by a typical pelagic (e.g. Wilson, 2009) or surface (e.g. Farley et al., 2005) trawl sample at each station.

Oceanographic predictor indices were not included in transect-based analyses due to the concern that station-based values from field samples interpolated from a 37-km sample resolution to a 0.5-km analytic resolution would not represent oceanographic conditions experienced by capelin during acoustic sampling. Heterogeneity in patterns associated with water masses, primary production, and zooplankton communities over the CGOA shelf (e.g. Coyle et al., 2013; Hopcroft et al., 2016; Waite and Mueter, 2013) can occur at scales less than the spatial (37-km) and temporal (approximately 4 hours to 4 days) sampling resolution of station-based data. Since the goal of this study is to examine the influence of physical and biological factors on capelin distributions using assumed instantaneous field observations of capelin and their environment, oceanographic indices were only included in station-based analyses.

To characterize environmental conditions where capelin occurred, all predictor indices are summarized relative to the presence or absence of capelin. Capelin densities were also

plotted relative to each oceanographic index. For each biological predictor index, I qualitatively assessed similarity between patterns at transect- and station-based resolutions by comparing the relative difference in summarized predictor values (i.e. median values, range between 25$^{th}$ and 75$^{th}$ quantiles) when capelin were present versus absent.

### 3.2.5 **Modeling approach**

*3.2.5.1. Model structure*

A spatial generalized linear mixed effects model (spatial GLMM) adapted from Thorson et al. (2015a) was used to predict capelin occurrence and density using fixed effects for predictor indices (Table 3.1), and random effects for spatial covariance at each sample location. Treating spatial covariance as a random effect enables a stochastic process to represent the cumulative effect of physical and biological factors on capelin distributions that are not directly measured (Dormann et al., 2007; Thorson et al., 2015b).

Probability of occurrence, $\hat{p}_i$, for sample $i$ is estimated as

$$\Pr[P = 1] = \hat{p}_i = \left(1 - e^{-e^{\lambda_i^{(p)}}}\right) \tag{3.1}$$

where $P$ is fitted to a Bernoulli distribution with a complementary log-log link (i.e. clog-log) (Hardin and Hilbe, 2007). The asymmetrical shape of the clog-log link function is better-suited to model binary responses with a disproportionately greater number of zeros relative to ones (Hardin and Hilbe, 2007). The linear predictor, $\lambda_i^{(p)}$, for sample $i$ combines fixed and random effects as

$$\lambda_i^{(p)} = \sum_{k=1}^{n_k} x_{i,k}\hat{\beta}_k^{(p)} + \hat{\omega}^{(p)}(s_i) \tag{3.2}$$

where $x_{i,k}$ is covariate $k$ for sample $i$, $\hat{\beta}_k^{(p)}$ is the parameter for covariate $k$ estimated as a fixed effect, and $\hat{\omega}^{(p)}(s_i)$ is the spatial residual at location $s_i$ estimated as a random effect. Spatial covariances are represented by a Gaussian Markov random field as

$$\hat{\omega}^{(p)} \sim MVN\left(0, \Sigma_{\omega}^{(p)}\right) \tag{3.3}$$

where $MVN$ is a multivariate normal distribution fixed at 0, and $\Sigma_{\omega}^{(p)}$ is the covariance of the random field at each sample location (i.e. spatial residuals) following a Matérn distribution with smoothness $v = 1$ (Thorson et al., 2015b, 2015c). The properties of the random are represented by the marginal standard deviation and the geostatistical range; the former indicates the standard deviation at any location when simulating a new realization from the random field and the latter indicates the distance at which correlations decline to 10% (*cf.* Thorson et al., 2015a).

Capelin nonzero density, $d_j$, for sample $j$ (where capelin $s_A > 0$) is estimated as

$$\Pr[D = d \mid D > 0] = \text{Gamma}(d_j, \sigma^{-2}, \exp\left(\lambda_j^{(d)}\right)\sigma^2) \tag{3.4}$$

where $D$ is fitted to a gamma distribution with shape $\sigma^{-2}$ and scale $\exp\left(\lambda_j^{(d)}\right)\sigma^2$, and $\sigma$ is the coefficient of variation for measurement error. The linear combination of fixed and spatial random effects, $\lambda_j^{(d)}$, for sample $j$, is approximated with a log link as

$$\lambda_j^{(d)} = \sum_{k=1}^{n_k} x_{j,k}\hat{\beta}_k^{(d)} + \hat{\omega}^{(d)}(s_j) \tag{3.5}$$

where $x_{j,k}$ is covariate $k$ for sample $j$, $\hat{\beta}_k^{(d)}$ is the estimated parameter for covariate $k$, and $\hat{\omega}^{(d)}(s_j)$ is the estimated spatial residual at location $s_j$.

Following Thorson et al. (2015b), I used the stochastic partial differential equation (SPDE) approximation (Lindgren et al., 2011) to estimate the conditional probability of the spatial covariance matrix, $\Sigma_{\omega}$. The three components of the precision matrix used in the SPDE

approximation (*cf.* Lindgren et al., 2011) were derived using the R package *INLA* (http://www.r-inla.org, Rue et al., 2009). Template Model Builder (TMB, Kristensen et al., 2016) was used to estimate all parameters using maximum marginal likelihood. TMB calculates the marginal likelihood of fixed effects when integrated across random effects using the Laplace approximation (Skaug and Fournier, 2006). The marginal likelihood was then optimized using a conventional nonlinear optimizer in the R statistical environment (http://www.R-project.org, R Core Development Team, 2013) to estimate fixed effects by maximizing the log-marginal likelihood (Thorson et al., 2015b, 2015c).

*3.2.5.2. Data analyses and model selection*

To quantify the influence of physical and biological factors on capelin distributions, a multistep approach was used to first quantify changes in nonzero density (i.e. where fish were present) relative to bottom depth by year and season, and then to identify which predictor indices (Table 3.1) best explained variance in capelin occurrence and density in summer 2013. The first step was based on Chapter 2's preliminary analysis of capelin distributions in summer and fall of 2011 and summer 2013 that showed average densities between major depth contours were higher at depths less than 100 m bottom depth relative to densities over deeper waters in summer of both years, and that overall densities were higher in 2013 compared to 2011. To assess if the spatial GLMM would estimate similar depth-related differences in density between seasons and years across a continuous bathymetric gradient, capelin nonzero densities were quantified relative to bottom depth (*BtmD*), season (*fSn)*, and year (*fYr*) using continuous transect data (i.e. 0.5 km resolution). The linear predictor, $\lambda_j^{(a)}$, from Eq. 3.5 included interaction terms for *BtmD*fSn* and *BtmD*fYr* to allow slopes to vary between surveys. Because capelin distributions

were assumed independent among surveys, spatial effects, $\omega_z$, estimated in Eq. 3.3 required a separate covariance matrix, $\Sigma_{\omega,z}$, for each survey, $z$.

In addition to examining differences in density relative to bottom depth, year, and season, length distributions of capelin over banks and troughs were also compared among surveys. Length measurements from midwater and surface trawl catches were pooled by survey and bottom depth factor (*fBT*, Table 3.1).

All subsequent analyses that assess the influence of physical and biological factors on capelin distributions were limited to data from the summer 2013 survey due to the relatively high proportion of acoustic samples located over the CGOA shelf classified as unknown backscatter in 2011 (Fig. 3.1), and the availability of age-0 pollock and macrozooplankton acoustic data (see Chapter 2 for details). The high proportion of unknown backscatter in 2011 resulted from a low number of trawl samples used to verify observed acoustic targets, which would potentially confound estimates of capelin occurrence due to the inability to differentiate between true and false (i.e. sample) zeroes of capelin density.

To identify which physical and biological factors explained variance in capelin distributions, model selection was used to identify the best combination of fixed and random effects that predict occurrence and density at station- and transect-based analysis resolutions. All predictor indices were organized into candidate models for each response variable and independent covariates at both analysis resolutions (Table 3.1). Each candidate model's name indicates its analysis resolution ("s"=station, "t"=transect), response variable ("P"=presence/absence, "D"=density), and sequential number for each combination of independent covariates. Collinearity among potential predictors was assessed using pairwise correlations (Pearson correlation coefficients, $r$ ) and variance inflation factors (VIF) (Zuur et al.,

2010, 2009). Candidate models were initially organized using pairwise comparisons, in which covariate pairs were considered independent if the magnitude of $r$ was less than |0.5| (Zuur et al., 2009). To assess multicollinearity among two or more predictors, VIFs were calculated for each candidate model (Kutner et al., 2004). If one or more predictors had a VIF greater than 2 (Burnham and Anderson, 2002), then the covariate with the highest VIF was dropped. VIFs for the remaining covariates were recalculated, and the process was repeated until all remaining covariates had VIF values less than 2 (Zuur et al., 2010). All predictor indices were assigned to at least one candidate model for analyses of occurrence and density at each analysis resolution. To allow direct comparison of parameter estimates among candidate models for the same response variable and analysis resolution, predictor indices were standardized (i.e. subtract mean and divide by standard deviation) prior to analysis.

Model selection for fixed effects used the stepwise backward approach and Akaike information criterion values corrected for finite sample size (AICc) (Burnham and Anderson, 2002). For each candidate model, the full model was run and AICc calculated using the R package *TMBhelper* (https://github.com/kaskr). The predictor with the highest Wald Z-test p-value was dropped, the model was re-run, and the AICc value recalculated. The reduced model AICc was subtracted from the full model AICc (hereafter ΔAICc). If ΔAICc was greater than 2, then the process was repeated until ΔAICc was less than 2 from the previous step, or all potential predictors had been dropped. The reduced model with a ΔAICc value less than 2 from the previous step is referred to as the final model. Model selection for random effects was based on the relationship of the parameter estimate and its standard error. If the parameter estimate was within one standard error of having no effect, then I inferred that the random effect explained little variance in the model and could be dropped. Sign deviance residuals (*cf.* Hardin and Hilbe,

2007) from models in which spatial effects were dropped were plotted against latitude and longitude to confirm that residuals did not contain any additional spatial structure (Zuur et al., 2009, 2010).

For each response variable and analysis resolution, the best model was determined by: the lowest AICc value from the final model of each candidate model; visual inspection of model fit; and proportion of explained deviance (i.e. pseudo $R^2$) (Zuur et al., 2012, 2009). To visually assess model fit, I compared predicted to observed occurrence probabilities using a diagnostic function adapted from the R package *SpatialDeltaGLMM* (https://github.com/James-Thorson). Observed occurrence probabilities were calculated from binary data by sorting predicted probabilities in 0.1 increments and then averaging the corresponding observed binary responses within each of the 0.1 bins (i.e. the average of observed 0s and 1s within each 0.1 increment of predicted occurrence probabilities). For density models, standard diagnostic plots (e.g. residual scatter plots and Q-Q plots) were used to assess model fits (Zuur et al., 2009).

To examine the relative importance of physical and biological factors that explained variance in capelin distributions at different analysis resolutions, the best models for transect-based analyses were compared to station-based models comprised of only continuous predictors. Comparisons of parameter estimates between response variables and/or analysis resolutions were qualitatively evaluated using: predictors retained in final reduced models at each resolution; signs of parameter estimates; and magnitudes of parameter estimates relative to other parameters in the same model. To facilitate direct comparison of parameter estimates among continuous covariates within each model, each predictor index was standardized by subtracting values from its mean and dividing by one standard deviation prior to running the model.

## 3.3 RESULTS

Capelin were present in approximately 23% of 6224 acoustic samples (0.5 km data resolution) collected over the CGOA shelf during GOAIERP surveys in 2011 and 2013 (Fig. 3.1). Among the 97 stations sampled, capelin were present at 27.8%, including 6 of 32 stations sampled in summer 2011, 9 of 28 in fall 2011 (including 3 based on acoustic data classified as mixed forage fish species), and 12 of 37 in summer 2013. The absence of capelin could not be confirmed at 70% of the stations sampled in 2011 due to the presence of acoustic samples with backscatter classified as unknown. All stations sampled in 2013 were included in the analysis as the presence or absence of capelin could be determined for all acoustic samples located within 0.5 km of each station (i.e. no backscatter associated with these samples were classified as unknown).

### 3.3.1 Distribution relative to bottom depth, season, and year

Model estimates indicated that capelin nonzero densities were higher in 2013 than in 2011 (Fig. 3.2A-C). Differences in density relative to bottom depth were observed between seasons, and to a lesser extent between years, as indicated by model interaction terms (Table 3.2). In summers of both years, densities declined from shallow to deeper waters over the CGOA shelf, although at a slower rate in 2013 as indicated by the coefficient value for the bottom depth (*BtmD*) and year (*fYr*) interaction term ($\hat{\beta}_{BtmD*fYr:2013}$=0.12). In contrast, densities in fall 2011 were lower over shallow waters compared to summer observations, and increased over deeper bottom depths. The spatial GLMM explained approximately 83% of the variation in capelin densities. Diagnostic plots indicate that densities are underestimated,

primarily at lower values, but more than 96% of standardized, sign deviance residuals varied within ± 2 units and lacked trends when compared to predicted densities (Fig. 3.2D-F).

Distributions of capelin in both 2011 and 2013 suggested that the 100-m depth contour was an informative delineation. A pronounced shift from relatively high to low densities was evident over depths greater than 100 m in summer of both years (2011: mean log $\widehat{D}_{<100\ \mathrm{m}}$=4.7 ± 0.3 $m^2\ nmi^{-2}$, mean log $\widehat{D}_{\geq 100\ \mathrm{m}}$=3.1 ± 0.4; 2013: mean log $\widehat{D}_{<100\ \mathrm{m}}$=6.9 ± 0.4 $m^2\ nmi^{-2}$, mean log $\widehat{D}_{\geq 100\ \mathrm{m}}$=4.6 ± 0.3) (Fig. 3.2A-C). Acoustic measurements also showed that capelin were concentrated over shallow waters between 50 to 100 m in all surveys (Fig. 3.1-2). Based on these patterns, trawl data were partitioned at the 100-m depth contour to examine differences in capelin length frequencies between banks (<100 m) and troughs (≥100 m over the CGOA shelf). Differences in fork length distributions between banks and troughs were evident in all surveys (Fig. 3.3), with modes and mean lengths smaller over banks. Using Brown's (2002) age-length relationship, observed length modes indicated that banks were primarily occupied by age-1 capelin while age-2+ capelin were more prevalent in deeper, trough waters.

### 3.3.2 **Relative importance of physical and biological factors**

*3.3.2.1. Summary of predictor indices*

Due to strong collinearity among predictor indices, bottom depth (*BtmD*) was not included as a continuous predictor in candidate models for station- or transect-based analyses. A binary bottom depth factor, *fBT*, was created using the 100-m depth contour to represent the edge of banks to categorize sample location as occurring over banks (<100 m) or troughs (≥100 m). The depth factor accounted for observed differences in density relative to bottom depth (Fig. 3.2) by allowing the intercept value to be lower for trough samples.

Station-based oceanographic samples collected in summer and fall 2011 and summer 2013 are summarized (Fig. 3.4) relative to capelin presence (box plots) and density (scatter plots). Visual inspection of scatter plots indicated that there were categorical differences in oceanographic samples relative to non-zero densities between banks ($n$=18) and troughs ($n$=9). Non-zero density samples of capelin occurred in waters over banks with cooler surface (*TmpS*) and warmer bottom (*TmpB*) temperatures, reduced thermal stratification (*TmpD*), lower bottom salinity (*SalB*), and higher integrated chlorophyll-*a* concentrations (*Chla*) compared to oceanographic conditions in troughs. Oceanographic conditions in summers were similar between years. In fall 2011, water temperatures were cooler and more stratified over banks and troughs compared to summer of that year.

Characterization of oceanographic conditions where capelin were present relative to conditions at stations where they were absent was limited to observations from summer 2013 due to the high occurrence of unknown backscatter in both 2011 surveys. Visual inspection of boxplots (Fig. 3.4) indicated that stations where capelin were present had relatively warmer bottom temperatures, lower thermal stratification, and higher chlorophyll concentrations compared to stations where capelin were absent.

Distributions of capelin density in summer 2013 and acoustic-based, biological predictors at transect- and station-based analysis resolutions are shown in Fig. 3.5, along with summary boxplots of continuous biological predictors and the *Edge* index to highlight differences in predictor values based on the presence or absence of capelin, analysis resolution, and bottom depth strata. When all samples for each predictor index were pooled across bottom depths, relationships between median values for *Edge*, *Pred*, and *Prey* indices and capelin presence/absence are similar at both analysis resolutions: median values for *Edge* were higher

where capelin were present compared to where they were absent, and median values for *Pred* and *Prey* were lower where capelin were present. In contrast, the relationship between median values for *Comp* based on capelin presence/absence switched between analysis resolutions: median *Comp* was higher where capelin were present at the transect resolution, but was lower at the station resolution. Overlap in the 25$^{th}$ and 75$^{th}$ quantiles for each predictor index among presence and absence values highlight the limitations of comparing samples pooled across all bottom depths. When samples were partitioned between bottom depth categories, differences in median values relative to capelin presence/absence were more pronounced at both resolutions for *Edge* samples in troughs and *Comp* samples over banks (Fig. 3.5). The relationship between medians for *Pred* relative to capelin presence/absence were opposite between banks (higher where capelin were present) and troughs (lower where capelin were present). Differences in medians for *Prey* based on capelin presence/absence were lower when samples were stratified by depth, although the difference in median values between banks/trough samples was larger and the range between 25$^{th}$ and 75$^{th}$ quantile values was reduced. These results indicate that relationships between capelin distributions, biological predictors, and the *Edge* index are sensitive to analysis resolution and/or bottom depth strata.

*3.3.2.2. Station-based analyses*

For all station-based candidate models, derived quantities for the geostatistical range and marginal standard deviation for the spatial random field were near zero. Spatial random effects were subsequently dropped and a generalized linear model (GLM) was used to estimate the probability of capelin occurrence and density. Visual inspection of residuals plotted against latitude and longitude indicated no apparent spatial structure (not shown).

Station-based analyses of capelin occurrence among 5 candidate models (Table 3.3) indicate that model s.P.1 is the best model based on AICc selection. Model s.P.1 predicts that the probability of capelin occurrence in summer 2013 increases with warmer bottom temperature (*TmpB*) and greater distance from the edge of banks (*Edge*), explaining 17.6% of observed variance. In all other candidate models bottom depth factor (*fBT*) is retained in the final model indicating that occurrence probabilities are consistently lower in troughs. The *Edge* predictor is retained in three of four candidate models that included *fBT*, including two models where predator density (*Pred*) is also retained in the final model. Thermal stratification (*TmpD*) and integrated chlorophyll-*a* concentration (*Chla*) are retained in their final models. When included, higher occurrence probabilities are associated with increasing *Edge*, *TmpB*, *Chla*, and *Pred* and decreasing *TmpD* values. Potential predictors that are not retained in the final model for any candidate models include surface temperature (*TmpS*), bottom salinity (*SalB*), competitor density (*Comp*), and prey density (*Prey*).

The relative importance of each standardized predictor within a model was examined by comparing the magnitude of its coefficient with estimates of other predictors included in the final model. In model s.P.1, *TmpB* explains more of the variance relative to *Edge* ($\hat{\beta}_{TmpB}$=0.95; $\hat{\beta}_{Edge}$=0.56), whereas in models s.P.2-4, *Edge* has a relatively higher explanatory power compared to the other continuous predictors. To evaluate model fits, predicted occurrence probabilities were visually compared to observed probabilities (Fig. 3.6A). Model s.P.1 tended to over-estimate occurrence probabilities where capelin were least likely to occur (minimum predicted encounter probability = 0.09), but otherwise model fit was acceptable given that the diagnostic is sensitive to small sample sizes at the resolution (0.1 increments of occurrence probabilities) used in the analysis.

In contrast to occurrence model results, models s.D.1 and s.D.2 (hereafter s.D.1/2 when referring to the same final model for both candidate models) predict that capelin density will be higher at stations located closer to the edge of banks; explaining 43.1% of observed variance. Model s.D.6 is the next best model based on AICc, explaining 37.3% of variance and predicts an increase in density when thermal stratification (*TmpD*) is reduced. Comparison of model diagnostics indicates that model s.D.1/2 fits the data relatively well compared to model s.D.6, but consistently overestimated density (Fig. 3.6B-D). Model diagnostics reveal that predicted densities from other candidate models fit the observed data poorly (not shown). This includes models s.D.3-4 (*TmpS* and *fBT* in final model), which explains 41.4% of the variation and has a similar CV value as the best model ($CV_{s.D.1\text{-}2}$=1.09; $CV_{s.D.3\text{-}4}$=1.1), but did not fit the data well as revealed in the diagnostics for these models.

*3.3.2.3. Transect-based analyses*

Model selection for transect-based analysis of capelin occurrence (Table 3.4) indicates that the best model to estimate probability of occurrence includes spatial random effects, a negative bottom depth factor (i.e. occurrence probabilities lower for trough samples), and positive coefficients for predator density (*Pred*), competitor density (*Comp*), and prey density (*Prey*). Model t.P.1 explains 71.8% of variance in occurrence, with nearly all of the explained variance attributed to spatial effects. The minor contribution of biological predictors is evident by low parameter estimate values ($\hat{\beta}$ range 0.2 to 0.26), indicating no clear differences in explanatory power. Visual inspection of the diagnostic plot (Fig. 3.6A) indicates that predicted occurrence probabilities were over-estimated where capelin are least likely to occur, but overall the model fit to the observed distribution is acceptable based on all observed occurrence probabilities falling within the 95% confidence interval for predicted occurrence probabilities.

At the transect-based analysis resolution, the best model based on AICc of capelin density (t.D.1) includes spatial random effects, a negative bottom depth factor, and the edge of banks (*Edge*), *Pred*, and *Comp* predictors (Table 3.4). Model t.D.1 explains 79.6% of observed variance and predicts that densities will increase with closer proximity to bank edges and increasing densities of predators and competitors. Unlike the transect-based occurrence model, there are clear differences in explanatory power among predictor indices. The *Edge* predictor ($\hat{\beta}$=-0.61) contributes more to model predictions of capelin densities than biological predictors *Pred* ($\hat{\beta}$=0.1) and *Comp* ($\hat{\beta}$=0.18). Visual inspection of diagnostic plots (Fig. 3.6B-D) shows a relatively good fit and no trends in the residuals, but that predicted densities are under-estimated.

Given the observed differences in capelin densities over banks compared to those in troughs (Fig. 3.4-5), the spatial GLMM used for transect-based analyses was modified by expanding Eq. 3.2 to estimate an interaction between the *Edge* and biological predictors with the bottom depth factor (hereafter depth-stratified model). By allowing intercepts and slopes to vary based on the sample's location, the model accounts for depth-specific differences in the influence of each covariate. Model selection results for the depth-stratified model are mixed (Table 3.5). Explained deviance and model fit improved in the depth-stratified occurrence model (t.P_bt), but increases are modest compared to the simpler transect-based model t.P.1 (explained deviance increased by 0.1%; AICc value increased by 6.2). In comparison, for the depth-stratified density model the explained deviance increased by 0.4%, the residual CV was reduced by 0.01, and the AICc value was reduced by 13.7. The improvement in AICc is notable considering the metric penalizes the addition of four new parameters in the depth-stratified model (Hardin and Hilbe, 2007).

The depth-stratified models also highlight differences in the relative influence of predictors on capelin distributions between bottom depth strata. Parameter estimates for the competitor density (*Comp*) predictor over banks are larger and have smaller standard errors in both occurrence ($Comp_b$: $\hat{\beta}$=0.27, SE=0.18; $Comp_t$: $\hat{\beta}$=0.07, SE=0.22) and density ($Comp_b$: $\hat{\beta}$=0.26, SE=0.13; $Comp_t$: $\hat{\beta}$=-0.06, SE=0.14) models, indicating that the explanatory power of *Comp* is both stronger and more stable over banks compared to troughs. The predator density (*Pred*) predictor over banks is retained in the occurrence model but dropped from the density model, while the *Pred* predictor for troughs is dropped from the occurrence model but retained in the density model. The explanatory power of the depth-stratified *Pred* predictor is greater relative to the other covariates in the depth-stratified model compared to the simpler, transect-based models (Tables 4-5).

### 3.3.3 **Resolution-dependent model differences**

Comparison of model selection results from station- to transect-based analyses for candidate models with continuous predictors revealed differences in retained predictors and the relative magnitudes of their estimates (Fig. 3.7). It should be noted that the best station-based occurrence model, s.P.1, was not included in this comparison because it included oceanographic predictors. The final station-based occurrence model (s.P.3) retains *Edge* and *Pred*, with the *Edge* variable explaining more of the variance ($\hat{\beta}_{Edge}$=0.78, $\hat{\beta}_{Pred}$=0.31). In contrast, the final transect-based occurrence model (t.P.1) does not retain the *Edge* predictor and there is no difference in the explanatory power among biological predictors *Pred*, *Comp*, and *Prey*.

In density models s.D.2 and t.D.1, *Edge* is retained in final models at both resolutions. Although *Pred* and *Comp* are also retained in the transect-based density model, the explanatory

power of the *Edge* predictor is higher ($\hat{\beta}_{Edge}$=-0.61, $\hat{\beta}_{Pred}$=0.1, $\hat{\beta}_{Comp}$=0.18). Overall, these results indicate that *Edge* is important at both resolutions, while the influence of biological predictors is sensitive to analysis resolution.

## 3.4 DISCUSSION

### 3.4.1 Relative importance of environmental factors

Model selection results indicate that the probability of capelin occurrence increases in waters with warmer bottom temperatures and higher chlorophyll concentrations, and that capelin density increases at shorter distances from bank edges and reduced thermal stratification. These results demonstrate that capelin distributions are influenced by processes associated with increased vertical mixing in association with bathymetry. Warmer bottom temperatures, increased chlorophyll concentrations, and reduced thermal stratification are all characteristic of increased vertical mixing in the northern GOA (Stabeno et al., 2016a). Throughout summer, primary production is sustained over the CGOA shelf by strong tidal pumping that supplies nutrients from bottom water originating in troughs to the euphotic zone over banks and near their edges (Cheng et al., 2012; Ladd et al., 2005; Mordy et al., 2016). Mixing and primary production are locally enhanced over and near CGOA banks due to increased current velocities that result from the interaction of tidal currents and the Alaska Coastal Current (ACC) with steep walls along troughs (Mordy et al., 2016; Stabeno et al., 2016a). Primary production is further enhanced by increases in ACC transport, which supplies shelf waters with iron originating primarily from river discharge (Cheng et al., 2012; Lippiatt et al., 2010; Stabeno et al., 2004). The distribution and species composition of zooplankton that capelin consume over the GOA shelf is correlated with water temperature, salinity, and primary production (Coyle et al., 2013;

Coyle and Pinchuk, 2005, 2003). Capelin diets primarily consist of copepods and euphausiids (Logerwell et al., 2010; Wilson et al., 2006), whose distributions are associated with different oceanographic and bathymetric features. Neritic copepods (e.g. *Pseudocalanus* spp., *Metridia pacifica*, and *Calanus marshallae*) are associated with ACC waters over the inner shelf while oceanic copepods (e.g. *Neocalanus cristatus* and *Eucalanus bungii*) primarily occur over the outer shelf and deeper slope waters (Coyle and Pinchuk, 2005). Euphausiids are also associated with the ACC (i.e. *Thysanoessa* spp.) and oceanic waters over the outer shelf and slope (*Euphausia pacifica*), but primarily in waters greater than 100 m depth (Pinchuk et al., 2008). Acoustics-based distributions of euphausiids across the GOA shelf indicate that they concentrate over deeper waters in troughs and sea valleys (Simonsen et al., 2016), characterized by higher current velocities compared to shallow banks and coastal waters (Wilson et al., 2009).

These findings build on earlier studies over the CGOA shelf that attribute variability in capelin distributions to a variety of factors. Hollowed et al. (2007) hypothesized that capelin distributions in Barnabas and Chiniak Troughs were limited by oceanographic conditions. Logerwell et al. (2007) suggested that capelin preferred warmer, well-mixed waters associated with the ACC that contained large copepod species in late-summer when age-1 and -2 pollock were not present to compete for shared prey resources. This study's station-based analyses support Logerwell et al.'s (2007) hypothesis that capelin were more likely to occur in well-mixed and productive shallow waters, but I believe that this association is characteristic for distributions of age-1 capelin. The results also indicate that age-2+ capelin primarily occupied cold, stratified waters in troughs, similar to distributions observed by Hollowed et al. (2007), and Logerwell et al. (2010, 2007).

Results of this study do not support the hypothesis of Logerwell et al. (2010) that capelin distributions are influenced by competitive interactions with age-0 pollock. Field observations combined with diet analyses for capelin and age-0 pollock led Logerwell et al. (2010) to speculate that all but the largest capelin were being outcompeted by age-0 pollock for euphausiids, and that capelin switched to alternate prey and expanded their distributions to match the wide availability of copepods. In contrast, this study's transect-based model results showed a positive relationship between capelin and age-0 pollock, and that the competitor index was not retained in any station-based models. This result indicates that capelin distributions were not negatively influenced by competitive interactions between species at either analysis resolution, and that the importance of the relationship differed between analysis resolutions. Interestingly, in both the depth-stratified, transect-based occurrence and density models, the explanatory power of the competitor index was higher over banks, compared to troughs. The positive relationship between capelin and age-0 pollock suggests that these species were likely responding to similar environmental cues over banks, which may be associated with utilization of shared resources that are not limiting. Age-0 pollock primarily consumed small and large copepods over the CGOA shelf in August 2013 (Moss et al., 2016a), consistent with the observation that diets of capelin less than 9.5 cm standard length were also dominated by copepods in 2004 and 2005 (Logerwell et al., 2010). A lack of difference between capelin vertical distribution patterns in 2011 when pollock were absent and during 2013 when pollock were abundant (Chapter 2) further suggests that capelin vertical movements were not influenced by competitive interactions with pollock in summer. These results do not indicate how the relationship might change in the fall when euphausiids would comprise a greater proportion of diets for larger age-0 pollock as reported in Logerwell et al. (2010) and Wilson et al. (2006).

Comparison of bank and trough parameter estimates for the competitor index in the depth-stratified transect-based models highlight differences among capelin age-classes. The depth-stratified model was able to differentiate a strong, positive relationship between age-0 pollock and age-1 capelin density over banks, and a relatively weak, negative relationship with larger, age-2+ capelin in troughs. Age-specific differences in prey and predator predictors also support hypothesized differences in prey preferences. The positive relationship between capelin density and macrozooplankton was relatively weak over banks compared to troughs. This is consistent with age-2+ capelin consuming larger zooplankton prey in troughs, such as euphausiids (Logerwell et al., 2010; Wilson et al., 2006). Capelin were positively related to predator density in transect-based models for occurrence and density, with predator density more influential in predicting capelin densities in troughs. The positive relationship between the predator index and capelin in both station- and transect-based models indicates that capelin distributions do not appear to be influenced by predation or avoidance behavior.

Observed differences in capelin length frequency distributions and literature-based, diet information leads to the hypothesis that in summer age-1 capelin concentrate over shallow banks on the CGOA shelf in waters that are well-mixed and more productive to feed on abundant copepods. Age-2+ capelin primarily occupy deeper trough waters where they consume larger prey, such as euphausiids. Distributions of both age groups over the shelf will likely be driven by changes in the composition and availability of their prey. These results are consistent with "bottom-up control" (e.g. Speckman et al., 2005), but do not indicate specific mechanisms that determine capelin distributions. To better understand mechanisms responsible for structuring capelin distributions over the GOA shelf, future studies should include age-based differences in distribution patterns (*e.g.* following Thorson et al., 2017 for pollock).

Observations from inshore Alaskan waters and Atlantic capelin populations support the hypothesis that capelin respond to oceanographically-induced changes in prey availability. During summer in southeast Alaska, Arimitsu et al. (2008) reported high densities of immature capelin and spawning adults in productive areas of Glacier Bay that were adjacent to edges of deep basins where interactions between tidal currents and shallow sills generate upwelling. In the North Atlantic, age-1 and -2 capelin were distributed in well-mixed, zooplankton-rich waters over the shelf north of Iceland and on the East Greenland plateau, where primary production is sustained by infusions of warm, nutrient-rich water from the Atlantic (Vilhjálmsson, 2002). In the Barents Sea, immature capelin distributions are associated with the receding edge of sea ice throughout summer, where primary and secondary production occur in waters near the ice edge as it retreats northward (Gjøsæter, 1998).

### 3.4.2 **Analysis resolution and modeling approach**

Integrating continuous acoustic sampling across bathymetric gradients with systematic oceanographic sampling at discrete stations allowed us to identify scale-dependent relationships among environmental factors and capelin distributions. Previous studies have identified scale-dependent relationships between capelin and their predators, including cod (Rose and Leggett, 1990) and seabirds (Fauchald et al., 2000; Piatt, 1990). Recognizing that capelin abundance was relatively high in 2013 compared to 2011 (Chapter 2) and that the magnitude and direction of predator-prey relationships have the potential to be both density- and scale-dependent (Fauchald, 2009), future studies should examine how interannual variability in capelin abundance is related to distributions of their prey, predators, and potential competitors.

Examination of autocorrelated samples at a high (0.5 km) resolution was possible by treating spatial covariance among autocorrelated samples as a random effect in the spatial GLMM. Traditional approaches for analyzing spatial data typically resample response variable data at coarser resolutions, or use nested hierarchical approaches to remove spatial structure to meet assumptions of independence among samples (Fauchald et al., 2000; Legendre and Fortin, 1989; Zuur et al., 2009). Treating spatial covariance as a random effect allowed unobserved extrinsic (e.g. density-independent response to environmental conditions) and/or intrinsic (e.g. density-dependent schooling behavior) processes that caused autocorrelation among samples to be included in the prediction of capelin distributions (Beale et al., 2010; Thorson et al., 2015b, 2015c). The spatial GLMM facilitated examination of the relative importance of environmental factors to explain variability in capelin distributions at biologically relevant spatial scales. Compared to station-based models, the spatial GLMM coefficient values for fixed covariates were smaller in transect-based models as spatial residuals accounted for most of the variance. Smaller parameter values were an expected result as variance related to spatial relationships are partitioned between random and fixed effects in the spatial GLMM, while variance is only attributed to fixed covariates in the non-spatial GLM used in conventional station-based analyses (Beale et al., 2010).

These findings also highlight the importance of considering length/age-based differences in distributions that may be influenced by different physical and biological processes. Given differences in length frequency distributions from trawl samples between banks and troughs, I inferred that age-1 fish primarily occupied banks while age-2+ fish were more prevalent in troughs. Age-based differences in capelin distributions and apparent differences in oceanographic properties between banks and troughs suggest that capelin occupy different water

masses based on life stage. It is not surprising that there were differences in the magnitudes and signs of parameter estimates for bank and trough coefficients in the depth-stratified transect-based models. Differences among the bank/trough coefficients indicate that the relative influence of environmental factors on the distribution of capelin is associated with the age-structure of the observed population. Stratifying predictor indices by bottom depth categories also reduced collinearity among oceanographic (not shown) and biological predictors, facilitating model selection of depth-stratified candidate models that were comprised of all potential predictors. This streamlined identification of covariates that best fit the data and explained the most deviance in capelin distributions by eliminating the step of comparing multiple candidate models.

### 3.4.3 **Study limitations**

Examining the relationship between physical and biological factors on capelin distributions was limited in this study to a single year. Oceanographic conditions over the GOA shelf in 2013 are believed to represent average conditions (Hopcroft et al., 2016), while capelin densities were above average relative to other time series (Ormseth, 2012). It is premature to speculate how capelin would respond to environmental perturbations at different population abundance levels. Nonetheless, these results provide guidance to future studies that investigate how capelin distributions are influenced by environmental variability as a function of data resolution and how model structure potentially affects analysis results.

Results of this study may have been influenced by the sampling and environmental indices used as potential predictors. The relatively high proportion of acoustic data classified as unknown in summer and fall 2011 increased uncertainty when differentiating absences (i.e. true

zeroes) from undetected capelin (i.e. sampling zeroes). The analysis of 2011 survey data was limited to only samples where capelin were present when quantifying changes in density relative to bottom depth by year and season. Exclusion of 2011 data from regression analyses prevented running depth-stratified models at the station resolution due to insufficient sample sizes.

Differences in capelin density between banks and troughs may also be due to fish that were located deeper in the water column with corresponding lower acoustic target strengths (TS). The vertical position of capelin was significantly shallower over banks (median center of mass = 55 m) compared to troughs (median center of mass ≥ 110 m) in both years (Chapter 2). Because capelin have a physostomous swimbladder (Fahlén, 1968), compression of their swimbladder at greater depths results in gas loss that cannot be replaced at depth, thereby reducing their backscattering cross-section ($\sigma_{bs}$, e.g. Gorska and Ona, 2003), and resulting in lower acoustic densities (Blaxter and Batty, 1990; Jørgensen, 2003). A depth-dependent TS correction factor is not available for capelin (De Robertis et al., 2017b), and I did not adjust acoustic densities for the potential depth bias. Nonetheless, I believe that the magnitude of the bias is relatively low and constant due to differences in acoustic observations of school morphology and trawl catches. Pronounced morphological differences were observed in capelin densities: schools located over banks were 5 to 20 m in height compared to small, discrete schools in troughs that were rarely greater than 5 m in height. Trawl samples support this conclusion, as midwater catches were consistently higher over banks (1000s to 10,000s of capelin per haul) than in troughs (100s to 1000s of fish), even though selectivity of the Cantrawl net is higher for capelin larger than 80 mm (De Robertis et al., 2017a).

The acoustic-based macrozooplankton index was intended as a proxy for relative densities of zooplankton biomass, but was likely biased toward species primarily consumed by

age-2+ capelin. Copepods are important prey for age-1 and -2+ capelin (Logerwell et al., 2010; Wilson et al., 2006), but are relatively weak scatterers at the frequencies (38 and 120 kHz) used in this study (Matsukura et al., 2009). Larger zooplankton species that are consumed by age-2+ capelin, such as euphausiids and amphipods, have higher TS values (De Robertis et al., 2010; Kang et al., 2002; Murase et al., 2009). As a result, measures of acoustic copepod density may be masked by backscatter associated with euphausiids and amphipods, making the macrozooplankton index a poor measure of copepod biomass (Witteveen et al., 2015). Net-based measures of copepod biomass (*sensu* Coyle and Pinchuk, 2003; Wilson, 2009) were not available at approximately half of sampled stations and were not included in this analysis.

Predator density was based on the piscivores classification category from Chapter 2 (Table 2.2), where backscatter originated from large aggregations of adult groundfish, but also included age-1+ groundfish that may forage at a similar trophic level as capelin. Trawl samples indicated that age-2+ capelin often co-occurred with juvenile pollock (likely age-1 and -2 based on lengths, Brodeur and Wilson, 1996) in troughs. Even though age-1 and -2 pollock may consume similar prey resources as age-2+ capelin (Logerwell et al., 2007), they were classified as piscivorous fish due to insufficient trawl samples to differentiate them from larger pollock. Positive covariance between capelin distributions and the predator index may be partially attributed to both species responding to similar foraging cues, not unlike the positive relationship observed between age-1 capelin and age-0 pollock over banks. This potential bias does not affect my findings that capelin distributions were not likely influenced by predator density in summer 2013.

### 3.4.4 **Summary**

This study's integrated sampling design allowed us to quantify the relative importance of physical and biological environmental factors when characterizing distributions of a mobile, pelagic species at two spatial resolutions. Capelin distributions on the CGOA shelf were primarily concentrated over shallow submarine banks in areas of enhanced vertical mixing and primary production. In summer 2013, capelin were predicted to occur across the shelf in waters with relatively warmer bottom temperatures, with highest densities occurring over banks or in close proximity to bank edges. The strong association between capelin density and proximity to banks was apparent at both analysis resolutions. The relative importance of biological indices as predictors of occurrence and density differed between sample resolutions and bottom depth strata. These findings indicate that in summer age-1 capelin concentrate over shallow banks on the CGOA shelf in waters that are well-mixed and more productive (Cheng et al., 2012; Mordy et al., 2016), and where copepods are likely to be abundant (Coyle et al., 2013). Age-2+ capelin primarily occupy deeper trough waters where they likely consume larger zooplankton prey, such as euphausiids (Wilson et al., 2009). Recognizing that the influence of environmental processes on capelin distributions may vary based on the age-structure of the observed population, I recommend that studies investigating mechanisms responsible for structuring capelin distributions include size- and/or age-specific analyses.

## 3.5 TABLES

**Table 3.1** – List of response and predictor indices used as potential predictors in station-based ("S") and transect-based ("T") models. Units in ().

| **Response variable** | **Abbreviation** | **Data Source** | **Model** |
|---|---|---|---|
| Capelin presence (binary)<br>Absent (0): $s_A = 0$<br>Present (1): $s_A > 0$ | $P$ | Derived from acoustics [1] | S, T |
| Capelin positive density ($s_A > 0$) | $D$ | Acoustics [1] | S, T |

| **Predictor variable** | **Abbreviation** | **Data Source** | **Model** |
|---|---|---|---|
| Bottom depth (m) | *BtmD* | Acoustics [1] | T |
| Bottom depth factor (binary)<br>0 = bank (< 100 m),<br>1 = trough (100 – 500 m) | *fBT* | Derived from acoustics [1] | S, T |
| Distance from 100 m depth contour (km) | *Edge* | Derived from bathymetry [2] | S, T |
| Surface temperature (° C) | *TmpS* | CTD profile [3] | S |
| Bottom temperature * (° C) | *TmpB* | CTD profile [3] | S |
| Surface-bottom temp. difference $\Delta_{TmpS\text{-}TmpB}$ (° C) | *TmpD* | Derived from CTD profile [3] | S |
| Bottom salinity * (psu) | *SalB* | CTD profile [3] | S |
| Integrated chlorophyll-α from 0-50 m (mg $m^{-2}$) | *Chla* | *In situ* bottle samples [4] | S |
| Predator: piscivorous, semi-pelagic fish ($s_A$) | *Pred* | Acoustics [1] | S, T |
| Competitor: age-0 pollock ($s_A$) | *Comp* | Acoustics [1] | S, T |
| Prey: macrozooplankton ($s_A$) | *Prey* | Acoustics [1] | S, T |

* Measurement taken 10 m above bottom or 200 m, whichever was shallower
[1] Chapter 2
[2] Zimmermann and Prescott 2015
[3] Stabeno et al., 2016b
[4] Strom et al., 2016

**Table 3.2** – Final parameter estimates (Est) and standard errors (SE) for transect-based analysis of capelin positive density relative to bottom depth (*BtmD*), season (*fSn*), year (*fYr*), and their interactions in summer (s11) and fall (f11) 2011 and summer 2013 (s13). Derived parameters for the spatial random field, including the geostatistical range (km) and the marginal standard deviation, were estimated for each survey. CV is the coefficient of variation for measurement errors. Type indicates if the parameter is estimated as a fixed effect (F) or is calculated as a derived quantity from other fixed effects that are not as easily interpreted (D).

| Parameter | Est | SE | Type |
|---|---|---|---|
| *B0* | 3.04 | 0.22 | F |
| *BtmD* | -1.53 | 0.27 | F |
| *fYr*:2013 | 2.49 | 0.26 | F |
| *fSn*:Fall | 0.14 | 0.33 | F |
| *BtmD*fYr*:2013 | 0.12 | 0.29 | F |
| *BtmD*fSn*:Fall | 1.96 | 0.43 | F |
| $Range_{s11}$ | 3.71 | 0.60 | D |
| $Range_{f11}$ | 5.11 | 0.98 | D |
| $Range_{s13}$ | 3.54 | 0.48 | D |
| Marginal $SD_{s11}$ | 4.28 | * 0.43 | D |
| Marginal $SD_{f11}$ | 4.17 | * 0.43 | D |
| Marginal $SD_{s13}$ | 6.30 | * 0.45 | D |
| CV | 1.00 | 0.02 | D |

**Table 3.3** – Final model estimates for station-based samples from summer 2013 survey, with best models based on $AIC_C$ in bold. Model names indicate analysis resolution (s=station), response variable (P=binary presence/absence, D=positive density), and covariate combination number. Fixed Effects include parameter estimates (and standard errors) for intercepts and predictor indices (Table 3.1). Spatial Est. indicates derived quantities representing the geostatistical range (Rng, km) and marginal standard deviation (SD) for the spatial random field. 'X' indicates parameter included in full model, CV is the coefficient of variation for measurement errors in positive density models, Delta AICc from best model in set (AICc for best model), Dev is the proportion of explained variance (i.e. pseudo $R^2$).

**Table 3.3 (cont'd)**

| Model | *N* | Fixed Effects (SE) | | | | | | | | | | | Spatial Est. | | CV | Delta | Dev |
|---|---|---|---|---|---|---|---|---|---|---|---|---|---|---|---|---|---|
| | | *B0* | *fBT* | *Edge* | *TmpS* | *TmpB* | *TmpD* | *SalB* | *Chla* | *Pred* | *Comp* | *Prey* | Rng | SD | (SE) | AICc | (%) |
| **s.P.1** | **37** | **-1.11 (0.35)** | X | **0.56 (0.3)** | X | **0.95 (0.39)** | | | | X | X | | X | X | NA | **0.00 (45.17)** | **17.6** |
| s.P.5 | 37 | -0.45 (0.36) | -1.05 (0.62) | X | | | | X | | X | X | | X | X | NA | 2.71 | 6.7 |
| s.P.2 | 37 | -0.3 (0.46) | -1.55 (0.9) | 0.65 (0.32) | X | | | | 0.36 (0.35) | X | X | | X | X | NA | 2.78 | 17.0 |
| s.P.3 | 37 | 0.01 (0.4) | -2.18 (0.89) | 0.78 (0.35) | X | | | | | 0.31 (0.31) | X | X | X | X | NA | 2.84 | 16.9 |
| s.P.4 | 37 | -0.32 (0.55) | -1.59 (1.04) | 0.85 (0.38) | | | -0.48 (0.5) | | | 0.31 (0.32) | X | | X | X | NA | 4.5 | 19.1 |
| **s.D.1** | **12** | **5.98 (0.31)** | X | **-1.31 (0.35)** | | | | | X | X | | | X | X | **1.09 (0.19)** | **0.00 (176.32)** | **43.1** |
| **s.D.2** | **12** | **5.98 (0.31)** | X | **-1.31 (0.35)** | | | | | | X | X | | X | X | **1.09 (0.19)** | **0.00** | **43.1** |
| s.D.6 | 12 | 6.05 (0.33) | X | | | | -1.8 (0.48) | | | X | X | | X | X | 1.14 (0.2) | 1.39 | 37.3 |
| s.D.7 | 12 | 6.13 (0.34) | X | | | | | -1.17 (0.4) | | X | X | | X | X | 1.19 (0.21) | 2.81 | 30.7 |
| s.D.5 | 12 | 6.84 (0.44) | -1.89 (0.76) | | | X | | | | X | X | | X | X | 1.24 (0.21) | 4.12 | 24.2 |
| s.D.8 | 12 | 6.84 (0.44) | -1.89 (0.76) | | | | | | | X | X | X | X | X | 1.24 (0.21) | 4.12 | 24.2 |
| s.D.3 | 12 | 6.69 (0.39) | -2.06 (0.69) | | -0.91 (0.38) | | | | X | X | | | X | X | 1.1 (0.19) | 5.13 | 41.4 |
| s.D.4 | 12 | 6.69 (0.39) | -2.06 (0.69) | | -0.91 (0.38) | | | | | X | | X | X | X | 1.1 (0.19) | 5.13 | 41.4 |

**Table 3.4** – Final model estimates for transect-based samples from summer 2013 survey, with best models based on $AIC_C$ in bold. Model names indicate analysis resolution (t=transect), response variable (P=binary presence/absence, D=positive density), and model combination number. Fixed Effects include parameter estimates (and standard errors) for intercepts and predictor indices (Table 3.1). Spatial Est. indicates derived quantities representing the geostatistical range (Rng, km) and marginal standard deviation (SD) for the spatial random field. 'X' indicates parameter included in full model, CV is the coefficient of variation for measurement errors in positive density models, Delta AICc from best model in set (AICc for best model), Dev is the proportion of explained variance (i.e. pseudo $R^2$).

| **Model** | ***N*** | **Fixed Effects (SE)** | | | | | | **Spatial Est.** | | **CV** | **Delta** | **Dev** |
|---|---|---|---|---|---|---|---|---|---|---|---|---|
| | | *B0* | *fBT* | *Edge* | *Pred* | *Comp* | *Prey* | Rng | SD | **(SE)** | **AICc** | **(%)** |
| **t.P.1** | **2268** | **-8.66** | **-1.44** | **X** | **0.22** | **0.20** | **0.26** | **23.93** | **13.37** | NA | **0.00** | **71.8** |
| | | **(1.88)** | **(1.34)** | | **(0.19)** | **(0.14)** | **(0.16)** | **(3.86)** | **(2.52)** | | **(790.1)** | |
| **t.D.1** | **669** | **5.67** | **-1.79** | **-0.61** | **0.1** | **0.18** | | **5.40** | **4.13** | **0.97** | **0.00** | **79.6** |
| | | **(0.27)** | **(0.4)** | **(0.22)** | **(0.09)** | **(0.1)** | | **(0.78)** | **(0.31)** | **(0.03)** | **(8501.4)** | |
| **t.D.2** | 669 | 6.00 | -2.39 | | 0.08 | 0.20 | 0.11 | 5.68 | 4.23 | 0.97 | 5.9 | 79.6 |
| | | (0.25) | (0.37) | | (0.09) | (0.1) | (0.08) | (0.84) | (0.31) | (0.03) | | |

**Table 3.5** – Final model estimates for depth-stratified transect-based samples from summer 2013 survey, with best models based on $AIC_C$ in bold. Fixed Effects include parameter estimates (and standard errors) for intercepts and predictor indices (Table 3.1). Model names indicate analysis resolution (t=transect), response variable (P=binary presence/absence, D=positive density, and depth-stratified parameters (bt). Spatial Est. indicates derived quantities representing the geostatistical range (Rng, km) and marginal standard deviation (SD) for the spatial random field. 'X' indicates parameter included in full model, CV is the coefficient of variation for measurement errors in positive density models, AICc for best model, Dev is the proportion of explained variance (i.e. pseudo $R^2$).

| **Model** | ***N*** | **Fixed Effects (SE)** | | | | | | | | | | **Spatial Est.** | | **CV** | | **Dev** |
|---|---|---|---|---|---|---|---|---|---|---|---|---|---|---|---|---|
| | | *B0* | *fBT* | $Edge_b$ | $Edge_t$ | $Pred_b$ | $Pred_t$ | $Comp_b$ | $Comp_t$ | $Prey_b$ | $Prey_t$ | Rng | SD | **(SE)** | **AICc** | **(%)** |
| **t.P_bt** | **2268** | **-5.85 (4.59)** | **-4.26 (4.09)** | **2.83 (4.06)** | **-0.28 (1.22)** | **0.31 (0.22)** | **X** | **0.27 (0.18)** | **0.07 (0.22)** | **0.23 (0.18)** | **0.32 (0.32)** | **24.13 (3.64)** | **13.09 (2.51)** | NA | **796.1** | **71.9** |
| **t.D_bt** | **669** | **6.66 (0.54)** | **-3.15 (0.64)** | **0.77 (0.69)** | **-0.9 (0.23)** | **X** | **0.4 (0.16)** | **0.26 (0.13)** | **-0.06 (0.14)** | **0.12 (0.09)** | **0.31 (0.2)** | **5.27 (0.74)** | **4.04 (0.31)** | **0.96 (0.03)** | **8493.4** | **80.0** |

## 3.6 FIGURES

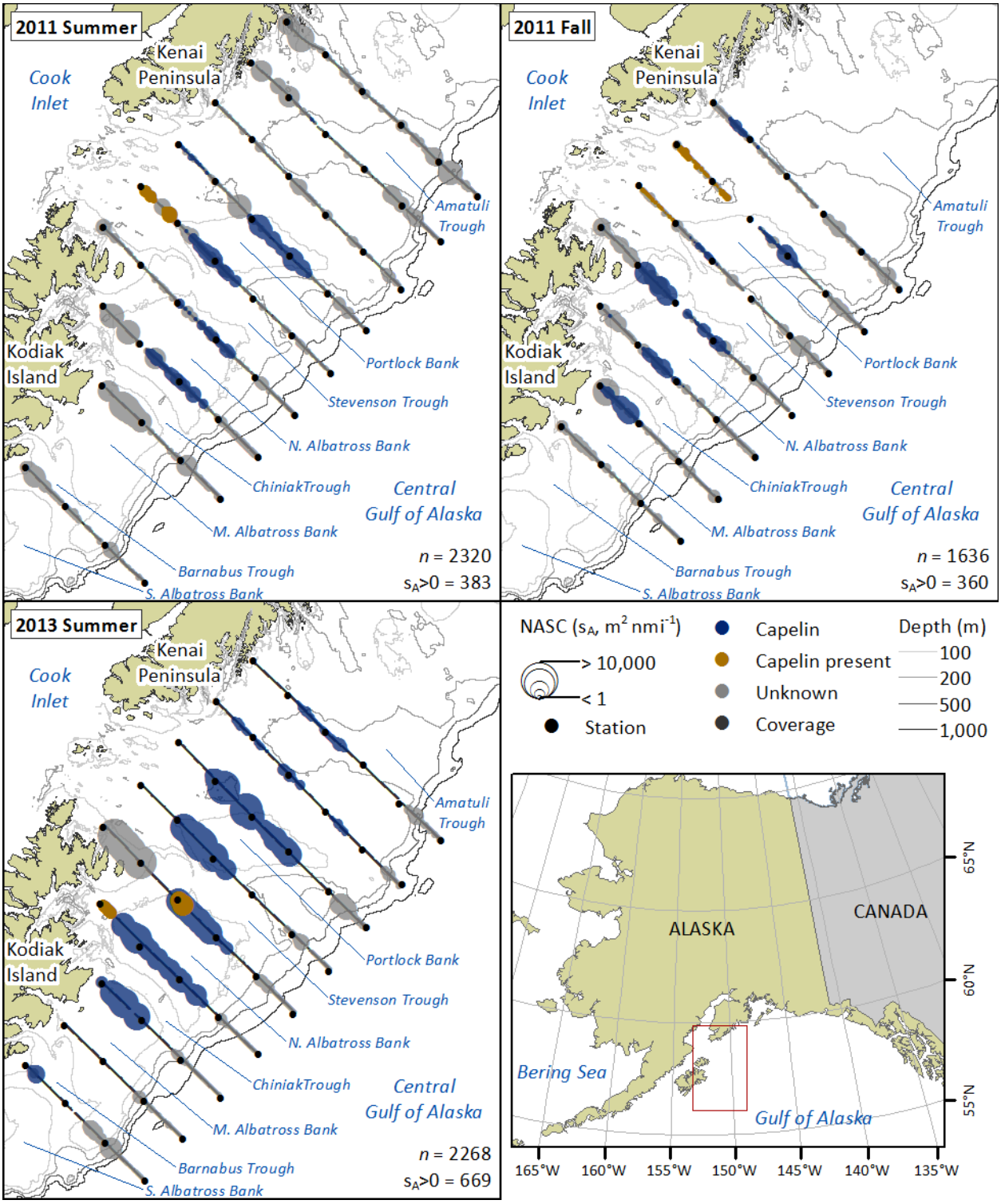
2011 Summer
Kenai Peninsula
Cook Inlet
Amatuli Trough
Kodiak Island
Portlock Bank
Stevenson Trough
N. Albatross Bank
ChiniakTrough
Central Gulf of Alaska
M. Albatross Bank
Barnabus Trough
S. Albatross Bank
n = 2320
sA>0 = 383
2011 Fall
n = 1636
sA>0 = 360
2013 Summer
n = 2268
sA>0 = 669
NASC (sA, m2 nmi-1)
> 10,000
< 1
Station
Capelin
Capelin present
Unknown
Coverage
Depth (m)
100
200
500
1,000
ALASKA
CANADA
Bering Sea
Gulf of Alaska
65°N
60°N
55°N
165°W
160°W
155°W
150°W
145°W
140°W
135°W

**Figure 3.1** – Distributions of capelin acoustic density, NASC ($s_A$, $m^2$ $nmi^{-2}$), in summer and fall 2011 and summer 2013, and locations of oceanography stations. Inset (red box) indicates CGOA study area. Acoustic data are categorized to indicate capelin density ("Capelin") or presence within multi-species aggregations ("Capelin present"), and "Unknown" indicates backscatter that could not be identified, "Coverage" indicates acoustic sampling, "*n*" indicates total number of 0.5 km acoustic samples (located < 500 m bottom depth) by survey, and "$s_A > 0$" indicates number of capelin positive density samples.

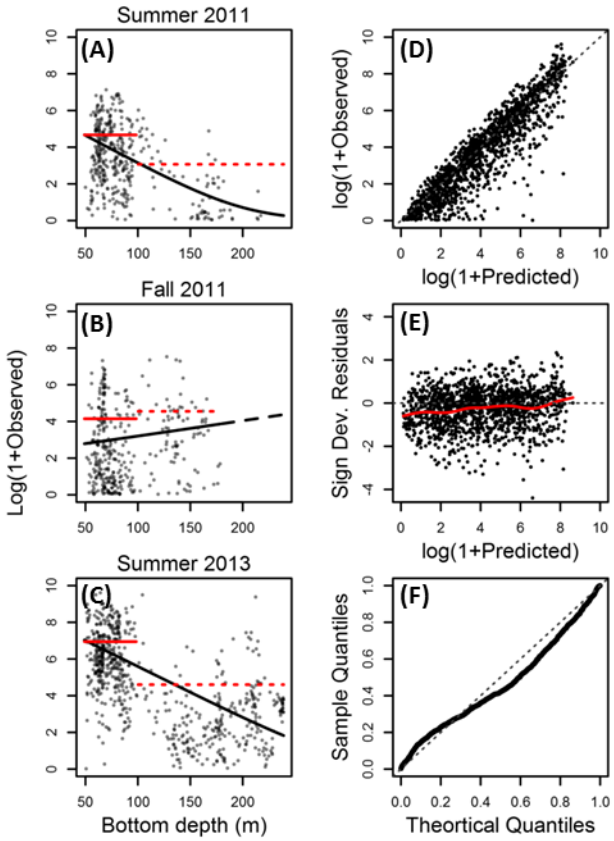


**Figure 3.2** – Scatter plots of observed capelin acoustic positive density, $s_A$, relative to bottom depth in (A) summer 2011, (B) fall 2011, and (C) summer 2013; solid black lines represent predicted density across depth range of capelin occurrence, while the dashed line extends predicted density to maximum bottom depth among all surveys; red lines represent mean predicted density over banks (< 100 m, solid lines) and troughs (≥ 100 m, dotted lines). Model diagnostic plots: (D) observed versus predicted density, where dotted line represents y=x relationship; (E) standardized sign deviance residuals versus predicted density, where red line represents a smooth spline fitted to residuals; (F) Q-Q plot showing sample versus theoretical quantiles of gamma distribution.

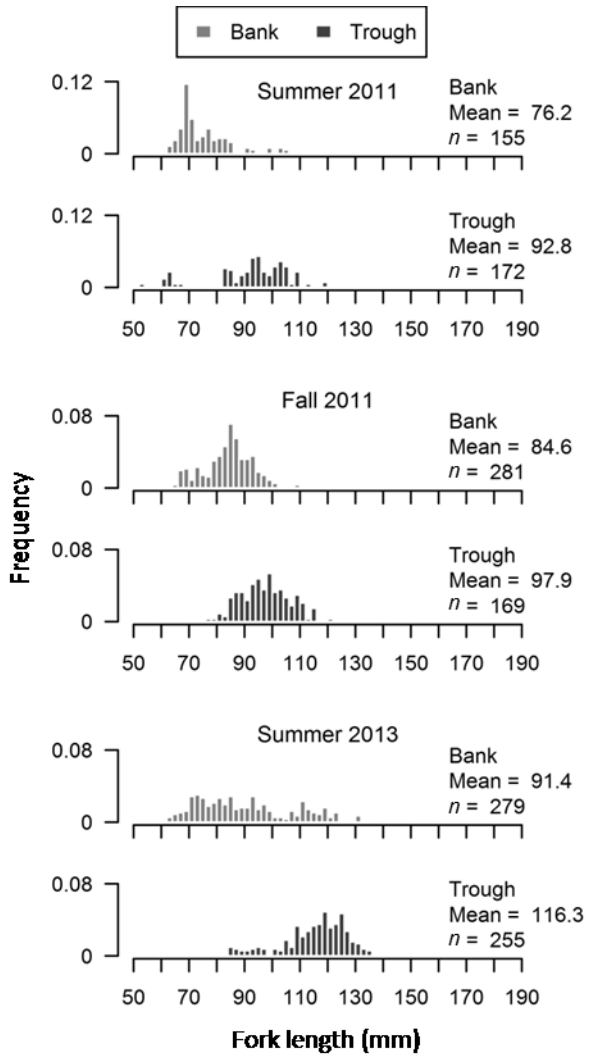


**Figure 3.3** – Frequency distributions of capelin fork length from trawl samples by year, season, and bottom depth factor ("Bank" = < 100 m bottom depth; "Trough" = ≥ 100 m). *n* indicates number of length measurements.

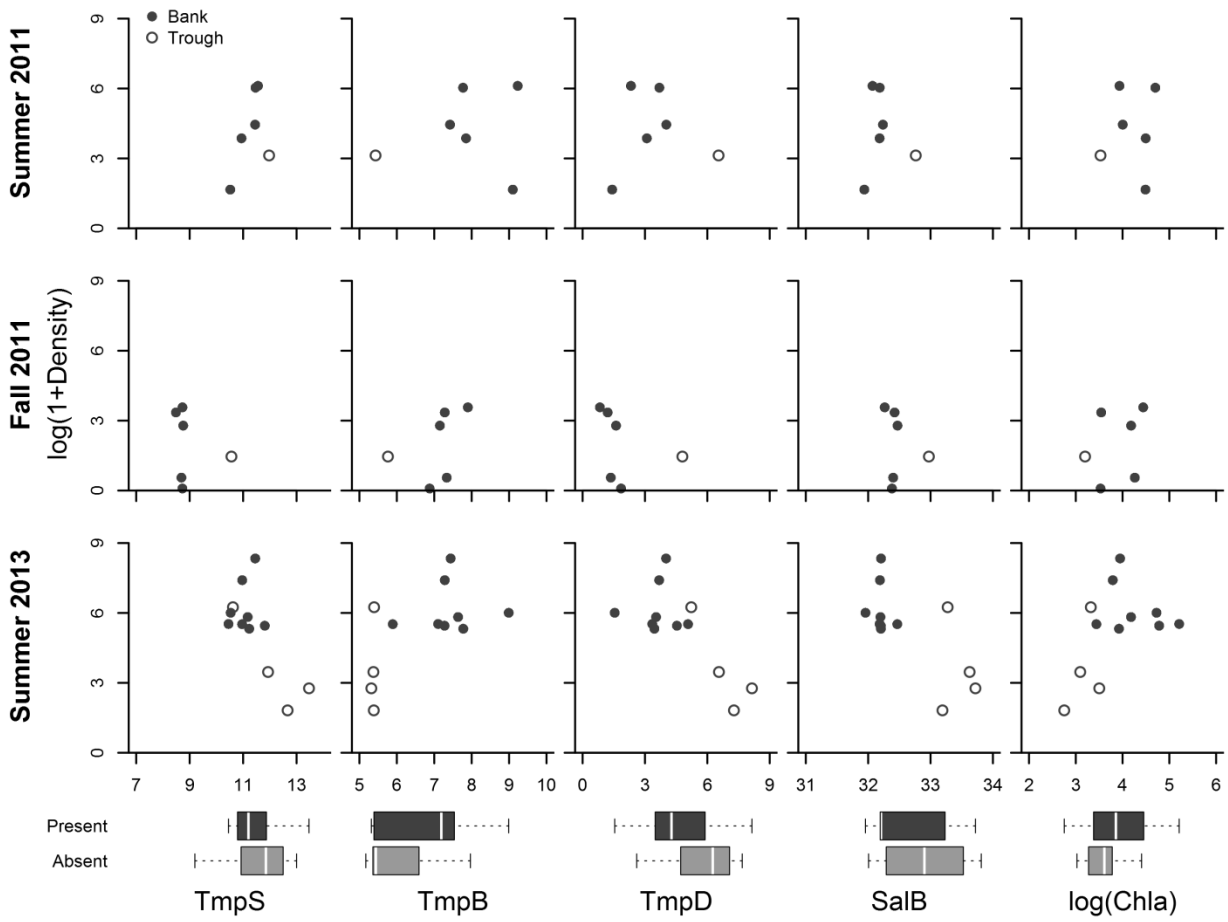


**Figure 3.4** – Station-based oceanographic predictor indices summarized by year and season. Scatter plots show capelin positive density, *D*, relative to each oceanographic index: "TmpS"=surface temperature (° C); "TmpB"=bottom temperature (° C); "TmpD"=surface-bottom temperature difference (° C); "SalB"=bottom salinity (psu); "Chla"=integrated chlorophyll-α (mg $m^{-2}$). Sample location is indicated by closed circles (banks) and open circles (troughs). For summer 2013, horizontal box plots summarize each index based on presence ($s_A > 0$, dark gray) or absence ($s_A = 0$, light gray) of capelin, *P*, at the station.

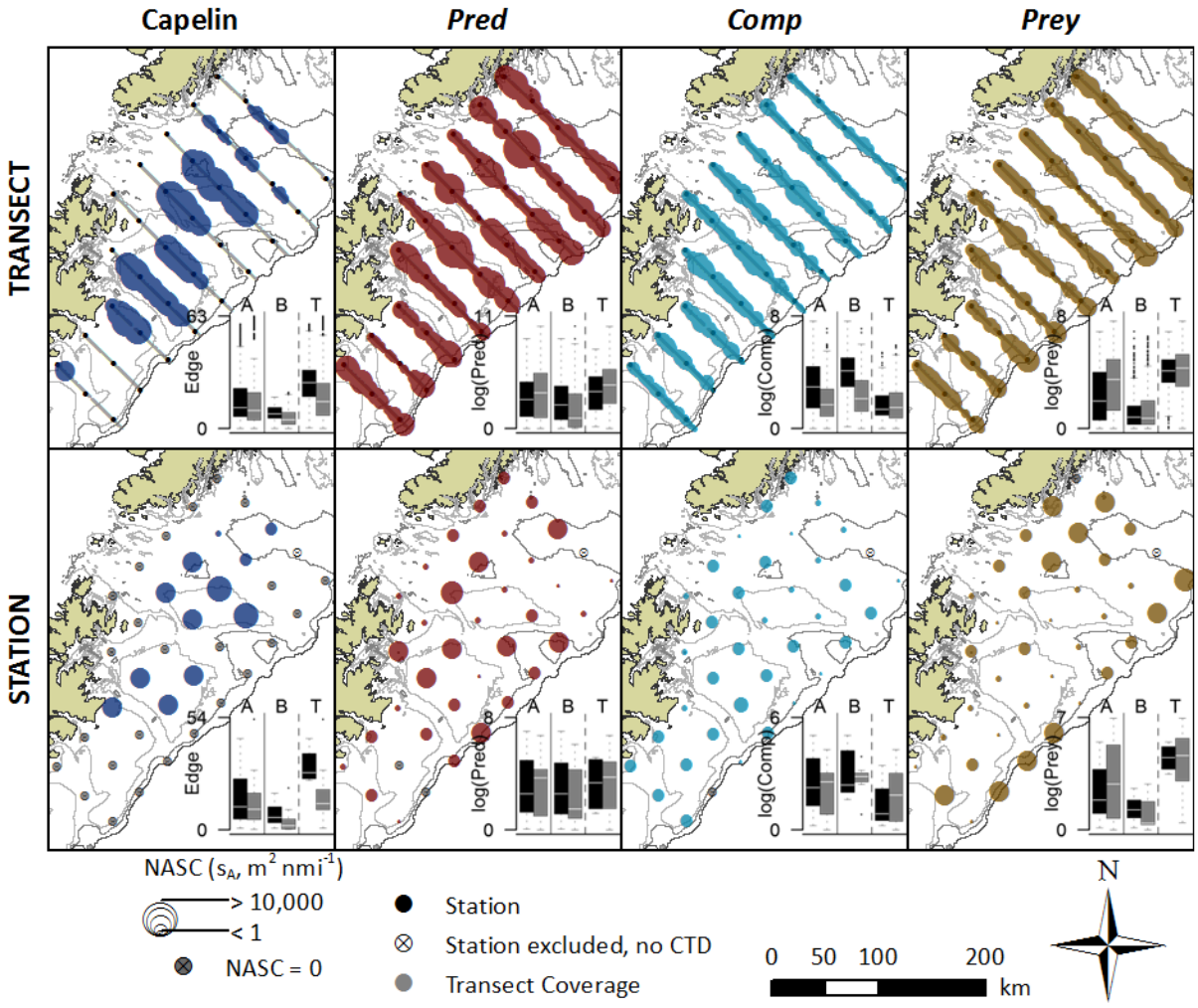


**Figure 3.5** – Acoustic densities of capelin and predictor indices for potential predators ("Pred", semi-pelagic piscivorous fish), competitors ("Comp", age-0 pollock), and prey ("Prey", macrozooplankton) at transect (top row) and station (bottom row) analysis resolutions from the summer 2013 survey. Inset boxplots summarize predictor indices by depth factor ("A"=all samples; "B"=bank; "T"=trough) where capelin were present (black box) and absent (gray box) for each analysis resolution. Boxplots within capelin column (far left) summarize the "Edge" predictor index, a measure of each sample's distance from the 100 m depth contour representing the edge of banks and troughs.

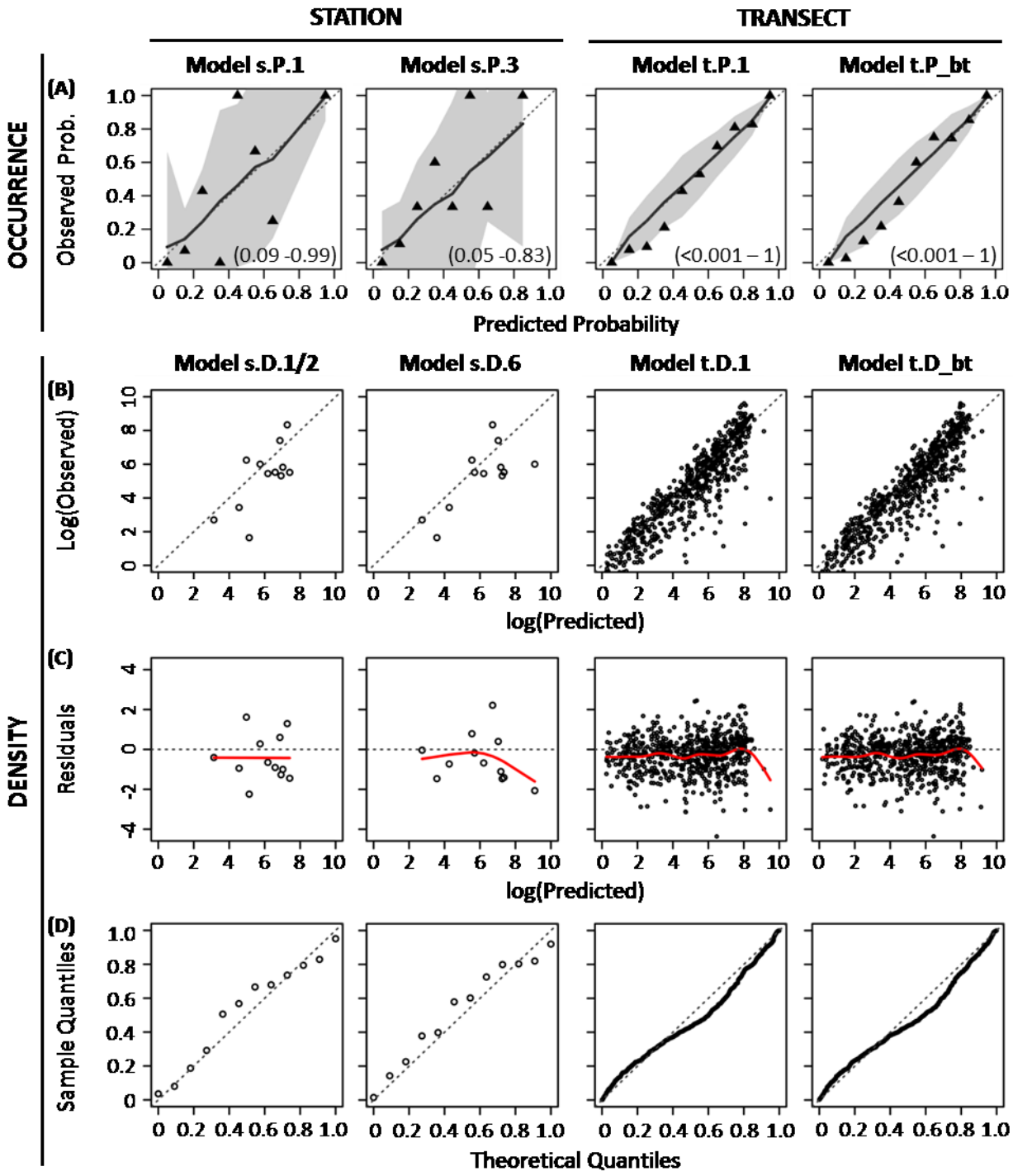


**Figure 3.6** – Diagnostic plots for final station- and transect-based models of capelin occurrence (row A) and positive density (rows B-D) in summer 2013. Row A) predicted vs. observed occurrence probabilities, with predicted probabilities indicated by black line (shaded area=95%

confidence interval) and mean observed probabilities by triangles. Range of predicted probabilities are in parentheses. For positive density models, row B) scatter plots of observed versus predicted density; dotted line represents y=x relationship; C) scatter plots of standardized sign deviance residuals vs. predicted density with a smooth spline fitted to the data (red line); dotted line represents y=0; D) Q-Q plots show sample quantiles vs. theoretical quantiles of gamma distribution. See Tables 3.3-5 for model name definitions (note: "Model s.D.1/2" shows final model fits for candidate models s.D.1 and s.D.2).

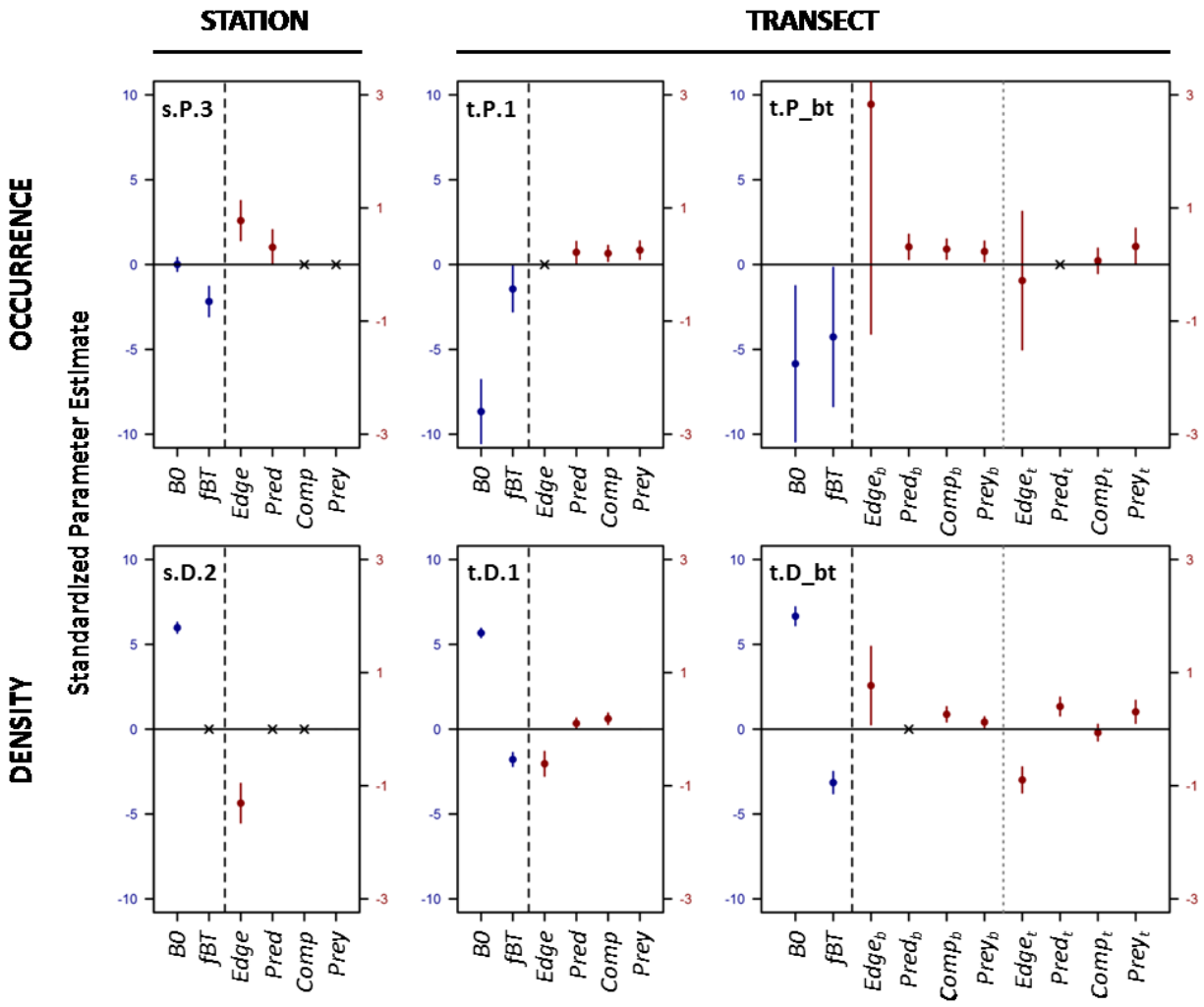


**Figure 3.7** –Standardized parameter estimates and standard errors for fixed effects by model for capelin occurrence (upper plots) and positive density (lower plots) in summer 2013. Parameter scale indicated by color: intercept (*BO*) and depth factor (*fBT*) are on left Y-axis in blue, environmental covariates (see Table 1 for covariate definitions) are on right Y-axis in red. "X" indicates covariates that were dropped from full model. Note *BO* is always included and not subject to model selection using AICc.

# Chapter 4. EFFECTS OF TEMPERATURE ON THE DISTRIBUTION AND DENSITY OF CAPELIN IN THE GULF OF ALASKA

## 4.1 INTRODUCTION

Marine food webs, fisheries, and fishery-dependent communities in the northern hemisphere are projected to be affected by climate-related changes to primary production (Arrigo and van Dijken, 2011), species distributions (Hollowed et al., 2013b; Pershing et al., 2015), community composition (Grebmeier et al., 2006), and the partitioning of energy between demersal and pelagic communities (Grebmeier et al., 2006; Moore and Stabeno, 2015). The potential for these ecological, economic, and social effects highlight the need for resource managers to improve understanding of how climate-related perturbations in ocean conditions and long-term warming affect the distribution and abundance of small pelagic fishes (Hollowed et al., 2013a) that modulate the transfer of energy from primary producers to upper trophic species (Pikitch et al., 2012).

Capelin (*Mallotus villosus*) is an important small pelagic fishes in boreal marine ecosystems. Distributed in all oceans in the northern hemisphere at latitudes of ~45 to 80° N (Carscadden et al., 2013; Logerwell et al., 2015; Pahlke, 1985), capelin occupy waters that extend from the nearshore, across the continental shelf, and to the upper slope. Spatial and temporal changes in capelin distributions and density affect their availability as prey to piscivorous seabirds, marine mammals, and commercially important fish species (Ciannelli and Bailey, 2005; Sydeman et al., 2017; Vilhjálmsson, 2002).

Temperature variability and climate-related effects on marine ecosystems have been directly and indirectly associated with fluctuations in distributions and abundances of capelin in the Pacific (Anderson and Piatt, 1999; Andrews et al., 2015), Arctic (Carscadden et al., 2013a; Logerwell et al., 2015), and Atlantic (Carscadden et al., 2013a; Ingvaldsen and Gjøsæter, 2013; Rose, 2005) Oceans. Despite having a wide thermal tolerance (-1.5 to 14° C), small changes in sea temperatures (~1° C) have been associated with changes in capelin distributions that spanned 100s km (Rose, 2005). Temperature has also been associated with changes in the timing and path of migrations to spawning areas around Iceland (Olafsdottir and Rose, 2012, 2013), as well as with spawn timing and the selection of spawning habitat in the Northwest Atlantic (Carscadden et al., 1989; Davoren et al., 2012; Nakashima and Wheeler, 2002). There is strong evidence that capelin distributions and population dynamics are affected by indirect effects of temperature variability linked to changes in predator distributions and abundance (Hjermann et al., 2004), and to changes in zooplankton prey distributions, abundance, and/or species composition related to temperature regime shifts (Orlova et al., 2010) or sea ice dynamics (Buren et al., 2014).

Large-scale increases in sea temperature have been associated with a northward shift in capelin distributions around Iceland (Carscadden et al., 2013a; Valdimarsson et al., 2012). Capelin distributions in the Barents and Bering Seas are also predicted to shift northward into the Arctic (Carscadden et al., 2013a; Hollowed et al., 2013b; Huse and Ellingsen, 2008) in response to projected increases in sea temperatures and loss of sea ice (IPCC, 2007). In the North Pacific, empirical evidence partially supports this predicted northward shift, where the southern range of capelin in the epipelagic zone (< 30 m) of the eastern Bering Sea contracted from the Aleutian Islands in cold years to northward of ~60° N in warm years (Andrews et al., 2015). Limited field

studies in the Chukchi and Beaufort Seas have observed variability in capelin range and abundance, but interannual differences in distribution and density were not directly associated with water temperatures (De Robertis et al., 2017b; Logerwell et al., 2015).

In contrast to most capelin populations that are expected to shift northward during periods of increased warming, capelin in the Gulf of Alaska (GOA) are potentially more vulnerable to anomalous warming events (*i.e.* marine heatwaves) and long-term increases in sea temperature. Northward movement in the GOA is impeded above 60° N by the Alaska coast (Fig. 4.1), potentially limiting availability of suitable habitat during periods of increased sea temperatures. While capelin are distributed across the GOA shelf, the core of the population is believed to occupy the shelf south and east of the Kodiak Archipelago (Ormseth et al., 2016). Waters around Kodiak are highly productive throughout summer relative to the GOA shelf (Stabeno et al., 2016a; Waite and Mueter, 2013), and this area may function as a summer feeding ground for age-1+ GOA capelin (Chapter 2). A previous collapse of the GOA population coincided with warm temperature anomalies in the GOA that occurred after the late 1970s climate regime shift (Anderson and Piatt, 1999; Francis et al., 1998). As the population recovered, increasing catch rates of capelin in the National Marine Fisheries Service Alaska Fisheries Science Center (AFSC) Groundfish Assessment Program's summer GOA Continental Shelf and Slope bottom trawl (BT) survey indicated that capelin distributions expanded across the GOA from the Kodiak region (Mueter and Norcross, 2002; Ormseth, 2012). Given that the area occupied by capelin is expected to contract with decreasing population abundance (Carscadden et al., 2013a), temperature-related reductions in suitable habitat may lead to distributional shifts, reduced biomass, and/or collapse of the GOA population if sufficient cold-water refugia (*e.g.* Arimitsu et al., 2008) are not available.

Compared to Atlantic populations, there are limited data available to examine spatial and temporal changes in Pacific capelin distributions and abundances relative to temperature in the GOA. This lack of information is attributed to the absence of a directed capelin fishery in the North Pacific, and to the fact that existing abundance surveys for demersal fish species (*e.g.* the AFSC BT survey) are poorly suited to accurately detect changes in capelin and other small pelagic species' distributions (Ormseth, 2012). Net-based (Rhea-Fournier et al., 2016) and integrated acoustic-trawl (*e.g.* Hollowed et al., 2007; Logerwell et al., 2007, 2010; Chapter 2) surveys have been conducted in the GOA to sample capelin and other small pelagic fishes. Regional changes in distributions and abundances of capelin are not readily detected using these data due to the following: gear-related sampling bias in net-based surveys that sample discreet water depths using surface (Parker-Stetter et al., 2013; Rhea-Fournier et al., 2016) or bottom (Hollowed et al., 2012; Mueter and Norcross, 2002) trawls; limited spatial coverage relative to capelin range (Hollowed et al., 2007; Logerwell et al., 2007, 2010); limited program duration (~2-3 years) (*i.e.* GOAIERP, Chapter 2) and/or lack of standardized sampling procedures among surveys.

The goal of this study is to investigate responses of age-1+ capelin to temperature-related changes in the GOA shelf ecosystem using seven years of late summer data collected from 2000 to 2013 during a survey designed to sample age-0 walleye pollock (*Gadus chalcogrammus*, hereafter pollock). The specific objectives of this study are to: 1) quantify spatiotemporal changes in capelin occurrence and positive catch rates related to *in situ* measurements of temperature-related covariates, 2) characterize interannual variability in capelin distributions and mean density to quantify shifts in capelin distributions and relative abundance during relatively

warm and cold years, and 3) measure correlations between annual estimates of mean capelin density and an alternate GOA-based capelin index, and also large-scale climate indices.

## 4.2 METHODS

This study used data from a net-based, fisheries oceanographic survey conducted by the AFSC Ecosystems and Fisheries-Oceanography Coordinated Investigations (EcoFOCI) Program. The primary objectives of the EcoFOCI late-summer small-mesh trawl survey are to monitor the distribution and abundance of age-0 pollock prior to the onset of winter, and to investigate the influence of oceanographic conditions and zooplankton prey resources on variability in densities of pollock and other small pelagic fishes.

### 4.2.1 Study area and survey design

Initiated in 2000, the EcoFOCI trawl survey has been conducted biennially during odd years in late-summer (August-September) over the continental shelf in the western GOA (hereafter WGOA region) between Shelikof Strait and the Shumagin Islands (Fig. 4.1). In 2005, a second survey area was added in the central GOA (hereafter CGOA region) that sampled the shelf along the southeast side of Kodiak Island. In both regions, the shelf is relatively wide (> 200 km) and characterized by complex circulation patterns and bathymetric (*e.g.* submarine banks, troughs, and a sea valley) features (Mordy et al., 2016; Stabeno et al., 2016a). Predetermined stations were occupied within each region to sample fish communities and water properties. Surveys were conducted 24 h $d^{-1}$ by the NOAA Ship *Miller Freeman* (2000-2009) and NOAA Ship *Oscar Dyson* (2013).

*4.2.2. Data collection*

Seven years of survey data from the EcoFOCI trawl survey conducted during the period of 2000 to 2013 were analyzed for this study: 2000 and all odd years except 2011. The 2011 survey was excluded from the analysis because it was conducted one month later than the other surveys and only sampled a limited portion of the CGOA region due to logistic constraints. Fish were sampled using a 47 m long Stauffer (*i.e.* anchovy) midwater trawl (*cf.* Wilson et al., 1996) with a 3 mm codend liner, and fished using 1.5 x 2.1 m steel-V otter doors (566 kg each). Using net mensuration equations from Wilson et al., (1996), the net opening vertical height averaged 8.7 ± 0.1 m (mean ± SE) and the horizontal spread averaged 15.1 ± 0.02 m. Trawls were towed obliquely through the water column at a vessel speed of 1.3 to 1.5 $ms^{-1}$ (2.5 to 3 knots) to a maximum headrope depth of 20 m above the seafloor or 200 m, whichever was shallowest, and retrieved at a rate of 10 m $min^{-1}$ (Wilson, 2009). Headrope depth was monitored in real time with a Furuno CN24-40 net sounder or Simrad ITI trawl sonar. Trawl catches were sorted by species, enumerated, and weighed. For each species, standard length (SL) was measured for up to 100 fish (Wilson, 2009). Catch-per-unit-effort (CPUE) for capelin biomass density ($b$, g $m^{-2}$) for each trawl sample was standardized by

$$b = W \times \frac{D_{max}}{V} \tag{4.1}$$

where $W$ is the total catch biomass (g), $D_{max}$ is the maximum depth of the trawl (m) and $V$ is the water volume filtered ($m^3$). Water volume filtered was estimated using mean trawl mouth opening ($m^2$) and vessel distance (m) traveled between deployment and recovery of trawl doors following Wilson (2009).

Water temperature was measured at each station using a Sea-Bird Electronics (SBE) 19 SeaCat conductivity-temperature-depth (CTD) profiler attached to either a 1 $m^2$ Tucker trawl (2000-2007) or a 60 cm paired bongo net (2013). Both the Tucker trawl and paired bongo were

towed obliquely at a wire angle of 45° to a maximum depth of 10 m above the seafloor or 200 m, whichever was shallowest, and retrieved at a rate of 20 m $min^{-1}$. The CTD was used to monitor net depth, and the CTD profile was collected within an hour of the Stauffer trawl. At stations where the SBE 19 SeaCat was not deployed, a temperature profile was sampled using a SBE 39 temperature-pressure recorder attached to the headrope of the Stauffer trawl. Water temperature and pressure (*i.e.* depth) measurements from the CTD and SBE 39 were used from the up-cast of each tow, and integrated in 1 m depth increments.

### 4.2.2 **Modeling approach**

A geostatistical delta-generalized linear mixed model (hereafter delta-GLMM) adapted from Thorson et al. (2015b) was used to predict capelin occurrence and positive catch rates (*i.e.* non-zero densities). A delta (*i.e.* hurdle) model framework estimates the probability of occurrence separately from estimating catch rates where fish were present (Maunder and Punt, 2004). The first component of the delta model (Eq. 4.2) estimates the probability of occurrence, $p_i$, for sample $i$ by fitting a Bernoulli distribution to a binary response (0, 1) for $b_i$, where non-zero (*i.e.* $b_i > 0$) catches are set to 1. A gamma distribution is then fitted to the non-zero catches for $b_i$ to estimate positive catch rates, $r_i$

$$\Pr(b_i = B) = \begin{cases} p_i & \text{if } B = 0 \\ (1 - p_i)\ \text{Gamma}(b_i, \sigma^{-2}, r_i\sigma^2)\} & \text{if } B > 0 \end{cases} \quad (4.2)$$

where $\sigma^{-2}$ and $r_i\sigma^2$ are the shape and scale parameters of the gamma distribution, and $\sigma^2$is the positive catch rate variance.

Following Shelton et al. (2014), the delta-GLMM is a "semi-parametric" model that includes intercepts for each year, environmental covariates, and random effects for spatial and spatiotemporal covariance at each spatial location (*i.e.* knot, $s$) (Table 4.1). Treating spatial and

spatiotemporal covariance as random effects enables the use of a stochastic process to represent the cumulative effect of physical and ecological factors on capelin distributions that are not directly measured (Dormann et al., 2007; Thorson et al., 2015c). Both spatial and spatiotemporal covariance are represented by a Gaussian Markov random field (GRF) as

$$\omega \sim MVN(0, \boldsymbol{\Sigma}_{\omega}) \tag{4.3a}$$

$$\varepsilon_t \sim MVN(0, \boldsymbol{\Sigma}_{\varepsilon}) \tag{4.3b}$$

where $MVN$ is a multivariate normal distribution fixed at 0, $\boldsymbol{\Sigma}_{\omega}$ is the covariance of the random field at each sample's spatial location $s_i$ (*i.e.* spatial residuals) following a Matérn distribution with smoothness $v = 1$, and $\boldsymbol{\Sigma}_{\varepsilon}$ is the covariance of the random field at each location in year $t_i$ (*i.e.* spatiotemporal residuals) (Thorson et al., 2015b, 2015c). Covariance between each pair of spatial locations is specified to be stationary and assumed to be isotropic (Thorson et al., 2015c). The stochastic partial differential equation (SPDE) approximation (Lindgren et al., 2011) was used to estimate the conditional probability of $\boldsymbol{\Sigma}_{\omega}$ and $\boldsymbol{\Sigma}_{\varepsilon}$. The three components of the precision matrix used in the SPDE approximation (*cf.* Lindgren et al., 2011) were computed within the R statistical environment (http://www.R-project.org; R Core Development Team, 2015) using the R package *INLA* (http://www.r-inla.org, Rue et al., 2009). Unique random fields for spatial and spatiotemporal covariance were created to estimate $p$ and $r$ (Table 4.1). The number of spatial locations ($s$) was determined by excluding samples that were not located within 37 km (~20 nmi) of at least one other sample from a different year.

To account for potential differences in capelin catch rates relative to the time of day a sample was collected, day and night samples were treated as separate categories (hereafter day-night category) within a joint modeling framework. Previous studies have adapted the delta-GLMM framework to jointly estimate abundance and range shifts using biomass data for

multiple length categories from a single species (Thorson et al., 2017), and multiple species (Thorson et al., 2016). Thorson et al. (2015a) showed that jointly estimating the distributions of multiple rockfish species within a spatial GLMM improved accuracy in predicted catches compared to modeling each species individually. Assuming that the day or night category does not influence spatial correlations related to capelin occurrence and positive catch rates, this study included locations from all day and night samples in the same triangulated mesh (Fig. 4.2) to create the precision matrix that estimates $\mathbf{\Sigma}_\omega$ and $\mathbf{\Sigma}_\varepsilon$. Parameters for fixed and random effects and derived quantities are estimated separately for each day-night category, sharing only the spatial mesh and range of spatial and spatiotemporal residuals ($\kappa$).

To estimate probability of occurrence, a logit link is used to linearize $p_i$

$$logit(p_i) = \alpha_{c(i),t(i)} + \sum_{k=1}^{n_x} \alpha_{c,k} X^{(p)}(s_i, t_i, k_i) + \omega^{(p)}(s_i, c_i) + \varepsilon^{(p)}(s_i, c_i, t_i) \quad (4.4)$$

where $\alpha_{c(i),t(i)}$ is the intercept for each year $t_i$ and day-night category $c_i$, $\alpha_{c,k}$ are the parameter estimates for each day-night category for the effects of covariates $X^{(p)}(s_i, t_i, k_i)$ on the probability of occurrence at a given location and year, $\omega^{(p)}(s_i, c_i)$ is the spatial residual for a given location and day-night category, and $\varepsilon^{(p)}(s_i, c_i, t_i)$ is the spatiotemporal residual for a given location, day-night category, and year. Covariate inputs to the probability of occurrence component of the delta-GLMM ($X^{(p)}$) included two categorical factors for survey region (*i.e.* CGOA or WGOA, Fig. 4.1) and bottom depth (*i.e.* bank or trough, defined in Table 4.1), and a combination of continuous, temperature-based covariates

$$X^{(p)}(s_i, c_i, t_i) = Reg_{s(i)} + fBT_{s(i)} + x_j(s_i, t_i, k_i) \quad (4.5)$$

where $Reg_{s(i)}$ is the region factor and $fBT_{s(i)}$ the bottom depth factor at a given spatial location, and $x_j(s_i, t_i, k_i)$ is the combined effect of temperature-based covariates at a given location and year (Eq. 4.6a-c). Temperature-based covariates refer to any of the following variables derived

from *in situ* temperature profiles (Table 4.1): local temperature ($Temp_L$, the mean water column temperature from the surface to 200 m or 10 m off bottom, whichever was shallower), water column stratification ($\Delta Temp_{1m-btm}$, represented by the difference between temperature at 1 m and the bottom), regional temperature ($Temp_R$, the average water temperature of all locations within a region and bottom depth factor in a given year), and relative local temperature ($\Delta Temp_{L-R}$, represented by the difference in local and regional temperatures). Temperature profiles were averaged for the upper 200 m of the water column to account for uncertainty in capelin vertical distributions during 24-hr sampling by the EcoFOCI survey. Capelin in the CGOA and Southeast Alaska vary their vertical position relative to bottom depth and occupy a wide range of depths during daytime (Chapter 2). The magnitude and direction of capelin diel vertical movements can also vary by year (Mowbray, 2002) and age-class (Gjøsæter, 1998) in late summer and fall. Therefore a mean water column temperature was assumed to be a more robust measure of thermal exposure to capelin over a 24-hr period compared to measurements from a discrete depth (*e.g.* surface or bottom temperature).

Temperature-based covariates were grouped in one of three combinations ($x_j$, hereafter covariate combination) to minimize collinearity among the variables,

$$x_1(s_i, t_i, k_i) = Temp_L(s_i, t_i) + Temp_L^2(s_i, t_i) \quad (4.6a)$$

$$x_2(s_i, t_i, k_i) = \Delta Temp_{1m-btm}(s_i, t_i) \quad (4.6b)$$

$$x_3(s_i, t_i, k_i) = Temp_R(s_i, t_i) + \Delta Temp_{L-R}(s_i, t_i) \quad (4.6c)$$

where $x_1(s_i, t_i, k_i)$ is the local temperature, $Temp_L(s_i, t_i)$, and its quadratic term, $Temp_L^2(s_i, t_i)$, (hereafter absolute temperature) at a given location and year, $x_2(s_i, t_i, k_i)$ is water column stratification ,$\Delta Temp_{1m-btm}(s_i, t_i)$, (hereafter stratification) at a given location and year, and

$x_3(s_i, t_i, k_i)$ is the regional temperature, $Temp_R(s_i, t_i)$, and relative local temperature, $\Delta Temp_{L-R}(s_i, t_i)$, (hereafter relative temperature) at a given location and year.

To account for potential differences in the relative influence of temperature-related covariates on capelin over banks and troughs (Chapter 3), Eq. 4.5 was expanded to include an interaction between the covariate combination, $x_j$, with the bottom depth factor ($fBT$). Referred to as a depth-stratified model, a set of coefficients for one of the three potential covariate combinations was estimated for samples located over banks, and a separate set of coefficients was estimated for samples located in troughs. Estimation of depth-stratified parameters is designed to account for potential differences in oceanographic properties among bottom depth factors that influence distributions of capelin. The model does not require the same covariate combination to be estimated for bank and trough samples

$$X^{(p)}(s_i, c_i, t_i) = Reg_{s(i)} + fBT_{s(i)} + x_j^{(B)}(s_i, t_i, k_i) + x_j^{(T)}(s_i, t_i, k_i) \quad (4.7)$$

where $x_j^{(B)}(s_i, t_i, k_i)$ is the covariate combination for samples at a given location and year over banks, $x_j^{(T)}(s_i, t_i, k_i)$ is the covariate combination for samples located in troughs, and the region and bottom depth factors are estimated using all samples.

To estimate positive catch rates (*i.e.* non-zero densities), a log link is used to linearize $r_i$

$$log(r_i) = \beta_{c(i),t(i)} + \sum_{k=1}^{n_x} \beta_{c,k} X^{(r)}(s_i, t_i, k_i) + \omega^{(r)}(s_i, c_i) + \varepsilon^{(r)}(s_i, c_i, t_i) \quad (4.8)$$

where parameters are defined identically to those used to calculate $logit(p_i)$ in the occurrence sub-model (Eq. 4.4): $\beta$ represents coefficients for intercepts and fixed effects of covariates $X^{(r)}$ on catch rates in the same way as $\alpha$, and random effects for spatial ($\omega^{(r)}$) and spatiotemporal ($\varepsilon^{(r)}$) residuals are calculated identically to $\omega^{(p)}$ and $\varepsilon^{(p)}$ for spatial locations where fish were

present. Similarly, parameters for $X^{(r)}$ are defined identically to those used to calculate $X^{(p)}$ in Eq. 4.5 and Eq. 4.7 for the occurrence sub-model.

Parameter estimation using maximum marginal likelihood was conducted within the R environment using Template Model Builder (TMB, Kristensen et al., 2016) with the R package *VAST*, version 1.1.0 (https://github.com/James-Thorson/VAST; Thorson and Barnett, 2017). TMB calculates the marginal likelihood of fixed effects when integrated across random effects using the Laplace approximation (Skaug and Fournier, 2006). The marginal likelihood was then optimized using a conventional nonlinear optimizer in the R environment to estimate fixed effects by maximizing the log-marginal likelihood (Thorson et al., 2015b, 2015c).

### 4.2.3 **Data analyses**

This study's analyses are designed to examine the influence of temperature-related covariates on capelin horizontal distributions and density to infer the response of GOA capelin to temperature variations in the pelagic environment. The first two study objectives examine four potential movements that could be inferred as a cumulative response of capelin to temperature variability: a shift between shallow banks and deeper troughs, a shift in distribution to cooler or warmer water over banks or in troughs, an across-shelf (southeast to northwest) shift between inshore and offshore areas of the GOA shelf, and an along-shelf (southwest to northeast) shift between lower and higher latitudes. Objective 1 examines the first two potential movement responses by quantifying differences in distributions between banks and troughs (*i.e.* the bottom depth factor), and the influence of temperature-related covariates on capelin occurrence and positive catch rates within each bottom depth factor. Objective 2 characterizes interannual variability in distributions using spatial statistics to examine across- and along-shelf distribution

shifts. Objective 2 also quantifies interannual variability in mean capelin densities to examine changes in relative abundance within and between the WGOA and CGOA regions during warm and cold years. Objective 3 measures correlations between mean capelin densities with another GOA-based capelin abundance index and climate indices to assess consistency and strength of relationships.

*4.2.4.1. Evaluating potential day-night bias*

Day and night capelin CPUEs were examined to evaluate if bias existed between time of day and catch rate during the EcoFOCI trawl survey's 24-hr sampling. This preliminary assessment was conducted because a previous analysis of the EcoFOCI trawl survey from 2000-03 (Wilson, 2009) reported that capelin densities were significantly higher at night compared to samples collected during the day. Sample time of day was categorized into day or night based on solar altitude (Table 4.1), calculated as a function of location and time using the R package *oce* version 0.9-21 (https://github.com/dankelley/oce). A solar altitude higher than 0° above the horizon was classified as day, and lower than 6° below horizon (*i.e.* civil twilight, as defined by the United States Naval Observatory; http://aa.usno.navy.mil/faq/docs/RST_defs.php) was considered night. Trawl samples that occurred during twilight (0 to -6°) were excluded from the analysis ($n$=29 out of 552 samples). Samples were summarized by year, region, and bottom depth factor to quantify differences in day and night capelin CPUEs within and between strata. Stations with paired day-night trawl samples, in which stations were sampled both during day and night within 24 hours during the 2000-2003 surveys, were compared to determine if a correction factor could be calculated to adjust day and night catch rates (*e.g.* Casey and Myers, 1998).

Day and night samples were analyzed separately in single-category delta-GLMM models with no covariate inputs ($X^{(p)}$ and $X^{(r)}$ set to 0), and then jointly as multiple categories within a delta-GLMM (hereafter multi-category, delta GLMM) to assess differences in model performance. Differences among the single-category and multi-category models were assessed by comparison of variance parameters for fixed and random effects (Table 4.1) and evaluation of model fits based on visual inspection of diagnostic plots for both components of the delta model. Model diagnostic plots included comparison of predicted occurrence probabilities ($p_i$) to observed occurrence probabilities, Q-Q plots, and sign deviance residual scatter plots for positive catch rates (Hardin and Hilbe, 2007; Zuur et al., 2009). Observed occurrence probabilities were converted to a 0 to 1 percentile from binary values of presence/absence ($b_i > 0 = 1$, otherwise 0) by sorting and averaging by their respective $p_i$ values in 0.05 increments.

*4.2.4.2. Influence of temperature variability on capelin distributions*

The influence of temperature variability on capelin occurrence and positive catch rates was quantified by comparing candidate models comprised of one of the 3 covariate combinations, $x_j$ (Eq. 4.6a-c) for each component of the multi-category, delta-GLMM. A candidate model was comprised of a separate covariate combination in the occurrence ($x_j^{(p)}$) and positive catch rates ($x_j^{(r)}$) submodels. Depth-stratified candidate models also included separate covariate combinations for banks ($x_j^{(B)}$) and troughs ($x_j^{(T)}$) for each sub-model. A total of 90 candidate models were assessed, including 9 candidate models with one covariate combination for each sub-model (3-$x_j^{(p)}$ x 3-$x_j^{(r)}$), and 81 depth-stratified, candidate models that were comprised of a set of 4 separate covariate combinations, one for banks and troughs within each sub-model (3-$x_j^{(p,B)}$ x 3-$x_j^{(p,T)}$ x 3-$x_j^{(r,B)}$ x 3-$x_j^{(r,T)}$).

Candidate models are named using the number for one of three possible covariate combinations (represented as $j$ in Eq. 4.6a-c) that were assessed in the occurrence ($x_j^{(p)}$) and positive catch rates ($x_j^{(r)}$) sub-models (separated by a "."), and whether or not it was a depth-stratified model (represented by "-"). For example, model M:1.2 is a multi-category model ("M") that included the absolute temperature covariate combination ("1"=$x_1$) in the occurrence sub-model and the stratification covariate ("2"=$x_2$) in the positive catch rates sub-model. Model M:1-3.2-2 is depth-stratified, multi-category model that included depth-stratified coefficients (*i.e.* interactions with $fBT$) in the occurrence sub-model for absolute temperature covariates for bank samples and relative temperature covariates for trough samples ("1-3"), and depth-stratified coefficients in the positive catch rates sub-model for stratification covariates for bank and trough samples ("2-2").

The best combination of temperature-based covariates among the 90 candidate models was determined using Akaike information criterion values corrected for finite sample size (AICc) (Burnham and Anderson, 2002). Predictions for capelin occurrence and positive catch rates from the "best" model (*i.e.* lowest AICc) were plotted by day-night category with temperature-based covariates included in the model. A bivariate loess smoother was fitted to the scatterplot to visualize the relationship.

*4.2.4.3. Interannual variability in capelin distributions and relative abundance*

Interannual differences in capelin distributions and mean densities were examined within and between the WGOA and CGOA regions using predicted catch rates from the "best" model. Predicted catch rates where fish were absent were set to zero, and then day and night catch rates were transformed to a common scale by dividing values by one standard deviation for the sample's respective day-night category. Scaled catch rates were mapped over bathymetric

features using the R package *marmap* version 0.9.6 (https://github.com/ericpante/marmap), which uses NOAA bathymetry data from the ETOPO1 Global Relief Model. Center of gravity (CG) and inertia, the mean location of the population and the dispersion of the population around its CG (Woillez et al., 2007), were used to characterize interannual differences in distributions within and between the regions. Using scaled, predicted catch rates for all samples, CG and inertia were calculated by year within each region and across both regions using the R package *RGeostats* version 11.1.2 (Renard et al., 2017; http://rgeostats.free.fr/). Annual estimates of capelin mean density, the average of predicted catch rates within each region by year and day-night category, were calculated to infer interannual differences in relative abundance.

*4.2.4.4. Measuring correlations between capelin densities with other capelin and climate indices*

Correlations were measured between this study's annual estimates of capelin mean density with another GOA-based capelin relative abundance index and large-scale climate indices. Used as ecosystem indicators for the GOA by the North Pacific Fisheries Management Council (Zador and Yasumishii, 2016), the three time series include: the capelin dynamic factor analysis (capelin DFA, NPFMC, 2016; http://access.afsc.noaa.gov/reem/ecoweb/) index, the Pacific Decadal Oscillation (PDO, Mantua et al., 1997; http://jisao.washington.edu/pdo/) , and the Multivariate El Niño Southern Oscillation (ENSO) Index (MEI, Wolter and Timlin, 1993, 1998; https://www.esrl.noaa.gov/psd/enso/mei/table.html). The capelin DFA integrates multiple data series related to seabird chick diets (black-legged kittiwakes, *Rissa tridactyla*; common murres, *Uria aalge*; rhinoceros auklets, *Cerorhinca monocerata*; and tufted puffins, *Fratercula cirrhata*) and groundfish stomach contents (arrowtooth flounder, *Atherestes stomias*; Pacific cod, *Gadus macrocephalus*; P. halibut, *Hippoglossus stenolepis*; walleye pollock, *G. chalcogrammus*) to calculate an annual estimate of capelin relative abundance. The PDO index represents the first

principal component of North Pacific sea surface temperature (SST) anomalies above 20° N. A winter PDO index was calculated by averaging monthly, standardized values from December through February. The MEI represents the first principal component of six variables observed over the tropical Pacific: sea-level pressure, zonal and meridional surface winds, SST, surface air temperature, and total cloudiness fraction of the sky. A winter index was based on averaged MEI values from December and January. Both the PDO and MEI time series have been shown to be strongly correlated with physical dynamics of the GOA that are correlated with biologically-relevant processes (Hermann et al., 2016).

Pearson correlation coefficients were calculated for predicted mean capelin density from the WGOA region with the capelin DFA and climate time series. Correlations were not measured for the CGOA region since only data from four years are analyzed in this study. To account for potential lagged responses between relative abundance and climate time series, correlations were measured between mean capelin density and each index lagged by 0, 1, and 2 years prior to the Eco-FOCI surveys.

## 4.3 RESULTS

### 4.3.1 Data summary

The GOA underwent a period of warming from 2001-2005 that was then followed by cooler temperatures (Fig. 4.3). In the WGOA, mean local water temperatures ($Temp_L$) averaged 8.6 ± 0.1° C (mean ± SE) across all years, varying from a low of 7.6 ± 0.2° C in 2013 to a high of 9.5 ± 0.2° C in 2003. The average water temperature in the CGOA from 2005 to 2013 was 8.4 ± 0.1° C, with 2013 being the coolest year (7.9 ± 0.2° C) and 2005 the warmest (9.4 ± 0.2° C). Temperatures were relatively higher over banks compared to troughs, but the overall warming

and cooling pattern observed during the seven data years was still apparent in both bottom depth categories. While temperatures over WGOA banks steadily declined from 2005 to 2013, temperatures dropped in the CGOA by 1.5° C from 2005 to 2007 but then remained within 0.1° C in 2009 and 2013. The contrast in cooling rates between the regions resulted in temperatures over CGOA banks that were lower than the WGOA by 1.2° C in 2007 and 0.7° C in 2009. In comparison, temperature differences between regions were less pronounced in troughs during these years (0.5° C in 2007, 0.3° C in 2009).

Water column stratification ($\Delta Temp_{1m-btm}$) also varied among years (Fig. 4.3), but was not closely associated with interannual differences in temperature. In the WGOA, $\Delta Temp_{1m-btm}$ ranged from 3.7 to 4.5° C during the first six years that were sampled, but then increased sharply to a $\Delta Temp_{1m-btm}$ of 5.6° C in 2013. In contrast, stratification in the CGOA varied from a $\Delta Temp_{1m-btm}$ of 3.3° C (2009) to 4.4° C (2007). There were relatively large reductions in the magnitude of stratification (*i.e.* $\Delta Temp_{1m-btm}$ ± 1° C compared to other years) over CGOA banks in 2009 and CGOA troughs in 2009 and 2013, indicating increased mixing of the water column.

Capelin mean lengths from Stauffer trawl samples also varied among years, regions, and bottom depth categories (Fig. 4.4). Capelin lengths ranged from 40 to 142 mm SL ($n = 5986$), of which 99.5 % were longer than 60 mm. Length frequency distributions are assumed to be unbiased given that selectivity for capelin has not been assessed for the Stauffer trawl, although it is acknowledged that selectivity bias has been reported for capelin sampled by other mid-water nets (*e.g.* De Robertis et al., 2017a; Nakashima, 1990). Based on length-age relationships from Brown (2002), this minimum size indicates the Stauffer trawl sampled capelin that were one year or older. Larger fish (mean length ≥ 84.6 mm SL over banks, ≥ 88.3 mm in troughs) occurred in

the WGOA during the warmest years of 2001, 2003, and 2005 (Fig. 4.3), while the largest fish in the CGOA occurred during both a warm (2005) and a cool (2007) year. The smallest mean lengths observed in either region occurred in 2013 over WGOA banks (71.3 ± 1.0 mm, mean ± SE) and troughs (74.2 ± 0.8 mm), coinciding with the coldest mean temperatures and highest stratification levels compared to other years (Fig. 4.3). Despite relatively cooler temperatures in 2013 in both regions, mean length of capelin over CGOA banks was the same as in 2009. In most years, mean lengths were smaller over banks in both regions and there was only one distinct length mode in each bottom depth category. The one exception, in 2013, two distinct length modes occurred at approximately 90 and 110 mm.

### 4.3.2 **Evaluating potential day-night bias**

#### 4.3.2.1 *Characterizing variability in catch rates between day and night*

Differences in capelin occurrence (Table 4.2) and catch rates (Fig. 4.5) occurred between day and night and varied across years, regions, and bottom depth strata. Positive catches were observed more frequently at night (70% of night trawl samples) than during the day (43% of day trawl samples). In the WGOA, the proportion of non-zero samples was relatively higher in troughs (50% day, 78% night) compared to over banks (30% day, 52% night). In contrast, the occurrence of capelin over CGOA banks during the day (31%) was less than half that occurred at night (75%). Occurrence was relatively high over CGOA troughs with less of a difference from day to night (66% day, 73% night) compared to CGOA banks. Capelin CPUEs were also typically higher at night (Fig. 4.5), sometimes by more than an order of magnitude (*e.g.* WGOA banks in 2000-2005), while at other times there was no discernible difference between night and day CPUEs (*e.g.* CGOA trough in 2007-2009). In both regions, the magnitude of differences in

CPUEs between day and night varied among years over banks and troughs. These differences varied during years of low (2000-2003) and high (2005, 2007) CPUEs. Comparison of over 100 stations with paired day-night samples from the 2000-2003 surveys did not reveal a clear relationship that could be used to calculate a correction factor between day and night CPUEs (not shown). Therefore, day and night CPUEs were treated as separate indices throughout the rest of this study.

*4.3.2.2 Comparison of single- and multi-category models*

The multi-category model improves precision and overall model performance compared to the single-category day and night models. In both single-category models, most variance parameter estimates are either higher than the matching parameter in the multi-category model or estimated as 0 for a measure of variation of spatial or spatiotemporal residuals ($\tau$). A 0 value indicates that random effects associated with that parameter do not contribute to the model (Table 4.3). Compared to the multi-category model, the day-only model has relatively higher variance ($\sigma^2$) and variation of spatiotemporal residuals ($\tau_\varepsilon^{(r)}$) in the positive catch rate sub-model, a larger range of spatial and spatiotemporal residuals in the occurrence sub-model ($\kappa^{(p)}$), and produces estimates of 0 for $\tau_\varepsilon^{(p)}$ in the occurrence sub-model and for the variation of spatial residuals ($\tau_\omega^{(r)}$) in the positive catch rate sub-model. All variance parameter estimates for the night-only model are either higher or 0 relative to the multi-category model. The improved (*i.e.* lower) estimates for 9 of the 10 parameters related to spatial and spatiotemporal random effects ($\tau$ and $\kappa$) is attributed to minimizing gaps in the spatial mesh (Fig. 4.2) used to create the precision matrix that estimates covariance among locations within the random fields ($\mathbf{\Sigma}_\omega$ and $\mathbf{\Sigma}_\varepsilon$).

Visual inspection of model diagnostics (Fig. 4.6) indicates that the night-only model estimated occurrence probabilities have lower precision than both the day-only and multi-category models. Poor precision in the night-only model is based on the relatively large confidence interval for predicted probabilities and unbalanced fit to observed probabilities less than 0.5. The day-only model estimates for positive catch rates have lower precision compared to the night-only and multi-category models based on the relatively poor, unbalanced fit in the Q-Q plot and non-uniformly distributed residuals in the scatter plot (Zuur et al., 2009). In contrast, the multi-category model had the best fit to both observed occurrence probabilities and positive catch rates. These results support the use of the multi-category model to examine the influence of temperature-based covariates on capelin distributions.

### 4.3.3 **Influence of temperature variability on capelin distributions**

A total of 90 candidate models were analyzed to quantify the influence of temperature variability on capelin occurrence and positive catch rates (Table 4.4). The "best" model, M:2-1.2-2, predicts that the probability of capelin occurrence increases in waters over banks that are more stratified and in troughs where temperatures are approximately 8 to 9° C. Positive catch rates increase in more stratified waters over banks but less stratified waters within troughs (Fig. 4.7). The best model explained 54.84% of observed variability in capelin distributions (Table 4.4). Visual inspection of its diagnostic plots showed good fits to both components of the delta-GLMM (Fig. 4.6). Model selection results for other candidate models indicated that the depth-stratified models were more effective at explaining variability in capelin distributions than models that did not include an interaction with $fBT$ ($\Delta$AICc $\geq$ 26.01 from best model). The best model outperformed other depth-stratified models that were comprised of the same temperature-

based covariate combination for banks and troughs in both delta-GLMM sub-models (ΔAICc ≥ 10.09) or used the same covariate combination within each bottom depth category in both sub-models (ΔAICc ≥ 5.44).

Predicted capelin occurrence probabilities and positive catch rates from the best model were plotted to visualize relationships with temperature-based covariates and to examine potential differences between day-night, regions, and bottom depth categories (Fig. 4.7). During both day and night, inflections in fitted loess smooth lines (Zuur et al., 2009) indicated that increases in capelin occurrence over banks remained constant or declined in waters with a $\Delta Temp_{1m-btm}$ greater than 3° C, although occurrence probabilities over CGOA banks continued to increase at night in more stratified waters. Over troughs where capelin occurred in waters that ranged from 5.7 to 11.3 ° C, fitted smooth lines indicated that predicted capelin occurrence probabilities peaked between mean local temperatures of approximately 8 to 9° C in both regions and declined sharply in waters warmer than 10.5° C. Positive catch rates over banks declined sharply in well-mixed waters ($\Delta Temp_{1m-btm}$ < 1° C), but otherwise showed a linear increase in more stratified waters as indicated by the fitted smooth lines. Similarly, positive catch rates were highest in less stratified waters within troughs and exhibit a linear negative relationship with stratification. Occurrence probabilities are predicted to be higher within troughs compared to over banks during both day ($\alpha_{fBT}$ = 1.32) and night ($\alpha_{fBT}$ = 1.86), while regional differences ($\alpha_{Reg} \leq 0.33$) are relatively less important (Table 4.5). In contrast, capelin positive catch rates based on day samples are predicted to be much higher in the CGOA ($\beta_{Reg}$ = 1.64), with night catch rates predicted to be slightly higher in the WGOA ($\beta_{Reg}$ = -0.07). Similar to the occurrence sub-model, catch rates are predicted to be higher within troughs during the day ($\beta_{fBT}$ = 0.37) and at night ($\beta_{fBT}$ = 0.30). The large standard deviations relative to the $\beta_{fBT}$ coefficients

(Table 4.5) and lack of apparent differences in predicted catch rates (Fig. 4.7) indicate that this predictor is of lower importance than other covariates in explaining variability in capelin non-zero densities.

Comparison of day and night parameter estimates supports the underlying assumption of the multi-category model that temperature variability influences capelin horizontal distributions similarly during day and night. The sign of coefficients estimated for day and night match for all temperature-based covariates (Table 4.5). Differences in the signs of coefficients for intercepts in 5 of 7 years between day-night categories in the occurrence sub-model (Table 4.5) are attributed to changes in the proportion of non-zero samples among years, regions, and bottom depth strata that were not consistent between day and night samples (Table 4.2).

### 4.3.4 **Interannual differences in capelin distributions and relative abundance**

There were clear interannual differences in capelin distributions within and between regions. Capelin densities in 2000 to 2003 were low relative to later years during the day and at night (Fig. 4.8). In all years the frequency of non-zero catches was consistently lower during day compared to night (Table 4.2, Fig. 4.8). Non-zero catches were more frequent in both regions during 2005 and 2007, and there was a sharp decrease in non-zero catches in 2013 (30.8%) compared to 2009 (80.0%) within WGOA troughs that was not observed in the CGOA. Relatively high catch rates (*i.e.* scaled predicted CPUE $\geq 1$, equivalent to 332.1 kg km$^{-2}$ for day and 975.0 kg km$^{-2}$ for night) were also less common during the day ($n = 22$) than at night ($n = 34$). During the day, 77.3% of high catch rates primarily occurred in the CGOA. At night, the total number of high catches across years was more evenly distributed between regions (19:15 = number of high catches in WGOA:CGOA), although regional differences were observed in 2007

(6:1), 2009 (1:3), and 2013 (1:2). High catch rates often occurred over or near the edges of banks, and were rarely observed over the outer part of the shelf near the shelf break (Fig 4.8).

In all years, capelin distributions were centered over the inner shelf of both regions (Fig. 4.9A). In the WGOA, CGs were located west of the Semidi Islands along the north side of Semidi Bank in all years except 2013, when the CG was located approximately 50 km to the east. In the CGOA, CGs for all years showed that capelin were centered over Middle Albatross Bank (between Barnabus and Chiniak Troughs). With the exception of 2013 in the WGOA, the long axis of inertia in each year extended parallel to the coastlines of the Alaska Peninsula (WGOA) and east side of Kodiak Island (CGOA). Longitudinal variability was greater in the WGOA (range 86.1 km) compared to the CGOA (37.7 km), whereas latitudinal variability was greater in the CGOA (range 49.2 km, versus 33.5 km in WGOA). In the four years that both regions were surveyed, capelin CGs calculated for both regions combined (referred to as "GOA") shifted approximately 150 km east and 66.9 km north in 2013. Contraction of the axes of inertia in 2013 further highlights the lack of capelin in the WGOA during that year.

The predicted mean density of capelin in the GOA varied among years and regions (Fig. 4.10), indicating that a rise and fall in GOA capelin occurred during the study period. In both day and night indices, capelin mean densities in the WGOA were relatively low in 2000-2003 prior to increasing by at least an order of magnitude in 2005. During the day, mean densities in both regions reached a peak in 2007 (409.0 ± 251.8 kg $km^{-2}$ in WGOA, 353.9 ± 122.8 kg $km^{-2}$ in CGOA). Daytime mean density declined sharply in the WGOA in 2009 to levels similar to that observed in 2003 and earlier, reaching a low of 2.6 ± 1.0 kg $km^{-2}$ in 2013. In the CGOA, relatively high mean densities persisted through 2009 before declining to 53.7±16.1 kg $km^{-2}$ in 2013. Estimates of mean density for the night index showed a different pattern. In both regions,

the night mean density peaked in 2005 (2067.3 ± 660.1 kg km$^{-2}$ in WGOA, 1164.8 ± 260.2 kg km$^{-2}$ in CGOA). Mean density in the WGOA remained relatively high in 2007 and then declined in 2009 and 2013. In contrast, mean density in the CGOA dropped to the lowest level in 2007 (423.3 ± 187.1 kg km$^{-2}$) among the four years surveyed, and then increased to 733.4 ± 333.9 kg km$^{-2}$ in 2013. The 2007 CGOA mean density estimate may be biased low due to the exclusion of four twilight samples located over Albatross Bank that averaged 540.3 ± 270.1 kg km$^{-2}$.

### 4.3.5 **Correlations between mean capelin density with GOA ecosystem indicators**

Pearson correlation coefficients ($r$) with other GOA indices were measured using night mean capelin densities (Fig. 4.11). The lower frequency of non-zero catch rates in day catches suggested that mean density estimates based on day samples may be biased due to sampling zeroes (*i.e.* fish were present but not sampled by the net), therefore they were excluded from this analysis. Unexpectedly, WGOA night mean capelin densities were negatively correlated ($r_0$= -0.71) with the capelin dynamic factor analysis (DFA) index. The lowest estimates in the 34-year capelin DFA index occurred from 2004 to 2007 (< -1.25), coinciding with the highest capelin mean density estimates in both regions and day-night categories in this study. The second highest anomaly in the capelin DFA index occurred in 2013 (2.15), while results from this study indicated that capelin densities in 2013 were relatively low in the WGOA and moderately high in the CGOA.

Comparisons of WGOA night mean densities with the PDO and MEI showed strong positive relationships with climate values lagged by one year ($r_1$ = 0.8 with PDO, $r_1$ = 0.7 with MEI) (Fig 4.11). Correlations between capelin densities and PDO and MEI values lagged by 0 ($r_0$ = 0.1 with PDO, $r_o$ = 0.36 with MEI) and 2 ($r_2$ = 0.68 with PDO, $r_2$ = 0.31 with MEI) years

were all positive, but weaker compared to climate values lagged by 1 year. It should be noted that while the PDO and MEI values lagged by 1 year include anomalies from strong negative phases ($PDO_{2000}$= -1.49, $MEI_{2000}$= -1.14), there were no strong positive phases (*i.e.* PDO/MEI values > 1) within either time series. Although correlations between CGOA night mean densities and the capelin DFA and climate indices were not measured due to small sample size ($n$=4 years), CGOA densities were included in the plots. Trends in CGOA mean densities relative to the other time series are consistent with WGOA values, but higher variance among CGOA values relative to the capelin DFA and PDO values suggests that the magnitude of the relationships are weaker.

## 4.4 DISCUSSION

### 4.4.1 Accounting for sampling bias related to day-night categories

This study demonstrated that bias associated with the time of day that a sample was collected can be reduced through the use of a multi-category, spatiotemporal mixed model. Adapted from Thorson et al.'s (2015a) multispecies model, estimating capelin distributions simultaneously for day and night categories within a joint modeling framework improved precision of predicted occurrence probabilities and positive catch rates compared to modeling samples from each category in separate models. The sign of parameter estimates for day and night categories matched for all temperature-based covariates, supporting the assumption that the influence of temperature on capelin distributions is independent of day-night category. In most years, trends in mean densities were similar among day and night indices, although the magnitude of predicted positive catch rates were consistently lower during the day.

Differences in the frequency of non-zero samples and magnitude of capelin CPUEs between day and night samples are attributed to changes in diel vertical movement and aggregating behavior that reduced the availability of capelin to the Stauffer trawl during the day. Small, discrete schools or aggregations of fish located near the seafloor are presumed to have a lower availability to the Stauffer trawl compared to relatively large aggregations or low densities of fish that occupy upper portions of the water column and/or are located closer to the surface. The higher frequency of positive catches observed at night (70% of night samples) compared to during the day (43% of day samples) suggests that capelin behave like typical diel vertical migrators: forming aggregations at greater depths during the day that disperse to lower densities within a wider range of shallower depths at night (Gjøsæter, 1998). These results are consistent with observations from the Northwest Atlantic, where bottom trawl catches of capelin and Atlantic herring (*Clupea harengus*) were higher during the day when these pelagic species were vertically distributed closer to the bottom (Casey and Myers, 1998). However, non-linear, order of magnitude differences between day and night CPUEs among years, regions, and bottom depth categories (Fig. 4.5) suggest that capelin diel behavior in the GOA is complex. High spatial and temporal variability in vertical distributions of pelagic fishes during the day is not uncommon (*e.g.* Stockwell et al., 2007), and is a likely source of differences in day-night CPUEs observed in this study. Without *in situ* information on capelin vertical distributions from acoustic data, net catch rates could not be adjusted using a correction factor to account for differences in availability to the Stauffer trawl. Treating day and night catch rates as separate indices of relative abundance was sufficient to address study objectives.

Acoustic data used to characterize vertical distribution and aggregative behavior of capelin can be used to identify potential sources of variability that affect differences in net catch

rates between day and night. In Chapter 2, capelin were reported to occupy a wide range of water column depths (13 to 192 m) that were greater than 20 m above the seafloor, with a median vertical position that was shallower over banks (center of mass = 55 m) compared to troughs (center of mass ≥ 110 m). Morphological differences in capelin aggregations also occurred between bottom depth categories: aggregations over banks were typically 5 to 20 m in height compared to small, discrete schools less than 5 m in height in troughs. Small capelin aggregations were also observed within 5-10 m of the seafloor in Barnabus trough in late August 2013 and over the Southeast Alaska shelf in early September (D. McGowan, unpublished data). The size and location of near-bottom aggregations would reduce availability of capelin to the Stauffer trawl compared to shallower aggregations, increasing the likelihood of not sampling fish near bottom and increasing the number of sampling zeroes. In the Barents Sea, capelin aggregate near bottom during the day and ascend to shallower depths at night from spring through fall, with the magnitude of diel changes in vertical distributions varying seasonally and among age classes (Gjøsæter, 1998). Capelin reduce their diel vertical movements and remain closer to the bottom during summer when light levels are higher and occur during most of the diel cycle (Gjøsæter, 1998). Diel vertical movements are more evident in fall with higher changes in light intensity between day and night, especially among older capelin (Gjøsæter, 1998). High interannual variability in vertical position, direction of diel migrations, and proximity to the seafloor has also been reported for capelin off Newfoundland (Mowbray, 2002), potentially explaining the nonlinear differences among years in net catch rates for day and night observed in this study.

### 4.4.2 **Influence of temperature on capelin distributions**

Model selection results indicate that temperature-related covariates explain variability in capelin distributions over the GOA shelf, but that the relationship is complex and there are direct and indirect effects of temperature on occurrence and positive catch rates. The presence of capelin within troughs was related to local water temperature, with occurrence probabilities increasing as waters warmed to approximately 8 to 9° C and then dropping sharply as temperatures rose above 10.5° C. Local temperature was not a strong predictor of density, as increases in positive catch rates in troughs were associated with reduced stratification, a measure related to vertical mixing (and indirectly primary production) over the GOA shelf (Stabeno et al., 2016a). Primary production is enhanced at the head of troughs over the GOA shelf due to increased vertical mixing that results from the interaction of tidal currents and the Alaska Coastal Current with steep walls along troughs (Mordy et al., 2016; Stabeno et al., 2016a). This suggests that in troughs, capelin concentrated in areas of increased mixing (and higher production) that were within a mean temperature range of 5.7 to 11.3° C. Over banks, capelin occurrence and positive catch rates were associated with increased stratification. Although this is opposite to the predicted relationship for capelin with stratification in troughs, the result is not surprising given that the magnitude of stratification over banks was much lower than that in troughs, and that strong vertical mixing can potentially inhibit primary production over banks. Intense vertical mixing increases the supply of nutrients from troughs to the euphotic zone over banks (Cheng et al., 2012; Ladd et al., 2005; Mordy et al., 2016), but also simultaneously deepens the pycnocline and reduces phytoplankton densities in the euphotic zone, resulting in lower overall production (Cheng et al., 2012). Adjacent areas that are more stratified with a shallower pycnocline, such as along the edges of banks, would have relatively higher production. These model results, in

conjunction with observed distributions, suggest that capelin concentrate over or near the edges of GOA banks in waters that are relatively more stratified and associated with higher localized production.

The hypothesis that capelin concentrate over or near the edges of GOA banks is consistent with Chapter 3's results for distributions of capelin density over the CGOA shelf in August 2013 (just prior to the EcoFOCI sampling of the CGOA region) using acoustic-trawl data. Capelin occupied waters associated with warmer bottom temperatures and concentrated in close proximity to the edge of banks (*i.e.* the 100 m isobath) and in areas with reduced stratification. Results from Chapter 3 demonstrate that the sign and relative importance of bottom temperature and stratification on capelin occurrence and density are similar to this study's results for trough-based observations using an independent data set. This study's use of a depth-stratified model was able to differentiate how temperature-based covariates explain variability in capelin distributions in bank and trough habitats that have different oceanographic properties. The expanded domain and duration of this study also demonstrates that the influence of these covariates on capelin distributions is robust across the GOA.

This study examined temperature-related effects on capelin distributions. The response of capelin to temperature variability may be influenced by other environmental factors, such as physiological condition, prey availability, and predation risk. Growth, condition, feeding ecology, distribution, and population size of Atlantic capelin have all been shown to vary directly or indirectly to climate-related changes in sea temperatures (*e.g.* Buren et al., 2014; Mowbray, 2002; Orlova et al., 2010). Given a reduction in suitable habitat (Andrews et al., 2015), altered prey supply (Obradovich et al., 2014), or influx of predators (Hjermann et al., 2004), it's reasonable to assume that capelin will be more likely to occupy waters outside their preferred

thermal range if it would increase their net energy intake to optimize growth (Macarthur and Pianka 1966) and minimize exposure to predators (Gilliam and Fraser, 1987). Further examination of the combined effects of temperature with other environmental factors on capelin distribution and abundance is needed to understand the relative importance of mechanisms that influence how GOA capelin respond to different temperature regimes.

### 4.4.3 **Interannual variability in distributions and relative abundance**

Comparison of capelin mean densities with water temperatures averaged within each region indicates that there was not a clear relationship between interannual variation in capelin relative abundance and average annual temperature. Inferred from annual estimates of mean density from night catches, the relative abundance of capelin in the WGOA was highest when the mean water temperature was warmer than the 7-year average temperature (2005, 2007). Low capelin abundance also occurred in relatively warm years (2001, 2003). Unexpectedly, capelin abundance in the WGOA was low during all cold years (2000, 2009, 2013), which is contrary to other observations of capelin relative abundance from the Northeast Pacific (Anderson et al., 1997; Andrews et al., 2015). Low abundance in the WGOA in 2013 also coincided with a sharp increase in stratification and the lowest occurrence of non-zero samples in troughs. Similar to the WGOA, the highest mean density in the CGOA occurred during the region's warmest year (2005), but density was also relatively high during the coldest year (2013). Stratification also increased over CGOA banks in 2013, but not within troughs as mean densities remained relatively high across the region. Overall, interannual variation in mean density within each region was lower in the CGOA compared to the WGOA. Fluctuations in capelin relative

abundance appears to be independent of regional temperature in the CGOA, but high abundance in the WGOA only occurred during some (but not all) warm years.

These results suggest that the occurrence and density of capelin is relatively stable in the CGOA, while the WGOA is more likely to experience booms and busts in capelin abundance. Capelin were consistently located over Albatross bank in the four survey years examined in this study, and observations from other surveys support the premise that capelin are consistently distributed over the Kodiak shelf. Acoustic-based measurements from two independent surveys, the NOAA Alaska Fisheries Science Center (AFSC) Midwater Assessment and Conservation Engineering (MACE) Program's summer GOA pollock acoustic-trawl (AT) survey (Guttormsen and Yasenak, 2007; Jones et al., 2014, 2015, 2017) and the Gulf of Alaska Integrated Ecosystem Research Program's (GOAIERP) offshore upper trophic level survey (Chapter 2), observed aggregations of capelin over CGOA banks and/or within the troughs (often near the edges of the banks) in all years that they were conducted (MACE pollock AT survey: Jun-Aug in 2003, 2005, 2011, 2013; GOAIERP: Aug-Oct 2011, 2013). Additional acoustic-trawl surveys of limited spatial coverage that were conducted in the CGOA as part of process studies within Barnabus and Chiniak Troughs from 2000 to 2005 by the AFSC Fisheries Interaction Team (FIT) also reported capelin were consistently observed in all years (Hollowed et al., 2007; Logerwell et al., 2007, 2010).

The contrast in relative abundance between regions in 2013 (*i.e.* low in WGOA, moderate-to-high in CGOA) also resulted in the largest observed shift in capelin distributions northeastward towards Kodiak among the four years that were compared. Relatively high catch rates also occurred east of Kodiak over Portlock Bank and further to the northeast in 2013, but these observations were excluded from the CGOA domain because of the requirement that

samples from at least two years be located within 37 km of each spatial location to estimate spatiotemporal covariance. Both MACE and GOAIERP acoustic surveys also observed large capelin aggregations over Portlock Bank and lower densities of capelin over deeper shelf waters further to the east in 2013. These observations preclude determining if the changes in center of gravity and inertia in 2013 indicate a distributional shift to the east-northeast of the shelf, or a contraction of GOA capelin around Kodiak.

There are alternative explanations for the inconsistent relationship between interannual variations in relative abundance of GOA capelin and temperature within and between regions: displacement of capelin across the GOA shelf, expansion of capelin distributions during warm years and contraction during cold years, or spatiotemporal differences in capelin mortality rates due to shifts in predator distributions. Displacement of capelin along the GOA shelf, as indicated by differences in mean density between regions, would be consistent with observed spatial dynamics for capelin in the Barents Sea (Carscadden et al., 2013a), when increased flux of warm Atlantic water from the west and higher temperatures in the Barents Seas coincided with shifts in capelin distributions to cooler northern and eastern waters. The idea of expansion and contraction of GOA capelin from the Kodiak shelf is based on decadal variability in distributions of capelin catches during the AFSC BT survey, which showed increases in capelin CPUEs as the population expanded from the CGOA region across the GOA shelf since the 1980's (Mueter and Norcross, 2002; Ormseth, 2012). Interannual differences in capelin densities between regions may have also resulted from shifts in distributions of capelin predators (*e.g.* groundfish, Yang et al., 2005), resulting in variable capelin mortality rates and regional abundances. For example in the Eastern Bering Sea (EBS), predation on capelin by Pacific cod (*Gadus macrocephalus*) increased in years when distributions of cod extended further north over

the EBS shelf due to northward contraction of a cold water mass (*i.e.* the cold pool) that cod did not occupy (Ciannelli and Bailey, 2005). If movement of capelin between regions over the GOA shelf is limited, increases in predator abundance within one region may impact local capelin densities and abundance. Observations in the Barents Sea indicate that high predation can impact capelin abundance, when capelin recruitment was poor during years in which influxes of juvenile Atlantic herring (*Clupea harengus*) from the North Sea resulted in heavy predation on capelin larvae (Carscadden et al., 2013b; Hjermann et al., 2010, 2004).

To assess potential inaccuracies in this study's measure of relative abundance, mean density estimates from night catches were compared to other capelin indices to assess if trends in relative abundance were detected in multiple data sources. The capelin DFA index did not match this study's mean density estimates. The two indices had a strong negative relationship. Evaluation of acoustic-based estimates of capelin density from the five MACE summer pollock AT surveys and the two summer and fall GOAIERP surveys showed that differences in relative abundances between acoustic surveys and the EcoFOCI trawl survey were primarily due to differences in spatial coverage. Large aggregations of capelin sampled by the acoustic surveys in 2003 and 2013 were located outside of the EcoFOCI study area, while areas with high catch rates during the 2005 EcoFOCI survey were not sampled by the MACE pollock AT survey. When survey domains overlapped, distributions of acoustic- and net-based densities show similar patterns of relative abundance. Some of the variability in this study's mean density estimates can also be attributed to the exclusion of 31 twilight samples, including 11 with relatively high catch rates in the WGOA in 2009 and in the CGOA in 2007, 2009, and 2013. Capelin DFA anomalies were consistent with relative abundance estimates from both MACE and GOAIERP acoustic

surveys in 2013 and the MACE pollock AT survey in 2003, but were not in agreement in 2005, 2011, and 2015.

A key takeaway from this evaluation is that inconsistent and/or limited spatial coverage of GOA capelin will confound interpretations of annual variations in relative abundance and the boundaries of capelin distributions. O'Driscoll et al. (2002) demonstrated that acoustic sampling more accurately estimates biomass and relative abundance of patchily distributed capelin compared to net-based sampling due to density-dependent effects on catchability of large aggregations and differences in net selectivity among size classes of fish (*e.g.* De Robertis et al., 2017a; Williams et al., 2011). To detect changes in the boundaries of capelin distributions within a survey domain, O'Driscoll et al. (2002) concluded systematic sampling of the same grid of fixed locations with a trawl would be more effective because net-based sampling can detect low densities of fish that may be missed or misclassified by acoustic sampling (O'Driscoll et al., 2002).

Inconsistencies among net- and acoustic-based measures of capelin abundance with the diet-based capelin DFA index also point to limitations in using predator diets to assess changes in prey abundance. Diet-based indices, such as the capelin DFA, are more representative of occurrence probabilities rather than relative abundance given their limited sensitivity to detect changes in population abundance and susceptibility to bias related to changes in the abundance of other prey species or prey preferences among predators (Sydeman et al., 2017). Indices based on diets from central place foragers will also be sensitive to changes in prey availability that result from shifts in horizontal and vertical distributions that may be independent of prey abundance (Orians and Pearson, 1979).

### 4.4.4 **Correlations with GOA climate indices**

The strong correlation between WGOA mean capelin densities and one year lagged PDO and MEI indices implies that GOA capelin abundance may be more strongly influenced by environmental factors from the prior year than by processes operating during the year capelin were sampled. The PDO and MEI explained up to 30% of variability in the physical dynamics of the GOA that can be coupled to biologically-relevant processes (Hermann et al., 2016). Given that the Stauffer trawl samples age 1+ fish, interannual variability in capelin abundance may be more strongly influenced by environmental factors linked to climate-related processes that affect survival during early life stages during the first year of life. Determination of cohort size in Atlantic capelin varies among populations. Year-class strength was primarily determined by factors that determine survival of larval capelin within two weeks of spawning off Newfoundland, survival of age-0's by late summer in the Barents Sea, and survival of age-1's off Iceland (Carscadden et al., 2013b). The observed range of factors influencing recruitment in Atlantic capelin populations suggests that future GOA research should investigate potential biophysical coupling with spawning and larval abundance to identify mechanisms that influence recruitment variability.

### 4.4.5 **Summary**

This study investigated responses of capelin to temperature over the GOA shelf during warm and cold years. The influence of temperature-based covariates on variability in capelin distributions was quantified using a multi-category, spatiotemporal delta-GLMM that accounted for differences in capelin catch rates between day and night. Model results indicate that variability in capelin distributions over the GOA shelf is explained by a combination of factors

that are directly and indirectly related to temperature. Over shallow submarine banks, capelin concentrated in areas with relatively high water column stratification that are associated with high primary production due to relatively weaker vertical mixing. In troughs, capelin were most likely to occur in waters between 8 to 9° C and concentrated in areas that were less stratified and associated with higher production. During the seven years of survey data that were analyzed between 2000 and 2013, interannual variation in estimates of mean density indicate that the relative abundance of capelin was not directly related to regional mean temperatures, and that distributions shifted northeastward during the coldest year. This observed movement is in stark contrast to an expected expansion of capelin over the GOA shelf during cold years (*e.g.* Andrews et al., 2015; Ormseth, 2012) given the wide distribution of capelin across subarctic and arctic waters. Alternative explanations for observed differences within and between the WGOA and CGOA regions in distributions and relative abundance include displacement along the GOA shelf due to changes in temperature, expansion of GOA capelin across the shelf during warm years and contraction towards Kodiak during cold years, or spatiotemporal differences in capelin mortality due to shifts in predator distributions. Despite the lack of a clear relationship between capelin relative abundance and temperature, interannual variability in mean densities in the WGOA was strongly correlated with the PDO (and to a lesser extent the MEI) lagged by 1 year. This suggests that abundance of GOA capelin may be influenced by climate-related processes linked to North Pacific SST anomalies that affect capelin survival during their first year of life.

## 4.5 TABLES

**Table 4.1** – Glossary of indices, data, covariates, model parameters (fixed and random effects), and estimates used in analyses.

| Name | | Symbol (indices) |
|---|---|---|
| **Indices** | Observation | $i$ |
| | Spatial location (*i.e.* knot) | $s$ |
| | Year | $t$ |
| | Day-night category (Day > 0° solar altitude, Night < -6°) | $c$ |
| | Covariate | $k$ |
| | Temperature covariate combination (1 = absolute temperature, 2 = stratification, 3 = relative temperature) | $j$ |
| **Data and covariates** | | |
| | Observed CPUE (*i.e.* capelin biomass density, g $m^{-2}$) for sample *i* | $b_i$ |
| | Measured covariates | $X(s_i, t_i, k_i)$ |
| | Region category (WGOA, CGOA) | $Reg(s)$ |
| | Bottom depth category (Bank < 100 m, Trough ≥ 100 m) | $fBT(s)$ |
| | Local mean temperature (whole water column average) * | $Temp_L(s)$ |
| | Local mean temperature polynomial term | $Temp_L^2(s)$ |
| | Water column stratification ($Temp_{1m} - Temp_{btm}$) | $\Delta Temp_{1m-btm}(s)$ |
| | Regional temperature (mean $Temp_L$ by $Reg$, $fBT$, $t$) | $Temp_R(s)$ |
| | Relative local temperature ($Temp_L - Temp_R$) | $\Delta Temp_{L-R}(s)$ |
| **Fixed effects** (occurrence / positive catch rate) | | |
| | Intercept | $\alpha_{c,t}$ / $\beta_{c,t}$ |
| | Covariate effect | $\alpha_{c,k}$ / $\beta_{c,k}$ |
| | Variation of spatial residuals | $\tau_\omega^{(p)}(c)$ / $\tau_\omega^{(r)}(c)$ |
| | Variation of spatiotemporal residuals | $\tau_\varepsilon^{(p)}(c)$ / $\tau_\varepsilon^{(r)}(c)$ |
| | Range of spatial and spatiotemporal residuals | $\kappa^{(p)}$ / $\kappa^{(r)}$ |
| | Positive catch rate variance | $\sigma^2$ |
| **Random Effects** (occurrence / positive catch rate) | | |
| | Spatial variation | $\omega^{(p)}(s, c)$ / $\omega^{(r)}(s, c)$ |
| | Spatiotemporal variation | $\varepsilon^{(p)}(s, c, t)$ / $\varepsilon^{(r)}(s, c, t)$ |
| **Derived quantities** (occurrence / positive catch rate) | | |
| | Occurrence probability | $p_i$ |
| | Positive catch rates | $r_i$ |
| | Covariance of spatial residuals | $\boldsymbol{\Sigma}_\omega^{(p)}$ / $\boldsymbol{\Sigma}_\omega^{(r)}$ |
| | Covariance of spatiotemporal residuals | $\boldsymbol{\Sigma}_\varepsilon^{(p)}$ / $\boldsymbol{\Sigma}_\varepsilon^{(r)}$ |

* CTD profile measured temperature from 1 to 200 m or 10 m off bottom, whichever was shallower

**Table 4.2** – Number of trawl samples (*n*) summarized by year, region, bottom depth factor, and day-night category ("*D*"=day; "*N*"=night). The proportion of samples with positive catch rates for capelin is indicated within parentheses (%).

| | **WGOA: *n* = 386 (0.54 %)** | | | | **CGOA: *n* = 137 (0.58 %)** | | | |
|---|---|---|---|---|---|---|---|---|
| | Bank: 145 (0.40) | | Trough: 241 (0.63) | | Bank: 69 (0.46) | | Trough: 68 (0.69) | |
| | *D* | *N* | *D* | *N* | *D* | *N* | *D* | *N* |
| 2000 | 17 (0.47) | 17 (0.53) | 24 (0.38) | 25 (0.76) | - | - | - | - |
| 2001 | 16 (0.31) | 17 (0.41) | 26 (0.42) | 22 (0.73) | - | - | - | - |
| 2003 | 13 (0.15) | 11 (0.55) | 21 (0.71) | 20 (0.90) | - | - | - | - |
| 2005 | 8 (0.25) | 3 (1.00) | 10 (0.90) | 9 (1.00) | 9 (0.44) | 8 (0.75) | 7 (0.57) | 11 (0.91) |
| 2007 | 7 (0.29) | 4 (0.75) | 8 (0.63) | 9 (1.00) | 8 (0.25) | 6 (0.67) | 11 (0.45) | 7 (0.43) |
| 2009 | 10 (0.40) | 3 (0.33) | 10 (0.70) | 11 (0.91) | 10 (0.30) | 5 (0.60) | 7 (0.86) | 8 (0.75) |
| 2013 | 9 (0.11) | 10 (0.50) | 30 (0.27) | 16 (0.38) | 18 (0.28) | 5 (1.00) | 10 (0.80) | 7 (0.71) |
| **Total** | 80 (0.30) | 65 (0.52) | 129 (0.50) | 112 (0.78) | 45 (0.31) | 24 (0.75) | 35 (0.66) | 33 (0.73) |

**Table 4.3** – Model type, inputs, estimates of variance parameters, and fits for day and night single-category models and day-night multi-category model.

| **Model type** | | | | |
|---|---|---|---|---|
| Single- or multi-category | Single | Single | Multi | |
| Day-night category | Day | Night | Day | Night |
| **Model inputs** | | | | |
| Number samples | 289 | 234 | 523 | |
| Number spatial locations | 147 | 109 | 190 | |
| Number fixed effects | 21 | 21 | 40 | |
| Number random effects | 2608 | 2000 | 3296 | |
| **Variance parameters** | **Estimate (marginal SD)** | | | |
| $\tau_{\omega}^{(p)}(c)$ | 1.394 (0.341) | 12.599 (8.342) | 1.443 (0.343) | 2.212 (0.734) |
| $\tau_{\varepsilon}^{(p)}(c)$ | 0 (0.488) | 0 (3.792) | 0.723 (0.336) | 1.254 (0.753) |
| $\kappa^{(p)}$ | -3.085 (0.410) | -0.262 (0.648) | -3.063 (0.299) | |
| $\tau_{\omega}^{(r)}(c)$ | 0 (2.092) | 1.164 (4.173) | 0.388 (0.654) | 0.761 (0.706) |
| $\tau_{\varepsilon}^{(r)}(c)$ | 1.528 (0.312) | 5.245 (2.874) | 1.425 (0.285) | 1.406 (0.368) |
| $\kappa^{(r)}$ | -2.402 (0.448) | -0.659 (0.570) | -2.460 (0.331) | |
| $\sigma^2$ | 0.049 (0.114) | 0.267 (0.067) | 0.034 (0.115) | 0.219 (0.08) |
| **Model fit** | | | | |
| Negative log-likelihood | -24.336 | -172.574 | -186.146 | |
| Explained deviance | 72.4 % | 20.3 % | 44.7 % | |

**Table 4.4** – Temperature-based covariate combinations that comprised candidate models and model selection results for the multi-category delta-GLMM. Depth-stratified models, which estimate an interaction between continuous, temperature-based covariates and bottom depth factor (***fBT***), show three categories of models results (A-C) from the 81 potential depth-stratified candidate models. Results are also shown for candidate models that only assessed one covariate combination and did not estimate depth-stratified coefficients (D). Numbers under each bottom depth factor for the delta-GLMM Occurrence and Positive Catch rate sub-models correspond to the temperature-based covariate combination number for each candidate model that was assessed. Model performance is indicated by the difference in AICc values from the best model (ΔAICc) and explained deviance (Dev).

**Table 4.4 (cont'd)**

| **Temperature-based covariate combinations** | | |
|---|---|---|
| **Number** | **Descriptor** | **Covariates** |
| $x_1$ | Absolute temperature | $Temp_L + Temp_L^2$ |
| $x_2$ | Stratification | $\Delta Temp_{1m-btm}$ |
| $x_3$ | Relative temperature | $Temp_R + \Delta Temp_{L-R}$ |

**Model Selection Results**

| **Model Name** | **Occurrence** | | **Positive Catch** | | **# Parameters** | | **ΔAICc (Best AICc)** | **Dev (%)** |
|---|---|---|---|---|---|---|---|---|
| | Bank | Trough | Bank | Trough | Fixed | Random | | |
| **A.** *Depth-stratified models – best 3 among all potential candidate models* | | | | | | | | |
| M:2-1.2-2 | $x_2$ | $x_1$ | $x_2$ | $x_2$ | 58 | 3296 | 0 (420.02) | 54.84 |
| M:2-3.2-2 | $x_2$ | $x_3$ | $x_2$ | $x_2$ | 58 | 3296 | 2.07 | 54.53 |
| M:3-1.2-2 | $x_3$ | $x_1$ | $x_2$ | $x_2$ | 60 | 3296 | 4.17 | 54.81 |
| **B.** *Depth-stratified models – same covariate combination within bottom depth strata* | | | | | | | | |
| M:2-1.2-1 | $x_2$ | $x_1$ | $x_2$ | $x_1$ | 60 | 3296 | 5.44 | 54.63 |
| M:2-3.2-3 | $x_2$ | $x_3$ | $x_2$ | $x_3$ | 60 | 3296 | 6.85 | 54.42 |
| M:3-1.3-1 | $x_3$ | $x_1$ | $x_3$ | $x_1$ | 64 | 3296 | 14.91 | 54.41 |
| M:3-2.3-2 | $x_3$ | $x_2$ | $x_3$ | $x_2$ | 60 | 3296 | 16.11 | 53.04 |
| M:1-2.1-2 | $x_1$ | $x_2$ | $x_1$ | $x_2$ | 60 | 3296 | 21.14 | 52.29 |
| M:1-3.1-3 | $x_1$ | $x_3$ | $x_1$ | $x_3$ | 64 | 3296 | 25.69 | 52.81 |
| **C.** *Depth-stratified models – same covariate combination only* | | | | | | | | |
| M:2-2.2-2 | $x_2$ | $x_2$ | $x_2$ | $x_2$ | 56 | 3296 | 10.09 | 52.75 |
| M:3-3.3-3 | $x_3$ | $x_3$ | $x_3$ | $x_3$ | 64 | 3296 | 17.62 | 54.01 |
| M:1-1.1-1 | $x_1$ | $x_1$ | $x_1$ | $x_1$ | 64 | 3296 | 20.53 | 53.57 |
| **D.** *Same covariate combination, no interaction with depth factor* | | | | | | | | |
| M:2.2 | $x_2$ | | $x_2$ | | 52 | 3296 | 26.01 | 49.19 |
| M:1.1 | $x_1$ | | $x_1$ | | 56 | 3296 | 30.44 | 49.72 |
| M:3.3 | $x_3$ | | $x_3$ | | 56 | 3296 | 31.09 | 49.63 |

**Table 4.5** – Parameter estimates (Est.) and standard deviations (SD) for the best multi-category model (M:2-1.2-2).

| | **OCCURRENCE** | | | |
|---|---|---|---|---|
| | **Day** | | **Night** | |
| **Parameter** | Est. | SD | Est. | SD |
| $\alpha_{2000}$ | -1.27 | 0.73 | 0.56 | 0.98 |
| $\alpha_{2001}$ | -1.64 | 0.74 | -0.28 | 0.97 |
| $\alpha_{2003}$ | -0.87 | 0.75 | 0.88 | 1.11 |
| $\alpha_{2005}$ | -0.88 | 0.77 | 1.83 | 1.32 |
| $\alpha_{2007}$ | -1.76 | 0.81 | 0.59 | 1.14 |
| $\alpha_{2009}$ | -0.67 | 0.75 | 1.18 | 1.20 |
| $\alpha_{2013}$ | -2.06 | 0.75 | -0.61 | 0.97 |
| $\alpha_{Reg}$ | 0.33 | 0.79 | 0.17 | 1.13 |
| $\alpha_{fBT}$ | 1.32 | 0.41 | 1.86 | 0.71 |
| $\alpha_{\Delta Temp_{1m-btm}(\mathrm{B})}$ * | 0.66 | 0.33 | 1.07 | 0.52 |
| $\alpha_{Temp_L(\mathrm{T})}$ * | 1.18 | 0.69 | 3.43 | 1.47 |
| $\alpha_{Temp_L^2(\mathrm{T})}$ * | -0.69 | 0.41 | -1.42 | 0.76 |
| $\tau_{\omega}^{(p)}(c)$ | 1.28 | 0.39 | 1.56 | 0.77 |
| $\tau_{\varepsilon}^{(p)}(c)$ | 0.84 | 0.33 | 1.49 | 0.85 |
| $\kappa^{(p)}$ | -3.40 | 0.35 | | |
| | **POSITIVE CATCH RATES** | | | |
| | **Day** | | **Night** | |
| **Parameter** | Est. | SD | Est. | SD |
| $\beta_{2000}$ | -3.93 | 0.49 | -1.86 | 0.48 |
| $\beta_{2001}$ | -4.22 | 0.51 | -2.56 | 0.61 |
| $\beta_{2003}$ | -3.75 | 0.59 | -2.22 | 0.60 |
| $\beta_{2005}$ | -2.43 | 0.57 | 0.32 | 0.62 |
| $\beta_{2007}$ | -1.68 | 0.64 | -0.47 | 0.63 |
| $\beta_{2009}$ | -3.32 | 0.57 | -1.19 | 0.64 |
| $\beta_{2013}$ | -4.70 | 0.62 | -1.19 | 0.62 |
| $\beta_{Reg}$ | 1.64 | 0.44 | -0.07 | 0.48 |
| $\beta_{fBT}$ | 0.37 | 0.38 | 0.30 | 0.36 |
| $\beta_{\Delta Temp_{1m-btm}(\mathrm{B})}$ * | 0.87 | 0.45 | 0.71 | 0.36 |
| $\beta_{\Delta Temp_{1m-btm}(\mathrm{T})}$ * | -0.16 | 0.20 | -0.58 | 0.21 |
| $\sigma^2$ | 0.09 | 0.11 | 0.19 | 0.09 |
| $\tau_{\omega}^{(r)}(c)$ | 0.06 | 0.61 | 0.14 | 1.18 |
| $\tau_{\varepsilon}^{(r)}(c)$ | 1.15 | 0.27 | 1.46 | 0.25 |
| $\kappa^{(r)}$ | -2.64 | 0.39 | | |

* Indicates a depth-stratified coefficient (*i.e.* an interaction between the covariate with *fBT*), where (B) is for samples located over a bank and (T) for samples located over a trough.

## 4.6 FIGURES

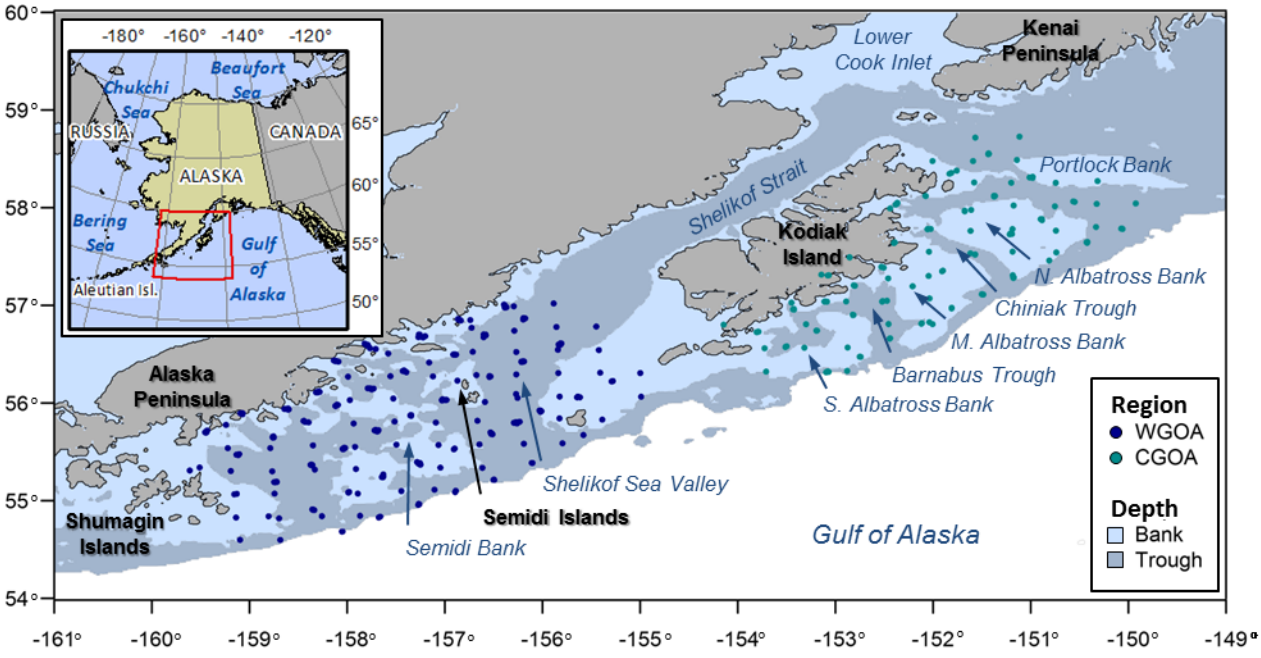


**Figure 4.1** – Survey domain and sample locations by region (CGOA, WGOA) and bottom depth category (Bank = < 100 m bottom depth, Trough = 100-500 m). The red box within the inset map of the Northeast Pacific outlines the survey domain. Key bathymetric (blue text) and geographic (black text) features mentioned in text are labeled.

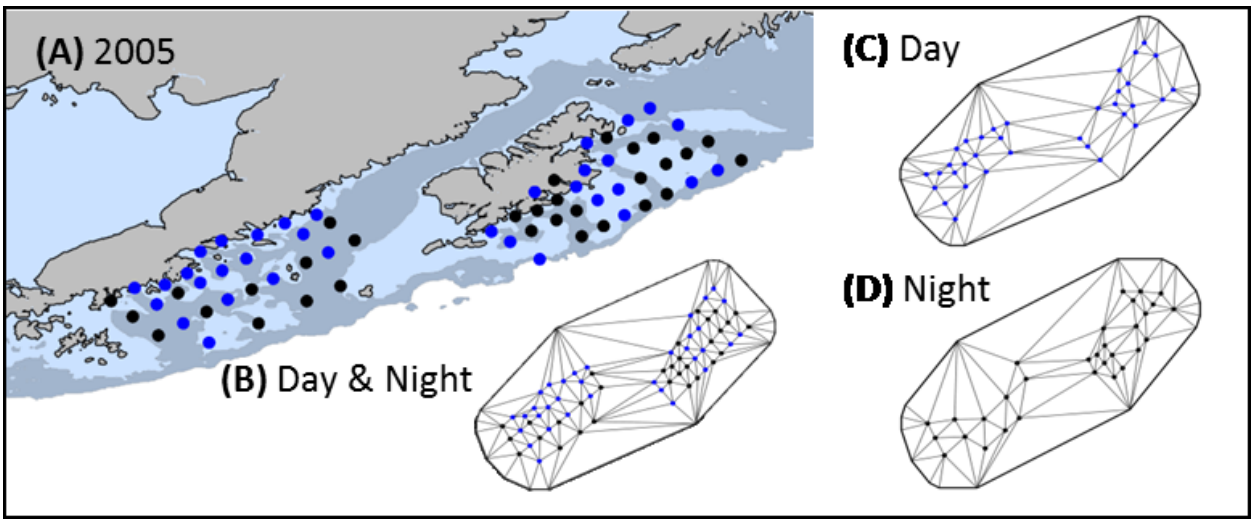


**Figure 4.2** – Example of samples stations and triangulated meshes used to create precision matrices to estimate conditional probabilities of $\boldsymbol{\Sigma}_{\boldsymbol{\omega}}$ and $\boldsymbol{\Sigma}_{\boldsymbol{\varepsilon}}$. Day (blue closed circles) and night (black closed circles) samples from the 2005 survey are used to demonstrate (A) the location of spatial knots within survey domain by day-night category. Example of triangulated meshes based on (B) day and night samples, (C) day samples only, and (D) night sample only.

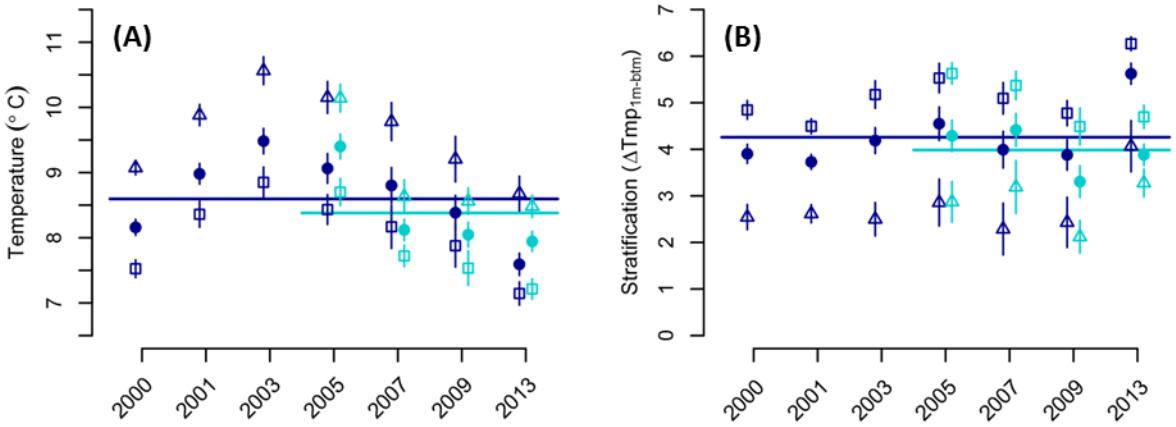


**Figure 4.3** – (A) Observed mean water column temperature ($\boldsymbol{Temp_L}$) and (B) stratification ($\Delta\boldsymbol{Temp_{1m-btm}}$) for each year. Mean values were estimated for samples within each region (WGOA = dark blue, CGOA = cyan) by bottom depth category (Bank = open triangles, Trough = open squares, Bank and Trough combined = close circles). Horizontal lines indicate average values for all WGOA (dark blue) and CGOA (cyan) samples. Note, mean values were not corrected for potential spatial autocorrelation and standard errors should be interpreted with caution.

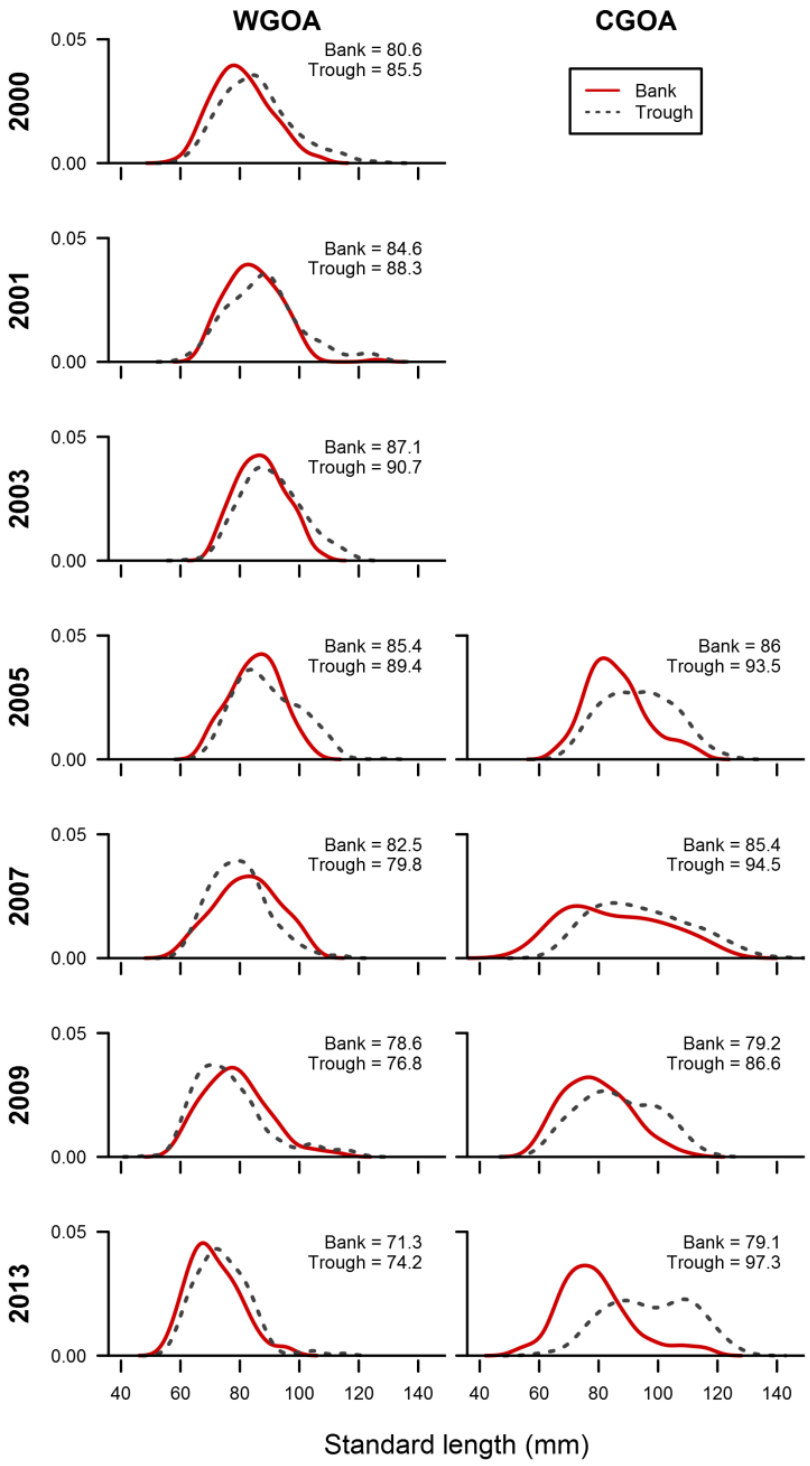


**Figure 4.4** – Kernel density plots for capelin length frequencies by year, region (WGOA, CGOA), and bottom depth category (***fBT***; Bank, Trough). Mean standard length (mm) are reported by ***fBT*** for each region.

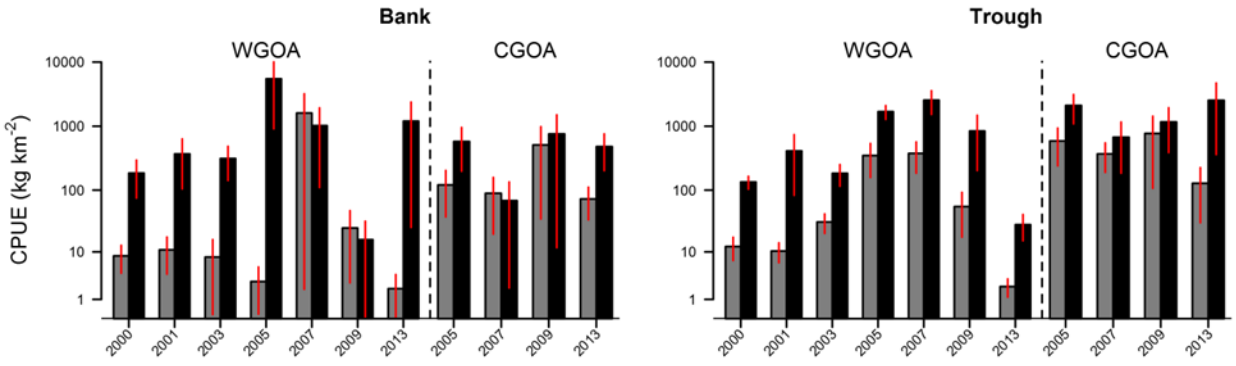


**Figure 4.5** – Observed mean capelin catch rates scaled to kg km$^{-2}$ by year, region (WGOA, CGOA), bottom depth category (Bank, Trough), and day-night category (day = gray bar, night= black bar). Note, mean CPUEs were not corrected for potential spatial autocorrelation and standard errors should be interpreted with caution.

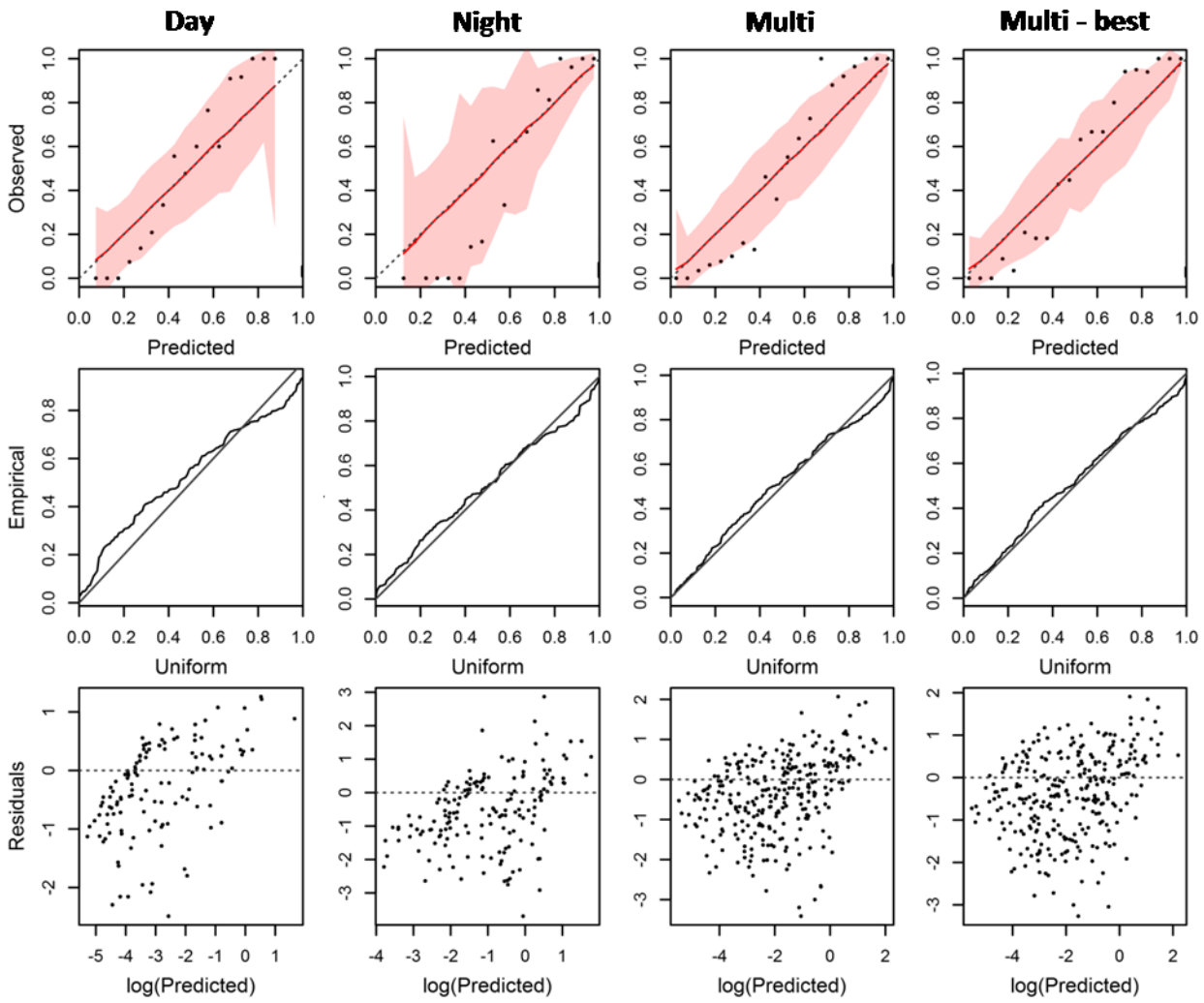


**Figure 4.6** – Model diagnostics for single-category ("Day", "Night") and multi-category ("Multi") models with no covariates, and for the best multi-category ("Multi-best") model with covariates. Upper row shows observed versus predicted occurrence probabilities, with predicted probabilities indicated by red line (shaded area=95% confidence interval) and mean observed probabilities by closed circles. Middle row shows Q-Q plots for empirical versus theoretical quantiles of gamma distribution for positive catch rates. Lower row shows standardized sign deviance residuals versus predicted positive catch rates.

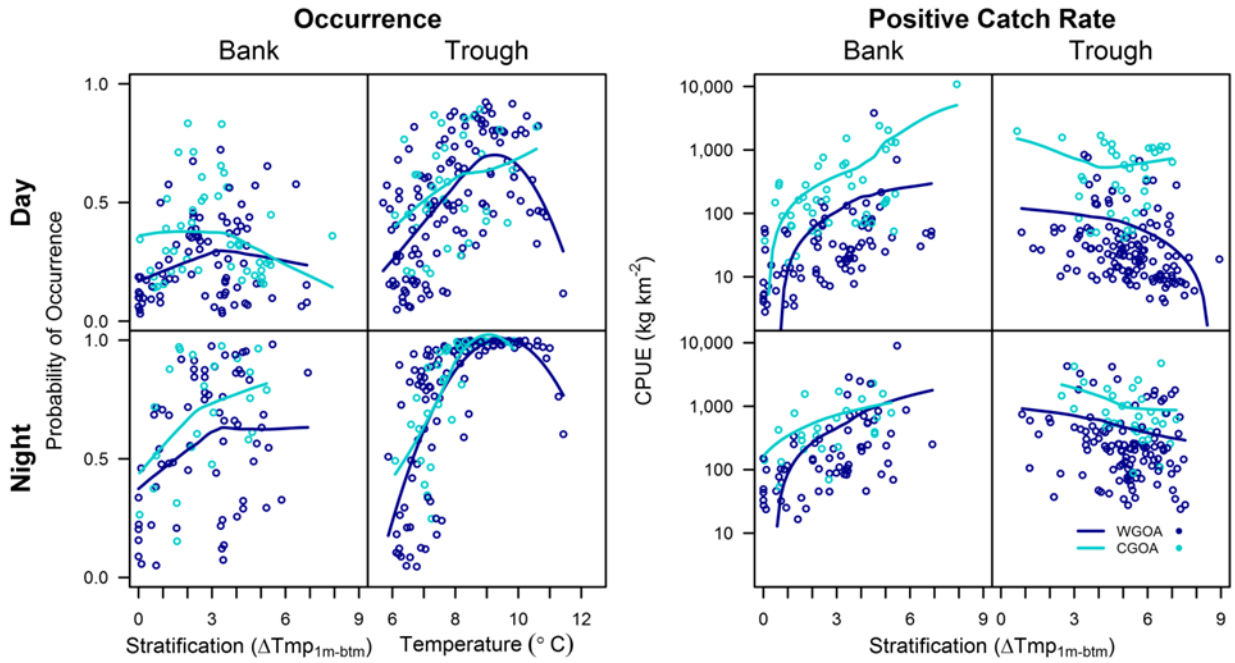


**Figure 4.7** – Predicted occurrence probabilities and positive catch rates (scaled to kg $km^{-2}$) for day and night categories by region and bottom depth category versus temperature-based covariates from the best multi-category candidate model (M:2-1.2-2).

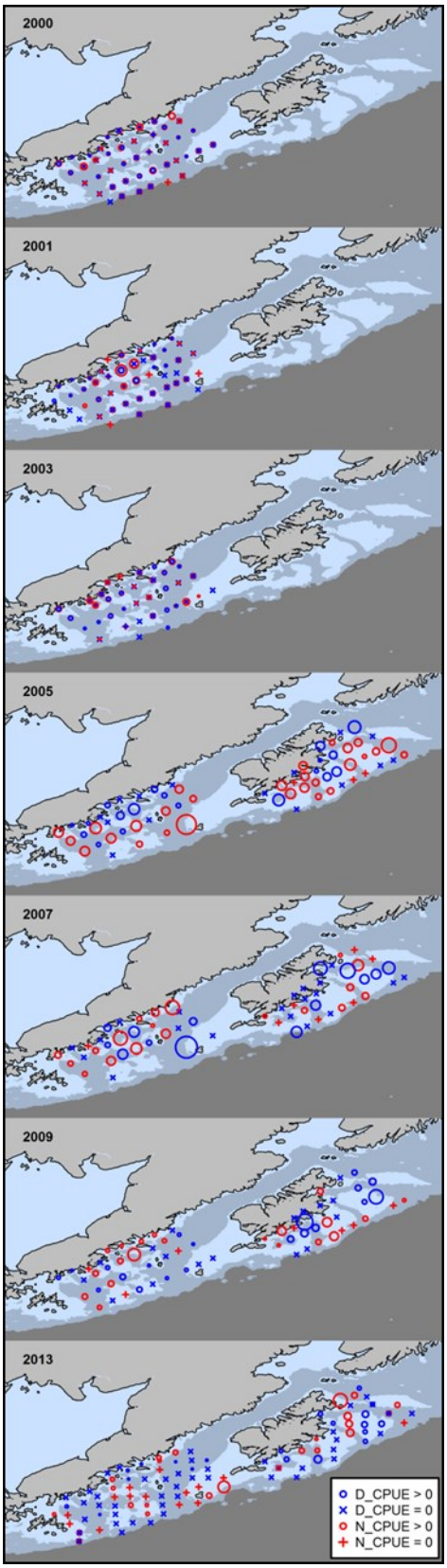


**Figure 4.8** – Distribution of standardized, predicted catch rates from the best multi-category candidate model (M:2-1.2-2) by day-night category ("D_CPUE" = catch rate for day, "N_CPUE" = catch rate for night) for each year. Circle diameter is proportional to the square root of the standardized catch rate.

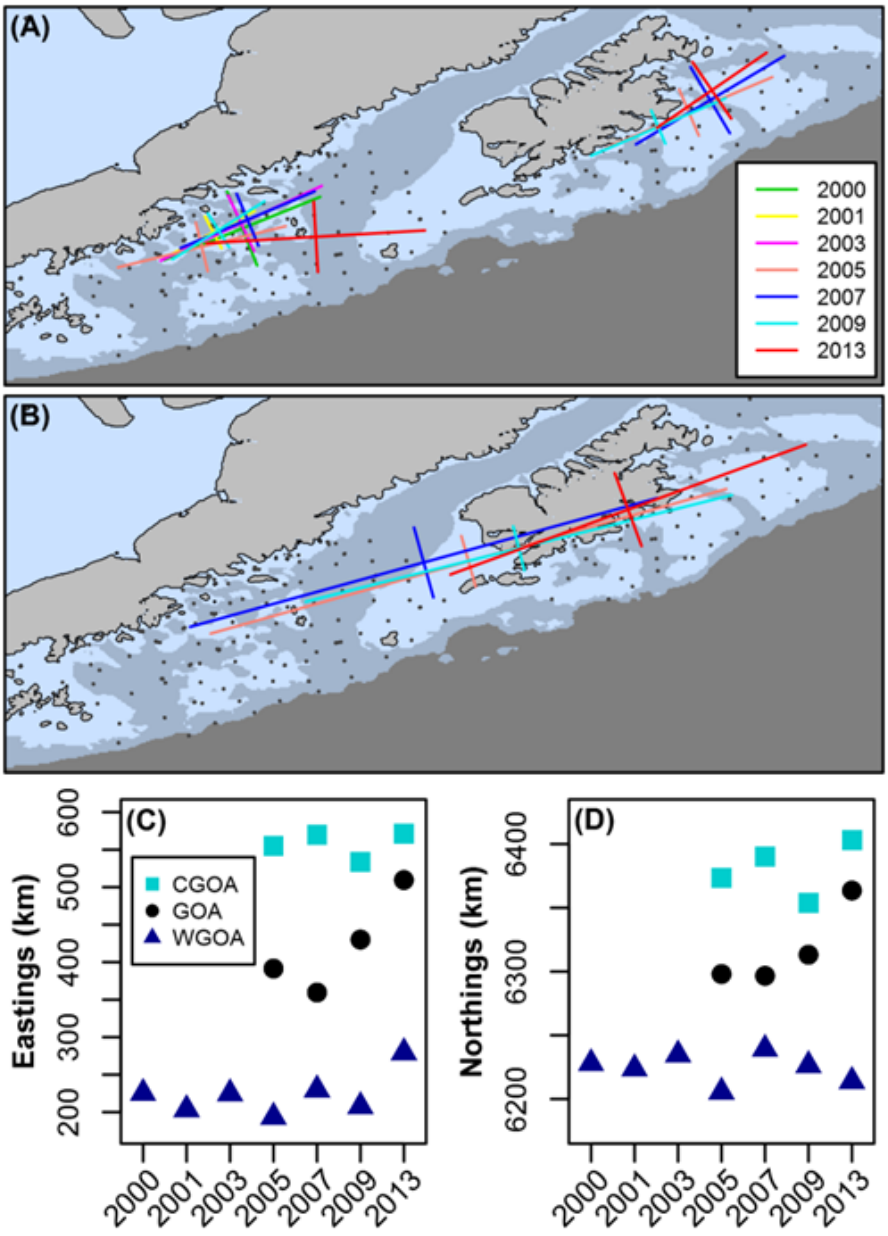


**Figure 4.9** – Center of gravity (line intersection) and inertia (line length) estimates by year for (A) samples within each region and (B) samples from both regions combined. Location of center of gravity estimates for each region (CGOA, WGOA) and both regions combined (GOA) by year along (C) longitudinal ("Eastings") and (D) and latitudinal ("Northings") axes.

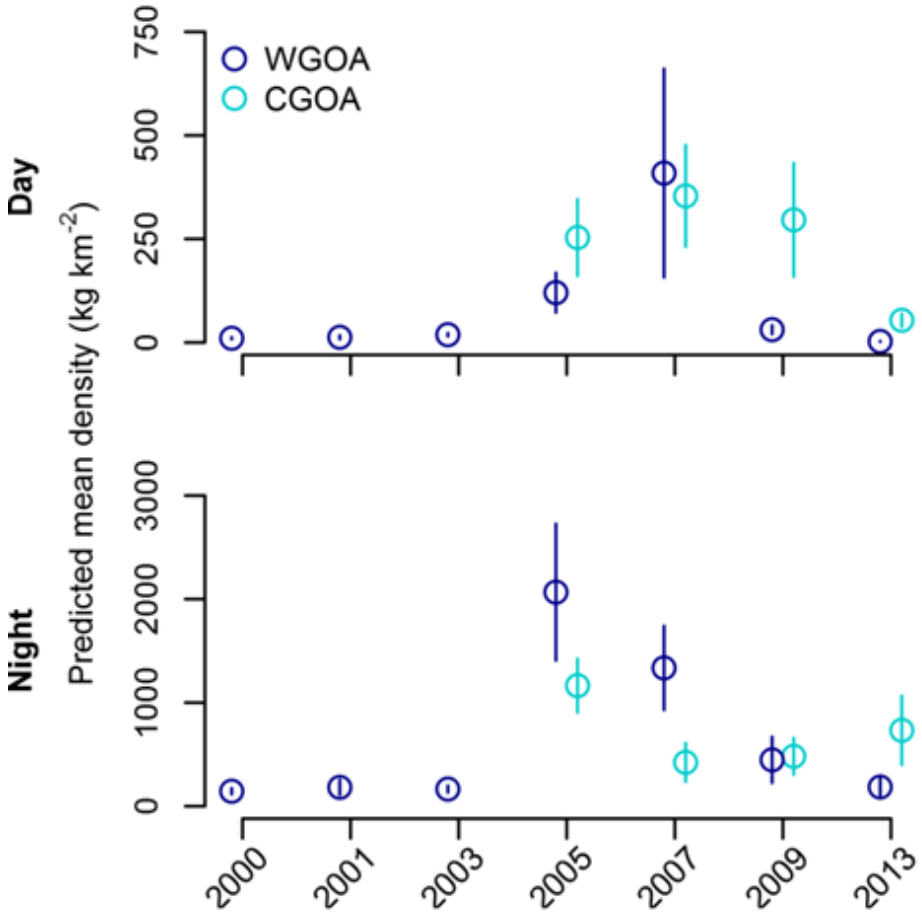


**Figure 4.10** – Predicted mean densities of capelin (scaled to kg km$^{-2}$) from the best multi-category candidate model (M:2-1.2-2) by year, region (WGOA, CGOA), and day-night category. Note, range and resolution of y-axes differ between plots.

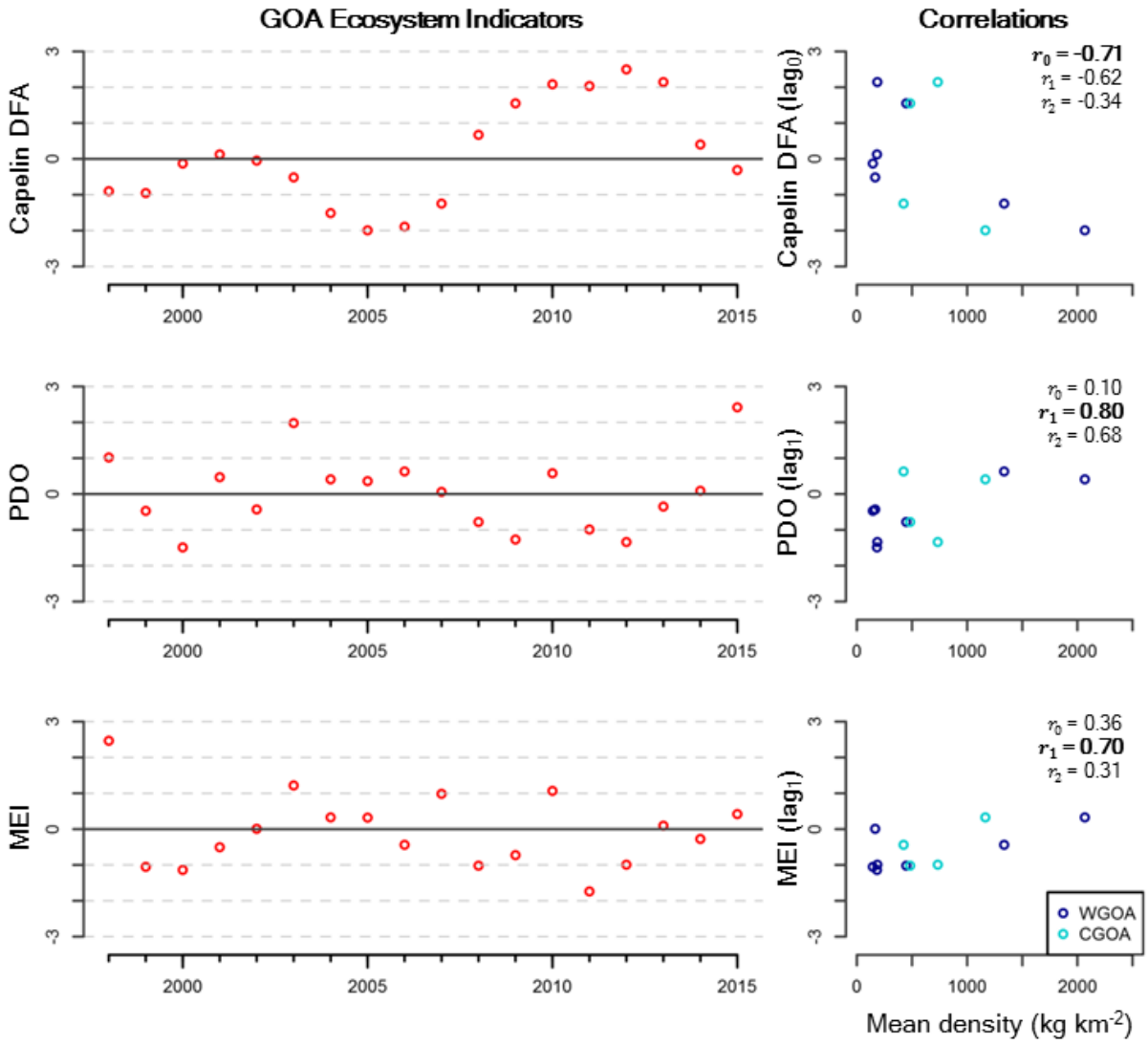


**Figure 4.11** – Correlations between predicted mean density of capelin (scaled to kg km$^{-2}$) for night samples from the best multi-category candidate model (M:2-1.2-2) with GOA ecosystem indicators (left column: capelin DFA index, PDO, MEI). Pearson correlation coefficient values indicate measure of correlation between WGOA capelin mean density with each ecosystem indicator index lagged by 0 ($\boldsymbol{r_0}$), 1 ($\boldsymbol{r_1}$), and 2 ($\boldsymbol{r_2}$) years prior to the survey year. The value in bold indicates the strongest relationship that is plotted in the scatterplots in the right column for indicator anomalies versus capelin mean densities for both regions.

# Chapter 5. SUMMARY AND RECOMMENDATIONS FOR MONITORING AND FUTURE RESEARCH FOR CAPELIN IN THE GULF OF ALASKA

## 5.1 INSIGHTS ON CAPELIN IN THE GOA

Results from this dissertation support Ormseth et al.'s (2016) observation that Gulf of Alaska (GOA) capelin have concentrated over the continental shelf to the south and east of the Kodiak Archipelago in the central GOA (CGOA) since at least the mid-2000s. Despite interannual fluctuations in relative abundance, capelin aggregations were consistently present over the Kodiak shelf from 2005 through 2013. Groundfish abundance surveys conducted in the GOA by the National Marine Fisheries Service Alaska Fisheries Science Center (AFSC) (*i.e.* the Groundfish Assessment Program's GOA Continental Shelf and Slope bottom trawl (BT) survey and the Midwater Assessment and Conservation Engineering (MACE) Program's summer pollock acoustic-trawl (AT) survey) that sample a larger, continuous area of the GOA shelf in summer also show that capelin have been concentrating over the Kodiak shelf since the 1990s (Guttormsen and Yasenak, 2007; Jones et al., 2014, 2015; Ormseth, 2014; Ormseth et al., 2016). If GOA capelin behave consistently with Atlantic capelin populations (Carscadden et al., 2013a), then I hypothesize that the CGOA region serves as a primary feeding area for age-1+ fish, and that interannual variability in the relative abundance of capelin from this area may be representative of capelin abundance in the GOA.

Capelin distributions and densities in the western GOA (WGOA) were more variable compared to the CGOA, suggesting that the WGOA is more likely to experience booms and busts in capelin abundance. Contrary to the expectation that abundances of a boreal species

would be higher in relatively cold years and occupy a larger area of the GOA shelf (*e.g.* Andrews et al., 2015), capelin abundance in the WGOA was only high during some (but not all) warm years, while fluctuations in capelin abundance was independent of regional temperature in the CGOA. Observed differences in distributions and relative abundance between the regions are hypothesized to be either displacement of capelin over the GOA shelf, expansion of capelin distributions during warm years and contraction during cold years, or spatiotemporal differences in capelin mortality rates due to shifts in predator distributions. Interannual variability in the relative abundance of capelin in the WGOA was strongly correlated with the winter Pacific Decadal Oscillation (PDO) index lagged by 1 year. This suggests that GOA capelin abundance may be influenced by climate-related processes that affect capelin survival during their first year of life. The determination of cohort size resulting from mortality during early life stages would be consistent with Atlantic capelin populations off Newfoundland and in the Barents Sea (Carscadden et al., 2013b). Continued monitoring is required to determine if observed regional differences in abundance and the association with the PDO are robust over time.

This dissertation improves our understanding of variability in capelin distributions associated with bathymetric features, environmental factors, and potential trophic interactions. In summer and fall, capelin primarily concentrated over or near edges of shallow submarine banks (< 100 m bottom depth). The close association between GOA capelin distributions and bathymetric features is similar to observations of capelin distributions in the Northwest Atlantic that were closely associated with tidal dynamics (Simard et al., 2002). Over the Kodiak shelf in summer, primary production is sustained by strong tidal pumping that supplies nutrients from cold, bottom water in troughs to the euphotic zone over banks and near their edges (Cheng et al., 2012; Ladd et al., 2005; Mordy et al., 2016). Model results from Chapters 3 and 4 indicate that

capelin distributions are influenced by vertical mixing in association with bathymetry. Over banks, capelin concentrated in waters with higher water column stratification and enhanced primary production relative to other areas over banks. The presence of capelin within troughs (≥ 100 m) was related to local water temperature, where occurrence probabilities increased as waters warmed to approximately 8 to 9° C, and then dropped as temperatures rose above 10.5° C. Local temperature was not a strong predictor of density, as increases in capelin catch rates in troughs were associated with reduced stratification. Consistency among results from Chapters 3 and 4 suggest that the influence of temperature-based covariates on capelin distributions is robust across years and GOA regions. Based on Chapter 3's model results, observed length frequency distributions, and previously published capelin diet compositions from the GOA (Logerwell et al., 2010; Wilson et al., 2006), I inferred that distributions of capelin over the shelf in summer 2013 were likely driven by changes in the availability and composition of their prey. Age-1 capelin concentrated over CGOA banks in waters that were well-mixed and more productive (relative to waters in troughs) to feed on abundant copepods, while age-2+ capelin primarily occupied deeper waters in troughs where they consumed larger euphausiid and amphipod prey. While capelin and age-0 pollock have previously been speculated to be potential competitors in the GOA (Logerwell et al., 2010; Wilson et al., 2006), results from this study do not provide evidence to support this hypothesis. Horizontal distributions of age-1 capelin were positively related to age-0 pollock densities over CGOA banks in summer 2013 (Chapter 3), and there was no apparent difference in vertical distributions of capelin when age-0 pollock were absent in 2011 or abundant in 2013 (Chapter 2). These results suggest that capelin distributions were not negatively influenced by age-0 pollock, and that these species were unlikely to be competing for shared prey resources in August 2013.

## 5.2 APPLICATIONS TO IMPROVED MONITORING OF GOA CAPELIN AND OTHER FORAGE SPECIES

Although the goals of this dissertation were not related to evaluating current sampling efforts for capelin and other forage species in the GOA, recommendations can be drawn from this study for survey design of forage fish and interdisciplinary, ecosystem monitoring (*e.g.* Eriksen et al., 2017). The GOA Integrated Ecosystem Research Program (GOAIERP) represented the largest commitment to date of resources dedicated to sampling age-0 groundfish species and their environment in the GOA (http://www.nprb.org/gulf-of-alaska-project). The offshore survey's original design of systematic oceanographic sampling coupled with surface trawling at equally-spaced stations was enhanced by the addition of active acoustic sampling that is better suited for detecting patchily distributed aggregations of pelagic fish throughout the water column and across bathymetric gradients (*e.g.* O'Driscoll et al., 2002). Inclusion of acoustic sampling to the GOAIERP survey included a key design change drawn from lessons learned during the Bering Sea IERP, where planning of cruise tracks changed from the Bering-Aleutian Salmon International Survey (BASIS) design of sampling a grid of stations (*e.g.* Farley et al., 2005) to sampling along a set of continuous, parallel transects oriented orthogonal to bathymetric gradients with embedded, pre-determined stations (*e.g.* Parker-Stetter et al., 2013). Considerable ship time was dedicated to sampling at stations, requiring increased spacing between acoustic transects and limiting the amount of time dedicated for midwater trawls to verify species and length compositions of acoustic targets. This approach resulted in a high proportion of acoustic data being classified as unknown during the 2011 surveys that limited most of Chapter 3's analyses to only 2013 data. Adjustments made to the sampling protocol for

the 2013 survey resulted in improved coverage of GOAIERP focal species (*i.e.* age-0 pollock) and capelin while reducing the proportion of acoustic data classified in mixed-species categories or as unknown. Improved communication among PIs facilitated greater flexibility to increase sampling effort in areas where forage fish concentrated and to sample opportunistic acoustic targets while mitigating unanticipated logistic constraints. Classification of acoustic data in 2013 was also aided by the increased pairing of midwater with surface trawls to resolve the contribution of epipelagic fish and invertebrates (*i.e.* surface contamination) to midwater samples. By employing a multi-gear approach, where each sampling gear provides information on biases associated with other gears (*e.g.* Kotwicki et al., 2015), changes in distribution and abundance of capelin and other forage fish species can be detected and quantified.

Based on the findings from the GOA and Bering Sea IERPs and long-term monitoring of Atlantic capelin populations, I recommend that monitoring efficiency of capelin in the GOA will be improved by the integration of active acoustic sampling with existing net-based, fisheries-oceanographic surveys in the GOA, including the GOA Assessment survey (*cf.* Ormseth et al., 2016) and the Ecosystems and Fisheries-Oceanography Coordinated Investigations Program (EcoFOCI) late-summer small-mesh trawl survey. As demonstrated by O'Driscoll et al. (2002), estimation of capelin biomass is more accurate using acoustic sampling, while systematic, net-based sampling is better suited for detecting changes in the boundaries of capelin distributions, as long as the net samples the full range of capelin vertical distributions. Results from Chapter 2 show that continuous acoustic sampling is essential to sample patchy forage fish distributions that are aggregated at scales less than 1 km.

Additional modifications to net-based surveys designed to improve coverage of capelin and other forage fish include modifying the spacing between stations along transects, the

orientation and spacing between transects, and time of year the survey is conducted. Results in Chapter 2 showed that capelin and age-0 pollock horizontal and vertical distributions were strongly associated with bottom depth, suggesting that the location of stations along each transect should be determined by depth strata (*e.g.* 50, 100, 200, 500, 1000 m depth contours), rather than being equally spaced. Acoustic transects should be oriented orthogonal to the strongest bathymetric gradients (Simmonds and MacLennan, 2005), alternating between across-shelf (perpendicular to coastline) and along-shelf when necessary to improve coverage over banks, troughs, and sea valleys (*e.g.* AFSC summer GOA pollock AT survey, Jones et al., 2014) ). In this study, the resolution used to characterize capelin distributions was determined by identifying variance peaks in capelin densities. To detect changes in capelin distributions, spacing between transects should be determined by half the distance of the peak mode of spatial scales determined by wavelet and Ripley's K analyses (*i.e.* the Nyquist frequency; Spellerberg, 1991). Chapter 2 results showed that the peak mode for capelin densities measured along transects spaced 37 km apart in 2011 and 2013 was 46 km using wavelets, while the peak mode measured along- and across-transects by Ripley's K was 41.5 km. These results indicate that inter-transect spacing should be no more than 23 km apart over the CGOA shelf, which is similar to the 27.78 km (15 nm) resolution used in the Barents Sea to achieve acceptable precision of capelin abundance estimates (Eriksen et al., 2017). The optimal time of year to monitor capelin distributions and abundance in the GOA is between July and August to align with other GOA-based surveys for managed species. Currently the GOA Assessment Survey is conducted during this period while the EcoFOCI trawl survey occurs primarily in September. A summer survey would coincide with groundfish abundance surveys (*i.e.* AFSC pollock AT survey, AFSC and Alaska Department of Fish and Game bottom trawl surveys, and AFSC longline survey), as well as

breeding season surveys of seabirds (Dragoo et al., 2015) and pinnipeds (Womble et al., 2009; Womble and Sigler, 2006). Temporal overlap among these surveys would allow spatiotemporal variations in capelin abundance to be related to diet-based characterizations of predator foraging habits and energy intake (*e.g.* Kettle et al., 2015; Yang et al., 2005), and changes in predator abundances, distributions, growth, and reproductive success. A summer survey would also be consistent with international efforts to survey capelin populations off Iceland and in the Barents Sea when immature age-1+ fish are distributed offshore (Carscadden et al., 2013b). The above recommendations are also applicable to the design of a future capelin-focused survey in the GOA if resources are available.

Whether or not acoustic data collection is incorporated into the GOA Assessment and EcoFOCI trawl surveys, net selectivity data for the Cantrawl and Stauffer trawls are needed to quantify sampling bias in species and length compositions of trawl catches. De Robertis et al. (2017a) showed species and length selectivity bias in Cantrawl catches of pelagic species, including capelin, from the Chukchi Sea that misrepresents the epipelagic (upper 20 m) assemblage. In this study, due to the lack of net selectivity data for the Cantrawl in the GOA, mixed-species trawl samples could not be used to apportion acoustic data from the GOAIERP surveys to single-species or -length categories by percent catch composition. As a result, classification of acoustic data was limited by the availability of homogenous trawl samples, in which one species and/or length category accounted for at least 90% of the catch (Chapter 2). Large proportions of acoustic data (primarily in 2011 and in the eastern GOA region) were apportioned to mixed-species categories or classified as unknown. These data constraints limited Chapter 2's analyses to using non-zero, acoustic densities for forage fish categories, and limited most of Chapter 3's analyses to data from the CGOA in summer 2013 when classification of

acoustic data was improved due to the reallocation of ship-time to opportunistically collect additional midwater trawl samples. If acoustic sampling is integrated into the GOA Assessment and/or EcoFOCI trawl surveys, net selectivity data for the Cantrawl and/or Stauffer trawls are needed to facilitate improved classification of acoustic data using mixed-species and -length samples and to estimate length-dependent selectivity for capelin and other abundant species to account for trawl bias when estimating biomass from acoustic densities (*e.g.* De Robertis et al., 2017a; Nakashima, 1990; Williams et al., 2011). In addition, non-linear differences in capelin catch rates between day and night trawl samples in Chapter 4 indicate net selectivity data for the Stauffer trawl are necessary to assess bias associated with the time of day samples are collected during the EcoFOCI trawl survey.

## 5.3 APPLICATIONS TO ECOLOGICAL INVESTIGATIONS OF CAPELIN AND OTHER FORAGE SPECIES

To aid future studies on capelin and other forage species using GOA-based survey data, I recommend: the use of generalized linear mixed models (GLMM), that include random effects for spatial and/or spatiotemporal covariance among samples, to quantify sources of variability in distributions of fish or macrozooplankton; inclusion of an interaction term for bottom depth categories (*e.g.* banks and troughs) with environmental covariates in linear models; and the use of a multi-category, joint model for analyzing distributions from surveys that sample 24 hours per day (*e.g.* EcoFOCI trawl survey). These recommendations result from analytic challenges encountered during this study that primarily resulted from how data were collected during the GOAIERP and EcoFOCI trawl surveys. Analytic methods used in this dissertation included existing and new techniques that allowed greater flexibility to quantify spatial and temporal

variability in capelin distributions and to examine how capelin occurrence and density are influenced by physical and ecological factors at different spatial scales.

Spatial GLMMs were used to facilitate examination of the relative importance of environmental factors explaining variability in capelin distributions at resolutions that maximize variance in capelin patterns while accounting for spatial autocorrelation (Chapter 3). Wavelets were used to objectively identify variance peaks in acoustic-based distributions of capelin and other forage fish species from the GOAIERP surveys that were used to determine resolutions for data analyses (Chapter 2). One of the spatial resolutions identified by the wavelet analysis of GOAIERP acoustic data was 0.5 km, at which samples were spatially autocorrelated. The spatial GLMM treats spatial covariance as a random effect, which allows unobserved extrinsic (e.g. density-independent response to environmental conditions) and/or intrinsic (e.g. density-dependent schooling behavior) processes that cause autocorrelation among samples to be included in the prediction of fish distributions and abundance (Beale et al., 2010; Thorson et al., 2015b, 2015c). By incorporating spatial autocorrelation within the model structure as random effects, statistical inference on the effects of environmental covariates can be drawn from unbiased model outputs. The combined approach of using wavelets to identify data resolutions with spatial and/or spatiotemporal GLMMs to analyze spatially-indexed fish or macrozooplankton data serves as a template for future investigations of scale-dependent relationships among acoustic- or net-based measurements of marine nekton with environmental covariates.

Results from Chapter 3 and 4 demonstrated the importance of accounting for differences in oceanographic conditions associated with bathymetric features by including an interaction term for bottom depth categories (*e.g.* banks and troughs) with environmental covariates

(hereafter a depth-stratified model). This study used depth-stratified models to analyze two independent data sets, and was able to differentiate how temperature-based covariates explain variability in capelin distributions in bank and trough habitats that have different oceanographic properties. A depth-stratified model accounts for depth-specific differences in the influence of each covariate by allowing intercepts and slopes to vary based on the sample's location. While this approach increases the number of fixed effects in the model, potentially requiring larger sample sizes, the added model complexity facilitates easy interpretation of parameter estimates to quantify the relative importance of each predictor on distributions and abundance of a species of interest.

If using survey data collected over a 24-hour period (*e.g.* the EcoFOCI trawl survey), this study demonstrated how a multi-species model (*e.g.* Ovaskainen et al., 2016; Thorson et al., 2015a) can be adapted to account for bias associated with the time of day that a sample was collected. In Chapter 4, capelin distributions were jointly modeled from day and night samples in a multi-category, spatiotemporal delta-GLMM (*e.g.* Thorson et al., 2015b, 2017) to account for observed differences between day and night catches in the frequency of zero samples and positive catch rates from the EcoFOCI trawl survey. Initial attempts to correct the non-linear differences in day and night catches were unsuccessful given the lack of net selectivity data for the Stauffer trawl and/or acoustic data describing diel vertical movements and schooling behavior that could be used to quantify availability to the trawl (*e.g.* Casey and Myers, 1998; Kotwicki et al., 2015). Use of the multi-category model resulted in improved precision of predicted occurrence probabilities and positive catch rates compared to modeling samples from day and night categories in separate models.

## 5.4 RECOMMENDATIONS FOR FUTURE RESEARCH

These recommendations aim to increase knowledge of capelin in the GOA and to inform resource managers on the response of capelin to climate-related changes in ocean conditions, anomalous warming events, and long-term warming. The resilience of capelin to increases in temperature and subsequent changes to the GOA marine ecosystem is unknown. Examinations of relationships between climate-related processes and capelin population dynamics are needed to identify recruitment bottlenecks. To address gaps in our knowledge of capelin in the GOA, I recommend: development of an abundance index for capelin in the GOA based on spatially-indexed densities; quantify the influence of environmental factors on spatial and temporal variability in distributions of larval capelin; examine connectivity between inshore spawning areas and offshore distributions of larval capelin.

Until existing surveys in the GOA are modified to improve monitoring of capelin (see section 5.2) or a new survey designed for capelin is deemed necessary by resource managers, I recommend that the EcoFOCI trawl survey is the best available index to serve as an indicator of capelin relative abundance in the GOA. The EcoFOCI trawl survey has: consistent spatial and temporal coverage for an extended period, consistent presence of capelin within the survey domain, near-complete coverage of capelin vertical distributions, and collection of *in situ* measurements of water column properties and zooplankton prey fields that can be used to investigate potential sources of spatiotemporal variations in capelin abundance. As described in Section 5.2, additional work is needed to quantify potential biases and limitations of the EcoFOCI trawl survey design. Quantification of Stauffer trawl net selectivity is needed to assess sampling bias among length classes of capelin, other fish species, and differences between day and night to adjust net catch compositions (*e.g.* De Robertis et al., 2017; Williams et al., 2011).

Acoustic data have been collected during surveys in most years, but has yet to be analyzed. To facilitate biomass estimates of capelin and other small pelagic species (*e.g.* O'Driscoll et al., 2002) and ecosystem monitoring surveys (*e.g.* Eriksen et al., 2017), full integration of active acoustic sampling within the existing EcoFOCI trawl survey, including the use of transects with embedded stations and midwater trawls to verify acoustic targets, is required to provide data confirming to international standards. Archived acoustic data should be examined to assess sampling bias associated with sampling time of day, including visual examination of zero catches to confirm the presence or absence of capelin acoustic targets, and incorporating measures of selectivity (*e.g.* De Robertis et al., 2017; Williams et al., 2011) and availability (*e.g.* Casey and Myers, 1998; Kotwicki et al., 2015) of capelin to the Stauffer trawl to correct net catch rates.

How well the EcoFOCI trawl survey represents interannual fluctuations in age-1+ capelin abundance across the GOA should be assessed relative to other available survey data. This study compared capelin distributions from the EcoFOCI trawl survey to other GOA surveys (*i.e.* AFSC pollock AT survey, GOAIERP acoustic survey, AFSC BT survey) and the capelin dynamic factor analysis (DFA) index. A more comprehensive synthesis of these data is needed to compare spatial patterns of capelin densities while accounting for any sampling biases that exist within each survey. Characterizing capelin spatial patterns from multiple sources will improve identification of high density areas and delineate capelin range boundaries.

Given that this study found a strong correlation between mean densities of age-1+ capelin with the PDO lagged by one year, there is a clear need to investigate relationships between environmental factors linked to climate processes with spawning and abundances of larvae. Cohort size in capelin populations off Newfoundland and in the Barents Sea are determined by factors that affect mortality during the first year of life (Carscadden et al., 2013b). Interannual

variations in the relative abundance of GOA capelin larvae may forecast age-1 abundance fluctuations the following year. Quantification of spatiotemporal variability of distributions of larval capelin and length frequencies is also needed to update Doyle et al.'s (2002) description of capelin phenology in the CGOA from the late 1970s. Interannual variations in densities of larval capelin within and between the CGOA and WGOA regions should also be compared to densities of age-1+ fish in subsequent years to determine if observed differences within and between regions persist through the life of a cohort.

Connectivity between inshore spawning locations and offshore nursery and foraging areas is poorly understood, but can be investigated using information that describes the timing and locations of capelin spawning data in the GOA with larval capelin distributions from ichthyoplankton and trawl survey data. Timing and locations of capelin spawning in the GOA have been reported for Kodiak (Blackburn et al., 1981; Doyle et al., 2002; Pahlke, 1985), Prince William Sound (Brown, 2002), and within Glacier Bay in Southeast Alaska (Arimitsu et al., 2008). Current trajectories derived from satellite-tracked drifters suggest that passive particles released during summer in the northern GOA will likely pass through the CGOA and/or WGOA regions (Stabeno et al., 2016a). Weak currents around banks in both regions may favor retention of larvae in areas associated with high primary production (Cheng et al., 2012; Mordy et al., 2016; Waite and Mueter, 2013). Particle trajectories simulated in an individual-based model (IBM) linked to a physical hydrodynamic model could be used to assess spatial and temporal connectivity between spawning locations along the GOA coast with offshore areas sampled by the EcoFOCI trawl survey in late summer (*e.g.* Parada et al., 2015). IBM trajectories should also provide insight into changes in larval transport related to variability in the Alaska Coastal Current (ACC). Interannual variations and differences among GOA regions in larval and age-1+

capelin abundance may be linked to fluctuations in ACC transport that result in shifts in the proportion of ACC water transported over the Kodiak shelf in the CGOA region compared to transport through Kennedy-Stevenson Entrance and the Shelikof sea valley into the WGOA (Stabeno et al., 2016a). Links between physical processes that influence ACC flow and capelin cohort strength may lead to additional ecosystem indicators for the GOA.

There is evidence of juvenile and non-spawning, adult capelin occurring within inshore waters and coastal embayments in the GOA during summer (*e.g.* Glacier Bay, Arimitsu et al., 2008). An unknown proportion of capelin in the GOA may belong to discrete, inshore populations that do not migrate from the GOA shelf. Inshore capelin stocks have been documented within fjords along the northern Norwegian coast that are believed to be mostly isolated spatially (but not genetically) from the offshore stock in the Barents Sea (Gjøsæter, 1998). Although the population structure of capelin in the N. Pacific is unknown, it is unlikely that these inshore capelin are reproductively isolated from capelin located offshore given that circulation patterns within Prince William Sound (Halverson, 2014; Royer et al., 1990; Vaughan et al., 2001) and Southeast Alaska (Stabeno et al., 2016a; Weingartner et al., 2009) are well connected with the GOA shelf. If true, it is not known the extent to which inshore capelin contribute to offshore capelin abundance. Arimitsu et al. (2008) hypothesized that waters near tidewater glaciers may serve as cold-water refugia for capelin during periods of warm ocean temperatures, such as the GOA's recent marine heatwave (Bond et al., 2015). If inshore capelin contribute to offshore capelin abundance, then they may serve an important role in sustaining or rebuilding capelin across the GOA following declines in the offshore spawning biomass population.

At this time, the net contribution of capelin to the GOA ecosystem is unknown. The role of capelin as an energy conduit between primary producers and upper tropic piscivores is not disputed. The lack of a commercial fishery has impeded the impetus to increase knowledge of capelin ecology in the GOA and the Northeast Pacific. The increased mandate of ecosystem-based management of Alaska's marine resources justifies increased resources for dedicated research on capelin and other non-commercial forage species.

# REFERENCES


Acevedo-Gutiérrez, A., Croll, D.A., Tershy, B.R., 2002. High feeding costs limit dive time in the largest whales. J. Exp. Biol. 205, 1747–1753.

Anderson, P.J., Blackburn, J.E., Johnson, B.A., 1997. Declines of forage species in the Gulf of Alaska, 1972-95, as indicator of regime shift, in: Forage Fishes in Marine Ecosystems. Alaska Sea Grant College Program, Fairbanks, Alaska, USA, pp. 531–543.

Anderson, P.J., Piatt, J.F., 1999. Community reorganization in the Gulf of Alaska following ocean climate regime shift. Mar. Ecol. Prog. Ser. 189, 117–123.

Andrews, A.G., Strasburger, W.W., Farley, E.V., Murphy, J.M., Coyle, K.O., 2015. Effects of warm and cold climate conditions on capelin (*Mallotus villosus*) and Pacific herring (*Clupea pallasii*) in the eastern Bering Sea. Deep Sea Res. Part II. https://doi.org/10.1016/j.dsr2.2015.10.008

Anselin, L., 1995. Local indicators of spatial association—LISA. Geogr. Anal. 27, 93–115. https://doi.org/10.1111/j.1538-4632.1995.tb00338.x

Arimitsu, M.L., Piatt, J.F., Litzow, M.A., Abookire, A.A., Romano, M.D., Robards, M.D., 2008. Distribution and spawning dynamics of capelin (*Mallotus villosus*) in Glacier Bay, Alaska: A cold water refugium. Fish. Oceanogr. 17, 137–146. https://doi.org/10.1111/j.1365-2419.2008.00470.x

Arrigo, K.R., van Dijken, G.L., 2011. Secular trends in Arctic Ocean net primary production. J. Geophys. Res. Oceans 116, C09011. https://doi.org/10.1029/2011JC007151

Ashmole, N.P., 1963. The regulation of numbers of tropical oceanic birds. Ibis 103b, 458–473. https://doi.org/10.1111/j.1474-919X.1963.tb06766.x

Bailey, K.M., 1989. Interaction between the vertical distribution of juvenile walleye pollock *Theragra chalcogramma* in the eastern Bering Sea, and cannibalism. Mar. Ecol. Prog. Ser. 53, 205–213.

Barange, M., 1994. Acoustic identification, classification and structure of biological patchiness on the edge of the Agulhas Bank and its relation to frontal features. South Afr. J. Mar. Sci. 14, 333–347. https://doi.org/10.2989/025776194784286969

Batten, S.D., Raitsos, D.E., Danielson, S., Hopcroft, R., Coyle, K., McQuatters-Gollop, A., 2017. Interannual variability in lower trophic levels on the Alaskan Shelf. Deep Sea Res. Part II. https://doi.org/10.1016/j.dsr2.2017.04.023

Beale, C.M., Lennon, J.J., Yearsley, J.M., Brewer, M.J., Elston, D.A., 2010. Regression analysis of spatial data. Ecol. Lett. 13, 246–264. https://doi.org/10.1111/j.1461-0248.2009.01422.x

Beamish, R.J., McCaughran, D., King, J.R., Sweeting, R.M., McFarlane, G.A., 2000. Estimating the abundance of juvenile coho salmon in the Strait of Georgia by means of surface trawls. North Am. J. Fish. Manag. 20, 369–375. https://doi.org/10.1577/1548-8675(2000)020<0369:ETAOJC>2.3.CO;2

Benoit-Bird, K.J., Battaile, B.C., Heppell, S.A., Hoover, B., Irons, D., Jones, N., Kuletz, K.J., Nordstrom, C.A., Paredes, R., Suryan, R.M., Waluk, C.M., Trites, A.W., 2013. Prey patch patterns predict habitat use by top marine predators with diverse foraging strategies. PLoS ONE 8, e53348. https://doi.org/10.1371/journal.pone.0053348

Bertrand, A., Ballón, M., Chaigneau, A., 2010. Acoustic observation of living organisms reveals the upper limit of the oxygen minimum zone. PLoS ONE 5, e10330. https://doi.org/10.1371/journal.pone.0010330

Bertrand, A., Segura, M., Gutierrez, M., Vasquez, L., 2004. From small-scale habitat loopholes to decadal cycles: A habitat-based hypothesis explaining fluctuation in pelagic fish populations off Peru. Fish Fish. 5, 296–316. https://doi.org/10.1111/j.1467-2679.2004.00165.x

Blackburn, J.E., Anderson, P.J., 1997. Pacific sand lance growth, seasonal availability, movements, catch variability, and food in the Kodiak-Cook Inlet area of Alaska (No. AK-SG-97-01), Forage Fishes in Marine Ecosystems. Alaska Sea Grant College Program, Fairbanks, Alaska, USA.

Blackburn, J.E., Jackson, P.B., Warner, I.M., Dick, M.H., 1981. Survey for spawning forage fish on the east side of the Kodiak Archipelago by air and boat during spring and summer 1979. Final Report (No. PB-87-195210/XAB). National Ocean Service, Ocean Assessments Div., Anchorage, AK.

Blaxter, J.H.S., Batty, R.S., 1990. Swimbladder "behaviour" and target strength. Rapp. Procès-Verbaux La Réun. Cons. Int. Pour Explor. Mer 189, 233–244.

Bond, N.A., Cronin, M.F., Freeland, H., Mantua, N., 2015. Causes and impacts of the 2014 warm anomaly in the NE Pacific. Geophys. Res. Lett. 42, 2015GL063306. https://doi.org/10.1002/2015GL063306

Bradshaw, G.A., Spies, T.A., 1992. Characterizing canopy gap structure in forests using wavelet analysis. J. Ecol. 80, 205–215. https://doi.org/10.2307/2261007

Brodeur, R.D., Wilson, M.T., 1996a. A review of the distribution, ecology and population dynamics of age-0 walleye pollock in the Gulf of Alaska. Fish. Oceanogr. 5, 148–166. https://doi.org/10.1111/j.1365-2419.1996.tb00089.x

Brodeur, R.D., Wilson, M.T., 1996b. Mesoscale acoustic patterns of juvenile walleye pollock (*Theragra chalcogramma*) in the western Gulf of Alaska. Can. J. Fish. Aquat. Sci. 53, 1951–1963. https://doi.org/10.1139/cjfas-53-9-1951

Brown, E.D., 2002. Life history, distribution, and size structure of Pacific capelin in Prince William Sound and the northern Gulf of Alaska. ICES J. Mar. Sci. 59, 983–996. https://doi.org/10.1006/jmsc.2002.1281

Buren, A.D., Koen-Alonso, M., Pepin, P., Mowbray, F., Nakashima, B., Stenson, G., Ollerhead, N., Montevecchi, W.A., 2014. Bottom-up regulation of capelin, a keystone forage species. PLoS ONE 9, e87589. https://doi.org/10.1371/journal.pone.0087589

Burnham, K.P., Anderson, D.R., 2002. Model Selection and Multimodel Inference: A Practical Information-Theoretic Approach, 2nd ed. Springer, New York, New York, USA.

Carlson, H.R., 1980. Seasonal distribution and environment of Pacific herring near Auke Bay, Lynn Canal, Southeastern Alaska. Trans. Am. Fish. Soc. 109, 71–78. https://doi.org/10.1577/1548-8659(1980)109<71:SDAEOP>2.0.CO;2

Carscadden, J.E., Frank, K.T., Miller, D.S., 1989. Capelin (*Mallotus villosus*) spawning on the southeast shoal: influence of physical factors past and present. Can. J. Fish. Aquat. Sci. 46, 1743–1754. https://doi.org/10.1139/f89-221

Carscadden, J.E., Gjøsæter, H., Vilhjálmsson, H., 2013a. A comparison of recent changes in distribution of capelin (*Mallotus villosus*) in the Barents Sea, around Iceland and in the Northwest Atlantic. Prog. Oceanogr., Nor.-Can. Comp. Mar. Ecosyst. (NORCAN) 114, 64–83. https://doi.org/10.1016/j.pocean.2013.05.005

Carscadden, J.E., Gjøsæter, H., Vilhjálmsson, H., 2013b. Recruitment in the Barents Sea, Icelandic, and eastern Newfoundland/Labrador capelin (*Mallotus villosus*) stocks. Prog. Oceanogr., Nor.-Can. Comp. Mar. Ecosyst. (NORCAN) 114, 84–96. https://doi.org/10.1016/j.pocean.2013.05.006

Carscadden, J.E., Montevecchi, W.A., Davoren, G.K., Nakashima, B.S., 2002. Trophic relationships among capelin ( Mallotus villosus ) and seabirds in a changing ecosystem. ICES J. Mar. Sci. 59, 1027–1033. https://doi.org/10.1006/jmsc.2002.1235

Carscadden, J.E., Vilhjálmsson, H., 2002. Capelin - what are they good for? Introduction. ICES J. Mar. Sci. J. Cons. 59, 863–869. https://doi.org/10.1006/jmsc.2002.1283

Casey, J.M., Myers, R.A., 1998. Diel variation in trawl catchability: is it as clear as day and night? Can. J. Fish. Aquat. Sci. 55, 2329–2340. https://doi.org/10.1139/f98-120

Chambers, J.M., Cleveland, W.S., Kleiner, B., Tukey, P.A., 1983. Graphical Methods for Data Analysis, The Wadsworth Statistics/Probability Series. Wadsworth International Group, Belmont, California.

Chavez, F.P., Ryan, J., Lluch-Cota, S.E., Ñiquen C., M., 2003. From anchovies to sardines and back: Multidecadal change in the Pacific Ocean. Science 299, 217–221. https://doi.org/10.1126/science.1075880

Cheng, W., Hermann, A.J., Coyle, K.O., Dobbins, E.L., Kachel, N.B., Stabeno, P.J., 2012. Macro- and micro-nutrient flux to a highly productive submarine bank in the Gulf of Alaska: A model-based analysis of daily and interannual variability. Prog. Oceanogr. 101, 63–77. https://doi.org/10.1016/j.pocean.2012.01.001

Ciannelli, L., Bailey, K.M., 2005. Landscape dynamics and resulting species interactions: the cod-capelin system in the southeastern Bering Sea. Mar. Ecol. Prog. Ser. 291, 227–236.

Coetzee, J., 2000. Use of a shoal analysis and patch estimation system (SHAPES) to characterise sardine schools. Aquat. Living Resour. 13, 1–10. https://doi.org/10.1016/S0990-7440(00)00139-X

Coyle, K.O., Gibson, G.A., Hedstrom, K., Hermann, A.J., Hopcroft, R.R., 2013. Zooplankton biomass, advection and production on the northern Gulf of Alaska shelf from simulations and field observations. J. Mar. Syst. 128, 185–207. https://doi.org/10.1016/j.jmarsys.2013.04.018

Coyle, K.O., Pinchuk, A.I., 2005. Seasonal cross-shelf distribution of major zooplankton taxa on the northern Gulf of Alaska shelf relative to water mass properties, species depth preferences and vertical migration behavior. Deep Sea Res. Part II 52, 217–245. https://doi.org/10.1016/j.dsr2.2004.09.025

Coyle, K.O., Pinchuk, A.I., 2003. Annual cycle of zooplankton abundance, biomass and production on the northern Gulf of Alaska shelf, October 1997 through October 2000. Fish. Oceanogr. 12, 327–338. https://doi.org/10.1046/j.1365-2419.2003.00256.x

Csepp, D.J., Vollenweider, J.J., Sigler, M.F., 2011. Seasonal abundance and distribution of pelagic and demersal fishes in southeastern Alaska. Fish. Res. 108, 307–320. https://doi.org/10.1016/j.fishres.2011.01.003

Cury, P.M., Bakun, A., Crawford, R.J.M., Jarre, A., Quinones, R.A., Shannon, L.J., Verheye, H.M., 2000. Small pelagics in upwelling systems: patterns of interaction and structural changes in “wasp-waist” ecosystems. ICES J. Mar. Sci. 57, 603–618. https://doi.org/10.1006/jmsc.2000.0712

Davison, P., 2011. The specific gravity of mesopelagic fish from the northeastern Pacific Ocean and its implications for acoustic backscatter. ICES J. Mar. Sci. J. Cons. 68, 2064–2074. https://doi.org/10.1093/icesjms/fsr140

Davison, P., Lara-Lopez, A., Anthony Koslow, J., 2015. Mesopelagic fish biomass in the southern California current ecosystem. Deep Sea Res. Part II 112, 129–142. https://doi.org/10.1016/j.dsr2.2014.10.007

Davoren, G.K., Penton, P., Burke, C., Montevecchi, W.A., 2012. Water temperature and timing of capelin spawning determine seabird diets. ICES J. Mar. Sci. 69, 1234–1241. https://doi.org/10.1093/icesjms/fss032

De Robertis, A., Higginbottom, I., 2007. A post-processing technique to estimate the signal-to-noise ratio and remove echosounder background noise. ICES J. Mar. Sci. J. Cons. 64, 1282–1291.

De Robertis, A., McKelvey, D.R., Ressler, P.H., 2010. Development and application of an empirical multifrequency method for backscatter classification. Can. J. Fish. Aquat. Sci. 67, 1459–1474. https://doi.org/10.1139/F10-075

De Robertis, A., Taylor, K., Williams, K., Wilson, C.D., 2017a. Species and size selectivity of two midwater trawls used in an acoustic survey of the Alaska Arctic. Deep Sea Res. Part II 135, 40–50. https://doi.org/10.1016/j.dsr2.2015.11.014

De Robertis, A., Taylor, K., Wilson, C.D., Farley, E.V., 2017b. Abundance and distribution of Arctic cod (*Boreogadus saida*) and other pelagic fishes over the U.S. Continental Shelf of the Northern Bering and Chukchi Seas. Deep Sea Res. Part II 135, 51–65. https://doi.org/10.1016/j.dsr2.2016.03.002

Dormann, C.F., McPherson, J.M., Araújo, M.B., Bivand, R., Bolliger, J., Carl, G., Davies, R.G., Hirzel, A., Jetz, W., Kissling, W., Kühn, I., Ohlemüller, R., Peres-Neto, P.R., Reineking, B., Schröder, B., Schurr, F.M., Wilson, R., 2007. Methods to account for spatial autocorrelation in the analysis of species distributional data: a review. Ecography 30, 609–628. https://doi.org/10.1111/j.2007.0906-7590.05171.x

Dorn, M., Aydin, K., Jones, S., Palsson, W., Spalinger, K., 2014. Assessment of walleye pollock stock in the Gulf of Alaska, Stock Assessment and Fishery Evaluation Report for the Groundfish Resources of the Gulf of Alaska. North Pacific Fishery Management Council, 605 W 4th Avenue, Suite 306 Anchorage, AK 99501.

Doyle, M.J., Busby, M.S., Duffy-Anderson, J.T., Picquelle, S.J., Matarese, A.C., 2002. Early life history of capelin (*Mallotus villosus*) in the northwest Gulf of Alaska: a historical perspective based on larval collections, October 1977–March 1979. ICES J. Mar. Sci. J. Cons. 59, 997–1005. https://doi.org/10.1006/jmsc.2002.1236

Dragoo, D.E., Renner, H.M., Irons, D.B., 2015. Breeding status and population trends of seabirds in Alaska, 2014 (Report No. AMNWR 2015/03). U.S. Fish and Wildlife Service, Alaska Maritime National Wildlife Refuge, 95 Sterling Highway, Suite 1 Homer, AK 99603.

Dragoo, D.E., Renner, H.M., Irons, D.B., 2012. Breeding status, population trends and diets of seabirds in Alaska, 2009 (Report No. AMNWR 2012/01). U.S. Fish and Wildlife Service, Alaska Maritime National Wildlife Refuge, 95 Sterling Highway, Suite 1 Homer, AK 99603.

Drinkwater, K.F., Beaugrand, G., Kaeriyama, M., Kim, S., Ottersen, G., Perry, R.I., Pörtner, H.-O., Polovina, J.J., Takasuka, A., 2010. On the processes linking climate to ecosystem changes. J. Mar. Syst., Impact of climate variability on marine ecosystems: A comparative approach 79, 374–388. https://doi.org/10.1016/j.jmarsys.2008.12.014

Duffy-Anderson, J.T., Barbeaux, S.J., Farley, E., Heintz, R., Horne, J.K., Parker-Stetter, S.L., Petrik, C., Siddon, E.C., Smart, T.I., 2015. The critical first year of life of walleye pollock (*Gadus chalcogrammus*) in the eastern Bering Sea: Implications for recruitment and future research. Deep Sea Res. Part II. https://doi.org/10.1016/j.dsr2.2015.02.001

Emmett, R.L., Brodeur, R.D., Orton, P.M., 2004. The vertical distribution of juvenile salmon (*Oncorhynchus* spp.) and associated fishes in the Columbia River plume. Fish. Oceanogr. 13, 392–402. https://doi.org/10.1111/j.1365-2419.2004.00294.x

Eriksen, E., Gjøsæter, H., Prozorkevich, D., Shamray, E., Dolgov, A., Skern-Mauritzen, M., Stiansen, J.E., Kovalev, Y., Sunnanå, K., 2017. From single species surveys towards monitoring of the Barents Sea ecosystem. Prog. Oceanogr. https://doi.org/10.1016/j.pocean.2017.09.007

Fahlén, G., 1968. The gas bladder as a hydrostatic organ in *Thymallus thymallus* L., *Osmerus eperlanus* L. and *Mallotus villosus* Müll. Fisk. Skr. Ser. Havunders. 14, 199–228.

Farley, E.V., Murphy, J.M., Wing, B.W., Moss, J.H., Middleton, A., 2005. Distribution, migration pathways, and size of western Alaska juvenile salmon along the eastern Bering Sea shelf. Alsk. Fish. Res. Bull. 11, 15–26.

Fauchald, P., 2010. Predator–prey reversal: a possible mechanism for ecosystem hysteresis in the North Sea? Ecology 91, 2191–2197. https://doi.org/10.1890/09-1500.1

Fauchald, P., 2009. Spatial interaction between seabirds and prey: review and synthesis. Mar. Ecol. Prog. Ser. 391, 139–151. https://doi.org/10.3354/meps07818

Fauchald, P., Erikstad, K.E., 2002. Scale-dependent predator-prey interactions: the aggregative response of seabirds to prey under variable prey abundance and patchiness. Mar. Ecol. Prog. Ser. 231, 279–291. https://doi.org/10.3354/meps231279

Fauchald, P., Erikstad, K.E., Skarsfjord, H., 2000. Scale-dependent predator-prey interactions: The hierarchical spatial distribution of seabirds and prey. Ecology 81, 773–783. https://doi.org/10.2307/177376

Foote, K.G., Knudsen, H.P., Vestnes, G., MacLennan, D.N., Simmonds, E.J., 1987. Calibration of Acoustic Instruments for Fish Density Estimation: a Practical Guide (Cooperative Research Report No. 144). International Council for the Exploration of the Sea.

Fortin, M.-J., Dale, M.R.T., 2005. Spatial Analysis: A Guide for Ecologists. Cambridge University Press.

Francis, R.C., Hare, S.R., Hollowed, A.B., Wooster, W.S., 1998. Effects of interdecadal climate variability on the oceanic ecosystems of the NE Pacific. Fish. Oceanogr. 7, 1–21. https://doi.org/10.1046/j.1365-2419.1998.00052.x

Francis, R.C., Hixon, M.A., Clarke, M.E., Murawski, S.A., Ralston, S., 2007. Ten commandments for ecosystem-based fisheries scientists. Fisheries 32, 217–233. https://doi.org/10.1577/1548-8446(2007)32[217:TCFBFS]2.0.CO;2

Frank, K.T., Carscadden, J.E., Simon, J.E., 1996. Recent excursions of capelin (*Mallotus villosus*) to the Scotian Shelf and Flemish Cap during anomalous hydrographic conditions. Can. J. Fish. Aquat. Sci. 53, 1473–1486. https://doi.org/10.1139/f96-078

Frank, K.T., Petrie, B., Fisher, J., Leggett, W.C., 2011. Transient dynamics of an altered large marine ecosystem. Nature 477, 86–98. https://doi.org/10.1038/nature10285

Freon, P., Cury, P., Shannon, L., Roy, C., 2005. Sustainable exploitation of small pelagic fish stocks challenged by environmental and ecosystem changes: a review. Bull. Mar. Sci. 76, 385–462.

Funk, F., 1990. Migration of Pacific herring in the eastern Bering Sea as inferred from 1983-88 joint venture and foreign observer information (Regional Information Report No. 5J90-04). Alaska Department of Fish and Game, Juneau, Alaska.

Gilliam, J.F., Fraser, D.F., 1987. Habitat selection under predation hazard: test of a model with foraging minnows. Ecology 68, 1856–1862. https://doi.org/10.2307/1939877

Gjøsæter, H., 1998. The population biology and exploitation of capelin (*Mallotus villosus*) in the Barents Sea. Sarsia 83, 453–496.

Gjøsæter, H., Bogstad, B., Tjelmeland, S., 2009. Ecosystem effects of the three capelin stock collapses in the Barents Sea. Mar. Biol. Res. 5, 40–53. https://doi.org/10.1080/17451000802454866

Gjøsæter, H., Dalpadado, P., Hassel, A., 2002. Growth of Barents Sea capelin (*Mallotus villosus*) in relation to zooplankton abundance. ICES J. Mar. Sci. 59, 959–967. https://doi.org/10.1006/jmsc.2002.1240

Gorska, N., Ona, E., 2003. Modelling the acoustic effect of swimbladder compression in herring. ICES J. Mar. Sci. 60, 548–554. https://doi.org/10.1016/S1054-3139(03)00050-X

Grados, D., Fablet, R., Ballon, M., Bez, N., Castillo, R., Lezama-Ochoa, A., Bertrand, A., 2012. Multiscale characterization of spatial relationships among oxycline depth, macrozooplankton, and forage fish off Peru using geostatistics, principal coordinates of neighbor matrices (PCNMs), and wavelets. Can. J. Fish. Aquat. Sci. 69, 740–754. https://doi.org/10.1139/F2012-017

Grebmeier, J.M., Overland, J.E., Moore, S.E., Farley, E.V., Carmack, E.C., Cooper, L.W., Frey, K.E., Helle, J.H., McLaughlin, F.A., McNutt, S.L., 2006. A major ecosystem shift in the northern Bering Sea. Science 311, 1461–1464. https://doi.org/10.1126/science.1121365

Greenstreet, S.P.R., Armstrong, E., Mosegaard, H., Jensen, H., Gibb, I.M., Fraser, H.M., Scott, B.E., Holland, G.J., Sharples, J., 2006. Variation in the abundance of sandeels *Ammodytes marinus* off southeast Scotland: an evaluation of area-closure fisheries management and stock abundance assessment methods. ICES J. Mar. Sci. J. Cons. 63, 1530–1550. https://doi.org/10.1016/j.icesjms.2006.05.009

Guttormsen, M.A., Yasenak, P.T., 2007. Results of the 2003 and 2005 echo integration-trawl surveys in the Gulf of Alaska during summer, Cruises MF2003-09 and OD2005-01 (No. AFSC Processed Rep. 2007-04). Alaska Fisheries Science Center, NOAA, National Marine Fisheries Service, 7600 Sand Point Way NE, Seattle WA 98115.

Halverson, M.J., 2014. Atmospheric and tidal forcing of the exchange between Prince William Sound and the Gulf of Alaska. Dyn. Atmospheres Oceans 65, 86–106. https://doi.org/10.1016/j.dynatmoce.2013.12.001

Hardin, J.W., Hilbe, J.M., 2007. Generalized Linear Models and Extensions, Second Edition. Stata Press, College Station, Texas.

Hay, D.E., Toresen, R., Stephenson, R., Thompson, M., Claytor, R., Funk, F., Ivshina, E., Jakobsson, J., Kobayashi, T., McQuinn, I., Melvin, G., Molloy, J., Naumenko, N., Oda, K.T., Parmanne, R., Power, M., Radchenko, V., Schweigert, J., Simmonds, J., Sjöstrand, B., Stevenson, D.K., Tanasichuk, R., Tang, Q., Watters, D.L., Wheeler, J., 2001. Taking stock: an inventory and review of world herring stocks in 2000, in: Herring: Expectations for a New Millennium. Alaska Sea Grant College Program, Fairbanks, Alaska, USA, pp. 381–454.

Haynes, T.B., Robinson, C.K.L., Dearden, P., 2008. Modelling nearshore intertidal habitat use of young-of-the-year Pacific sand lance (*Ammodytes hexapterus*) in Barkley Sound, British Columbia, Canada. Environ. Biol. Fishes 83, 473–484. https://doi.org/10.1007/s10641-008-9374-2

Hebert, K.P., 2014. Operational plan: Southeast Alaska herring stock assessment surveys and sampling, 2014 (Regional Operational Plan No. CF.1J.14-01). Alaska Department of Fish and Game, Division of Commercial Fisheries, Juneau, Alaska.

Hermann, A.J., Ladd, C., Cheng, W., Curchitser, E.N., Hedstrom, K., 2016. A model-based examination of multivariate physical modes in the Gulf of Alaska. Deep Sea Res. Part II 132, 68–89. https://doi.org/10.1016/j.dsr2.2016.04.005

Hinckley, S., Bailey, K., Picquelle, S., Schumacher, J., Stabeno, P., 1991. Transport, distribution, and abundance of larval and juvenile walleye pollock (*Theragra chalcogramma*) in the Western Gulf of Alaska. Can. J. Fish. Aquat. Sci. 48, 91–98. https://doi.org/10.1139/f91-013

Hjermann, D.Ø., Bogstad, B., Dingsør, G.E., Gjøsæter, H., Ottersen, G., Eikeset, A.M., Stenseth, N.C., 2010. Trophic interactions affecting a key ecosystem component: a multistage analysis of the recruitment of the Barents Sea capelin (*Mallotus villosus*). Can. J. Fish. Aquat. Sci. 67, 1363–1375. https://doi.org/10.1139/F10-064

Hjermann, D.Ø., Stenseth, N.C., Ottersen, G., 2004. Indirect climatic forcing of the Barents Sea capelin: a cohort effect. Mar. Ecol. Prog. Ser. 273, 229–238.

Hjort, J., 1914. Fluctuations in the great fisheries of northern Europe. Rapp. Cons. Explor. Mer 20, 1–228.

Hobson, E.S., 1986. Predation on the Pacific sand lance, *Ammodytes hexapterus* (Pisces: Ammodytidae), during the transition between day and night in southeastern Alaska. Copeia 1986, 223–226. https://doi.org/10.2307/1444914

Hollowed, A.B., Barange, M., Beamish, R.J., Brander, K., Cochrane, K., Drinkwater, K., Foreman, M.G.G., Hare, J.A., Holt, J., Ito, S., Kim, S., King, J.R., Loeng, H., MacKenzie, B.R., Mueter, F.J., Okey, T.A., Peck, M.A., Radchenko, V.I., Rice, J.C., Schirripa, M.J., Yatsu, A., Yamanaka, Y., 2013a. Projected impacts of climate change on marine fish and fisheries. ICES J. Mar. Sci. J. Cons. 70, 1023–1037. https://doi.org/10.1093/icesjms/fst081

Hollowed, A.B., Barbeaux, S.J., Cokelet, E.D., Farley, E., Kotwicki, S., Ressler, P.H., Spital, C., Wilson, C.D., 2012. Effects of climate variations on pelagic ocean habitats and their role in structuring forage fish distributions in the Bering Sea. Deep Sea Res. Part II 65–70, 230–250. https://doi.org/10.1016/j.dsr2.2012.02.008

Hollowed, A.B., Planque, B., Loeng, H., 2013b. Potential movement of fish and shellfish stocks from the sub-Arctic to the Arctic Ocean. Fish. Oceanogr. 22, 355–370. https://doi.org/10.1111/fog.12027

Hollowed, A.B., Wilson, C.D., Stabeno, P.J., Salo, S.A., 2007. Effect of ocean conditions on the cross-shelf distribution of walleye pollock (*Theragra chalcogramma*) and capelin (*Mallotus villosus*). Fish. Oceanogr. 16, 142–154. https://doi.org/10.1111/j.1365-2419.2006.00418.x

Hollowell, G., Otis, E.O., Ford, E., 2015. 2014 Lower Cook Inlet area finfish management report (Fishery Management Report No. No 15-32). Alaska Department of Fish and Game, Anchorage, Alaska.

Hopcroft, R.R., Aguilar-Islas, A.M., Ladd, C., Matarese, A.C., Mordy, C.W., Rember, R., Stabeno, P.J., Strom, S.L., 2016. The Role of Cross-shelf and Along-shelf Transports as Controlling Mechanisms for Nutrients, Plankton and Larval Fish in the Coastal Gulf of Alaska (NPRB GOA Project G83 & G85 Lower Trophic Level Final Report). North Pacific Research Board, Anchorage, AK.

Horne, J.K., Schneider, D.C., 1994. Analysis of scale-dependent processes with dimensionless ratios. Oikos 70, 201–211. https://doi.org/10.2307/3545631

Hrabik, T.R., Jensen, O.P., Martell, S.J.D., Walters, C.J., Kitchell, J.F., 2006. Diel vertical migration in the Lake Superior pelagic community. I. Changes in vertical migration of coregonids in response to varying predation risk. Can. J. Fish. Aquat. Sci. 63, 2286–2295. https://doi.org/10.1139/f06-124

Hunt, G.L., Mehlum, F., Russell, R.W., Irons, D., Decker, M.B., Becker, P.H., 1999. Physical processes, prey abundance, and the foraging ecology of seabirds, in: Proceedings of the International Ornithological Congress. pp. 2040–2056.

Huse, G., Ellingsen, I., 2008. Capelin migrations and climate change – a modelling analysis. Clim. Change 87, 177–197. https://doi.org/10.1007/s10584-007-9347-z

Ingvaldsen, R.B., Gjøsæter, H., 2013. Responses in spatial distribution of Barents Sea capelin to changes in stock size, ocean temperature and ice cover. Mar. Biol. Res. 9, 867–877. https://doi.org/10.1080/17451000.2013.775450

IPCC, 2007. Climate Change 2007: Synthesis Report, in: Pachauri, R.K., Reisinger, A., Core Writing Team (Eds.), Contribution of Working Groups I, II, and III to the Fourth Assessment Report of the Intergovernmental Panel on Climate Change. IPCC, Geneva, Switzerland, p. 104.

Johnson, S.W., Thedinga, J.F., Munk, K.M., 2008. Distribution and use of shallow-water habitats by Pacific sand lances in southeastern Alaska. Trans. Am. Fish. Soc. 137, 1455–1463. https://doi.org/10.1577/T07-194.1

Jones, D.T., Ressler, P.H., Stienessen, S.C., McCarthy, A.L., Simonsen, K.A., 2014. Results of the acoustic-trawl survey of walleye pollock (*Gadus chalcogrammus*) in the Gulf of Alaska, June-August 2013 (DY2013-07) (AFSC Processed Rep. No. 2014-06). Alaska Fish. Sci. Cent., NOAA, Natl. Mar. Fish. Serv., 7600 Sand Point Way NE, Seattle WA 98115.

Jones, D.T., Stienessen, S.C., Lauffenburger., N., 2017. Results of the acoustic-trawl survey of walleye pollock (*Gadus chalcogrammus*) in the Gulf of Alaska, June-August 2015 (DY2015-06) (AFSC Processed Rep. No. 2017-03). Alaska Fish. Sci. Cent., NOAA, Natl. Mar. Fish. Serv., 7600 Sand Point Way NE, Seattle WA 98115.

Jones, D.T., Stienessen, S.C., Simonsen, K.A., Guttormsen, M.A., 2015. Results of the acoustic-trawl survey of walleye pollock (*Gadus chalcogrammus*) in the Gulf of Alaska, June-August 2011 (DY2011-03) (AFSC Processed Rep. No. 2015-04). Alaska Fish. Sci. Cent., NOAA, Natl. Mar. Fish. Serv., 7600 Sand Point Way NE, Seattle WA 98115.

Jørgensen, R., 2003. The effects of swimbladder size, condition and gonads on the acoustic target strength of mature capelin. ICES J. Mar. Sci. 60, 1056–1062. https://doi.org/10.1016/S1054-3139(03)00115-2

Kang, M., Furusawa, M., Miyashita, K., 2002. Effective and accurate use of difference in mean volume backscattering strength to identify fish and plankton. ICES J. Mar. Sci. 59, 794–804. https://doi.org/10.1006/jmsc.2002.1229

Keith, G.J., Ryan, T.E., Kloser, R.J., 2005. ES60adjust. jar. Java software utility to remove a systematic error in Simrad ES60 data.

Kettle, A.B., Bargmann, N., Winnard, S., 2015. Biological monitoring at East Amatuli Island, Alaska in 2014 (Report No. AMNWR 2015/06). U.S. Fish and Wildlife Service, Alaska Maritime National Wildlife Refuge, 95 Sterling Highway, Suite 1 Homer, AK 99603.

Kornilovs, G., Sidrevics, L., Dippner, J.W., 2001. Fish and zooplankton interaction in the Central Baltic Sea. ICES J. Mar. Sci. 58, 579–588. https://doi.org/10.1006/jmsc.2001.1062

Kotwicki, S., Horne, J.K., Punt, A.E., Ianelli, J.N., 2015. Factors affecting the availability of walleye pollock to acoustic and bottom trawl survey gear. ICES J. Mar. Sci. 72, 1425–1439. https://doi.org/10.1093/icesjms/fsv011

Kristensen, K., Nielsen, A., Berg, C.W., Skaug, H., Bell, B., 2016. TMB: Automatic differentiation and Laplace approximation. J. Stat. Softw. 70, 1–21. https://doi.org/doi: 10.18637/jss.v070.i05

Kutner, M., Nachtsheim, C., Neter, J., Li, W., 2004. Applied Linear Statistical Models, 5th ed. McGraw Hill.

Ladd, C., 2007. Interannual variability of the Gulf of Alaska eddy field. Geophys. Res. Lett. 34, L11605.

Ladd, C., Cheng, W., 2016. Gap winds and their effects on regional oceanography Part I: Cross Sound, Alaska. Deep Sea Res. Part II 132, 41–53. https://doi.org/10.1016/j.dsr2.2015.08.006

Ladd, C., Cheng, W., Salo, S., 2016. Gap winds and their effects on regional oceanography Part II: Kodiak Island, Alaska. Deep Sea Res. Part II 132, 54–67. https://doi.org/10.1016/j.dsr2.2015.08.005

Ladd, C., Mordy, C.W., Kachel, N.B., Stabeno, P.J., 2007. Northern Gulf of Alaska eddies and associated anomalies. Deep Sea Res. Part Oceanogr. Res. Pap. 54, 487–509.

Ladd, C., Stabeno, P., Cokelet, E., 2005. A note on cross-shelf exchange in the northern Gulf of Alaska. Deep Sea Res. Part II 52, 667–679.

Legendre, P., Fortin, M., 1989. Spatial pattern and ecological analysis. Vegetatio 80, 107–138. https://doi.org/10.1007/BF00048036

Lewis, S., Sherratt, T.N., Hamer, K.C., Wanless, S., 2001. Evidence of intra-specific competition for food in a pelagic seabird. Nature 412, 816–819. https://doi.org/10.1038/35090566

Li, K., Doubleday, A.J., Galbraith, M.D., Hopcroft, R.R., 2016. High abundance of salps in the coastal Gulf of Alaska during 2011: A first record of bloom occurrence for the northern Gulf. Deep Sea Res. Part II 132, 136–145. https://doi.org/10.1016/j.dsr2.2016.04.009

Lindgren, F., Rue, H., Lindström, J., 2011. An explicit link between Gaussian fields and Gaussian Markov random fields: the stochastic partial differential equation approach. J. R. Stat. Soc. Ser. B Stat. Methodol. 73, 423–498. https://doi.org/10.1111/j.1467-9868.2011.00777.x

Link, J.S., 2002. What does ecosystem-based fisheries management mean. Fisheries 27, 18–21.

Lippiatt, S.M., Lohan, M.C., Bruland, K.W., 2010. The distribution of reactive iron in northern Gulf of Alaska coastal waters. Mar. Chem. 121, 187–199.

Livingston, P.A., Aydin, K., Boldt, J., Ianelli, J., Jurado-Molina, J., 2005. A framework for ecosystem impacts assessment using an indicator approach. ICES J. Mar. Sci. 62, 592–597. https://doi.org/10.1016/j.icesjms.2004.12.016

Logerwell, E., Busby, M., Carothers, C., Cotton, S., Duffy-Anderson, J., Farley, E., Goddard, P., Heintz, R., Holladay, B., Horne, J., Johnson, S., Lauth, B., Moulton, L., Neff, D., Norcross, B., Parker-Stetter, S., Seigle, J., Sformo, T., 2015. Fish communities across a spectrum of habitats in the western Beaufort Sea and Chukchi Sea. Prog. Oceanogr., Synthesis of Arctic Research (SOAR) 136, 115–132. https://doi.org/10.1016/j.pocean.2015.05.013

Logerwell, E.A., Duffy-Anderson, J., Wilson, M., McKelvey, D., 2010. The influence of pelagic habitat selection and interspecific competition on productivity of juvenile walleye pollock (*Theragra chalcogramma*) and capelin (*Mallotus villosus*) in the Gulf of Alaska. Fish. Oceanogr. 19, 262–278. https://doi.org/10.1111/j.1365-2419.2010.00542.x

Logerwell, E.A., Stabeno, P.J., Wilson, C.D., Hollowed, A.B., 2007. The effect of oceanographic variability and interspecific competition on juvenile pollock (*Theragra chalcogramma*) and capelin (*Mallotus villosus*) distributions on the Gulf of Alaska shelf. Deep Sea Res. Part II 54, 2849–2868. https://doi.org/10.1016/j.dsr2.2007.08.008

Macarthur, R.H., Pianka, E.R., 1966. On optimal use of a patchy environment. Am. Nat. 100, 603–613. https://doi.org/10.1086/282454

MacCall, A.D., 1990. Dynamic geography of marine fish populations. Washington Sea Grant Program Seattle, Washington.

MacLennan, D.N., Fernandes, P.G., Dalen, J., 2002. A consistent approach to definitions and symbols in fisheries acoustics. ICES J. Mar. Sci. J. Cons. 59, 365–369. https://doi.org/10.1006/jmsc.2001.1158

Mantua, N.J., Hare, S.R., Zhang, Y., Wallace, J.M., Francis, R.C., 1997. A Pacific interdecadal climate oscillation with impacts on salmon production. Bull. Am. Meteorol. Soc. 78, 1069–1079. https://doi.org/10.1175/1520-0477(1997)078<1069:APICOW>2.0.CO;2

Matsukura, R., Yasuma, H., Murase, H., Yonezaki, S., Funamoto, T., Honda, S., Miyashita, K., 2009. Measurements of density contrast and sound-speed contrast for target strength estimation of Neocalanus copepods (*Neocalanus cristatus* and *Neocalanus plumchrus*) in the North Pacific Ocean. Fish. Sci. 75, 1377. https://doi.org/10.1007/s12562-009-0172-3

Maunder, M.N., Punt, A.E., 2004. Standardizing catch and effort data: a review of recent approaches. Fish. Res., Models in Fisheries Research: GLMs, GAMS and GLMMs 70, 141–159. https://doi.org/10.1016/j.fishres.2004.08.002

McGill, R., Tukey, J.W., Larsen, W.A., 1978. Variations of box plots. Am. Stat. 32, 12–16. https://doi.org/10.2307/2683468

McKelvey, D.R., Wilson, C.D., 2006. Discriminant classification of fish and zooplankton backscattering at 38 and 120 kHz. Trans. Am. Fish. Soc. 135, 488–499. https://doi.org/10.1577/T04-140.1

McQuinn, I.H., 2009. Pelagic fish outburst or suprabenthic habitat occupation: legacy of the Atlantic cod (Gadus morhua) collapse in eastern Canada. Can. J. Fish. Aquat. Sci. 66, 2256–2262. https://doi.org/10.1139/F09-143

Mecklenburg, C.W., Mecklenburg, T.A., Thorsteinson, L.K., 2002. Fishes of Alaska. American Fisheries Society, Bethesda, Md.

Merrick, R.L., Chumbley, M.K., Byrd, G.V., 1997. Diet diversity of Steller sea lions (*Eumetopias jubatus*) and their population decline in Alaska: a potential relationship. Can. J. Fish. Aquat. Sci. 54, 1342–1348. https://doi.org/10.1139/f97-037

Meyer, T.L., Cooper, R.A., Langton, R.W., 1979. Relative abundance, behavior, and food habits of the American sand lance, *Ammodytes americanus*, from the Gulf of Maine. Fish. Bull. 77, 243–253.

Mi, X.C., Ren, H.B., Ouyang, Z.S., Wei, W., Ma, K.P., 2005. The use of the Mexican Hat and the Morlet wavelets for detection of ecological patterns. Plant Ecol. 179, 1–19. https://doi.org/10.1007/s11258-004-5089-4

Micheli, F., 1999. Eutrophication, fisheries, and consumer-resource dynamics in marine pelagic ecosystems. Science 285, 1396–1398. https://doi.org/10.1126/science.285.5432.1396

Moore, S.E., Stabeno, P.J., 2015. Synthesis of Arctic Research (SOAR) in marine ecosystems of the Pacific Arctic. Prog. Oceanogr., Synthesis of Arctic Research (SOAR) 136, 1–11. https://doi.org/10.1016/j.pocean.2015.05.017

Mordy, C.W., Stabeno, P.J., Kachel, N.B., Kachel, D., Ladd, C., Zimmermann, M., Doyle, M.J., 2016. Appendix 1: importance of canyons to the northern Gulf of Alaska ecosystem, In: *The Role of Cross-shelf and Along-shelf Transports as Controlling Mechanisms for Nutrients, Plankton and Larval Fish in the Coastal Gulf of Alaska* (NPRB GOA Project G83 & G85 Lower Trophic Level Final Report). North Pacific Research Board, Anchorage, AK.

Moss, J.H., Heintz, R.A., Zaleski, M., 2016a. Chapter 10 - Interannual and regional variability in the distribution, feeding, and energetic health of age-0 walleye pollock (*Gadus chalcogrammus*) and pacific cod (*Gadus macrocephalus*) in the Gulf of Alaska, In: *Surviving the Gauntlet: a Comparative Study of the Pelagic, Demersal, and Spatial Linkages that Determine Groundfish Recruitment and Diversity in the Gulf of Alaska Ecosystem* (NPRB GOA Project G84 Upper Trophic Level Final Report). North Pacific Research Board, Anchorage, AK.

Moss, J.H., Shotwell, S.K., Heintz, R.A., Atkinson, S., Debenham, C., Fournier, W., Golden, N., Heifetz, J., Mueter, F.J., Pirtle, J.L., Reid, J.A., Slater, L., Sreenivasan, A., Will, A., Zaleski, M., Zimmermann, M., 2016b. Surviving the Gauntlet: a Comparative Study of the Pelagic, Demersal, and Spatial Linkages that Determine Groundfish Recruitment and Diversity in the Gulf of Alaska Ecosystem (NPRB GOA Project G84 Upper Trophic Level Final Report). North Pacific Research Board, Anchorage, AK.

Mowbray, F., 2002. Changes in the vertical distribution of capelin (*Mallotus villosus*) off Newfoundland. ICES J. Mar. Sci. 59, 942–949. https://doi.org/10.1006/jmsc.2002.1259

Mueter, F., Norcross, B., 2002. Spatial and temporal patterns in the demersal fish community on the shelf and upper slope regions of the Gulf of Alaska. Fish. Bull. 100, 559–581.

Murase, H., Ichihara, M., Yasuma, H., Watanabe, H., Yonezaki, S., Nagashima, H., Kawahara, S., Miyashita, K., 2009. Acoustic characterization of biological backscatterings in the Kuroshio-Oyashio inter-frontal zone and subarctic waters of the western North Pacific in spring. Fish. Oceanogr. 18, 386–401. https://doi.org/10.1111/j.1365-2419.2009.00519.x

Nakashima, B.S., 1990. Escapement from a Diamond IX midwater trawl during acoustic surveys for capelin (*Mallotus villosus*) in the Northwest Atlantic. ICES J. Mar. Sci. 47, 76–82. https://doi.org/10.1093/icesjms/47.1.76

Nakashima, B.S., Wheeler, J.P., 2002. Capelin (*Mallotus villosus*) spawning behaviour in Newfoundland waters–the interaction between beach and demersal spawning. ICES J. Mar. Sci. 59, 909–916. https://doi.org/10.1006/jmsc.2002.1261

National Atlas of the United States, 2014. 1:1,000,000-Scale Coastline of the United States.

Obradovich, S.G., Carruthers, E.H., Rose, G.A., 2014. Bottom-up limits to Newfoundland capelin (*Mallotus villosus*) rebuilding: the euphausiid hypothesis. ICES J. Mar. Sci. J. Cons. 71, 775–783. https://doi.org/10.1093/icesjms/fst184

O'Driscoll, R.L., Rose, G.A., Anderson, J.T., 2002. Counting capelin: a comparison of acoustic density and trawl catchability. ICES J. Mar. Sci. J. Cons. 59, 1062–1071. https://doi.org/10.1006/jmsc.2002.1262

Olafsdottir, A.H., Rose, G.A., 2013. Staged spawning migration in Icelandic capelin (*Mallotus villosus*): effects of temperature, stock size and maturity. Fish. Oceanogr. 22, 446–458. https://doi.org/10.1111/fog.12032

Olafsdottir, A.H., Rose, G.A., 2012. Influences of temperature, bathymetry and fronts on spawning migration routes of Icelandic capelin (*Mallotus villosus*). Fish. Oceanogr. 21, 182–198. https://doi.org/10.1111/j.1365-2419.2012.00618.x

Ona, E., Mitson, R.B., 1996. Acoustic sampling and signal processing near the seabed: the deadzone revisited. ICES J. Mar. Sci. J. Cons. 53, 677–690. https://doi.org/10.1006/jmsc.1996.0087

Orians, G.H., Pearson, N.E., 1979. On the theory of central place foraging, in: Horn, D.J., Stairs, G.R., Mitchell, R.D. (Eds.), Analysis of Ecological Systems. Ohio State University Press, Columbus, OH, pp. 155–177.

Orlova, E.L., Rudneva, G.B., Renaud, P.E., Eiane, K., Savinov, V., Yurko, A.S., 2010. Climate impacts on feeding and condition of capelin *Mallotus villosus* in the Barents Sea: evidence and mechanisms from a 30 year data set. Aquat. Biol. 10, 105–118. https://doi.org/10.3354/ab00265

Ormseth, O., 2014. Appendix 2. Forage species report for the Gulf of Alaska (Stock Assessment and Fishery Evaluation Report for the Groundfish Resources of the Gulf of Alaska). North Pacific Fishery Management Council, 605 W. 4th Avenue, Suite 306, Anchorage, AK 99301.

Ormseth, O., 2012. Appendix 2. Preliminary assessment of forage species in the Gulf of Alaska (Stock Assessment and Fishery Evaluation Report for the Groundfish Resources of the Gulf of Alaska). North Pacific Fishery Management Council, 605 W. 4th Avenue, Suite 306, Anchorage, AK 99301.

Ormseth, O., Moss, J.H., McGowan, D.W., 2016. Appendix. Forage species report for the Gulf of Alaska (Stock Assessment and Fishery Evaluation Report for the Groundfish Resources of the Gulf of Alaska). North Pacific Fishery Management Council, 605 W. 4th Avenue, Suite 306, Anchorage, AK 99301.

Ormseth, O.A., Budge, S., De Robertis, A., Horne, J., McGowan, D., Rand, K., Wang, S., 2016. Temporal and spatial axes of variability in the structure of Gulf of Alaska forage fish communities (No. NPRB GOA Project G82 Middle Trophic Level Final Report), Gulf of Alaska Integrated Ecosystem Research Program. North Pacific Research Board.

Orsi, J., Wertheimer, A., 1995. Marine vertical distribution of juvenile chinook and coho salmon in southeastern Alaska. Trans. Am. Fish. Soc. 124, 159–169. https://doi.org/10.1577/1548-8659(1995)124<0159:MVDOJC>2.3.CO;2

Ostrand, W.D., Gotthardt, T.A., Howlin, S., Robards, M.D., Orr, J.W., 2005. Habitat selection models for Pacific sand lance (*Ammodytes hexapterus*) in Prince William Sound, Alaska. Northwest. Nat. 86, 131–143. https://doi.org/10.1898/1051-1733(2005)086[0131:SMFPSL]2.0.CO;2

Ovaskainen, O., Roy, D.B., Fox, R., Anderson, B.J., 2016. Uncovering hidden spatial structure in species communities with spatially explicit joint species distribution models. Methods Ecol. Evol. 7, 428–436. https://doi.org/10.1111/2041-210X.12502

Pahlke, K.A., 1985. Preliminary studies of capelin (*Mallotus villosus*) in Alaskan waters. Alaska Department of Fish and Game.

Parada, C., Hinckley, S., Horne, J., Mazur, M., Hermann, A., Curchister, E., 2016. Modeling connectivity of walleye pollock in the Gulf of Alaska: Are there any linkages to the Bering Sea and Aleutian Islands? Deep Sea Res. Part II 132, 227–239. https://doi.org/10.1016/j.dsr2.2015.12.010

Parker-Stetter, S., Urmy, S., Horne, J., Eisner, L., Farley, E., 2016. Factors affecting summer distributions of Bering Sea forage fish species: assessing competing hypotheses. Deep Sea Res. Part II. https://doi.org/10.1016/j.dsr2.2016.06.013i

Parker-Stetter, S.L., Horne, J.K., Farley, E.V., Barbee, D.H., Andrews III, A.G., Eisner, L.B., Nomura, J.M., 2013. Summer distributions of forage fish in the eastern Bering Sea. Deep Sea Res. Part II 94, 211–230. https://doi.org/10.1016/j.dsr2.2013.04.022

Parker-Stetter, S.L., Horne, J.K., Urmy, S.S., Heintz, R.A., Eisner, L.B., Farley, E.V., 2015. Vertical distribution of age-0 pollock during late-summer: Biophysical coupling or ontogeny? Mar. Coast. Fish. 7, 349–369. https://doi.org/10.1080/19425120.2015.1057307

Perrette, M., Yool, A., Quartly, G.D., Popova, E.E., 2011. Near-ubiquity of ice-edge blooms in the Arctic. Biogeosciences Katlenburg-Lindau 8, 515.

Perry, A.L., Low, P.J., Ellis, J.R., Reynolds, J.D., 2005. Climate change and distribution shifts in marine fishes. Science 308, 1912–1915. https://doi.org/10.1126/science.1111322

Pershing, A.J., Alexander, M.A., Hernandez, C.M., Kerr, L.A., Bris, A.L., Mills, K.E., Nye, J.A., Record, N.R., Scannell, H.A., Scott, J.D., Sherwood, G.D., Thomas, A.C., 2015. Slow adaptation in the face of rapid warming leads to collapse of the Gulf of Maine cod fishery. Science aac9819. https://doi.org/10.1126/science.aac9819

Piatt, J.F., 1990. The aggregative response of common murres and Atlantic puffins to schools of capelin. Stud. Avian Ecol. 14, 36–51.

Piatt, J.F., Anderson, P.J., 1996. Response of common murres to the Exxon Valdez oil spill and long-term changes in the Gulf of Alaska marine ecosystem, in: American Fisheries Society Symposium. Presented at the Proceedings of the Exxon Valdez Oil Spill Symposium: held at Anchorage, Alaska, USA, 2–5 February 1993, American Fisheries Society, Bethesda, MD, pp. 720–737.

Piatt, J.F., Harding, A.M.A., Shultz, M., Speckman, S.G., Pelt, T.I. van, Drew, G.S., Kettle, A.B., 2007. Seabirds as indicators of marine food supplies: Cairns revisited. Mar. Ecol. Prog. Ser. 352, 221–234. https://doi.org/10.3354/meps07078

Pikitch, E.K., Boersma, P.D., Boyd, I.L., Conover, D.O., Cury, P., Essington, T., Heppell, S.S., Houde, E.D., Mangel, M., Pauly, D., Plaganyi, E., Sainsbury, K., Steneck, R.S., 2012. Little fish, big impact: managing a crucial link in ocean food webs. Lenfest Ocean Program, Washington, DC.

Pikitch, E.K., Rountos, K.J., Essington, T.E., Santora, C., Pauly, D., Watson, R., Sumaila, U.R., Boersma, P.D., Boyd, I.L., Conover, D.O., Cury, P., Heppell, S.S., Houde, E.D., Mangel, M., Plagányi, É., Sainsbury, K., Steneck, R.S., Geers, T.M., Gownaris, N., Munch, S.B., 2014. The global contribution of forage fish to marine fisheries and ecosystems. Fish Fish. 15, 43–64. https://doi.org/10.1111/faf.12004

Pikitch, E.K., Santora, C., Babcock, E.A., Bakun, A., Bonfil, R., Conover, D.O., Dayton, P., Doukakis, P., Fluharty, D., Heneman, B., Houde, E.D., Link, J., Livingston, P.A., Mangel, M., McAllister, M.K., Pope, J., Sainsbury, K.J., 2004. Ecosystem-based fishery management. Science 305, 346–347. https://doi.org/10.1126/science.1098222

Pinchuk, A.I., Coyle, K.O., Hopcroft, R.R., 2008. Climate-related variability in abundance and reproduction of euphausiids in the northern Gulf of Alaska in 1998–2003. Prog. Oceanogr. 77, 203–216. https://doi.org/10.1016/j.pocean.2008.03.012

R Core Development Team, 2015. R: A Language and Environment for Statistical Computing. R Foundation for Statistical Computing, Vienna, Austria.

Renard, D., Bez, N., Desassis, N., Beucher, H., Ors, F., Freulon, X., 2017. RGeostats: The Geostatistical R package 11.1.2. MINES ParisTech / ARMINES.

Ressler, P.H., De Robertis, A., Warren, J.D., Smith, J.N., Kotwicki, S., 2012. Developing an acoustic survey of euphausiids to understand trophic interactions in the Bering Sea ecosystem. Deep Sea Res. Part II 65–70, 184–195. https://doi.org/10.1016/j.dsr2.2012.02.015

Rhea-Fournier, W.J., Mueter, F.J., Moss, J.H., 2016. Chapter 1 - Young of the year groundfish in the epipelagic fish community of the Gulf of Alaska, In: *Surviving the Gauntlet: a Comparative Study of the Pelagic, Demersal, and Spatial Linkages that Determine Groundfish Recruitment and Diversity in the Gulf of Alaska Ecosystem* (NPRB GOA Project G84 Upper Trophic Level Final Report). North Pacific Research Board, Anchorage, AK.

Ripley, B.D., 1981. Spatial Statistics. Wiley, New York.

Robards, M.D., Abookire, A., Anson, J.M., Bodkin, J.L., Drew, G., Hooge, P., Piatt, J.F., Speckman, S.G., 2003. Ecology of selected marine communities in Glacier Bay: zooplankton, forage fish, seabirds and marine mammals. United States Geological Survey, Alaska Science Center, Biological Science Office, Anchorage, AK.

Rose, G.A., 2005. Capelin (*Mallotus villosus*) distribution and climate: a sea "canary" for marine ecosystem change. ICES J. Mar. Sci. J. Cons. 62, 1524–1530. https://doi.org/10.1016/j.icesjms.2005.05.008

Rose, G.A., Leggett, W.C., 1990. The importance of scale to predator-prey spatial correlations: an example of Atlantic fishes. Ecology 71, 33–43. https://doi.org/10.2307/1940245

Rose, G.A., O'Driscoll, R.L., 2002. Capelin are good for cod: can the northern stock rebuild without them? ICES J. Mar. Sci. 59, 1018–1026. https://doi.org/10.1006/jmsc.2002.1252

Royer, T.C., Vermersch, J.A., Weingartner, T.J., Niebauer, H.J., Muench, R.D., 1990. Ocean circulation influencing the "Exxon Valdez" oil spill. Oceanography 3, 3–10.

Rue, H., Martino, S., Chopin, N., 2009. Approximate Bayesian inference for latent Gaussian models by using integrated nested Laplace approximations. J. R. Stat. Soc. Ser. B Stat. Methodol. 71, 319–392. https://doi.org/10.1111/j.1467-9868.2008.00700.x

Saunders, S.C., Chen, J.Q., Drummer, T.D., Gustafson, E.J., Brosofske, K.D., 2005. Identifying scales of pattern in ecological data: a comparison of lacunarity, spectral and wavelet analyses. Ecol. Complex. 2, 87–105. https://doi.org/10.1016/j.ecocom.2004.11.002

Scheuerell, M.D., Schindler, D.E., 2003. Diel vertical migration by juvenile sockeye salmon: empirical evidence for the antipredation window. Ecology 84, 1713–1720. https://doi.org/10.1890/0012-9658(2003)084[1713:DVMBJS]2.0.CO;2

Schneider, D.C., 1994. Quantitative Ecology: Spatial and Temporal Scaling. Academic Press, San Diego.

Schwartzlose, R.A., Alheit, J., Bakun, A., Baumgartner, T.R., Cloete, R., Crawford, R.J.M., Fletcher, W.J., Green-Ruiz, Y., Hagen, E., Kawasaki, T., Lluch-Belda, D., Lluch-Cota, S.E., MacCall, A.D., Matsuura, Y., Nevarez-Martinez, M.O., Parrish, R.H., Roy, C., Serra, R., Shust, K.V., Ward, M.N., Zuzunaga, J.Z., 1999. Worldwide large-scale fluctuations of sardine and anchovy populations. South Afr. J. Mar. Sci. 21, 289–347.

Shelton, A.O., Thorson, J.T., Ward, E.J., Feist, B.E., 2014. Spatial semiparametric models improve estimates of species abundance and distribution. Can. J. Fish. Aquat. Sci. 71, 1655–1666. https://doi.org/10.1139/cjfas-2013-0508

Sigler, M.F., Csepp, D.J., 2007. Seasonal abundance of two important forage species in the North Pacific Ocean, Pacific herring and walleye pollock. Fish. Res. 83, 319–331. https://doi.org/10.1016/j.fishres.2006.10.007

Sigler, M.F., Womble, J.N., Vollenweider, J.J., 2004. Availability to Steller sea lions (*Eumetopias jubatus*) of a seasonal prey resource: a prespawning aggregation of eulachon (*Thaleichthys pacificus*). Can. J. Fish. Aquat. Sci. 61, 1475–1484.

Simard, Y., Lavoie, D., Saucier, F.J., 2002. Channel head dynamics: capelin (*Mallotus villosus*) aggregation in the tidally driven upwelling system of the Saguenay - St. Lawrence Marine Park's whale feeding ground. Can. J. Fish. Aquat. Sci. 59, 197–210. https://doi.org/10.1139/f01-210

Simmonds, E.J., MacLennan, D.N., 2005. Fisheries Acoustics: Theory And Practice, 2nd ed. Blackwell Science, Oxford, UK.

Simonsen, K.A., Ressler, P.H., Rooper, C.N., Zador, S.G., 2016. Spatio-temporal distribution of euphausiids: an important component to understanding ecosystem processes in the Gulf of Alaska and eastern Bering Sea. ICES J. Mar. Sci. 73, 2020–2036. https://doi.org/10.1093/icesjms/fsv272

Skaug, H.J., Fournier, D.A., 2006. Automatic approximation of the marginal likelihood in non-Gaussian hierarchical models. Comput. Stat. Data Anal. 51, 699–709. https://doi.org/10.1016/j.csda.2006.03.005

Slater, L., Fety, S., 2015. Biological monitoring at St. Lazaria Island, Alaska, in 2014 (Report No. AMNWR 2015/09). U.S. Fish and Wildlife Service, Alaska Maritime National Wildlife Refuge, 95 Sterling Highway, Suite 1 Homer, AK 99603.

Smart, T.I., Duffy-Anderson, J.T., Horne, J.K., 2012. Alternating temperature states influence walleye pollock early life stages in the southeastern Bering Sea. Mar. Ecol. Prog. Ser. 455, 257–267. https://doi.org/10.3354/meps09619

Smart, T.I., Siddon, E.C., Duffy-Anderson, J.T., 2013. Vertical distributions of the early life stages of walleye pollock (*Theragra chalcogramma*) in the Southeastern Bering Sea. Deep Sea Res. Part II 94, 201–210. https://doi.org/10.1016/j.dsr2.2013.03.030

Sogard, S.M., Olla, B.L., 1998. Behavior of juvenile sablefish, *Anoplopoma fimbria* (Pallas), in a thermal gradient: Balancing food and temperature requirements. J. Exp. Mar. Biol. Ecol. 222, 43–58. https://doi.org/10.1016/S0022-0981(97)00137-8

Speckman, S.G., Piatt, J.F., Minte-Vera, C.V., Parrish, J.K., 2005. Parallel structure among environmental gradients and three trophic levels in a subarctic estuary. Prog. Oceanogr. 66, 25–65. https://doi.org/10.1016/j.pocean.2005.04.001

Spellerberg, I.F., 1991. Monitoring Ecological Change, 1st ed. Cambridge University Press, Cambridge, U.K.

Springer, A.M., Speckman, S.G., 1997. A forage fish is what? Summary of the symposium (No. AK-SG-97-01), Forage Fishes in Marine Ecosystems. Alaska Sea Grant College Program, Fairbanks, Alaska, USA.

Stabeno, P., Bond, N., Hermann, A., Kachel, N., Mordy, C., Overland, J., 2004. Meteorology and oceanography of the Northern Gulf of Alaska. Cont. Shelf Res. 24, 859–897.

Stabeno, P.J., Bell, S., Cheng, W., Danielson, S., Kachel, N.B., Mordy, C.W., 2016a. Long-term observations of Alaska Coastal Current in the northern Gulf of Alaska. Deep Sea Res. Part II 132, 24–40. https://doi.org/10.1016/j.dsr2.2015.12.016

Stabeno, P.J., Bond, N.A., Kachel, N.B., Ladd, C., Mordy, C.W., Strom, S.L., 2016b. Southeast Alaskan shelf from southern tip of Baranof Island to Kayak Island: Currents, mixing and chlorophyll-a. Deep Sea Res. Part II 132, 6–23. https://doi.org/10.1016/j.dsr2.2015.06.018

Stockwell, J.D., Yule, D.L., Hrabik, T.R., Adams, J.V., Gorman, O.T., Holbrook, B.V., 2007. Vertical distribution of fish biomass in Lake Superior: implications for day bottom trawl surveys. North Am. J. Fish. Manag. 27, 735–749. https://doi.org/10.1577/M06-116.1

Strom, S.L., Fredrickson, K.A., Bright, K.J., 2016. Spring phytoplankton in the eastern coastal Gulf of Alaska: photosynthesis and production during high and low bloom years. Deep Sea Res. Part II 132, 107–121. https://doi.org/10.1016/j.dsr2.2015.05.003

Strom, S.L., Olson, M.B., Macri, E.L., Mordy, C.W., 2006. Cross-shelf gradients in phytoplankton community structure, nutrient utilization, and growth rate in the coastal Gulf of Alaska. Mar. Ecol. Prog. Ser. 328, 75–92. https://doi.org/10.3354/meps328075

Sydeman, W.J., Brodeur, R.D., Grimes, C.B., Bychkov, A.S., McKinnell, S., 2006. Marine habitat "hotspots" and their use by migratory species and top predators in the North Pacific Ocean: Introduction. Deep Sea Res. Part II 53, 247–249. https://doi.org/10.1016/j.dsr2.2006.03.001

Sydeman, W.J., Piatt, J.F., Thompson, S.A., García-Reyes, M., Hatch, S.A., Arimitsu, M.L., Slater, L., Williams, J.C., Rojek, N.A., Zador, S.G., Renner, H.M., 2017. Puffins reveal contrasting relationships between forage fish and ocean climate in the North Pacific. Fish. Oceanogr. 26, 379–395. https://doi.org/10.1111/fog.12204

Szuwalski, C.S., Vert-Pre, K.A., Punt, A.E., Branch, T.A., Hilborn, R., 2015. Examining common assumptions about recruitment: a meta-analysis of recruitment dynamics for worldwide marine fisheries. Fish Fish. 16, 633–648. https://doi.org/10.1111/faf.12083

Thorson, J.T., Barnett, L.A.K., 2017. Comparing estimates of abundance trends and distribution shifts using single- and multispecies models of fishes and biogenic habitat. ICES J. Mar. Sci. 74, 1311–1321. https://doi.org/10.1093/icesjms/fsw193

Thorson, J.T., Ianelli, J.N., Kotwicki, S., 2017. The relative influence of temperature and size-structure on fish distribution shifts: A case-study on walleye pollock in the Bering Sea. Fish Fish. 18, 1073–1084. https://doi.org/10.1111/faf.12225

Thorson, J.T., Ianelli, J.N., Larsen, E.A., Ries, L., Scheuerell, M.D., Szuwalski, C., Zipkin, E.F., 2016. Joint dynamic species distribution models: a tool for community ordination and spatio-temporal monitoring. Glob. Ecol. Biogeogr. 25(9), 1144-1158. https://doi.org/10.1111/geb.12464

Thorson, J.T., Scheuerell, M.D., Shelton, A.O., See, K.E., Skaug, H.J., Kristensen, K., 2015a. Spatial factor analysis: a new tool for estimating joint species distributions and correlations in species range. Methods Ecol. Evol. 6, 627–637. https://doi.org/10.1111/2041-210X.12359

Thorson, J.T., Shelton, A.O., Ward, E.J., Skaug, H.J., 2015b. Geostatistical delta-generalized linear mixed models improve precision for estimated abundance indices for West Coast groundfishes. ICES J. Mar. Sci. J. Cons. 72, 1297–1310. https://doi.org/10.1093/icesjms/fsu243

Thorson, J.T., Skaug, H.J., Kristensen, K., Shelton, A.O., Ward, E.J., Harms, J.H., Benante, J.A., 2015c. The importance of spatial models for estimating the strength of density dependence. Ecology 96, 1202–1212. https://doi.org/10.1890/14-0739.1

Torrence, C., Compo, G.P., 1998. A practical guide to wavelet analysis. Bull. Am. Meteorol. Soc. 79, 61–78. https://doi.org/10.1175/1520-0477(1998)079<0061:APGTWA>2.0.CO;2

Urmy, S.S., Horne, J.K., Barbee, D.H., 2012. Measuring the vertical distributional variability of pelagic fauna in Monterey Bay. ICES J. Mar. Sci. 69, 184–196. https://doi.org/10.1093/icesjms/fsr205

Valdimarsson, H., Astthorsson, O.S., Palsson, J., 2012. Hydrographic variability in Icelandic waters during recent decades and related changes in distribution of some fish species. ICES J. Mar. Sci. 69, 816–825. https://doi.org/10.1093/icesjms/fss027

Vaughan, S.L., Mooers, C.N.K., Gay, S.M., 2001. Physical variability in Prince William Sound during the SEA Study (1994–98). Fish. Oceanogr. 10, 58–80. https://doi.org/10.1046/j.1054-6006.2001.00034.x

Vilhjálmsson, H., 2002. Capelin (*Mallotus villosus*) in the Iceland–East Greenland–Jan Mayen ecosystem. ICES J. Mar. Sci. J. Cons. 59, 870–883. https://doi.org/10.1006/jmsc.2002.1233

Vilhjálmsson, H., 1994. The Icelandic Capelin Stock: Capelin, *Mallotus villosus* (Müller) in the Iceland-Greenland-Jan Mayen area. Rit Fiskid. 13, 1–281.

Vollenweider, J.J., Heintz, R.A., Schaufler, L., Bradshaw, R., 2011. Seasonal cycles in whole-body proximate composition and energy content of forage fish vary with water depth. Mar. Biol. 158, 413–427. https://doi.org/10.1007/s00227-010-1569-3

Waite, J.N., Mueter, F.J., 2013. Spatial and temporal variability of chlorophyll-*a* concentrations in the coastal Gulf of Alaska, 1998–2011, using cloud-free reconstructions of SeaWiFS and MODIS-Aqua data. Prog. Oceanogr. 116, 179–192. https://doi.org/10.1016/j.pocean.2013.07.006

Weingartner, T., Eisner, L., Eckert, G.L., Danielson, S., 2009. Southeast Alaska: oceanographic habitats and linkages. J. Biogeogr. 36, 387–400.

Whitehead, H., Carscadden, J.E., 1985. Predicting inshore whale abundance — whales and capelin off the Newfoundland coast. Can. J. Fish. Aquat. Sci. 42, 976–981. https://doi.org/10.1139/f85-122

Williams, K., Punt, A.E., Wilson, C.D., Horne, J.K., 2011. Length-selective retention of walleye pollock, *Theragra chalcogramma*, by midwater trawls. ICES J. Mar. Sci. J. Cons. 68, 119–129. https://doi.org/10.1093/icesjms/fsq155

Wilson, M.T., 2009. Ecology of small neritic fishes in the western Gulf of Alaska. I. Geographic distribution in relation to prey density and the physical environment. Mar. Ecol. Prog. Ser. 392, 223–237. https://doi.org/10.3354/meps08160

Wilson, M.T., Brodeur, R.D., Hinckley, S., 1996. Distribution and abundance of age-0 walleye pollock, *Theragra chalcogramma*, in the western Gulf of Alaska during September 1990 (NOAA AFSC Tech Rep No. 126). US Dept of Commerce, Alaska Fisheries Science Center, National Marine Fisheries Service, Seattle, WA.

Wilson, M.T., Jump, C.M., Buchheister, A., 2009. Ecology of small neritic fishes in the western Gulf of Alaska. II. Consumption of krill in relation to krill standing stock and the physical environment. Mar. Ecol. Prog. Ser. 392, 239–251. https://doi.org/10.3354/meps08237

Wilson, M.T., Jump, C.M., Duffy-Anderson, J.T., 2006. Comparative analysis of the feeding ecology of two pelagic forage fishes: capelin *Mallotus villosus* and walleye pollock *Theragra chalcogramma*. Mar. Ecol. Prog. Ser. 317, 245–258. https://doi.org/10.3354/meps317245

Wilson, R.P., Hustler, K., Ryan, P.G., Burger, A.E., Noldeke, E.C., 1992. Diving birds in cold water: do Archimedes and Boyle determine energetic costs? Am. Nat. 140, 179–200.

Witteveen, B.H., De Robertis, A., Guo, L., Wynne, K.M., 2015. Using dive behavior and active acoustics to assess prey use and partitioning by fin and humpback whales near Kodiak Island, Alaska. Mar. Mammal Sci. 31, 255–278. https://doi.org/10.1111/mms.12158

Woillez, M., Poulard, J.-C., Rivoirard, J., Petitgas, P., Bez, N., 2007. Indices for capturing spatial patterns and their evolution in time, with application to European hake (*Merluccius merluccius*) in the Bay of Biscay. ICES J. Mar. Sci. 64, 537–550. https://doi.org/10.1093/icesjms/fsm025

Wolter, K., Timlin, M.S., 1998. Measuring the strength of ENSO events: How does 1997/98 rank? Weather 53, 315–324. https://doi.org/10.1002/j.1477-8696.1998.tb06408.x

Wolter, K., Timlin, M.S., 1993. Monitoring ENSO in COADS with a seasonally adjusted principal component index, in: Proc. of the 17th Climate Diagnostics Workshop. Presented at the NOAA/NMC/CAC, NSSL, Oklahoma Clim. Survey, CIMMS and the School of Meteor., Univ. of Oklahoma, Norman, OK, pp. 52–57.

Womble, J.N., Sigler, M.F., 2006. Seasonal availability of abundant, energy-rich prey influences the abundance and diet of a marine predator, the Steller sea lion *Eumetopias juhatus*. Mar. Ecol. Prog. Ser. 325, 281–293. https://doi.org/10.3354/meps325281

Womble, J.N., Sigler, M.F., Willson, M.F., 2009. Linking seasonal distribution patterns with prey availability in a central-place forager, the Steller sea lion. J. Biogeogr. 36, 439–451. https://doi.org/10.1111/j.1365-2699.2007.01873.x

Yang, M.S., Aydin, K., Greig, A., Lang, G., Livingston, P., 2005. Historical Review of Capelin (*Mallotus villosus*) Consumption in the Gulf of Alaska and Eastern Bering Sea (No. NMFS-AFSC-155). National Marine Fisheries Service, Alaska Fisheries Science Center.

Zador, S., 2014. Ecosystem Considerations 2014 (Stock Assessment and Fishery Evaluation Report). North Pacific Fishery Management Council, 605 W. 4th Avenue, Suite 306, Anchorage, AK 99301.

Zador, S., 2013. Ecosystem Considerations 2013 (Stock Assessment and Fishery Evaluation Report). North Pacific Fishery Management Council, 605 W. 4th Avenue, Suite 306, Anchorage, AK 99301.

Zador, S., 2012. Ecosystem Considerations 2012 (Stock Assessment and Fishery Evaluation Report). North Pacific Fishery Management Council, 605 W. 4th Avenue, Suite 306, Anchorage, AK 99301.

Zador, S., Yasumishii, E.C., 2017. Ecosystem Considerations 2017: Status of the Gulf of Alaska Marine Ecosystem (Stock Assessment and Fishery Evaluation Report). North Pacific Fishery Management Council, 605 W. 4th Avenue, Suite 306, Anchorage, AK 99301.

Zador, S., Yasumishii, E.C., 2016. Ecosystem Considerations 2016: Status of the Gulf of Alaska Marine Ecosystem (Stock Assessment and Fishery Evaluation Report). North Pacific Fishery Management Council, 605 W. 4th Avenue, Suite 306, Anchorage, AK 99301.

Zar, J.H., 2010. Biostatistical analysis, 5th ed. Prentice-Hall/Pearson, Upper Saddle River, N.J.

Zimmermann, M., Prescott, M.M., 2015. Smooth sheet bathymetry of the central Gulf of Alaska (NOAA Technical Memorandum No. NMFS-AFSC-287). U.S. Deptartment of Commerce.

Zuur, A.F., Ieno, E.N., Elphick, C.S., 2010. A protocol for data exploration to avoid common statistical problems. Methods Ecol. Evol. 1, 3–14. https://doi.org/10.1111/j.2041-210X.2009.00001.x

Zuur, A.F., Ieno, E.N., Walker, N.J., Saveliev, A.A., Smith, G.D., 2009. Mixed Effects Models and Extensions in Ecology with R. Springer, New York, New York, USA.

Zuur, A.F., Saveliev, A.A., Ieno, E.N., 2012. Zero Inflated Models and Generalized Linear Mixed Models with R. Highland Statistics Ltd., Newburgh, United Kingdom.

# APPENDIX A: SUPPLEMENTARY MAPS FOR CHAPTER 2

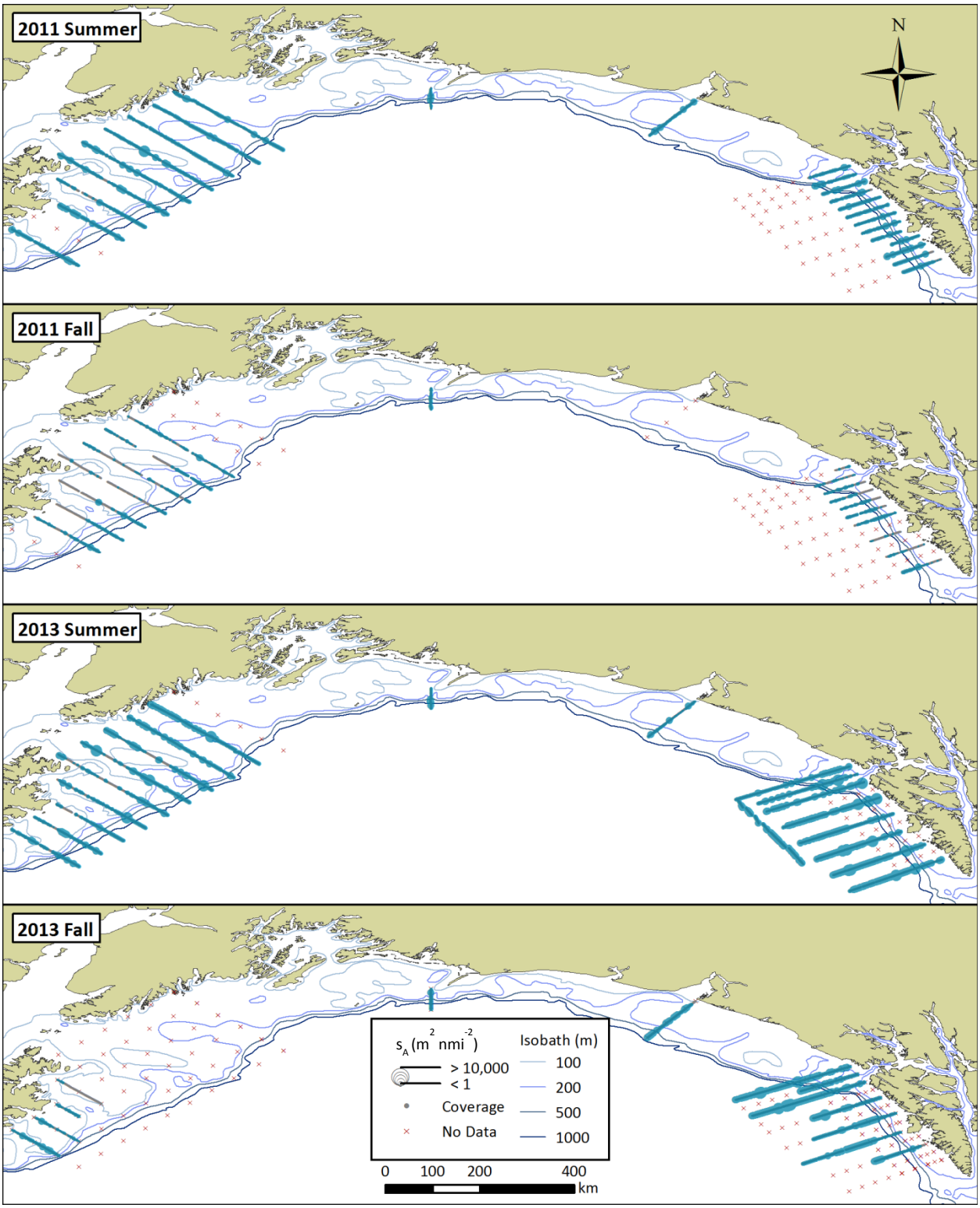


**Appendix A.1 –** Summer and fall distributions of backscatter assigned to the surface category in 2011 and 2013. Acoustic density estimates, $s_A$ ($m^2$ $nmi^{-2}$) are in 200 m horizontal bins.

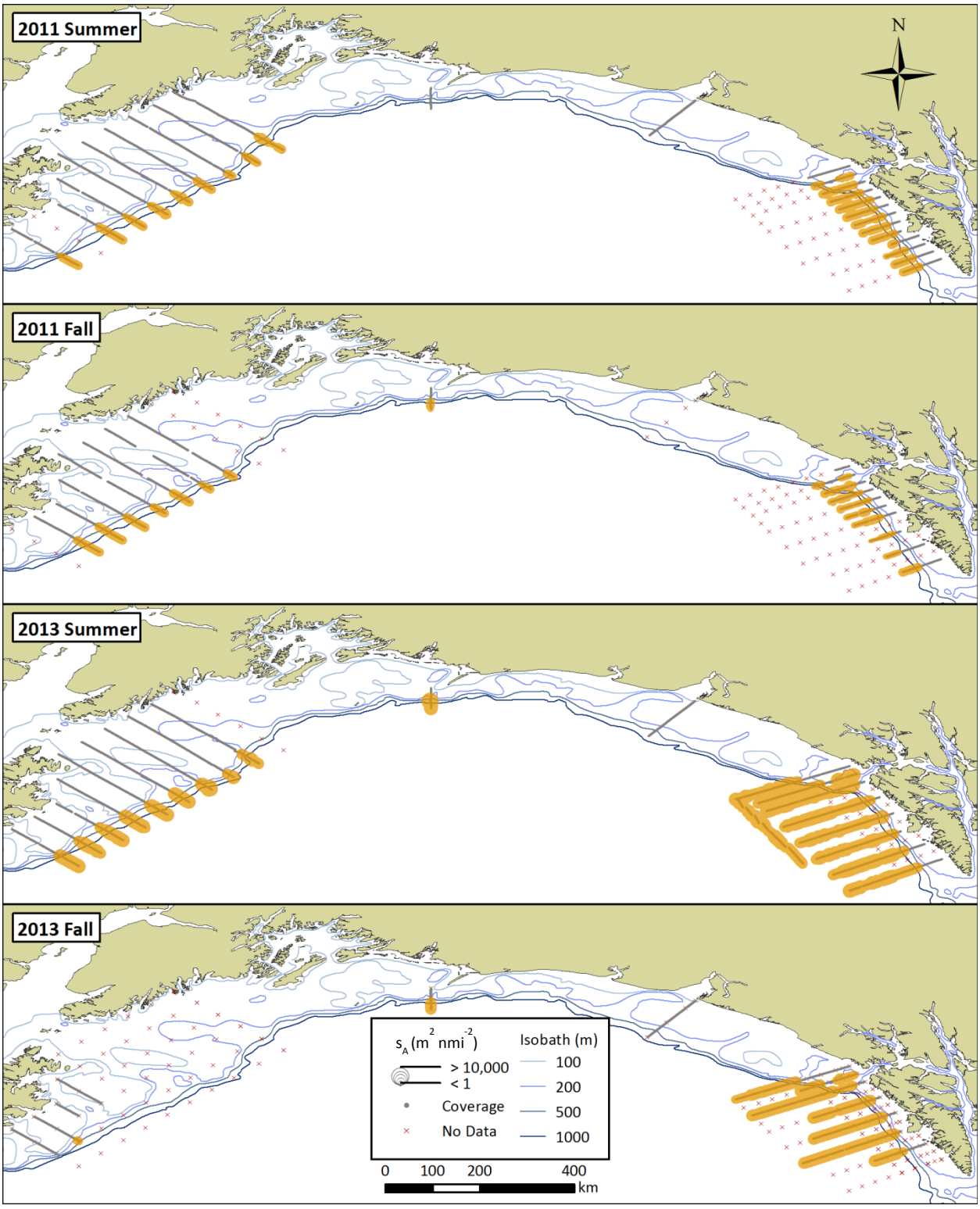


**Appendix A.2 –** Summer and fall distributions of backscatter assigned to the mesopelagic category in 2011 and 2013. Acoustic density estimates, $s_A$ ($m^2$ $nmi^{-2}$) are in 200 m horizontal bins.

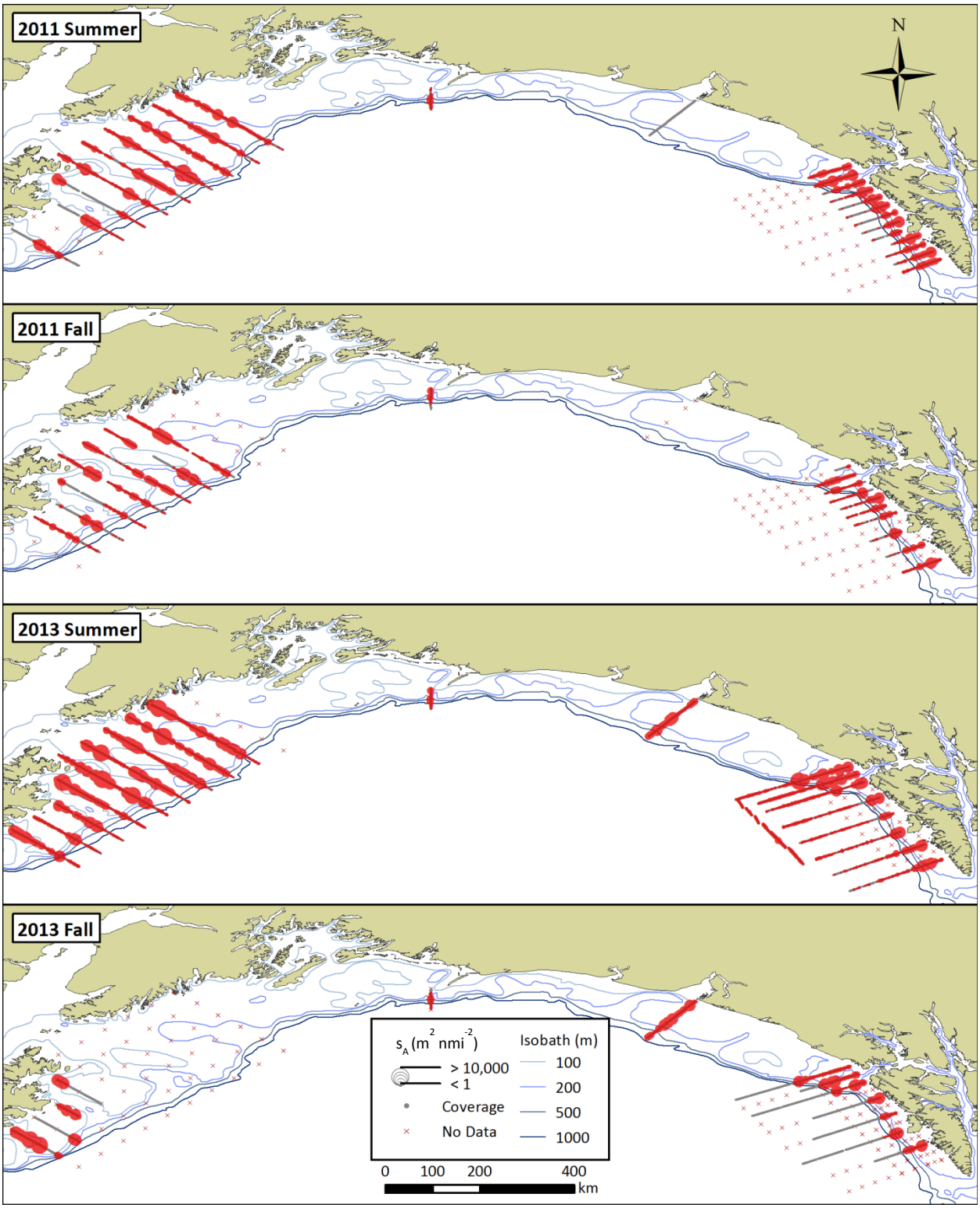


**Appendix A.3 –** Summer and fall distributions of backscatter assigned to the piscivores category in 2011 and 2013. Acoustic density estimates, $s_A$ ($m^2$ $nmi^{-2}$) are in 200 m horizontal bins.

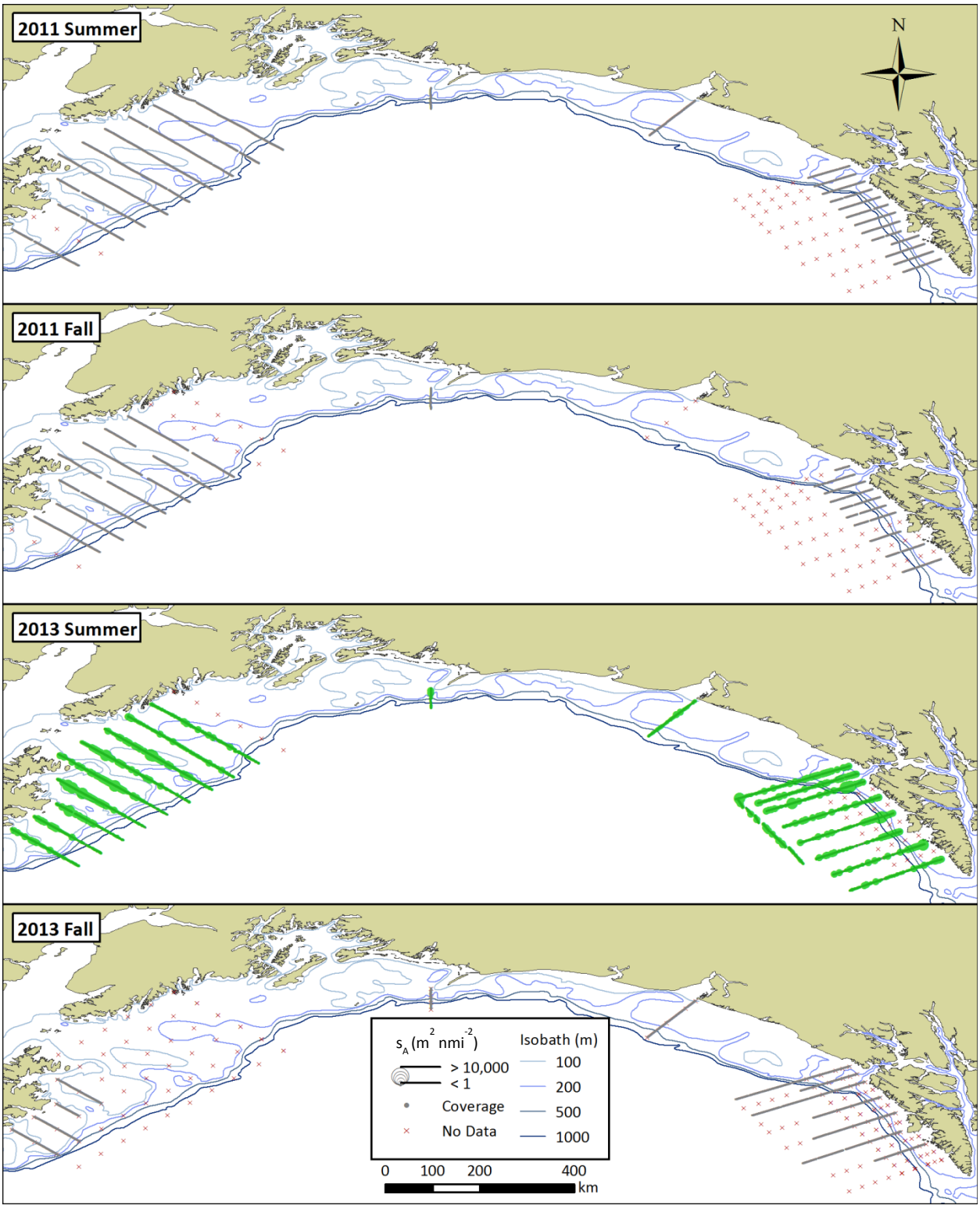


**Appendix A.4 –** Summer and fall distributions of backscatter assigned to the age-0 pollock category in 2011 and 2013. Acoustic density estimates, $s_A$ ($m^2$ $nmi^{-2}$) are in 200 m horizontal bins.

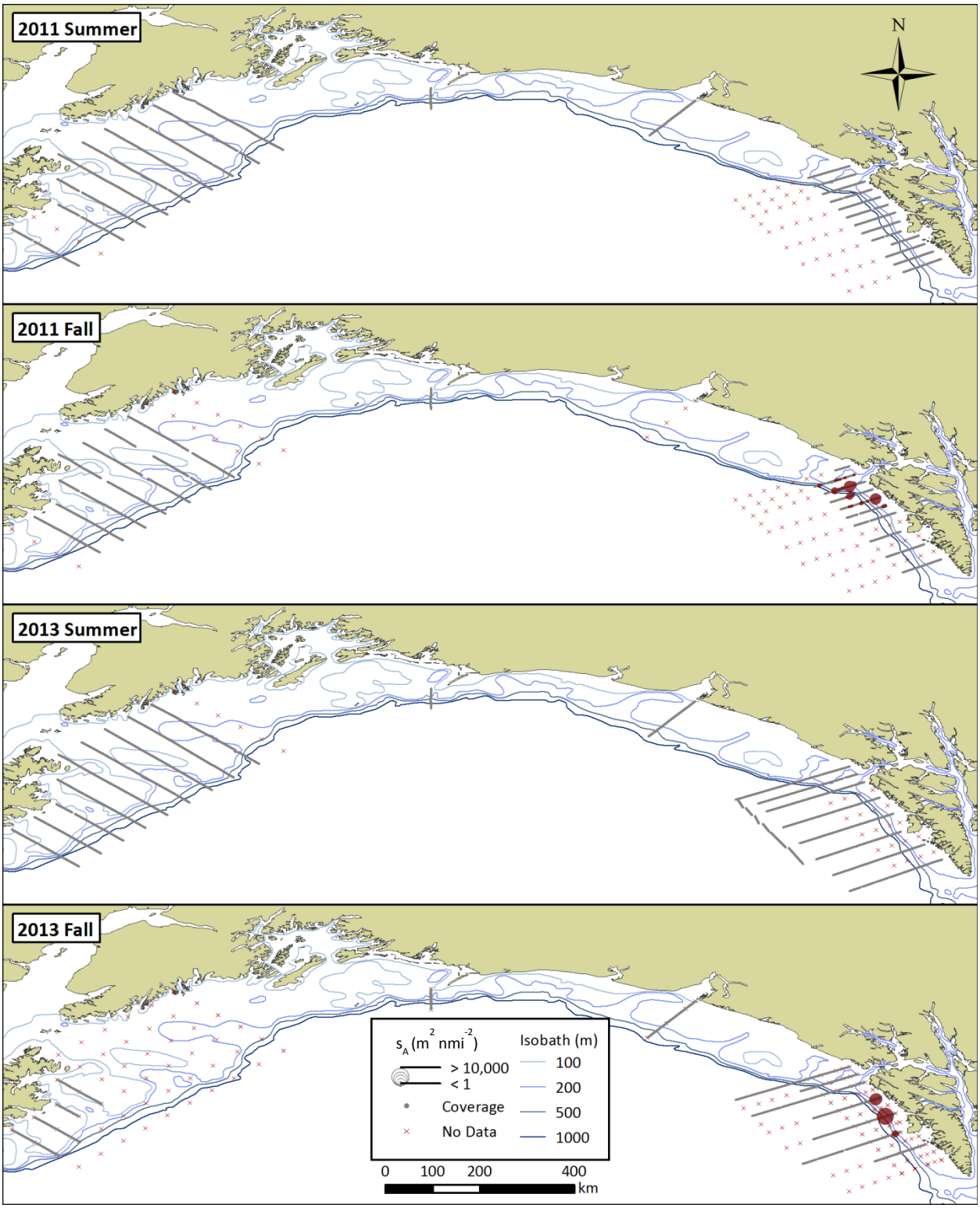


**Appendix A.5 –** Summer and fall distributions of backscatter assigned to the herring category in 2011 and 2013. Acoustic density estimates, $s_A$ ($m^2$ $nmi^{-2}$) are in 200 m horizontal bins.

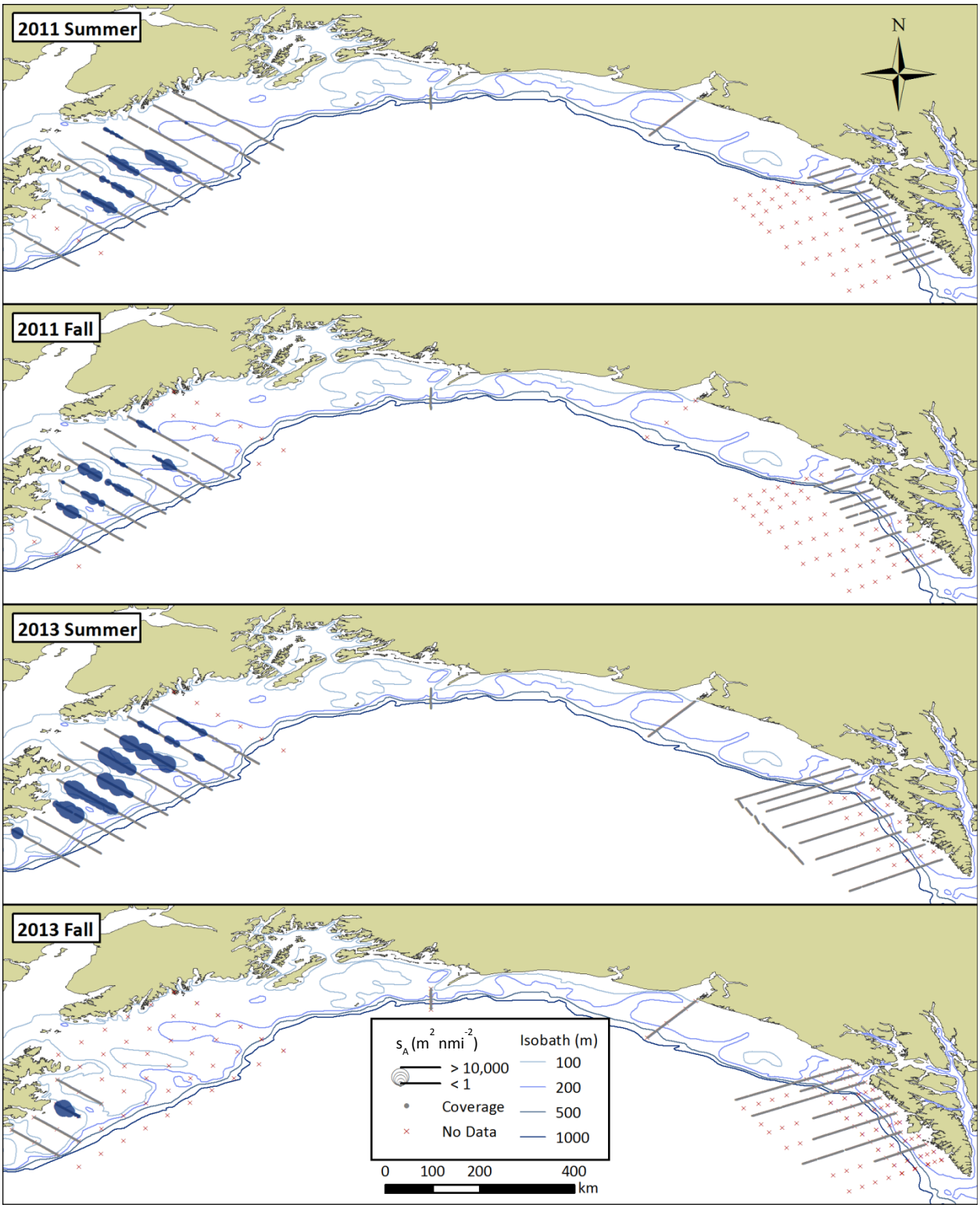


**Appendix A.6 –** Summer and fall distributions of backscatter assigned to the capelin category in 2011 and 2013. Acoustic density estimates, $s_A$ ($m^2$ $nmi^{-2}$) are in 200 m horizontal bins.

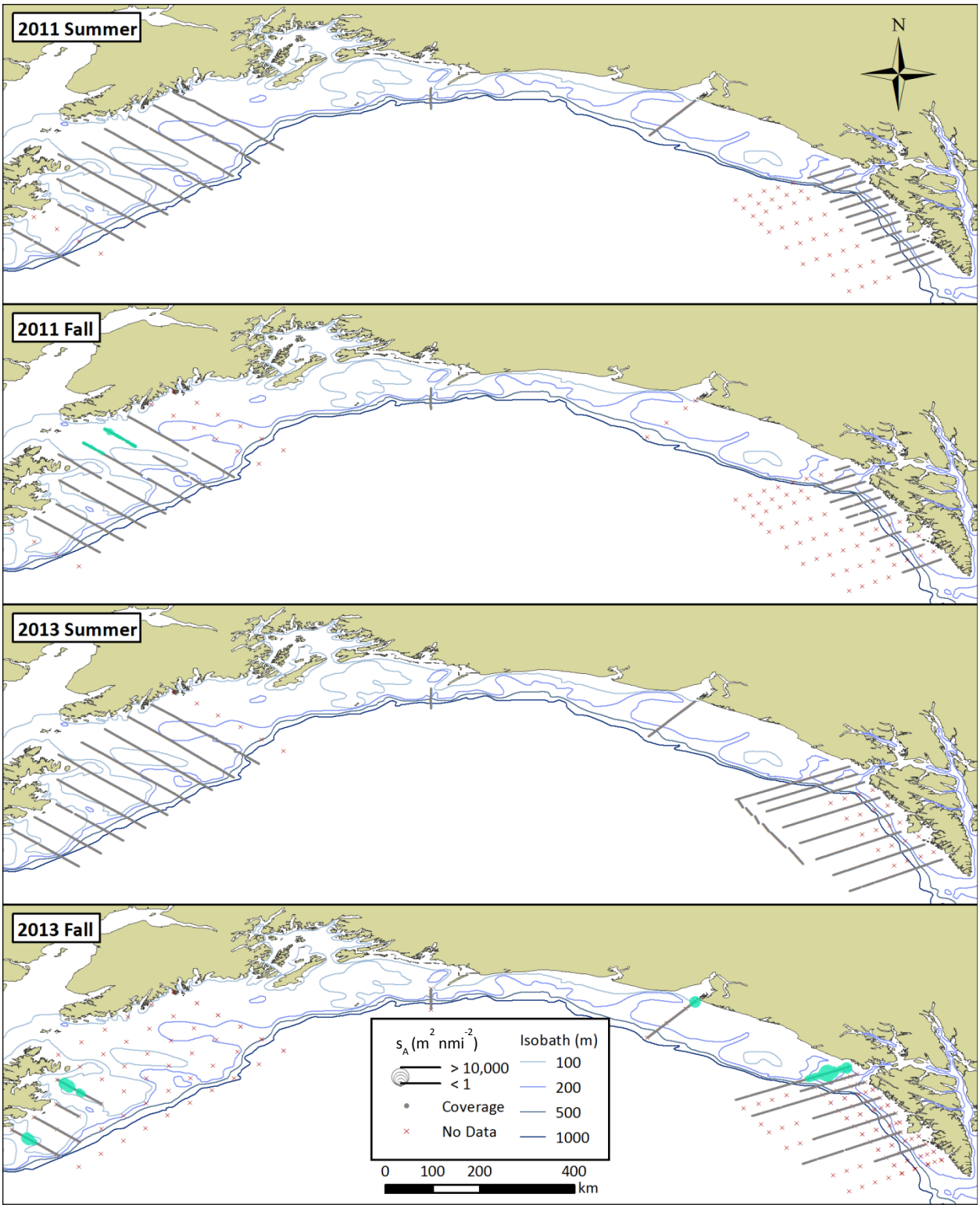


**Appendix A.7 –** Summer and fall distributions of backscatter assigned to the forage fish mix category in 2011 and 2013. Acoustic density estimates, $s_A$ ($m^2$ $nmi^{-2}$) are in 200 m horizontal bins.

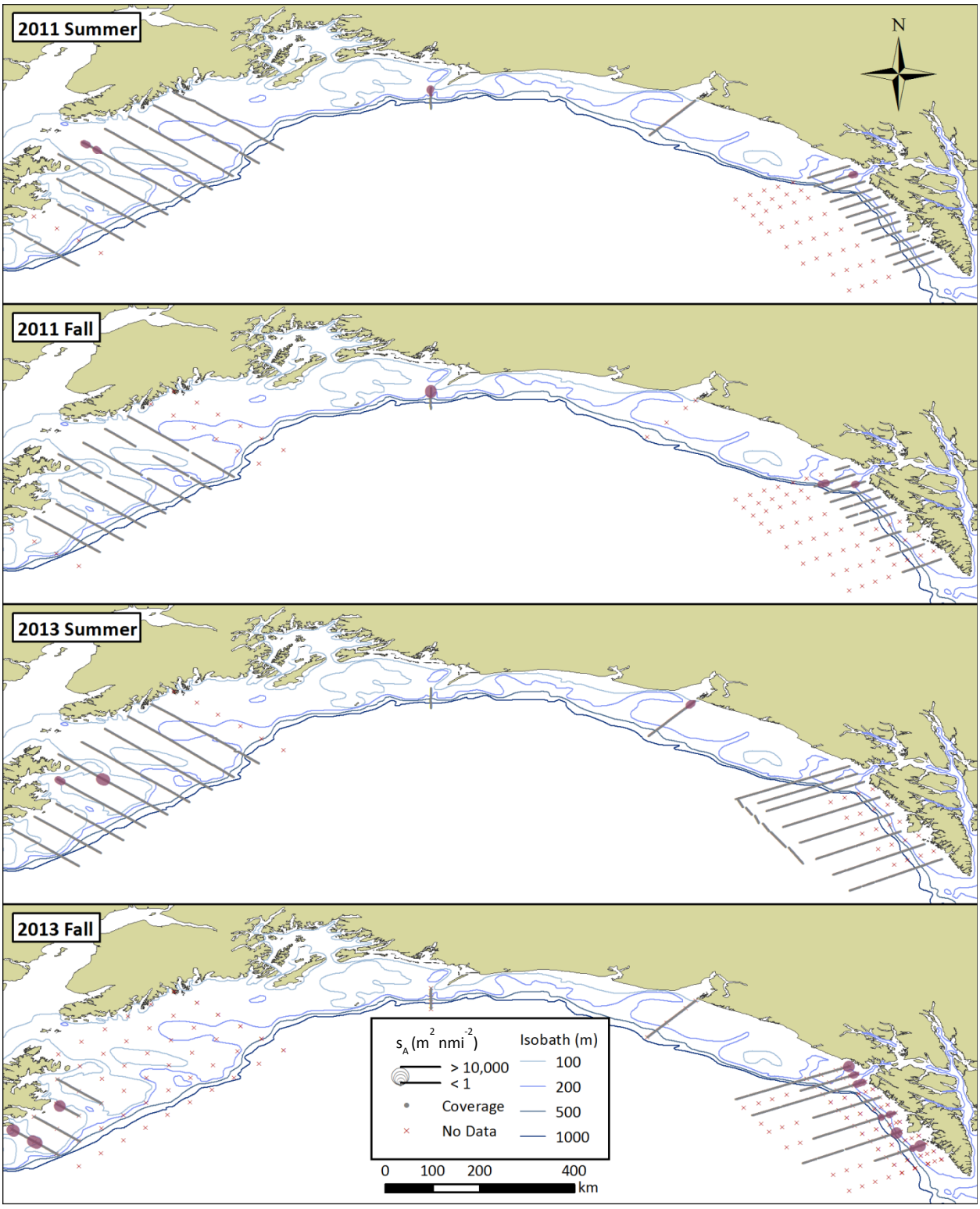


**Appendix A.8 –** Summer and fall distributions of backscatter assigned to the forage fish / piscivores mix category in 2011 and 2013. Acoustic density estimates, $s_A$ ($m^2$ $nmi^{-2}$) are in 200 m horizontal bins.

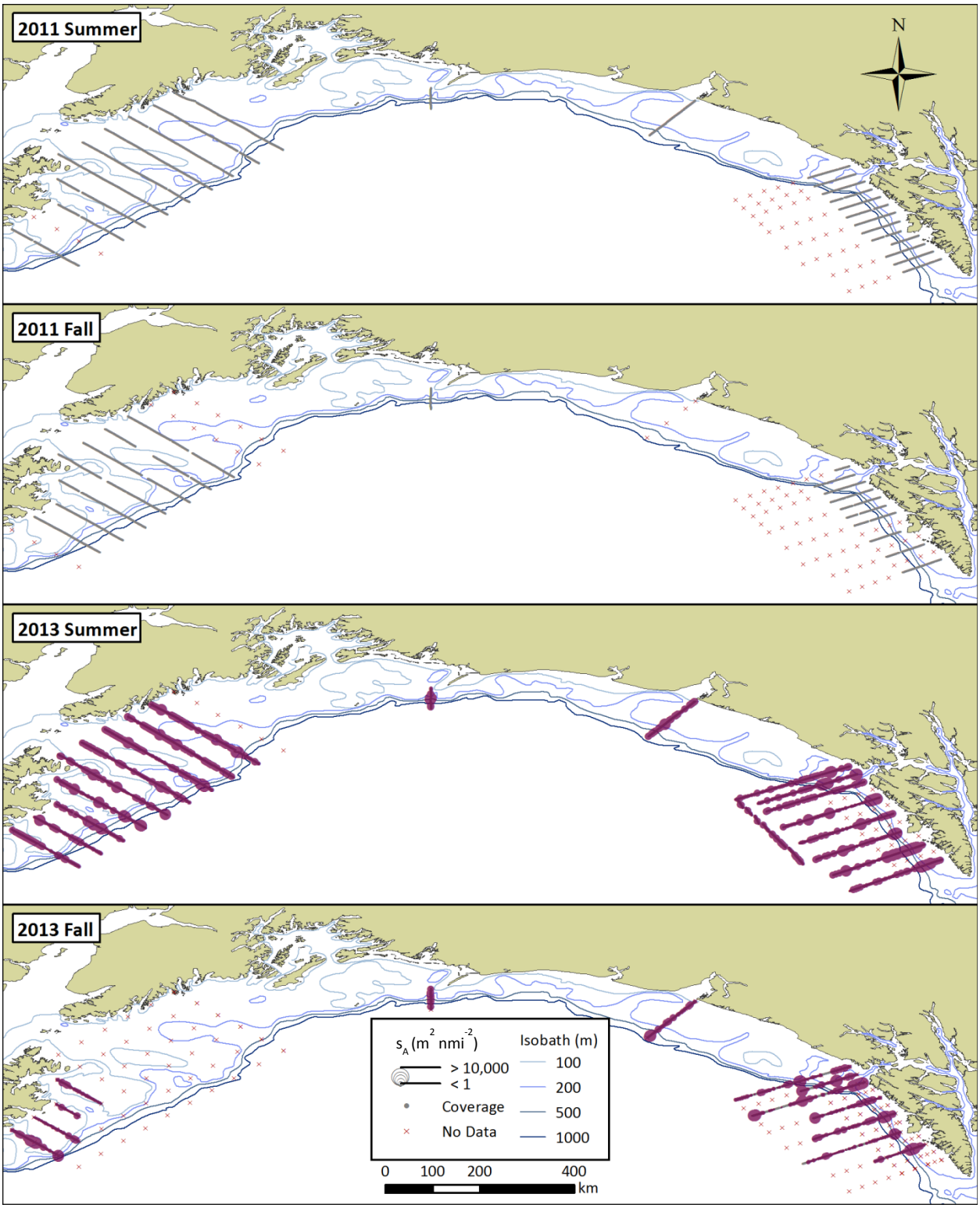


**Appendix A.9 –** Summer and fall distributions of backscatter assigned to the macrozooplankton category in 2011 and 2013. Acoustic density estimates, $s_A$ ($m^2$ $nmi^{-2}$) are in 200 m horizontal bins.

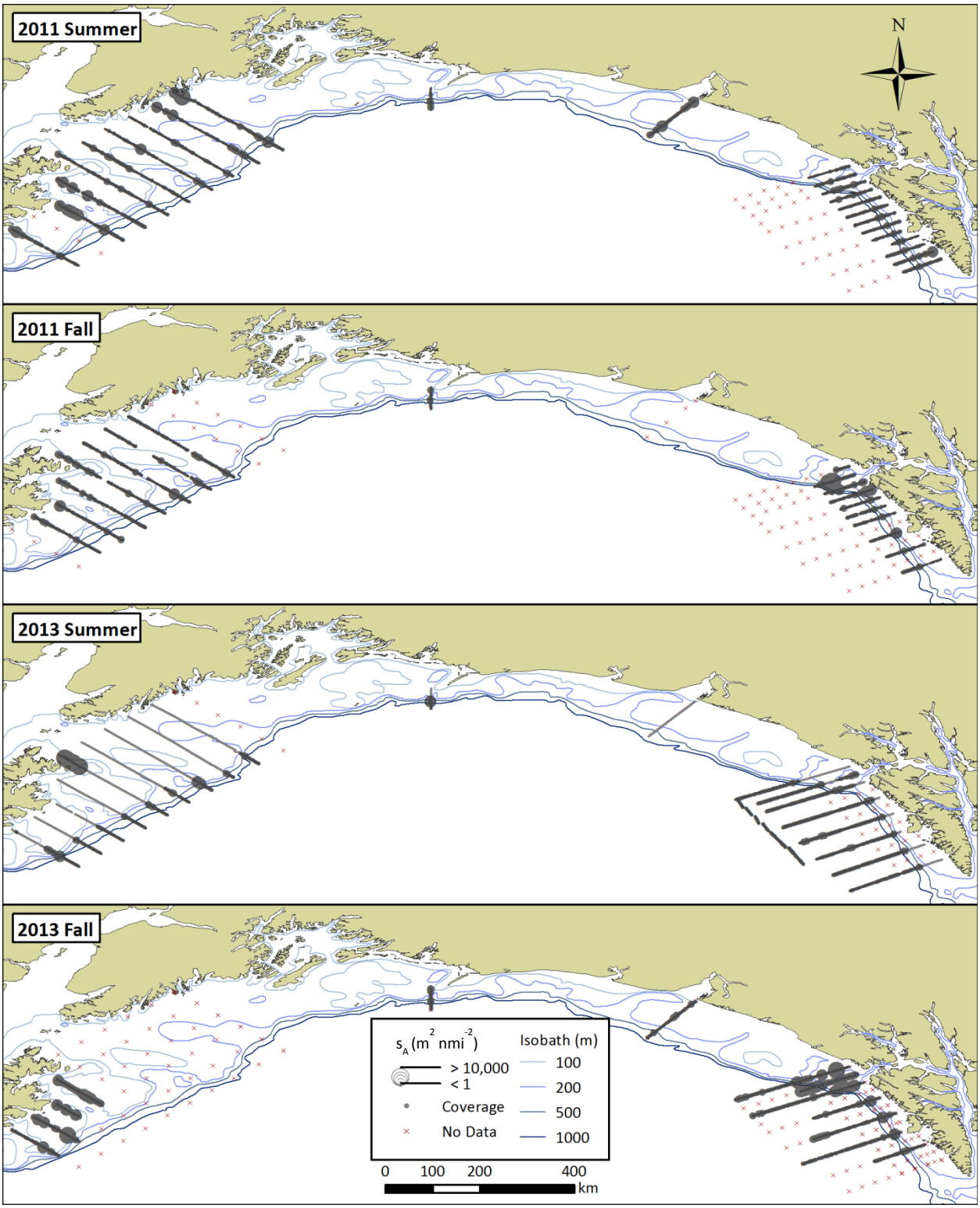


**Appendix A.10 –** Summer and fall distributions of backscatter assigned to the unknown category in 2011 and 2013. Acoustic density estimates, $s_A$ ($m^2$ $nmi^{-2}$) are in 200 m horizontal bins.